

Volcano-Climate Interactions in the Holocene

Claire Louise Cooper

Submitted in accordance with the requirements for the degree of

Doctor of Philosophy

The University of Leeds

School of Geography

School of Earth and Environment

February 2020

The candidate confirms that the work submitted is his/her/their own, except where work which has formed part of jointly authored publications has been included. The contribution of the candidate and the other authors to this work has been explicitly indicated below. The candidate confirms that appropriate credit has been given within the thesis where reference has been made to the work of others.

The following chapters contain jointly authored manuscripts where C.L.C. is the lead author:

Chapter 2: Evaluating the relationship between climate change and volcanism.

Cooper, C.L., Swindles, G.T., Savov, I.P., Schmidt, A. and Bacon, K.L., 2018.

Evaluating the relationship between climate change and volcanism. *Earth-Science Reviews*, 177, pp.238-247.

Contributions: C.L.C. conducted the research on existing literature, wrote the paper, and prepared all Figures. G.T.S. provided data included in Figure 3. G.T.S, I.P.S., A.S., and K.L.B. provided commentary and edits to the manuscript.

Chapter 3: Evaluating tephrochronology in the permafrost peatlands of Northern Sweden

Cooper, C.L., Swindles, G.T., Watson, E.J., Savov, I.P., Gałka, M., Gallego-Sala, A. and Borken, W., 2019. Evaluating tephrochronology in the permafrost peatlands of northern Sweden. *Quaternary Geochronology*, 50, pp.16-28.

Contributions: C.L.C. conducted tephra extraction and geochemical data analysis, performed assignment of tephra to source eruption, wrote the paper including discussion of preservation factors, and prepared Figures 2, 3, 4, 5, and 6, in addition to editing Figure 1. E.J.W, I.P.S. and G.T.S. performed sample collection, and E.J.W. conducted geochemical analysis on Marooned and Stordalen cores. G.M. and W.B. provided radiocarbon data, and A.G-S. provided ²¹⁰Pb data. G.T.S. and I.P.S. provided supervision of both C.L.C. and E.J.W. and contributed expertise. All authors reviewed the final manuscript.

Chapter 4: Standard chemical-based tephra extraction methods significantly alter the geochemistry of volcanic glass shards

Cooper, C.L., Savov, I.P. and Swindles, G.T., 2019. Standard chemical-based tephra extraction methods significantly alter the geochemistry of volcanic glass shards. *Journal of Quaternary Science*, 34, pp.697-707

Contributions: C.L.C. designed the experiment, conducted chemical extractions of tephra and conducted geochemical analysis, performed statistical analysis of results, wrote the paper, and produced all Figures. I.P.S. contributed to the experiment design, and assisted with the interpretation of results. G.T.S. assisted with statistical analysis and provided laboratory training and supervision. G.T.S. and I.P.S. provided commentary and edits to the final manuscript and Figures.

Chapter 5: Is there a climatic control on Icelandic volcanism?

Cooper, C.L., Savov, I.P., Patton, H., Hubbard, A., Ivanovic, R.F., Carrivick, J.L. and Swindles, G.T., 2019. Is there a climatic control on Icelandic volcanism?

Contributions: C.L.C. designed the study, compiled the Holocene database, produced all Figures, and wrote the paper. I.P.S. assisted in the design of the study and provided expertise on volcanic mechanics. H.P. and A.H. contributed the palaeoglacial modelling, with assistance and input from J.L.C. R.F.I. contributed the atmospheric modelling, with input from C.L.C. and G.T.S. G.T.S. provided an early version of the Holocene tephra database. All authors provided commentary and edits to the final manuscript and figures.

This copy has been supplied on the understanding that it is copyright material and that no quotation from the thesis may be published without proper acknowledgement.

The right of Claire Louise Cooper to be identified as Author of this work has been asserted by her in accordance with the Copyright, Designs and Patents Act 1988.

© 2020 The University of Leeds and Claire Louise Cooper

Acknowledgements

The road to the submission of this thesis has been far from direct, and there are many people I must thank for their unwavering support, and without whom I doubt this point could have been reached. First and foremost I give thanks to my primary supervisor Graeme Swindles, who introduced me to tephrochronology, Thai food, and the uniquely frustrating and rewarding world of academic publication. His optimism, encouragement, and ability to see manuscript potential in dozens upon dozens of tephra-devoid microscope slides were an unending source of inspiration and confidence. Likewise to my co-supervisor, Ivan Savov, whose support and enthusiasm for the volcanic side of things helped to keep me on track, and whose geochemical guidance was invaluable for my laboratory work.

Additionally, I received a great deal of help from Chris Hayward at the University of Edinburgh, both in the form of EPMA advice and in suggestions for so-bad-they're-good sci-fi films to watch while running the probe into the late hours of the night. I am also grateful to Matthew Percival and the histology laboratory team at St James' University Hospital for their help in unsticking several samples when it became clear that those slides contained the only useful tephra to be found in certain Swedish peat cores.

For support outside the university, I extend thanks to the entire Leeds Griffins Quidditch team. Through writing-related stress, slotting tournaments around lab work, and coping with several broken bones (only some of them mine), the joy, friendships, and constant undercurrent of fond exasperation were defining parts of my time at Leeds. For knitting circles where we discussed academic plans, for late night coding advice in Hyde Park, for evenings spent partly writing but mostly watching Doctor Who and Buffy the Vampire Slayer, I am grateful.

Thank you also to my family. For listening to my rants, both of excitement and frustration. For giving me advice and usually being right. For letting me know when I'm getting ahead of myself, and loving me anyway. It should go without saying, but this would not have been possible without you.

Last but not least, to my D&D group. I'm sorry I killed you all that one time.

Abstract

Efforts to understand the complex interactions between distinct earth systems are a vital part of the future of Earth Science. Recent advances in glaciology, atmospheric sciences, and natural hazard modelling have highlighted how variations in separate components on both a local and global scale can affect adjacent systems. Volcanic hazards have been demonstrated to be susceptible to external hydrological and cryospheric influences. It has previously been hypothesised that regional-scale changes to pressure regimes, such as might occur following rapid deglaciation leading to isostatic uplift, might be sufficient to cause widespread changes in eruption frequency in volcanic areas. This theory is often referred to as the 'unloading effect'.

Icelandic volcanic ash can be found in sites across western mainland Europe and the UK, preserved as tephra layers in terrestrial, lacustrine, and marine sediments. These layers provide temporal and geochemical information on the source eruption, and may also be used as a measure of the frequency of explosive eruptions (the most likely to disperse ash over a wide geographic area). However, as tephrochronology is a relatively new discipline, the methodologies and related applications are still in the process of development. This thesis addresses concerns related to the preservation potential and the impacts of commonly used chemical extraction methods of volcanic tephra. This is achieved through laboratory experimentation, EPMA analysis, and statistical evaluation performed on volcanic glasses of various compositions.

Additionally, this thesis presents an updated and expanded database of Holocene and Late Glacial tephra in Europe. The final chapter builds on this database in addition to incorporating palaeo-atmospheric and -glacial modelling to evaluate the potential of the unloading effect in Iceland within the last 12,500 years, finding that, while evidence for this effect occurring within the Holocene does exist, it is likely to be a secondary factor in determining eruption frequency.

Contents

Chapter 1: Introduction	1
1.1 Preface	1
1.2 Context of research & rationale.....	1
1.3 Primary research aim	4
1.4 Objectives.....	4
1.5 Thesis structure.....	5
Chapter 2: Evaluating the relationship between climate change and volcanism.....	8
2.1 Introduction	10
2.2 Volcanic Forcing of the Climate	12
2.2.1 Short-term events.....	12
2.2.2 Decadal to century-scale effects	15
2.3 The Potential for a Volcanic Response to Climate Change	18
2.3.1 Proposed mechanisms	18
2.3.1.1 Climate, glacier response and the Icelandic Low	18
2.3.1.2 The unloading effect	20
2.3.2 Evidence for a volcanic response	22
2.3.2.1 Tephrochronology and ‘cryptotephra’	22
2.3.2.2 Modelling efforts.....	24
2.4 Areas of Uncertainty	25
2.4.1 Gaps in the tephra record.....	25
2.4.2 Volcanic and tectonic processes	26
2.5 The Potential for Future Work.....	28
2.5.1 A more comprehensive record of past volcanism	28
2.5.2 Quantifying the unloading effect	29
2.6 Conclusions	30
Acknowledgements.....	32

References	33
Chapter 3: Evaluating tephrochronology in permafrost peatlands of Northern Sweden.....	48
3.1 Introduction	50
3.2 Materials and Methods.....	51
3.2.1 Study Area.....	51
3.2.2 Methods.....	53
3.3 Results.....	55
3.3.1 Tephrostratigraphies.....	55
3.3.1.1 MN85/Hekla 4.....	57
3.3.1.2 MN70/Hekla-Selsund	58
3.3.1.3 ST30/Hekla 1104 (Hekla 1).....	58
3.3.1.4 ST25/Hekla 1158	58
3.3.1.5 EA12/Askja 1875	58
3.3.1.6 NI5 (Unknown tephra)	59
3.4 Discussion.....	61
3.4.1 Tephra transport and preservation.....	61
3.4.2 Site analysis.....	62
3.4.2.1 Local climate and wind currents	62
3.4.2.2 Vegetation.....	65
3.4.2.3 Topography	65
3.4.2.4 Eruption conditions.....	66
3.4.2.5 Other factors	67
3.5 Conclusions	67
3.6 Acknowledgements.....	68
References	69
Chapter 4: Standard chemical-based tephra extraction methods significantly alter the geochemistry of volcanic glass shards.....	74

4.1	Introduction	76
4.2	Materials and Methods.....	78
4.2.1	Tephra samples	78
4.2.2	Processing methods	80
4.2.2.1	Control (No treatment)	80
4.2.2.2	Muffle furnace burning and dilute hydrochloric acid (Method 1) 80	
4.2.2.3	Acid digestion (Method 2)	80
4.2.2.4	Acid/base digestion (Method 3)	81
4.2.3	Electron Probe Microanalysis	82
4.2.4	Statistical Analysis – PERMANOVA	82
4.3	Results.....	83
4.3.1	Notes on removal of organic material	83
4.3.2	Glass Alteration.....	83
4.3.2.1	Glass Morphology	83
4.3.2.2	Geochemistry.....	85
4.3.2.3	PERMANOVA.....	88
4.5	Conclusions	100
	Acknowledgements.....	100
	Chapter 5: Is there a Climatic Control on Icelandic Volcanism?	107
5.1	Introduction	109
5.2	Methods.....	112
5.2.1	Tephra	112
5.2.2	Atmospheric-Ocean General Circulation Model.....	113
5.2.3	Ice Sheet Reconstruction	113
5.3	Results.....	114
5.3.1	A correlation between cooling events and lulls in volcanic activity? 114	

5.3.2	Analysing the glacial loading effect in Iceland	118
5.4	Discussion and Conclusions	121
	Acknowledgements.....	124
	References	125
Chapter 6:	Discussion & Conclusions	131
6.1	Research Synthesis.....	132
6.1.1.	Objective 1 – Establish the legitimacy of the methods used to examine the unloading effect in the Holocene.....	132
6.1.2.	Objective 2 – Has the unloading effect occurred in Europe within the Holocene?	136
6.2	Research Implications	139
6.2.1	Advances in methods and understanding.....	140
6.2.2	Novel approaches	140
6.3	Prospects for Future Research.....	140
	References	142
Appendix	144
Suppl. Chapter 3:	Evaluating tephrochronology in the permafrost peatlands of northern Sweden	144
Table A.1.1.	Radiocarbon dates of Abisko peat profiles	144
Table A.1.2.	²¹⁰ Pb dating of Abisko peat profiles	146
Table A.1.3.	Non-normalised major element glass geochemistry of Abisko peat profiles	149
Table A.1.4.	EMPA of Lipari and BCR-2G glass standards prior to Abisko glass shard analysis.....	153
Table A.1.5.	Site information	154
Suppl. Chapter 4:	Standard chemical-based tephra extraction methods significantly alter the geochemistry of volcanic glass shards	155
A.2.1.	PERMANOVA testing.....	155

Table A.2.1. Major element geochemistry of tephra analyses for each chemical treatment, normalised to 100%. Analyses with an original total oxide count of < 97 % have been removed.	157
Table A.2.2. Secondary glass standards for EPMA (non-normalised).....	184
Suppl. Chapter 5: Is there a Climatic Control on Icelandic volcanism?.....	186
Table A.3. NEVA database v.2.0.....	186

List of Figures

Chapter 1: Introduction

Figure 1. Conceptual model of the research project. Page 7.

Chapter 2: Evaluating the relationship between climate change and volcanism

Figure 1. Schematic of volcanic inputs to the atmosphere. Page 14.

Figure 2. Example pressure-temperature diagram illustrating how decompression may alter the geotherm of a magma body. Page 21.

Figure 3. Bi-plot geochemical analyses of three tephra samples collected from a peat bog in the Shetland Isles (Swindles, unpublished data), compared with the known geochemical signatures of seven historic Icelandic eruptions. Page 24.

Figure 4. Theoretical map of regions in which the unloading effect could currently occur. Page 29.

Chapter 3: Evaluating tephrochronology in the permafrost peatlands of Northern Sweden

Figure 1. Map of study area, showing local topography and the location of coring sites. Page 52.

Figure 2. Tephrostratigraphic profiles of Abisko peat cores. Page 56.

Figure 3. Age-depth models of Eagle, Nikka, and Stordalen peatland profiles. Page 57.

Figure 4. Geochemical bi-plots of glass shards found in the Marooned and Stordalen cores, showing the geochemical type-data envelopes of the eruptions to which they correlate. Page 60.

Figure 5. Spatial distribution patterns within Europe of four tephra layers found in the Abisko peatlands. Page 61.

Figure 6. Conceptual diagram of factors influencing tephra preservation in Abisko peatlands. Page 63.

Chapter 4: Standard chemical-based tephra extraction methods significantly alter the geochemistry of volcanic glass shards

Figure 1. SEM images of volcanic glass subjected to chemical treatments. Page 84.

Figure 2. TAS diagrams showing group variations in geochemical classifications following chemical treatments of volcanic glass. Page 85.

Figure 3. Boxplots and ternary diagrams displaying variations in major element geochemistry for four analysed glasses. Page 87.

Figure 4. Composite TAS diagram showing the range of reported Icelandic geochemistry against geochemical variations produced by chemical extraction in this study. Page 99.

Chapter 5: Is there a climatic control on Icelandic volcanism?

Figure 1. Time series diagram showing distal and proximal tephra deposits, palaeoclimate estimates as derived from physical proxies, and palaeoglacial and atmospheric modelling results. Page 116.

Figure 2. Conceptual model of ice sheet unloading on a volcanic system. Page 119.

Figure 3. Depth-time models of magma ascent for shallow bodies at 15 km, 20 km, and 25 km depth. Page 122.

Chapter 6: Discussion & Conclusions

n/a

Appendix

n/a

List of Tables

Chapter 4: Standard chemical-based tephra extraction methods significantly alter the geochemistry of volcanic glass shards

Table 1. A summary of the tephra samples analysed in this chapter. Page 79.

Table 2. PERMANOVA results. Page 90.

Table 3. Summary of variations in glass major oxide concentrations compared to control group. Page 95.

Appendix

Supplementary to Chapter 3

Table A.1.1. Radiocarbon dates of Abisko peat profiles

Table A. 1.2. ²¹⁰Pb dating of Abisko peat profiles

Table A.1.3. Non-normalised major element glass geochemistry of Abisko peat profiles

Table A.1.4. EMPA of Lipari and BCR-2G glass standards prior to Abisko glass shard analysis

Table A.1.5. Abisko study site information

Supplementary to Chapter 4

Table A.2.1. Major element geochemistry of tephra analyses for each chemical treatment, normalised to 100%

Table A.2.2. Secondary glass standards for EPMA (non-normalised)

Supplementary to Chapter 5

Table A.3. NEVA database v.2.0

Chapter 1: Introduction

1.1 Preface

This thesis examines the potential and the possible scientific pitfalls behind the controversial theory of magmatic response to isostatic rebound, hereafter referred to as the 'unloading theory'. The thesis takes the form of an anthology of several published works, each of which seek to assess the validity of various quantitative techniques typically used to provide physical evidence of the proposed phenomenon, including tephrochronology, geochemical analysis of cryptotephra (microscopic volcanic ash), and numeric modelling approaches.

This work represents a significant step forward in the interdisciplinary study of earth system interactions. Through solidifying the foundations of current understanding and identifying the uncertainties and inconsistencies in past and existing methods, we strengthen the scientific case for a climatic control on volcanic activity through glacial loading. Chapter 2 of this thesis consists of a literature review of current methods and understandings, while Chapters 3, 4, and 5 consist of original research. Chapter 6 is a discussion of the research findings.

1.2 Context of research & rationale

Recent advances in the natural sciences, particularly in earth system modelling, have allowed increased specialisation within individual disciplines, resulting in many advances in model development and a greater insight into systems in isolation (Steffen et al., 2006). However, it is also becoming increasingly apparent that even a detailed and comprehensive understanding of an individual system, such as a single glacier or a particular volcano, is insufficient to entirely predict the responses of that system to outside perturbation. Natural systems do not exist in segregation from their surroundings; the mass balance of a glacier will be affected by local climate fluctuations, which in turn will be impacted by regional or global atmosphere-ocean circulation. Likewise, activity at a given volcano is not only subject to local magma supply, but to variations in regional stress regimes, and to controls determined by the geographic setting, such as the presence of ice sheets or surface water (Kokelaar, 1986; Walter et al., 2007). In attempting to build a greater understanding of natural systems, it is therefore essential to fully consider

the interactions between different elements, particularly when considering processes conducted over geological timescales.

The 'unloading effect' is a prime example of a more holistic theory, which attempts to clarify the connection between regional stress fields in a glaciated environment and underlying/peripheral volcanic systems. The theory, discussed more extensively in the literature review (Chapter 2), posits that the removal of subaerial weight above a volcanic system would cause lithospheric decompression to a depth on the order of tens of kilometres (Jull & McKenzie, 1996; Maclennan et al., 2002; Pagli & Sigmundsson, 2008), resulting in a significant change in volcanic activity. Isostatic adjustment following the loading or unloading of glacial or marine weights is known to cause dramatic alterations to regional tectonic stress regimes (Peltier & Andrews, 1976) on the order of centuries to millennia (Klemann & Wolf, 1998; Larsen et al., 2005). It is therefore plausible that abrupt, rapid (< 500 year) climate fluctuations and subsequent changes in glacier mass would have a notable impact on sub-glacial and glacier-periphery volcanoes.

Iceland is uniquely situated as a case study for this research. Its unusual geological position on the confluence of a divergent tectonic plate boundary (the Atlantic mid-ocean ridge) and a deep mantle plume (Pálmason & Saemundsson, 1974; Ito et al., 1996) has produced several distinct zones of volcanic activity across the island. The Eastern Volcanic Zone (EVZ) contains the highest number of currently active systems (8) (Thordarson & Höskuldsson, 2008) and at the time of writing is the most active of the five widely recognised zones, having formed approximately 2-3 Mya (Scheiber-Enslin, 2011). The current landmass itself is geologically young, with the oldest rocks dated to ~16.5 million years. Iceland has been volcanically active throughout the Holocene, with an average eruption frequency of > 20 events per century (Thordarson & Höskuldsson, 2008). Iceland also displays an extremely wide variety in magmatic evolution and eruptive style. Although around 91% of Icelandic eruptions are mafic (the remaining 9% consisting of 6% intermediate and 3% silicic eruptions), the diversity of eruption types within a given volcanic zone remains high. The availability of marine, ground-, and surface water, often in the form of ice, allows for frequent hydromagmatic (phreatic) activity (Thordarson & Höskuldsson, 2008). This in turn promotes the occurrence of phreato-explosive eruptions in addition to 'dry' explosive events, contributing

to the high return interval for Icelandic ash fallout over northern Europe (44 ± 7 years) (Watson et al., 2017).

Additionally, Icelandic glacial activity following the breakup of the Icelandic Ice Sheet (IIS) at around 15 ka is characterised as being particularly dynamic (Geirsdóttir et al., 2009). At the time of writing, approximately 11% of the land surface of Iceland is covered by glaciers, though the collective mass balance of those glaciers has been almost continually negative since 1995 as a result of a warming climate (Björnsson & Pálsson, 2008). The clear interconnectivity between Iceland's cryosphere and geosphere, and the highly variable nature of both throughout the Holocene, make it the ideal location to form the foundation of this research.

A keystone of this investigation is the use of cryptotephra to estimate the frequency of explosive Icelandic eruptions. Cryptotephra, usually defined as microscopic volcanic particles $< 150 \mu\text{m}$ in diameter, is ejected into the atmosphere during eruption events, and may then be transported via air currents thousands of kilometres from their volcanic source. In Europe, Icelandic ash has been found as far from the source as northern Sweden and eastern Russia (Swindles et al., 2017). The fallout from these eruptions is then preserved in lake and peat sediments as distinct, discrete layers, which may be attributed to particular source volcanoes and, in many cases, particular eruption events through geochemical analysis and dating techniques. Previous studies have compiled these tephrochronological records of Iceland into the middle Atlantic period of the Holocene (~ 6500 ya) (Swindles et al., 2011; Watson et al., 2017). However, the research presented in this thesis extends the records through the Holocene into the Younger Dryas ($\sim 12,500$ ya).

Recent advances in climate science and related fields have led to a significant increase in public, political, and scientific interest in the impact of climatic shifts on geohazards. One result of this has been an increased emphasis on multidisciplinary research, which this study encapsulates. Its results have the potential to be of interest to researchers from a range of scientific backgrounds, including volcanologists, glaciologists, and atmospheric/climate modellers. While the studies described below focus on Iceland as a case study, the findings are also likely to be applicable in many other locations where ice and volcanic activity have existed concurrently in recent millennia, such as the Kamchatka peninsula in Far

East Russia, Alaska, parts of Antarctica, and the Southern and Austral Andean Volcanic Zones.

1.3 Primary research aim

The aim of this thesis is to examine the data commonly used in defence of the unloading theory, and having determined whether or not the data is valid- to assess the potential for a change in volcanic eruption frequency as a result of isostatic uplift.

1.4 Objectives

Objective 1: Establish the legitimacy of the methods used to examine the unloading effect in the Holocene

- Review the existing works and methods in this field and assess conflicting or complimentary data (Chapter 2)
- Examine the potential uncertainties and biases in the study of distal tephrochronology in Europe due to eruption parameters and local geography of preservation sites (Chapter 3)
- Evaluate the preservation and possible geochemical alteration of cryptotephra shards during chemical extraction methods (Chapters 3, 4)

Objective 2: Did the unloading effect occur in Iceland during the Holocene?

- Identify, through field and laboratory analysis, new cryptotephra records (Chapter 3)
- Collate and examine existing tephra records in Europe spanning the past 12,500 years, and combine with new tephra records to produce a comprehensive database of volcanic activity recorded in the European sedimentary record (Chapter 5)
- Model glacial responses to climatic variations based on contemporary data within the Holocene (11,700 yrs.), and, with reference to the tephrochronology database established above in addition to numeric models of potential magmatic stress regimes, assess the suitability of the unloading effect to address any observed correlations (Chapter 5)

1.5 Thesis structure

This thesis is presented in the standard format as described by the University of Leeds. Each of the following chapters, with the exception of Chapter 6: Discussions & Conclusions, takes the form of a manuscript, all of which have been published or favourably reviewed/accepted for publication in a peer-reviewed journal. Each chapter has a specific research focus and is entirely self-contained, typically separated into introduction, methods, results, discussion, and conclusions sections. Each chapter has an accompanying reference list. Figure 1 outlines the connections between chapters, and shows how they relate to the research objectives.

A summary of the subsequent chapters is as follows:

- *Chapter 2: Evaluating the relationship between climate change and volcanism.* A literature-based review of current scientific understandings and practices regarding the interaction of volcanic systems and the atmosphere.
- *Chapter 3: Evaluating tephrochronology in the permafrost peatlands of Northern Sweden.* Examining the potential pitfalls of distal tephrochronology using laboratory analyses of volcanic glass in peat cores from Abisko, Northern Sweden. This research fills a geographic gap in Icelandic tephrochronology, as most previous research was conducted in more southern locations.
- *Chapter 4: Standard chemical-based tephra extraction methods significantly alter the geochemistry of volcanic glass shards.* Through electron probe microanalysis (EPMA) of ten volcanic glasses subjected to four chemical treatments, this chapter shows that exposure to the concentrated acids and bases used in many standard tephra extraction methods may alter the chemical composition of those glasses, with implications for the validity of past tephrochronology studies.
- *Chapter 5: Is there a climatic control on Icelandic volcanism?* This chapter presents new correlations between Holocene and Late Glacial tephra records and reconstructions of Icelandic palaeoclimate, and, through

numerical simulations of glacial extent, shows how the unloading effect may have impacted Icelandic volcanoes within this time period.

- *Chapter 6: Discussion & Conclusions.* This chapter consolidates the major findings from each of the previous chapters, and provides a discussion of the implications, limitations, and potential directions of future research based on those conclusions.

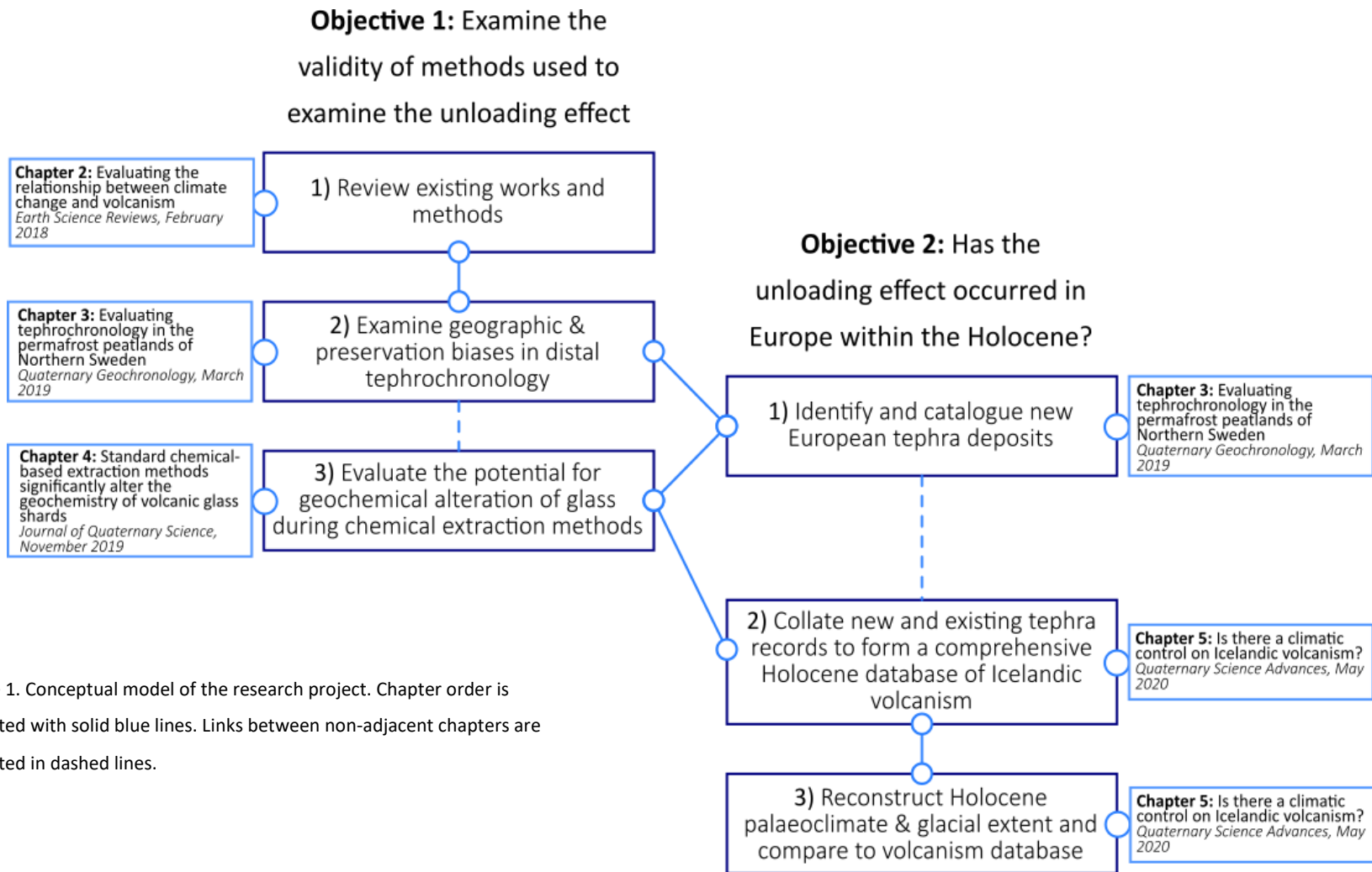


Figure 1. Conceptual model of the research project. Chapter order is indicated with solid blue lines. Links between non-adjacent chapters are indicated in dashed lines.

Chapter 2: Evaluating the relationship between climate change and volcanism

Claire L. Cooper^{a,b}, Graeme T. Swindles^a, Ivan P. Savov^b, Anja Schmidt^{c,d}, Karen L. Bacon^a

^aSchool of Geography, University of Leeds, Leeds, LS2 9JT, UK

^bSchool of Earth and Environment, University of Leeds, Leeds, LS2 9JT, UK

^cDepartment of Chemistry, University of Cambridge, Lensfield Rd, Cambridge CB2 1EW, UK

^dDepartment of Geography, University of Cambridge, Downing Place, Cambridge CB2 3EN, UK

Published in: Earth Science Reviews, 177, 238-247. 2018

Keywords: volcanism, climate, deglaciation, unloading effect, tephra

Abstract

Developing a comprehensive understanding of the interactions between the atmosphere and the geosphere is an ever-more pertinent issue as global average temperatures continue to rise. The possibility of more frequent volcanic eruptions and therefore more frequent volcanic ash clouds raises potential concerns for the general public and the aviation industry. This review describes the major processes involved in short- and long-term volcano--climate interactions with a focus on Iceland and northern Europe, illustrating a complex interconnected system, wherein volcanoes directly affect the climate and climate change may indirectly affect volcanic systems. In this paper we examine both the effect of volcanic inputs into the atmosphere on climate conditions, in addition to the reverse relationship – that is, how global temperature fluctuations may influence the occurrence of volcanic eruptions. Explosive volcanic eruptions can cause

surface cooling on regional and global scales through stratospheric injection of aerosols and fine ash particles, as documented in many historic eruptions, such as the Pinatubo eruption in 1991. The atmospheric effects of large-magnitude explosive eruptions are more pronounced when the eruptions occur in the tropics due to increased aerosol dispersal and effects on the meridional temperature gradient. Additionally, on a multi-centennial scale, global temperature increase may affect the frequency of large-magnitude eruptions through deglaciation. Many conceptual models use the example of Iceland to suggest that post-glacial isostatic rebound will significantly increase decompression melting, and may already be increasing the amount of melt stored beneath Vatnajökull and several smaller Icelandic glaciers. Evidence for such a relationship existing in the past may be found in cryptotephra records from peat and lake sediments across northern Europe. At present, such records are incomplete, containing spatial gaps. As a significant increase in volcanic activity in Iceland would result in more frequent ash clouds over Europe, disrupting aviation and transport, developing an understanding of the relationship between the global climate and volcanism will greatly improve our ability to forecast and prepare for future events.

2.1 Introduction

It is already well established that various aspects of the Earth system, such as the atmosphere, geosphere and cryosphere, regularly interact through the exchange of materials and energy (Webster, 1994; Pielke et al, 1998). The global impact of large eruptions, such as the 1991 eruption of Mt. Pinatubo (Philippines, VEI 6) (McCormick et al, 1995), the 1815 eruption of Tambora (Indonesia, VEI 7) (Stothers, 1984), or the 1783-1784 eruption of Laki (Iceland, VEI 6) (Thordarson & Self, 2003), can be clearly seen in historical and environmental records (Robock, 2000). Injection of large quantities of volcanogenic material, such as fine tephra or volcanic gases (e.g. sulphur dioxide, carbon dioxide, hydrogen sulphide), into the stratosphere or troposphere can cause so-called 'dust veil' events (Lamb, 1970) with the potential to dramatically alter the Earth's climate on a regional or global scale for short periods of time (typically on the scale of several years to decades). The year following the 1815 eruption of Mt Tambora, for example, is often referred to as the 'year without a summer' – global temperatures are estimated to have dropped by 0.4-0.7°C (Stothers, 1984), causing several weather anomalies (Raible et al, 2016), particularly across the northern hemisphere, and placing considerable strain on agriculture worldwide (Stothers, 1999).

The relationship between a changing global climate (specifically, one experiencing a warming period) and a potential increase in volcanic eruption frequency and/or intensity is relatively unexplored. McGuire (2010) suggests that periods of 'exceptional climate change' may be associated with increased levels of hazardous geological and geomorphological activity, based on early Holocene records and contemporary observations of glacier retreat, measurements of ground instability, and estimations of melt production beneath Iceland (Oerlemans et al, 1998; Óladóttir et al, 2011; Magnúsdóttir et al, 2013). An increase in volcanic activity as a response to a warming climate as a result of isostatic adjustment has previously been suggested by multiple studies (Jull & McKenzie, 1996; Pagli & Sigmundsson, 2008; Watson, 2016). Such an escalation would have significant ramifications for local communities, and an increase in the frequency of ash clouds would have consequences for global aviation. As of 2014, approximately 100,000 commercial flights occur per day worldwide (Air Transport Action Group, 2016). Jet aircraft are extremely vulnerable to damage caused by interactions with even low

concentrations of airborne ash particles, which may cause electronic failures, severe abrasion on the turbine fans (Grindle & Burcham Jr, 2003), and clogging of the engine through the melting and re-solidifying of ash particles (Dunn et al, 1993). Since 1976, approximately two severely damaging encounters between aircraft and volcanic ash clouds have occurred per year (Guffanti et al, 2010). Between 1944 and 2006, volcanic activity necessitated the closure of more than 100 airports in 28 countries on 171 separate occasions (Guffanti et al, 2009). The economic and social disruption caused by such events may be most clearly illustrated by reference to the relatively minor (VEI = 3) eruption of Eyjafjallajökull in Iceland in 2010, which resulted in the closure of a large region of airspace across the North Atlantic and Europe, causing the loss of approximately US\$ 1.7 billion in revenue to various airlines in the space of a week (Mazzocchi et al, 2010). Volcanic ash can also pose a hazard to human health and the health of crops and livestock, particularly with regards to respiratory systems (Horwell & Baxter, 2006), even at relatively small concentrations (Horwell, 2007).

Regional climate change can also increase the likelihood of destructive non-eruptive events in volcanic regions, such as mass movements, including lahars (Thouret & Lavigne, 2000; Pierson et al, 2014). Increased rainfall has previously been a significant factor in several such disasters, including the 1998 collapse at Casita volcano in Nicaragua (Kerle et al, 2003; Scott et al, 2005), and the 2005 lahar at Toliman volcano in Guatemala, which destroyed the town of Panabaj and caused the deaths of more than 1,200 people (Luna, 2007). Changes to depositional and runoff channels following such events also has implications for hazard and risk estimation and models (Hayes et al, 2002).

The 2010 eruption of Eyjafjallajökull sharpened the focus of scientific research into the understanding and mitigation of volcanic ash hazards, particularly with regards to northern Europe and volcanism in Iceland. Strong interest from the media and government departments prompted rapid development of many ash modelling and monitoring techniques, most notably in the UK and Western Europe (Wilkins et al, 2016; Marenco et al, 2016). The unusual geochemical profile of Iceland (a result of its unique geological location above a mid-oceanic spreading

ridge and a deep-seated mantle plume (hotspot); Oskarsson et al, 1985) and the relative wealth of data concerning eruptions in Iceland, in addition to the wide range of locations affected by Icelandic eruptions, make the region ideal for the study of evolving volcanic activity. Based largely on comparisons with known proximal deposits, Icelandic tephra have been identified in Scotland, England, Wales, Ireland, Germany, Sweden, Arctic Norway, Poland, Estonia and the Faroe Islands (Pilcher et al, 2005; Swindles et al, 2011; Lawson et al, 2012; Watson et al, 2017), forming a comprehensive record of Icelandic ash deposition across Europe. If the proposed relationship between periods of global warming and 'flare-ups' in volcanic activity can be shown to exist, the ramifications to modern society, particularly with regards to aviation and the agricultural industry, may be significant.

Understanding the intricacies of the links between the climate and volcanism requires investigation of both sides of the relationship. This review examines the established links between volcanism and subsequent surface cooling, in addition to assessing the potential for correlation between periods of climate warming and an increase in the frequency of volcanic eruptions, with a focus on Iceland and ash fallout across northern Europe. Iceland is frequently referred to as a case study, as much of the existing work pertinent to this review was conducted with a European focus.

2.2 Volcanic Forcing of the Climate

2.2.1 Short-term events

A link between large volcanic eruptions and variations in regional and global climate variability has been surmised to exist for at least several centuries. One of the earliest examples of scientific thought on the matter was published by Benjamin Franklin in 1784, following the catastrophic fissure eruption of Laki (also called Lakagigar) in Iceland in 1783 (Franklin, 1784). Franklin linked the observations of a 'haze' or 'mist' across much of Europe in the months following the onset of the Laki eruption to the significant temperature anomalies that characterised the winter of 1783. The mist Franklin referred to was caused by the release of approximately 122 megatons of sulphur dioxide (SO₂) from the Laki

fissure, 95 Mt of which were injected into the lower stratosphere, ensuring widespread atmospheric dispersal (Thordarson & Self, 2003). Once injected into the atmosphere, SO₂ is chemically converted via the OH radical or via aqueous phase reactions to form aerosol mixtures of sulphuric acid (H₂SO₄). This increase in aerosol particle concentrations in the upper troposphere and lower stratosphere is thought to have caused significant cooling for a period of several months as a result of aerosol particles leading to enhanced scattering of incoming solar radiation back to space (Jacoby et al, 1999; Thordarson & Self, 2003; Oman et al, 2006; Schmidt, 2013). In the lower atmosphere, sulphur aerosols may also act as cloud condensation nuclei (Schmidt et al, 2011), furthering the surface cooling effect. There is evidence to suggest that this alteration to surface temperatures may have caused a weakening of the monsoon circulation in 1783 and 1784 through a reduction of the summer temperature contrast between the mid-latitudes and the equator, resulting in abnormally low precipitation and drought in Africa and India (Oman et al, 2006).

Several other large eruptions have had notable effects on the global climate. The eruptions of Krakatoa (Indonesia, August 1883), Agung (Indonesia, February 1963) and El Chichón (Mexico, March 1982) each had a short-term (several months to years) impact on surface temperatures, atmospheric temperatures, precipitation patterns and other aspects of the climate system (Self et al, 1981; Robock, 2000). In each case, the eruptions in question were explosive in nature, with a VEI (a quantitative measurement of the volume of material ejected during an eruption; Newhall & Self, 1982) of 5 or greater; however, some explosive eruptions of a similar magnitude, such as the eruption of Mt St Helens in 1980, have only negligible atmospheric effects (Robock & Mass, 1982). The determining factor in an eruption's climatic impact, therefore, is not the volume of material ejected from the vent, but whether a significant amount of that material reaches the stratosphere (Robock, 2000; Self, 2006). Larger dust and ash fragments typically have a residence time on the order of a few months in the atmosphere (Robock, 2000), and their effects disappear once the particles fall out and settle. By contrast, SO₂ has a lifetime of hours to days in the troposphere, though this may extend to approximately three weeks if released into the stratosphere (Schmidt & Robock, 2015).

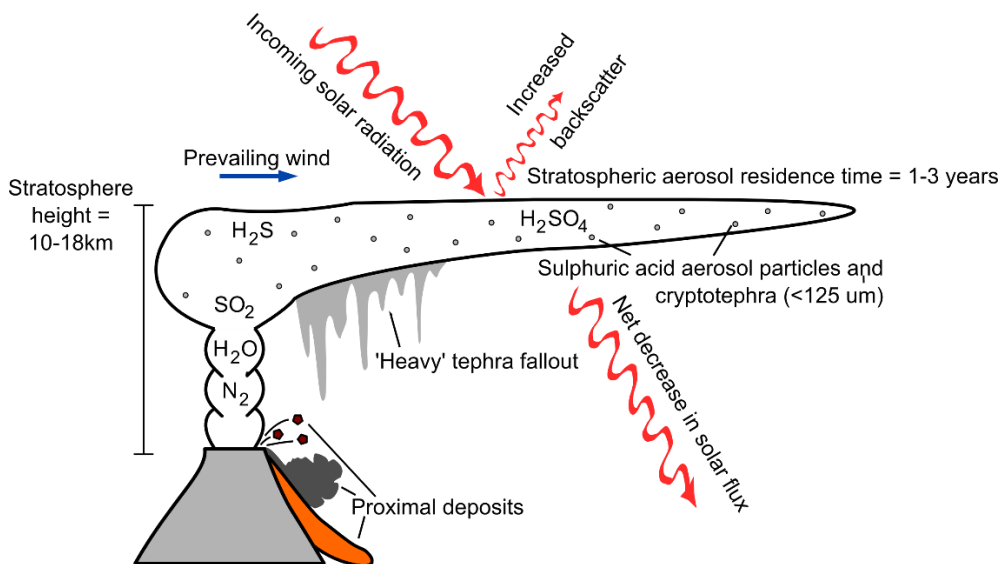


Figure 1. Schematic of volcanic inputs to the atmosphere. Most tephra particles will fall out within a time period of days to weeks, while lighter emissions may have a residence time of several months (in the case of tephra particles <125 μm in diameter) to years (stratospheric aerosols) (Robock, 2000). Chemical species with a naturally high atmospheric abundance (such as CO₂, H₂O and N₂) will have a much lesser effect than less abundant species, such as SO₂. Robock, 2000.

The contribution of volcanic gases to climate forcing is much more significant than that of ash particles. The most abundant volcanic gases emitted during an eruption are those that are already at relatively high concentrations in our atmosphere (such as H₂O, N₂ and CO₂), and as such have only a minimal effect on atmospheric composition and climate; however, other volcanic emissions, such as sulphur compounds (e.g. SO₂, H₂S) have a much greater impact. These gases react with ambient hydroxyl radicals (OH·) and H₂O molecules to form sulphuric acid aerosols. If carried into the stratosphere by a volcanic column, these particles rapidly achieve global coverage, sometimes circulating the globe in as little as 3 weeks (Robock & Matson, 1983; Bluth et al, 1992; Self, 2006). The dominant effect of such an aerosol cloud is to greatly (albeit briefly) increase the planetary albedo by backscattering incoming solar radiation, resulting in net cooling at the surface. On a similar timescale, the aerosol particles also act as a catalyst for ozone depletion reactions which may result in anomalous regions of net surface warming, particularly in polar and mid-latitude regions (Solomon, 1999). In addition, the presence of an aerosol cloud can lead to stratospheric heating due to absorption of thermal infrared and near-infrared solar radiation. However, the

global-mean net effect of such short-term aerosol releases is always one of mild surface cooling, typically less than 1°C lower than ambient conditions (Rampino et al, 1988; Santer et al, 2016).

The geographic location of the initial eruption also plays a factor in determining an eruption's atmospheric impact (Robock, 2000; Toohey et al, 2011). Large-scale patterns of air circulation enable a more global dispersal of aerosols from tropical eruptions, whereas airborne material from high-latitude eruptions is more likely to remain in the hemisphere into which it was injected (Oman et al, 2006). In addition, stratospheric heating can increase the meridional temperature gradient, strengthening the polar vortex and causing alterations in stratospheric circulation (Robock & Mao, 1992; Kirchner et al, 1995; Fischer et al, 2007). However, the complexities in the response of the atmosphere to the asymmetric cooling effects produced by volcanic eruptions are as yet poorly understood. The temperature anomalies that occur following volcanic aerosol injection are far from homogeneous (Haywood et al, 2013; Svensson et al, 2013; Ridley et al, 2015). Baldini et al (2015) suggest that high-latitude eruptions in either hemisphere may also have significant atmospheric effects by causing cooling in one hemisphere relative to the other, forcing migration of the Intertropical Convergence Zone (ITCZ). Current southward migration of the ITCZ in response to anthropogenic aerosol emissions is thought to be a major cause of frequent droughts experienced by the Sahel region of Africa (Hwang et al, 2013), and is a major control of air currents and associated precipitation in equatorial and low-latitude areas (Huang et al, 2001; Ridley et al, 2015).

2.2.2 Decadal to century-scale effects

In all observed incidences, volcanic aerosols are typically short-lived, with the result that their effects are generally only experienced on an interannual scale (Robock, 2000). However, there are suggestions that explosive volcanic eruptions may also have longer-lasting 'knock-on' effects. One such proposal is that large tropical eruptions may trigger the onset of certain ENSO (El Niño Southern Oscillation) states, and affect the magnitude of subsequent El Niño events, though the topic remains controversial (Self et al, 1997; Maher et al, 2015). Multiple

attempts have been made to establish a causative link between eruption events and the onset of El Niño cycles through analysis of proxy data (Adams et al, 2003) or numerical modelling (Meehl & Washington, 1996; Boer et al, 2000); however, while the analyses do suggest the possibility of a connection between explosive volcanism and ENSO phenomena, discrepancies in event timings and the influence of other factors on the likelihood of ENSO variations continue to cause uncertainty on the subject (Self et al, 1997; Emile-Geay et al, 2008).

Baldini et al (2015) used ice core, volcanological and speleothem data to suggest that unusually large volcanic events (i.e. VEI 5 or greater) might be at least partially responsible for abrupt millennial-scale shifts in the global climate characterised by rapid periods of warming in Greenland and apparently synchronous cooling in Antarctica, termed Dansgaard-Oeschger (DO) events. DO events are typically characterised by extremely rapid warming over a period of 20-50 years, followed by a period of relatively warmer climate which may last several centuries to millennia (Mogensen, 2009). The timing of DO events is largely constrained by the examination of oxygen isotopes from Greenland ice cores (Dansgaard et al, 1993), and multiple possible explanations for their occurrence have been suggested, including solar forcing, meltwater injections and oscillations in ocean-atmosphere interactions. Baldini et al (2015) argue that following an exceptionally large eruption, such as the supereruption of Lake Toba approximately at 75 kya, the ensuing atmospheric temperature asymmetry could have caused sufficient disruption to global circulation patterns to initiate a series of positive feedbacks, including sea ice expansion, increased surface albedo, and weakening of the Atlantic meridional overturning circulation (AMOC). Similar feedback loops thought to be triggered by volcanic eruptions have been implicated as factors in other Quaternary cooling events (Stuiver et al, 1995; Baldini et al, 2015). Miller et al (2012) also suggest that the onset of the Little Ice Age (approximately 1300 AD) may have been triggered by the occurrence of four sulphate-heavy eruptions in quick succession, based on measurements of stratospheric aerosol loadings by Gao et al (2008).

On a longer time scale, there is substantial evidence that the emplacement of unusually large igneous provinces (i.e. flood basalt volcanism) may be linked to periods of long-term global climate change. Most of these eruptions are

estimated to have occurred on a timescale of approximately 1 Myr (Hofmann et al, 1997), and are frequently linked to sudden shifts in the global climate, as well as to mass extinction events (McLean, 1985; Campbell et al, 1992; Courtillot & Renne, 2003; Bond & Wignall, 2014). During the formation of the Deccan Traps, for example, at the Cretaceous/Tertiary boundary at approximately 65 Ma, it is thought that around 5×10^{17} moles of CO_2 may have been released into the atmosphere at a rate of up to 9.6×10^{11} moles CO_2 per year (McLean, 1985). It has been estimated that the same eruption could also have released 10,000 Tg of SO_2 over a decade (Self et al, 2006). In addition, it is thought that flood basalt events (which may attain cumulative volumes of several thousand cubic kilometres; Coffin & Eldholm, 1994) may also cause significant contact metamorphism of overlying and underlying sedimentary rocks (such as carbonates, coal or shales), generating further quantities of greenhouse gases (Ganino & Arndt, 2009), particularly CO_2 . Estimating the climatic impact of flood basalt events is greatly complicated by the apparently contradictory effects of the two major gases released. While volcanic SO_2 generally has a cooling effect when converted to sulphuric acid aerosol in the stratosphere, as discussed above, CO_2 is a greenhouse gas, and in high enough atmospheric concentrations causes significant surface warming. However, whether sufficient concentrations of CO_2 could have been achieved during the emplacement of large igneous provinces remains disputed; while some models predict a net greenhouse effect (Caldeira & Rampino, 1990; Dessert et al, 2001), others argue that the volumes of CO_2 released would have been small in comparison to the natural atmospheric reservoir, particularly in ambient greenhouse conditions, such as those of the late Cretaceous (Self et al, 2006). Thus, in most cases the controlling factor in terms of atmospheric change is likely to be the quantity of SO_2 emissions, making the net effect likely to be one of cooling (Schmidt et al, 2016).

Flood basalt volcanism has also been suggested as a contributing factor in the mid-Jurassic Pliensbachian-Toarcian mass extinction event, most notable in the depletion of bivalves and other marine invertebrate species as a result of an oceanic anoxic event (OAE)(Aberhan & Fürsich, 2000). Pálffy and Smith (2000) link the event to the synchronous Karoo-Ferrar flood volcanism, which occurred in southern Gondwana (modern southern Africa/Antarctica) 184 - 179 Ma (Duncan

et al, 1997). Based on U-Pb ages for the flows within the Karoo Traps and ocean sediments from the Toarcian OAE, Pálffy and Smith (2000) suggest that heightened extinction rates were sustained for approximately 4 Ma, reaching a peak at 183 Ma. This correlates with the peak of flood volcanism, in which approximately $1 \times 10^6 \text{ km}^3$ of material is believed to have been extruded over the course of $\sim 1 \text{ Myr}$ (Duncan et al, 1997; Riley et al, 2006). Though the topic is still debated (Svensen et al, 2007; Ikeda & Hori, 2014), the OAE is thought to have been at least partially triggered by volcanic CO_2 release, coupled with multiple synchronous events, likely unrelated to volcanic activity, most notably massive methane hydrate dissociation (Hesselbo et al, 2000). The suggested contribution of multiple secondary factors to the extinction event, such as enhanced global mercury deposition (Percival et al, 2015) and a proliferation of endemic species during the late Pliensbachian (Aberhan & Fürsich, 2000), ties into the argument presented by Wignall (2005) - that while volcanic CO_2 emissions may initiate major perturbations to the global carbon cycle, other factors occurring either as a result of or unrelated to the initial eruption are likely to be necessary to cause major climatic change. Whether the emplacement of large igneous provinces may be ultimately responsible for, or merely a contributing factor to any subsequent mass extinction events remains to be determined. Nevertheless, it is clear that wide-scale interplay between the Earth's atmosphere and geosphere currently exists, and has existed in the past on a range of scales, and will continue to do so for the foreseeable future.

2.3 *The Potential for a Volcanic Response to Climate Change*

2.3.1 *Proposed mechanisms*

2.3.1.1 *Climate, glacier response and the Icelandic Low*

The majority of studies attempting to model the effect of a warming climate on volcanic eruption frequency are performed in the context of the Icelandic glaciers and volcanoes, though the same link may potentially exist in other locations (see section 5.2). The relatively rapid response of the Icelandic glaciers to fluctuations in oceanic currents is well documented (Bond et al, 1997; Rahmstorf, 2002; Björnsson & Pálsson, 2008). Numerous palaeoclimate proxies indicate multiple periods of oceanic cooling in the North Atlantic over the past 10 ka BP (Watson et

al, 2016b). In particular, decreased sediment productivity across multiple Icelandic lakes suggests a significant cooling event at approximately 6.4 ka BP (Geirsdóttir et al, 2013), and geochemical analysis of a Greenland ice core by Mayewski et al (1997) shows fluctuations in the concentration of sodium (Na^+), which may indicate a deepening of the Icelandic Low atmospheric system between 3.5-2.5 ka BP. The strengthening of regional wind speeds that would occur following the onset of a deeper Icelandic Low would result in enhanced transportation of sea salts, resulting in greater concentrations of Na^+ present in the ice core (Mayewski et al, 1997). However, ice core records of the Holocene indicate that variations in Earth's climate were of a lower amplitude than those seen during the Pleistocene, suggesting that the climate has been more stable in the past 10,000 years than at any point in the last 100,000 (O'Brien et al, 1995; Mayewski et al, 2004).

Evidence of glacial advance in the south, centre and north of Iceland coincides with the climatic cooling events described above (Gudmundsson, 1997; Kirkbride & Dugmore, 2001; Kirkbride & Dugmore, 2006). Kirkbride and Dugmore (2006) suggest that, as smaller glaciers are more susceptible to the impacts of climatic forcing, they may account for the vast majority of short-term glacial expansion effects. Larger ice sheets, such as Vatnajökull, the largest Icelandic glacier, have a longer response time when compared with smaller glaciers (Oerlemans & Fortuin, 1998) — the total lag time between significant climatic changes and glacial response typically ranges between 10 and 1000 years (Jóhannesson, 1985). A mass balance study of Icelandic glaciers over the 20th century by Björnsson et al (2013) found that regional temperature fluctuations correlated strongly with the rates of glacier retreat or growth. Between 1995 and 2010, the average Icelandic temperature increased by approximately 1°C (3 to 4 times higher than the hemispheric average; Jones et al, 2012), coinciding with a loss of 3.7% ice mass at Vatnajökull and an 11% loss at Hofsjökull (Björnsson et al, 2013). The authors attribute these changes to longer melting seasons, thinner snow accumulation resulting in lower glacier albedo, and a greater ratio of precipitation falling as rain rather than snow. Oerlemans & Fortuin (1992) noted that the greatest factor in determining a glacier's responsiveness to external forcing is the wetness of the climate, and several recent studies concur that Iceland's setting as an island

contributes to the relatively rapid response of its glaciers and ice sheets to climate change (Björnsson & Pálsson, 2008; Chandler et al, 2016a, 2016b.).

Possibly the most important factor in understanding and modelling the response of the cryosphere to a warming climate, particularly in northern Europe, is observing alterations to global thermohaline circulation patterns. The North Atlantic Deep Water (NADW) is a key component of this system. Benthic oxygen isotope, cadmium and ^{13}C data from sediment cores imply that a relative shallowing of the current coincides with warming phases, while ebbs may be linked to rapid cooling, such as the Younger Dryas (12.9 – 11.7 ka BP) (Boyle & Keigwin, 1987). Changes to thermohaline circulation patterns have been identified as 'a major factor in forcing the climate signal and in amplifying it' (Bond et al, 1997), and it is thought that even small perturbations to the system may have had the potential to cause regional temperature changes on the order of several degrees during the Late Glacial and Early Holocene periods (Rahmstorf, 1996). On a regional scale, many factors related to a warming climate have been identified as major drivers of terrestrial glacier retreat, though the components with the greatest impact are likely to be increased atmospheric temperatures, increased precipitation, and the growth of supraglacial lakes (Reynolds, 2000; Björnsson & Pálsson, 2008).

2.3.1.2 The unloading effect

The 'unloading effect' refers to crustal deformation (specifically uplift) as a response to deglaciation. Isostatic rebound occurs after a load (such as a large glacier) is removed from the lithosphere. This has been directly or indirectly observed in Iceland (Sigmundsson, 1991; Sigvaldason, 1992), northern Europe (Lambeck, Smither & Johnston, 1998) and North America (James & Morgan, 1990). It is also generally accepted that rapid decreases in pressure (rapid on a geological timescale - on the order of at least a few centuries) cause an increase in the extent of decompression melting of the mantle (Asimow et al, 1995), suggesting that an association between the two factors may be plausible.

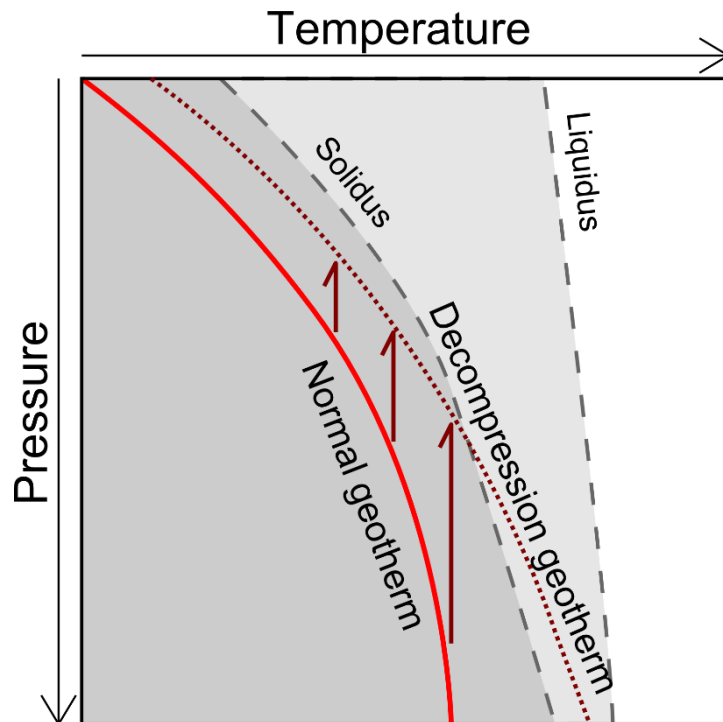


Figure 2. Example pressure-temperature diagram illustrating how decompression may alter the geotherm of a magma body, allowing for the production of greater quantities of partial melt. Rapid upwelling of the mantle causes a sudden decrease in pressure, altering the geothermal gradient to such a point that it intersects the solidus, allowing melting to begin.

The divergent plate boundary combined with hotspot activity beneath Iceland is already the source of large quantities of decompression melting (Slater et al, 2001). However, Jull and McKenzie (1996) estimate that the removal of 2 km of ice would increase the melt fraction by approximately 0.2 %, though the increase in melt generation as a response to unloading is non-linear. Schmidt et al (2013) go further, suggesting that the Icelandic uplift due to glacial isostatic adjustments (currently estimated at 25-29 mm/yr; Auriac et al, 2013) has resulted in an annual melt production increase of 100-135% since 1890. Much of this new magma is believed to be located beneath central Iceland, with approximately 20% hosted by the mantle beneath Vatnajökull, a region containing some of the island's most productive volcanic centres, such as Grímsvötn (Schmidt et al, 2013). Even on a smaller scale, minor alterations in the crustal stress fields surrounding shallow magma storage regions may have a significant impact on the likelihood of an eruption, particularly at volcanic centres with glacial caps (Albino et al, 2010). Watson et al (2016c) draws a correlation between the depth of the Icelandic Low

(as determined through analysis of the GISP2 Na⁺ record (Mayewski et al, 1997)) and the frequency of explosive Icelandic eruptions over the last 7,000 years. Their findings indicate that in both instances of Na⁺ increase, volcanic activity on Iceland decreased significantly. There was a lag of approximately 650 years between climate alteration and geodetic response, which the authors attribute to the delay in the glacial reaction, and the time taken for new excess magma due to adiabatic melt to reach the surface.

2.3.2 Evidence for a volcanic response

2.3.2.1 Tephrochronology and 'cryptotephra'

Many of the current research efforts investigating a geospheric response to global warming utilise the rapidly developing field of tephrochronology in an attempt to reconstruct the relative frequency of past volcanic events (Dugmore, 1989; Hall & Pilcher, 2002; Davies, 2015). 'Cryptotephra' refers to particles of volcanic ash which are not visible to the naked eye, typically being 125 µm (Lane et al, 2014; Stevenson et al, 2015; Watson et al, 2016b). These particles are often concentrated into layers within well-preserved sediment, such as in lake beds or peat bogs (Hall & Pilcher, 2002), and can provide useful isochrons across multiple sites within an area (Lane et al, 2014; Watson et al, 2016a).

Previously, cryptotephra has been used primarily as a dating and correlation tool in geological and archaeological fields (Balascio et al, 2011; Lowe, 2011; Schmid et al, 2017). However, more recent studies have focused on volcanological applications, such as the reconstruction of undocumented eruptions (Sun et al, 2016; Martin-Jones et al, 2017; Watson et al, 2016b), and -- on a wider scale -- the analysis of past patterns of volcanic eruptions (Connor et al, 2006), and the transportation of ash particles (Watson et al, 2016b). Watson et al (2017) use cryptotephra layers acquired from peat and lake sediments to estimate the recurrence interval of Icelandic ashfall across Northern Europe. Using data representing the past 1000 years, the study estimates an average return interval of approximately 44 years (a 20% chance of occurrence within a given 10-year period), based on samples from Germany, Scandinavia, Ireland, Great Britain, Poland and the Faroe islands (Swindles et al, 2011). Swindles et al (2011) report

an apparent increase in the number of ash-fall events affecting Europe over the past 1,500 years; however, it is unclear whether this is due to a true increase in volcanic activity during this period, or is an artefact of sampling intensity and improved methodology. It is also possible that more recent events are preferentially preserved in the geological record, and as such assessments of ashfall frequency based solely on tephra will always represent a minimum estimate (Watson et al, 2017)

The assignment of a given tephra or cryptotephra horizon to a particular eruption relies heavily on geochemical analysis of glass shards, in combination with other physical and historical constraints, such as ¹⁴C dating, wiggle-match dating techniques and ice core chronologies, where applicable (Lowe, 2011; Swindles et al, 2011; Lowe et al, 2013; Ramsey et al, 2015; Alloway et al, 2017). Examples of how geochemical analyses of tephra shards may be ‘fitted’ to existing chemical distributions of particular volcanic eruptions within a particular time frame are given in Figure 3. Various uncertainties still remain in the use of the technique, and the geochemical analysis of individual shards is not yet routine in tephra studies. However, by dating individual tephra layers, it is possible to estimate the relative frequency of volcanic events in a given area. In recent years, collaborative database resources such as TephraBase (www.tephrabase.org) have emerged in an effort to catalogue the glass shard geochemistry of historic eruptions, greatly smoothing the process of cryptotephra identification.

Analysis of cryptotephra layers can also provide other valuable insights into the processes and characteristics of prior eruptions. For example, the shape and vesicularity of ash shards may provide information about the conditions under which they were formed and transported (Heiken, 1974; Colucci et al, 2013). It is well recognised that the dominant shape of tephra shards (particularly regarding the ratio of the longest to the shortest axis) has a significant effect on the distance those shards may be transported before settling (Wilson & Huang, 1979; Folch, 2012). The concentrations of shards (also known as ‘tephra loading’) may be affected by the distance of the site from the source volcano, or by ambient

conditions at the time of emplacement (Langdon and Barber, 2004; Rea et al, 2012).

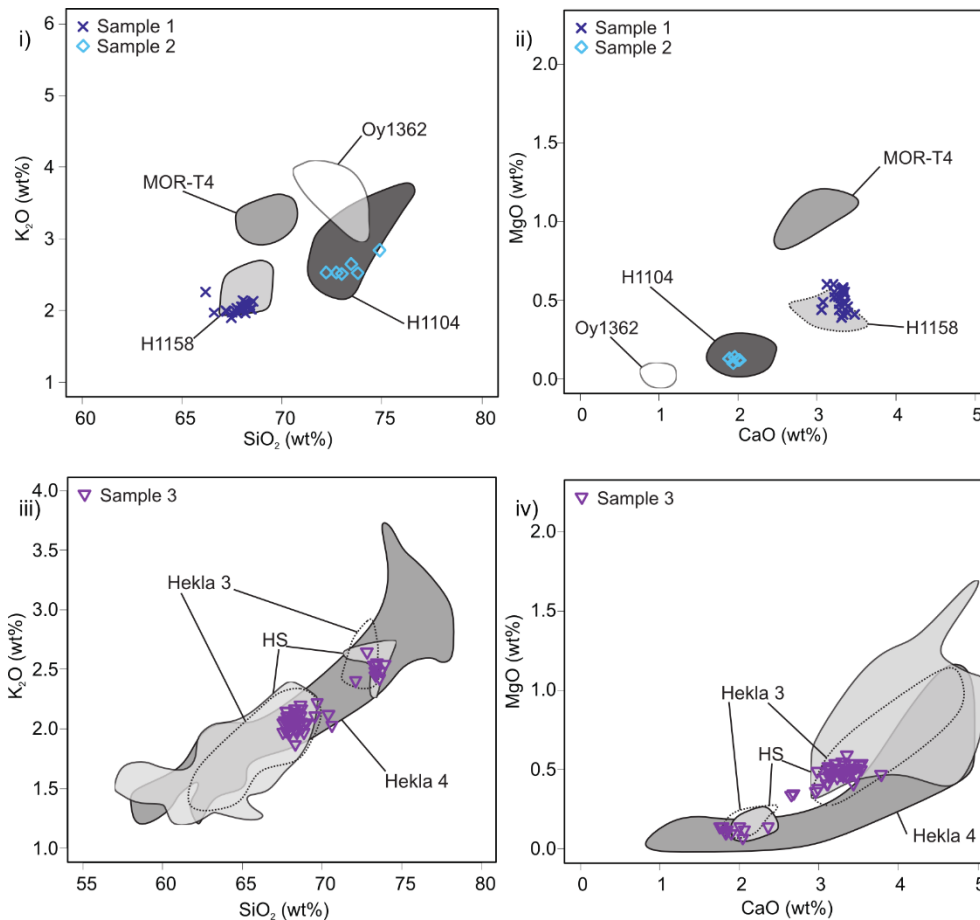


Figure 3. Bi-plot geochemical analyses of three tephra samples collected from a peat bog in the Shetland Isles (Swindles, unpublished data), compared with the known geochemical signatures of seven historic Icelandic eruptions (grey polygons) (Newton et al, 2007). This example illustrates how cryptotephra which falls into a particular geochemical 'envelope' may be ascribed to a single eruption. In this case, sample one (blue 'x's'; seen in plots (i) and (ii)) most closely matches the H1158 eruption (Hekla), sample 2 (cyan diamonds; plots (i) and (ii)) is most similar to H1104, and sample 3 (purple triangles; plots (iii) and (iv)) is similar to the Selsund (HS) 1800 - 1750 cal. BC eruption.

2.3.2.2 Modelling efforts

Many studies within the past two decades have attempted to evaluate the effect of ice loading on volcanic activity, both via numerical modelling or through evaluation of historical evidence. Jull & McKenzie (1996) endeavoured to model the effect mathematically, utilising data obtained from tephrochronology of the

Dyngjufjöll region of North Iceland. Their results indicated that the removal of 2 km of ice would have an effect approximately equivalent to a 0.6 km upwards shift in the melting column (although it should be noted that the thickest glacier currently in existence – the Taku glacier in Alaska – is less than 1.5 km thick (Robert & Hermans, 2000)). Jull & McKenzie go on to estimate that total deglaciation of Iceland would increase overall melt production rates by a factor of 30 over a period of 1000 years.

More recent studies have produced more conservative results. Pagli & Sigmundsson (2008) modelled the maintenance of isostatic equilibrium within the lithosphere using the assumption of an elastic plate overlying an isotropic, incompressible, viscoelastic half-space. Adopting contemporary measurements of ice loss and uplift beneath Vatnajökull (Pagli et al, 2007), the study found that, while present rates of ice thinning increase the volume of magma by approximately 0.014 km³/yr, the effects are confined within existing regions of volcanic activity. Their model also concluded that, although the rates of vertical uplift were likely to be greatest towards the centre of the ice cap, volcanoes peripheral to the glacier, such as Kverkfjöll or Bárðarbunga, experienced greater radial glacio-isostatic stresses and were more likely to alter their behaviour than those in a central location, such as Grímsvötn. Additionally, the existing tectonic stresses in the region (the western edge of Vatnajökull is situated above the axis of Iceland's Eastern Rift) play a role in determining the exact response of the volcanic systems (Pagli & Sigmundsson, 2008). However, while stating that the effects of increased melt production might be offset by intrusive processes and glacio-isostatic stresses, the study ultimately asserts that the likelihood of a large volcanic eruption within the region is increased by the retreat of the overlying glacier. The results of Jellinek et al (2004), Huybers & Langmuir (2009), Albino et al (2010) and Schmidt et al (2013) echo this inference.

2.4 Areas of Uncertainty

2.4.1 Gaps in the tephra record

The analysis of tephra and cryptotephra remains a relatively recent field of study. The current tephra record for Icelandic eruptions contains many spatial gaps,

introducing an element of uncertainty into the analyses of fallout areas and eruption frequencies. While it is possible that these gaps represent regions of minimal fallout (i.e. locations that may not commonly experience ashfall due to prevailing meteorological conditions), it is also highly likely that they are an artefact of research intensity (Watson, 2016a). Swindles et al (2011) present a database of Holocene tephra records across northern Europe, noting that the abundance of data recorded in Ireland and Scandinavia is much greater than in other regions. Lawson et al (2012) also provides an analysis of 22 Holocene tephra deposits found in north western Europe, again noting the geographical bias resulting in the underrepresentation of certain continental areas (such as Spain, southern Germany, Belgium and the Netherlands) while also indicating spatial gaps in northern Scandinavia and the western Baltic (Lawson et al, 2012), though recent efforts have focused on addressing this issue (Watson et al, 2016b). Additionally, there is a question of glass shard preservation and reworking following deposition - meteorological conditions, vegetation and (more recently) anthropogenic factors may affect the likelihood of ash fallout preservation (Watson, 2016c). The tephra chemistry may also play a role in preservation - basaltic glass is more readily dissolved by acidic depositional environments than rhyolitic, resulting in the preferential preservation of silicic eruptions (Lawson et al, 2012). To enable a complete understanding of the processes governing the emplacement of these deposits, it is imperative to establish whether these omissions indicate a true absence of tephra horizons in the locations in question, or if they are simply an artefact of sampling bias.

2.4.2 *Volcanic and tectonic processes*

Unfortunately, as our understanding of volcanic processes remains incomplete, so too does our ability to fully predict the response of volcanic systems to external stimuli. Taking Iceland as an example once again, there remains considerable uncertainty over the variability of rifting across the region (Saemundsson, 1974; Metzger & Jónsson, 2014), and whether large scale changes in the rate and geographical trends of the main axis of rifting might be linked to the presence of a deep mantle plume or 'hotspot' (Ofeigsson et al, 2013; Karson, 2016). The present-day rifting zone in eastern Iceland is thought to have become active at around 4-3 Ma (Saemundsson, 1974; Sinton et al, 2005), and to have remained

approximately static since that time, with the exception of a brief eastwards shift of the Spar fracture zone roughly 3 Ma (Meyer et al, 1972). It is thought that this section of the rifting zone may have migrated incrementally eastwards in order to accommodate westward drift of the lithospheric plates over a stationary plume. Periods of increase in rifting activity (such as the major rifting episodes known to have occurred at 12 ka, 11 ka, 10 ka and 3 ka) correspond with periods of enhanced eruption rates, particularly in Iceland's Northern and Western volcanic zones (Magnusdottir et al, 2013). Therefore, any major deviations in underlying tectonic and volcanic processes must be taken into account when attempting to assess the impact of deglaciation. Changes in the rate of rifting are likely to cause centennial variations in eruption frequency (Larsen et al, 1998), while fluctuations in mantle plume activity may cause multi-millennial changes (Óladóttir et al, 2011). However, Watson (2016c) argues that such pulses are unlikely to simultaneously affect multiple sites at varying distances from the central spreading ridge in precisely the same manner, hypothetically allowing the signal produced by ice loading to be separated from other factors.

Another issue raised in opposition to the hypothesis that the unloading effect might increase volcanic eruption frequency is that the pressure changes associated with ice retreat may also increase the capacity of the crust to capture melt. Hooper et al (2011) used a numerical model based on radar and GPS measurements of the Kverkfjöll volcanic system to show how relaxation of the stress fields surrounding the volcano might support magmatic intrusion rather than eruption of magma. However, their findings also indicated that dyke orientation is a major factor in determining crustal storage capacity, and that changes in crustal loading alter the conditions required for dyke initiation (Albino et al, 2010). The overall conclusion reached by Hooper et al (2011) was that, while deglaciation might increase magmatic storage capacity in the short term, ultimately increased mantle melting would become the dominant factor.

2.5 The Potential for Future Work

2.5.1 A more comprehensive record of past volcanism

While evidence of past volcanic eruptions are typically well-preserved in both the proximal record (i.e. in visible tephra layers and flow deposits), and often also in the distal record as cryptotephra, in many areas the dataset of past events may be considered to be incomplete. Though many sources suggest an apparent increase in the frequency of large volcanic events in Iceland over the past 2 ka (Zielinski et al, 2002; Óladóttir et al, 2011), it is highly possible that inference is largely a result of the preferential preservation of younger ash layers (Watson, 2016c), an increase in the number of studies, and recent improvements in research techniques, such as advances in geochemical analysis. A thorough campaign of investigation, centred particularly around the examination of the distal record and addressing the identified spatial gaps (as previously discussed), is necessary to confidently evaluate the past levels of volcanic activity, both in Iceland and in other locations. Efforts to this end are currently ongoing in northwestern and continental Europe (Swindles et al, 2011; Lawson et al, 2012; Watson et al, 2016b) and more recently in North America and Greenland (Pyne-O'Donnell et al, 2012; Mackay et al, 2016), but there is also great potential for such work to be conducted in other parts of the world, as evidenced by the discovery of Holocene cryptotephra in Peru (attributed to the Ecuadorian Eastern Cordillera) (Watson et al, 2015). A recent intensive study focusing on Japan (Kiyosugi et al, 2015) found that as much as 89% of VEI 4 events over the past 100 ka may be missing from the geological record, and the authors go on to estimate that under-recording of events may be 7.9-8.7 times higher in the global dataset.

However, the effect of deglaciation on volcanism in the near future is likely to be more substantial in the northern hemisphere, as glacier and ice sheet coverage in that hemisphere is more widespread. Additionally, while the focus has hitherto been on explosive events (as these are more likely to leave distal deposits in the geological record; Swindles et al, 2011), there is significant evidence that the greatest quantities of volcanic sulphate emissions may occur during large effusive eruptions (Krueger et al, 1996; Schmidt, 2013). Examining the aerosol contents

and acidity profiles of ice cores, typically from Greenland and Antarctica, can provide insights into the timing and subsequent climatic effects of volcanic eruptions (Robock & Free, 1995; Cole-Dai, 2010). Sigl et al (2015) use tephra analysis (among other methods) to constrain the dates of several sulphate peaks in the ice core record. Though explosive eruptions are more likely to deliver ash across multiple atmospheric layers and therefore present a greater danger to aviation, it may be of interest from a climatological perspective to compare the levels of climate forcing resulting from different eruption regimes and compositions.

2.5.2 Quantifying the unloading effect

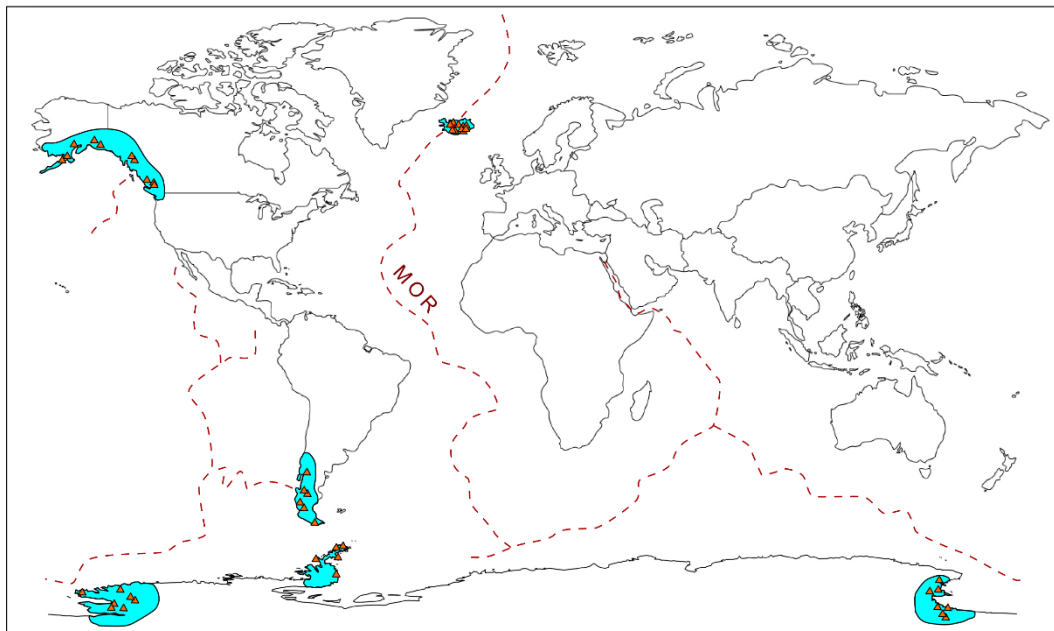


Figure 4. Multiple areas worldwide meet the following criteria: That they have 1. displayed significant volcanic activity within the past 11,500 years, and 2. currently have one or more large glaciers or ice sheets. These areas are typically within polar/sub-polar latitudes, and are marked in blue. Volcanoes active within the past 5,000 years are indicated with red triangles. Mid-oceanic ridges are marked with red dotted lines. The most significant identified regions in which the unloading effect may exert an influence are Alaska/western Canada, southern Chile/Argentina, Iceland, and several regions in coastal Antarctica, including the Antarctic Peninsula and the perimeter of the Ross Ice Shelf.

The issue of geographic sampling bias is also present in models of future changes related to glaciation. Most attempts to model a volcanic response to ice load variations focus on examples from Iceland (Sigmundsson, 1991; Sigvaldason, 1992; Pagli & Sigmundsson, 2008; Sigmundsson et al, 2010). A more global view of this effect may offer new insights, and may provide important data to advise policy beyond Europe's airspace. Through combining Smithsonian Global Volcanism Database and the Randolph Glacier Inventory (Global Land Ice Measurements from Space, 2017; see figure 4), it is possible to identify several areas worldwide in which:

- i. Significant volcanic activity has occurred during the Holocene
- ii. A glacier or large ice sheet (> 1000km²) currently exists

Assuming the current trends of atmospheric warming and glacier retreat continue (Rogelij, 2013), it is reasonable to hypothesise that these highlighted areas may experience a geospheric response to isostatic unloading. While the atmospheric and societal effects of this would in some cases be minimal - increased eruptions in the Antarctic regions, for example, are unlikely to have a significant climatic effect due to their high latitude (Oman et al, 2006), and their remoteness reduces the risk posed to commercial flights - in other areas, such as Canada and Alaska, the impact could be considerably greater, due to the importance of the region for trans-continental and trans-Pacific flights.

2.6 Conclusions

1. As the subject of rapid climate change becomes ever more pertinent to our society, it is increasingly important to understand how such changes may affect the other aspects that govern the workings of our planet. While the atmosphere, geosphere, cryosphere and other facets of the natural world may be considered separately for the purposes of scientific study, in truth none exist in isolation and each represents only part of a complex, interconnected system. The intricate economical and societal structures we have constructed around the aviation

industry alone necessitate a more in-depth knowledge of the interplay between volcanic systems and the climate, highlighting the need for further study.

2. Explosive volcanic eruptions may cause significant climatic cooling effects if sufficient quantities of sulphuric aerosol particles reach the stratosphere. It is thought that some eruptions, such as the 75 kya Toba event, may have caused a series of positive feedback loops, prolonging the initial cooling effect by several centuries and causing migration of the ITCZ with ensuing changes to circulation and precipitation patterns.

3. Though large-scale flood basalt eruptions are frequently linked to long-term climate change and mass extinction events, there is lively debate concerning the cooling influence of SO₂ release versus the greenhouse effect of CO₂. While it has been estimated that 5×10^{17} moles of CO₂ may have been emitted during the formation of the Deccan Traps, it has also been argued that this quantity would still have been small in comparison to ambient conditions, and that the effects of the conversion of SO₂ to sulphuric acid in the stratosphere would have outweighed any warming effects.

4. Isostatic rebound in response to glacial unloading is presented as a viable mechanism for a volcanic response to climate change. Adiabatic melting following deglaciation of Iceland is visible both in historical records and in present-day studies of Vatnajökull. It has been estimated that melt production may have increased between 100-135% since 1890.

5. Studies of tephra and cryptotephra provide invaluable insights into the frequency of volcanic ash cloud occurrences, and may also provide information on the nature of individual eruptions. Current studies of Icelandic ash deposition suggest that eruptions in Iceland which transport significant volumes of ash over continental Europe have a return interval of approximately 56 years, based on depositional records.

6. Numerical models of the 'unloading effect' confirm the hypothesis that crustal uplift in response to deglaciation is very likely to cause increased decompression melting. While increased fracturing and intrusion may provide greater storage capacity for upwelling material in the short-term, most models find that the likelihood of a large volcanic eruption is raised by the retreat of an overlying glacier.

Acknowledgements

This review was prepared while Claire Cooper held a Leeds Anniversary Research Scholarship at the University of Leeds, in addition to receiving funding from the Climate Research Bursary Fund, awarded by the Priestley International Centre for Climate.

References

1. Aberhan, M. and Fürsich, F.T., 2000. Mass origination versus mass extinction: the biological contribution to the Pliensbachian–Toarcian extinction event. *Journal of the Geological Society*, 157(1), 55-60.
2. Adams, J.B., Mann, M.E. and Ammann, C.M., 2003. Proxy evidence for an El Niño-like response to volcanic forcing. *Nature*, 426(6964), 274-278.
3. Air Transport Action Group. Aviation benefits beyond borders global summary 2016. 2016.
4. Albino, F., Pinel, V. and Sigmundsson, F., 2010. Influence of surface load variations on eruption likelihood: application to two Icelandic subglacial volcanoes, Grímsvötn and Katla. *Geophysical journal international*, 181(3), 1510-1524.
5. Alloway, B.V., Andreastuti, S., Setiawan, R., Miksic, J. and Hua, Q. 2017. Archaeological implications of a widespread 13th Century tephra marker across the central Indonesian Archipelago. *Quaternary Science Reviews*, 155, 86-99
6. Asimow, P.D., Hirschmann, M.M., Ghiorso, M.S., O'Hara, M.J. and Stolper, E.M., 1995. The effect of pressure-induced solid-solid phase transitions on decompression melting of the mantle. *Geochimica et Cosmochimica Acta*, 59(21), 4489-4506.
7. Auriac, A., Spaans, K.H., Sigmundsson, F., Hooper, A., Schmidt, P. and Lund, B. 2013. Iceland rising: solid Earth response to ice retreat inferred from satellite radar interferometry and viscoelastic modelling. *Journal of Geophysical Research: Solid Earth*, 118(4), 1331-1344
8. Balascio, N.L., Wickler, S., Narmo, L.E. and Bradley, R.S. 2011. Distal cryptotephra found in a Viking boathouse: the potential for tephrochronology in reconstructing the Iron Age in Norway. *Journal of Archaeological Science*, 38, 934-941
9. Baldini, J.U., Brown, R.J. and McElwaine, J.N., 2015. Was millennial scale climate change during the Last Glacial triggered by explosive volcanism?. *Scientific Reports*, 5.
10. Björnsson, H. and Pálsson, F., 2008. Icelandic glaciers. *Jökull*, 58, 365-386.
11. Björnsson, H. et al. 2013. Contribution of Icelandic ice caps to sea level rise: trends and variability since the Little Ice Age. *Geophysical Research Letters*, 40, 1546-1550

12. Bluth, G.J., Doiron, S.D., Schnetzler, C.C., Krueger, A.J. and Walter, L.S., 1992. Global tracking of the SO₂ clouds from the June, 1991 Mount Pinatubo eruptions. *Geophysical Research Letters*, 19(2), 151-154.
13. Boer, J. G., Flato, G., Reader, M. C. & Ramsden, D. 2000. A transient climate change simulation with greenhouse gas and aerosol forcing: Experimental design and comparison with the instrumental record for the 20th century. *Climate Dynamics*, 16, 405–425
14. Bond, G., Showers, W., Cheseby, M., Lotti, R., Almasi, P., Priore, P., Cullen, H., Hajdas, I. and Bonani, G., 1997. A pervasive millennial-scale cycle in North Atlantic Holocene and glacial climates. *Science*, 278(5341), 1257-1266.
15. Bond, D.P.G. and Wignall, P.B. 2014. Large igneous provinces and mass extinctions: An update. *Geological Society of America Special Papers*, 505, 29-55
16. Boyle, E.A. and Keigwin, L., 1987. North Atlantic thermohaline circulation during the past 20, 000 years linked to high-latitude surface temperature. *Nature*, 330(6143), 35-40.
17. Caldeira, K. and Rampino, M.R. 1990. Carbon dioxide emissions from Deccan volcanism and a K/T boundary greenhouse effect. *Geophysical Research Letters*, 17(9), 1299-1302.
18. Campbell, I.H., Czamanske, G.K., Fedorenko, V.A., Hill, R.I. and Stepanov, V., 1992. Synchronism of the Siberian Traps and the Permian-Triassic boundary. *Science*, 258(5089), 1760-1763.
19. Chandler, B.M.P., Evans, D.J.A. and Roberts, D.H. 2016a. Characteristics of recessional moraines at a temperate glacier in SE Iceland: insights into patterns, rates and drivers of glacier retreat. *Quaternary Science Reviews*, 135, 171-205
20. Chandler, B.M.P., Evans, D.J.A. and Roberts, D.H. 2016b. Recent retreat at a temperate Icelandic glacier in the context of the last ~80 years of climate change in the North Atlantic region. *Arktos*, 2(24)
21. Coffin, M.F. and Eldholm, O., 1994. Large igneous provinces: crustal structure, dimensions, and external consequences. *Reviews of Geophysics*, 32(1), 1-36.
22. Cole-Dai, J. 2010. Volcanoes and climate. *Wiley Interdisciplinary Reviews: Climate Change*, 1(6), 824-839
23. Collins, M., Knutti, R., Arblaster, J., Dufresne, J.L., Fichet, T., Friedlingstein, P., Gao, X., Gutowski, W.J., Johns, T., Krinner, G. and Shongwe, M., 2013. Long-term climate change: projections, commitments and irreversibility. In *Climate Change 2013-The Physical Science Basis: Contribution of Working*

- Group I to the Fifth Assessment Report of the Intergovernmental Panel on Climate Change (pp. 1029-1136). Cambridge University Press.
24. Colucci, S., Palladino, D.M., Mulukutla, G.K. and Proussevitch, A.A., 2013. 3-D reconstruction of ash vesicularity: insights into the origin of ash-rich explosive eruptions. *Journal of Volcanology and Geothermal Research*, 255, 98-107.
 25. Connor, C.B., McBirney, A.R. and Furlan, C., 2006. What is the probability of explosive eruption at a long-dormant volcano. *Statistics in Volcanology*, 1, 39-48.
 26. Courtillot, V.E. and Renne, P.R., 2003. On the ages of flood basalt events. *Comptes Rendus Geoscience*, 335(1), 113-140.
 27. Dansgaard, W., Johnsen, S.J., Clausen, H.B., Dahl-Jensen, D., Gundestrup, N.S., Hammer, C.U., Hvidberg, C.S., Steffensen, J.P., Sveinbjörnsdottir, A.E., Jouzel, J. and Bond, G., 1993. Evidence for general instability of past climate from a 250-kyr ice-core record. *Nature*, 364(6434), 218-220.
 28. Davies, S.M., 2015. Cryptotephra: the revolution in correlation and precision dating. *Journal of Quaternary Science*, 30, 114-130.
 29. Dessert, C., Dupré, B., Francois, L.M., Schott, J., Gaillardet, J., Chakrapani, G. and Bajpai, S., 2001. Erosion of Deccan Traps determined by river geochemistry: impact on the global climate and the $^{87}\text{Sr}/^{86}\text{Sr}$ ratio of seawater. *Earth and Planetary Science Letters*, 188(3), 459-474.
 30. Duncan, R.A., Hooper, P.R., Rehacek, J., Marsh, J. and Duncan, A.R., 1997. The timing and duration of the Karoo igneous event, southern Gondwana. Oregon State University Faculty Publications, College of Earth, Ocean and Atmospheric Sciences. DOI: 10.1029/97JB00972
 31. Dugmore, A., 1989. Icelandic volcanic ash in Scotland. *Scottish Geographical Magazine*, 105, 168-172.
 32. Dunn, J., Baran, A.J., Wade, D.P., and Tremba, E.L. 1993. Deposition of volcanic materials in the hot sections of two gas turbine engines. *Journal of Engineering for Gas Turbines and Power*, 115(3), 641-651
 33. Emile-Geay, J., Seager, R., Cane, M.A., Cook, E.R. and Haug, G.H., 2008. Volcanoes and ENSO over the past millennium. *Journal of Climate*, 21(13), 3134-3148.
 34. Fischer, E.M., Luterbacher, J., Zorita, E., Tett, S.F.B., Casty, C. and Wanner, H., 2007. European climate response to tropical volcanic eruptions over the last half millennium. *Geophysical Research Letters*, 34(5).

35. Folch, A., 2012. A review of tephra transport and dispersal models: evolution, current status, and future perspectives. *Journal of Volcanology and Geothermal Research*, 235, 96-115.
36. Franklin, B., 1784. Meteorological imaginations and conjectures. *Manchester Literary and Philosophical Society Memoirs and Proceedings*, 2, 122.
37. Ganino, C. and Arndt, N.T., 2009. Climate changes caused by degassing of sediments during the emplacement of large igneous provinces. *Geology*, 37(4), 323-326.
38. Gao, C., Robock, A. and Ammann, C., 2008. Volcanic forcing of climate over the past 1500 years: An improved ice core based index for climate models. *Journal of Geophysical Research: Atmospheres*, 113(D23).
39. Geirsdóttir, Á., Miller, G.H., Larsen, D.J. and Ólafsdóttir, S., 2013. Abrupt Holocene climate transitions in the northern North Atlantic region recorded by synchronized lacustrine records in Iceland. *Quaternary Science Reviews*, 70, 48-62.
40. Global Land Ice Measurements from Space, 2017. Randolph Glacier Inventory. v. 5.0. Downloaded 12 Jan 2017.
41. Global Volcanism Program, 2013. *Volcanoes of the World*, v. 4.5.3. Venzke, E (ed.). Smithsonian Institution. Downloaded 12 Jan 2017.
<http://dx.doi.org/10.5479/si.GVP.VOTW4-2013>
42. Grindle, T.J. and Burcham Jr, F.W., 2003. Engine damage to a NASA DC-8-72 airplane from a high-altitude encounter with a diffuse volcanic ash cloud. *NASA Technical Reports*, 20030068344
43. Gudmundsson, M.T., Sigmundsson, F. and Björnsson, H., 1997. Ice–volcano interaction of the 1996 Gjálp subglacial eruption, Vatnajökull, Iceland. *Nature*, 389(6654), 954-957.
44. Guffanti, M., Mayberry, G.C., Casadevall, T.J. and Wunderman, R., 2009. Volcanic hazards to airports. *Natural hazards*, 51(2), 287-302.
45. Guffanti, M., Casadevall, T.J. and Budding, K., 2010. Encounters of aircraft with volcanic ash clouds; a compilation of known incidents, 1953-2009 (No. 545). US Geological Survey.
46. Hall, V.A., Pilcher, J.R., 2002. Late-Quaternary Icelandic tephtras in Ireland and Great Britain: detection, characterization and usefulness. *Holocene*, 12, 223-230.
47. Haug, G.H., Hughen, K.A., Sigman, D.M., Peterson, L.C. and Röhl, U., 2001. Southward migration of the intertropical convergence zone through the Holocene. *Science*, 293(5533), 1304-1308.

48. Hayes, S.K., Montgomery, D.R. and Newhall, C.G., 2002. Fluvial sediment transport and deposition following the 1991 eruption of Mount Pinatubo. *Geomorphology*, 45(3), pp.211-224.
49. Haywood, J.M., Jones, A., Bellouin, N. and Stephenson, D., 2013. Asymmetric forcing from stratospheric aerosols impacts Sahelian rainfall. *Nature Climate Change*, 3(7), 660-665.
50. Heiken, G., 1974. An atlas of volcanic ash. NASA Technical Report, 19740017769
51. Hesselbo, S.P., Gröcke, D.R., Jenkyns, H.C., Bjerrum, C.J., Farrimond, P., Bell, H.S.M. and Green, O.R., 2000. Massive dissociation of gas hydrate during a Jurassic oceanic anoxic event. *Nature*, 406(6794), 392-395.
52. Hofmann, C., Courtillot, V., Feraud, G., Rochette, P., Yirgu, G., Ketefo, E. and Pik, R., 1997. Timing of the Ethiopian flood basalt event and implications for plume birth and global change. *Nature*, 389(6653), 838-841.
53. Hooper, A., Ófeigsson, B., Sigmundsson, F., Lund, B., Einarsson, P., Geirsson, H. and Sturkell, E., 2011. Increased capture of magma in the crust promoted by ice-cap retreat in Iceland. *Nature Geoscience*, 4(11), 783-786.
54. Horwell, C.J. and Baxter, P.J., 2006. The respiratory health hazards of volcanic ash: a review for volcanic risk mitigation. *Bulletin of Volcanology*, 69, 1-24.
55. Horwell, C.J., 2007. Grain-size analysis of volcanic ash for the rapid assessment of respiratory health hazard. *Journal of Environmental Monitoring*, 9(10), 1107-1115.
56. Huang, B., Pan, Z. and Schopf, P.S., 2001. The interannual variability in the Tropical Atlantic Ocean simulated by a regionally coupled ocean-atmosphere GCM. In US CLIVAR Atlantic workshop, June, 12-14.
57. Huybers, P. and Langmuir, C. 2009. Feedback between deglaciation, volcanism and atmospheric CO₂. *Earth and Planetary Science Letters*, 286(3-4), 479-491
58. Hwang, Y.T., Frierson, D.M. and Kang, S.M., 2013. Anthropogenic sulfate aerosol and the southward shift of tropical precipitation in the late 20th century. *Geophysical Research Letters*, 40(11), 2845-2850.
59. Ikeda, M. and Hori, R.S., 2014. Effects of Karoo–Ferrar volcanism and astronomical cycles on the Toarcian oceanic anoxic events (Early Jurassic). *Palaeogeography, Palaeoclimatology, Palaeoecology*, 410, 134-142.
60. Jacoby, G. C., K. W. Workman, and R. D. D'Arrigo (1999), Laki eruption of 1783, tree rings, and disaster for northwest Alaska Inuit. *Quaternary Science Reviews*, 18, 1365–1371.

61. James, T.S. and Morgan, W.J., 1990. Horizontal motions due to post-glacial rebound. *Geophysical Research Letters*, 17(7), 957-960.
62. Jellinek, A.M., Manga, M. and Saar, M.O., 2004. Did melting glaciers cause volcanic eruptions in eastern California? Probing the mechanics of dike formation. *Journal of Geophysical Research: Solid Earth*, 109(B9).
63. Jóhannesson, T., 1985. The response time of glaciers in Iceland to changes in climate. *Annals of Glaciology*, 8, 100-101.
64. Jones, P.D., Lister, D.H., Osborn, T.J., Harpham, C., Salmon, M. & Morice, C.P. 2012. Hemispheric and large-scale land-surface air temperature variations: An extensive revision and an update to 2010. *Journal of Geophysical Research: Atmospheres*, 117(D5)
65. Jull, M. and McKenzie, D., 1996. The effect of deglaciation on mantle melting beneath Iceland. *Journal of Geophysical Research: Solid Earth*, 101(B10), 21815-21828.
66. Karson, J.A., 2016. Crustal Accretion of Thick, Mafic Crust in Iceland: Implications for Volcanic Rifted Margins. *Canadian Journal of Earth Sciences*, 53(11), 1205-1215
67. Kerle, N., de Vries, B. V. W., & Oppenheimer, C., 2003. New insight into the factors leading to the 1998 flank collapse and lahar disaster at Casita volcano, Nicaragua. *Bulletin of volcanology*, 65(5), 331-345.
68. Kirchner, I., Stenchikov, G.L., Graf, H.F., Robock, A. and Antuña, J.C., 1999. Climate model simulation of winter warming and summer cooling following the 1991 Mount Pinatubo volcanic eruption. *Journal of Geophysical Research: Atmospheres*, 104(D16), 19039-19055.
69. Kirkbride, M.P. and Dugmore, A.J., 2001. Timing and significance of mid-Holocene glacier advances in northern and central Iceland. *Journal of Quaternary Science*, 16(2), 145-153.
70. Kirkbride, M.P. and Dugmore, A.J., 2006. Responses of mountain ice caps in central Iceland to Holocene climate change. *Quaternary Science Reviews*, 25(13), 1692-1707.
71. Kiyosugi, K., Connor, C., Sparks, R.S.J., Crosweller, H.S., Brown, S.K., Siebert, L., Wang, T. and Takarada, S. 2015. How many explosive eruptions are missing from the geologic record? Analysis of the quaternary record of large magnitude explosive eruptions in Japan. *Journal of Applied Volcanology*, 4(17)
72. Krueger, A.J., Schnetzler, C.C. and Walter, L.S., 1996. The December 1981 eruption of Nyamuragira volcano (Zaire), and the origin of the "mystery

- cloud" of early 1982. *Journal of Geophysical Research: Atmospheres*, 101(D10), 15191-15196.
73. Lamb, H.H., 1970. Volcanic dust in the atmosphere; with a chronology and assessment of its meteorological significance. *Philosophical Transactions of the Royal Society of London A: Mathematical, Physical and Engineering Sciences*, 266(1178), 425-533.
 74. Lambeck, K., Smither, C. and Johnston, P., 1998. Sea-level change, glacial rebound and mantle viscosity for northern Europe. *Geophysical Journal International*, 134(1), 102-144.
 75. Lane, C.S., Cullen, V.L., White, D., Bramham-Law, C.W.F. and Smith, V.C., 2014. Cryptotephra as a dating and correlation tool in archaeology. *Journal of Archaeological Science*, 42, 42-50.
 76. Langdon, P.G., Barber, K.E., 2004. Snapshots in time: precise correlations of peat-based proxy climate records in Scotland using mid-Holocene tephras. *Holocene*, 14, 21-33
 77. Larsen, G., Gudmundsson, M. T. & Björnsson, H. 1998. Eight centuries of periodic volcanism at the center of the Iceland hotspot revealed by glacier tephrostratigraphy. *Geology*, 26, 943-946
 78. Lawson, I.T., Swindles, G.T., Plunkett, G., Greenberg, D., 2012. The spatial distribution of Holocene cryptotephras in north-west Europe since 7 ka: implications for understanding ash fall events from Icelandic eruptions. *Quaternary Science Reviews*, 41, 57-66
 79. Lowe, D.J., 2011. Tephrochronology and its application: a review. *Quaternary Geochronology*, 6(2), 107-153.
 80. Lowe, D.J., Blaauw, M., Hogg, A.G. and Newnham, R.M. 2013. Ages of 24 widespread tephras erupted since 30,000 years ago in New Zealand, with re-evaluation of the timing and palaeoclimatic implications of the Lateglacial cool episode recorded at Kaipo bog. *Quaternary Science Reviews*, 74, 170-194
 81. Luna, B.Q. 2007. Assessment and modelling of two lahars caused by "Hurricane Stan" at Atitlan, Guatemala, October 2005. Doctoral Dissertation, University of Oslo.
 82. Mackay, H., Hughes, P.D., Jensen, B.J., Langdon, P.G., Pyne-O'Donnell, S.D., Plunkett, G., Froese, D.G., Coulter, S. and Gardner, J.E., 2016. A mid to late Holocene cryptotephra framework from eastern North America. *Quaternary Science Reviews*, 132, 101-113.
 83. Magnúsdóttir, S., Brandsdóttir, B., Driscoll, N.W. and Detrick, R.S., 2013. Tectonics of the Nafir-Skjálíandadjúp volcanic system, Tjörnes Fracture Zone,

- offshore North Iceland: A case of transtensional rifting along a divergent plate boundary. In AGU Fall Meeting Abstracts (Vol. 1, p. 2382).
84. Maher, N., McGregor, S., England, M.H. and Gupta, A.S., 2015. Effects of volcanism on tropical variability. *Geophysical Research Letters*, 42(14), 6024-6033.
 85. Marenco, F., Kent, J., Adam, M., Buxmann, J., Francis, P. and Haywood, J. 2016. Remote sensing of volcanic ash at the Met Office. *EPJ Web of Conferences*, 119, 07003
 86. Martin-Jones, C.M., Lane, C.S., Pearce, N.J.G., Smith, V.C., Lamb, H.F., Oppenheimer, C., Asrat, A. and Schaebitz, F., 2017. Glass compositions and tempo of post-17 ka eruptions from the Afar Triangle recorded in sediments from lakes Ashenge and Hayk, Ethiopia. *Quaternary Geochronology*, 37, 15-31
 87. Mayewski, P.A., Meeker, L.D., Twickler, M.S., Whitlow, S., Yang, Q., Lyons, W.B. and Prentice, M., 1997. Major features and forcing of high-latitude northern hemisphere atmospheric circulation using a 110,000-year-long glaciochemical series. *Journal of Geophysical Research: Oceans*, 102(C12), 26345-26366.
 88. Mayewski, P.A., Rohling, E.E., Stager, J.C., Karlén, W., Maasch, K.A., Meeker, L.D., Meyerson, E.A., Gasse, F., van Kreveld, S., Holmgren, K. and Lee-Thorp, J., 2004. Holocene climate variability. *Quaternary research*, 62(3), 243-255.
 89. Mazzocchi, M., Hansstein, F. and Ragona, M., 2010. The 2010 volcanic ash cloud and its financial impact on the European airline industry. In *CESifo Forum* (Vol. 11, No. 2, 92-100). Ifo Institute for Economic Research at the University of Munich.
 90. McCormick, M.P., Thomason, L.W. and Trepte, C.R., 1995. Atmospheric effects of the Mt Pinatubo eruption. *Nature*, 373(6513), 399-404.
 91. McGuire, B., 2010. Potential for a hazardous geospheric response to projected future climate changes. *Philosophical Transactions of the Royal Society A: Mathematical, Physical and Engineering Sciences*, 368(1919), 2317-2345.
 92. McLean, D.M., 1985. Deccan Traps mantle degassing in the terminal Cretaceous marine extinctions. *Cretaceous Research*, 6(3), 235-259.
 93. Meehl, G. A. & Washington, W. M. 1996. El Niño-like climate change in a model with increased atmospheric CO₂ concentrations. *Nature*, 382, 56-60
 94. Metzger, S. and Jónsson, S., 2014. Plate boundary deformation in North Iceland during 1992–2009 revealed by InSAR time-series analysis and GPS. *Tectonophysics*, 634, 127-138.

95. Meyer, O., Voppel, D., Fleischer, U., Closs, H. and Gerke, K., 1972. Results of bathymetric, magnetic and gravimetric measurements between Iceland and 70 N. *Deutsche Hydrografische Zeitschrift*, 25(5), 193-201.
96. Miller, G.H., Geirsdóttir, Á., Zhong, Y., Larsen, D.J., Otto-Bliesner, B.L., Holland, M.M., Bailey, D.A., Refsnider, K.A., Lehman, S.J., Southon, J.R. and Anderson, C., 2012. Abrupt onset of the Little Ice Age triggered by volcanism and sustained by sea-ice/ocean feedbacks. *Geophysical Research Letters*, 39(2).
97. Mogensen, I.A., 2009. Dansgaard-Oeschger Cycles. *Encyclopedia of Paleoclimatology and Ancient Environments*, 229-233. Springer. ISBN: 978-1-4020-4411-3
98. Newhall, C.G. and Self, S., 1982. The volcanic explosivity index (VEI) an estimate of explosive magnitude for historical volcanism. *Journal of Geophysical Research: Oceans*, 87(C2), 1231-1238.
99. Newton, A.J., Dugmore, A.J. and Gittings, B.M. (2007) Tephrobase: tephrochronology and the development of a centralised European database. *Journal of Quaternary Science*, 22, 737-743.
100. Nicholls, N., 1988. Low latitude volcanic eruptions and the El Niño-Southern Oscillation. *Journal of climatology*, 8(1), pp.91-95.
101. O'Brien, S.R., Mayewski, P.A., Meeker, L.D., Meese, D.A., Twickler, M.S. and Whitlow, S.I., 1995. Complexity of Holocene climate as reconstructed from a Greenland ice core. *Science*, 270(5244), 1962-1964
102. Oerlemans, J. and Fortuin, J.P.F. 1992. Sensitivity of glaciers and small ice caps to greenhouse warming. *Science*, 258(5079), 115-117
103. Oerlemans, J., Anderson, B., Hubbard, A., Huybrechts, P., Johannesson, T., Knap, W.H., Schmeits, M., Stroeven, A.P., Van de Wal, R.S.W., Wallinga, J. and Zuo, Z., 1998. Modelling the response of glaciers to climate warming. *Climate dynamics*, 14(4), 267-274.
104. Ofeigsson, B.G., Hreinsdóttir, S., Sigmundsson, F., Arnadóttir, T., Vogfjörð, K., Geirsson, H., Einarsson, P., Jonsson, S., Villemin, T., Fjalar Sigurdsson, S. and Roberts, M., 2013, April. Geodetic observations in Iceland: divergent plate boundary influenced by a hotspot. In *EGU General Assembly Conference Abstracts* (Vol. 15, p. 12560).
105. Óladóttir, B.A., Larsen, G. and Sigmarsson, O., 2011. Holocene volcanic activity at Grímsvötn, Bárðarbunga and Kverkfjöll subglacial centres beneath Vatnajökull, Iceland. *Bulletin of Volcanology*, 73(9), 1187-1208.

106. Oman, L., Robock, A., Stenchikov, G., Schmidt, G.A. and Ruedy, R., 2005. Climatic response to high-latitude volcanic eruptions. *Journal of Geophysical Research: Atmospheres*, 110(D13).
107. Oman, L., Robock, A., Stenchikov, G. L. and Thordarson, T., 2006. High-latitude eruptions cast shadow over the African monsoon and the flow of the Nile. *Geophysical Research Letters*, 33, L18711
108. Oskarsson, N., Steinthorsson, S. and Sigvaldason, G.E., 1985. Iceland geochemical anomaly: origin, volcanotectonics, chemical fractionation and isotope evolution of the crust. *Journal of Geophysical Research: Solid Earth*, 90(B12), 10011-10025.
109. Pagli, C., Sigmundsson, F., Lund, B., Sturkell, E., Geirsson, H., Einarsson, P., Árnadóttir, T. and Hreinsdóttir, S., 2007. Glacio-isostatic deformation around the Vatnajökull ice cap, Iceland, induced by recent climate warming: GPS observations and finite element modeling. *Journal of Geophysical Research: Solid Earth*, 112(B8).
110. Pagli, C. and Sigmundsson, F., 2008. Will present day glacier retreat increase volcanic activity? Stress induced by recent glacier retreat and its effect on magmatism at the Vatnajökull ice cap, Iceland. *Geophysical Research Letters*, 35(9).
111. Pálffy, J. and Smith, P.L., 2000. Synchrony between Early Jurassic extinction, oceanic anoxic event, and the Karoo-Ferrar flood basalt volcanism. *Geology*, 28(8), 747-750.
112. Percival, L.M.E., Witt, M.L.I., Mather, T.A., Hermoso, M., Jenkyns, H.C., Hesselbo, S.P., Al-Suwaidi, A.H., Storm, M.S., Xu, W. and Ruhl, M., 2015. Globally enhanced mercury deposition during the end-Pliensbachian extinction and Toarcian OAE: A link to the Karoo–Ferrar Large Igneous Province. *Earth and Planetary Science Letters*, 428, 267-280.
113. Pielke, R.A., Avissar, R., Raupach, M., Dolman, A.J., Zeng, X. and Denning, A.S., 1998. Interactions between the atmosphere and terrestrial ecosystems: influence on weather and climate. *Global Change Biology*, 4(5), 461-475.
114. Pierson, T.C., Wood, N.J. and Driedger, C.L., 2014. Reducing risk from lahar hazard: concepts, case studies, and roles for scientists. *Journal of Applied Volcanology*, 3(1), 16
115. Pilcher, J. et al. 2005. A Holocene tephra record from the Lofoten Islands, Arctic Norway. *Boreas*, 34, 136-156
116. Pyne-O'Donnell, S.D., Hughes, P.D., Froese, D.G., Jensen, B.J., Kuehn, S.C., Mallon, G., Amesbury, M.J., Charman, D.J., Daley, T.J., Loader, N.J. and

- Mauquoy, D., 2012. High-precision ultra-distal Holocene tephrochronology in North America. *Quaternary Science Reviews*, 52, 6-11.
117. Rahmstorf, S., 1996. Bifurcations of the Atlantic thermohaline circulation in response to changes in the hydrological cycle. *Oceanographic Literature Review*, 5(43), p.435.
118. Rahmstorf, S., 2002. Ocean circulation and climate during the past 120,000 years. *Nature*, 419(6903), 207-214.
119. Raible, C.C. et al. Tambora 1815 as a test case for high impact volcanic eruptions: Earth system effects. *WIREs: Climate Change*, 7(4), 569-589
120. Rampino, M.R., Self, S. and Stothers, R.B., 1988. Volcanic winters. *Annual Review of Earth and Planetary Sciences*, 16(1), 73-99.
121. Ramsey, C.B., Housley, R.A., Lane, C.S., Smith, V.C. and Pollard, A.M. 2015. The RESET tephra database and associated analytical tools. *Quaternary Science Reviews*, 118, 33-47
122. Rea, H.A., Swindles, G.T., Roe, H.M., 2012. The Hekla 1947 tephra in the north of Ireland: regional distribution, concentration and geochemistry. *Journal of Quaternary Science*, 27, 425-431
123. Reynolds, J.M., 2000. On the formation of supraglacial lakes on debris-covered glaciers. IAHS publication, 153-164.
124. Ridley, H.E., Asmerom, Y., Baldini, J.U., Breitenbach, S.F., Aquino, V.V., Pruffer, K.M., Culleton, B.J., Polyak, V., Lechleitner, F.A., Kennett, D.J. and Zhang, M., 2015. Aerosol forcing of the position of the intertropical convergence zone since AD 1550. *Nature Geoscience*, 8(3), 195-200.
125. Riley, T.R., Leat, P.T. and Curtis, M.L., 2006. Karoo large igneous province: Brevity, origin, and relation to mass extinction questioned by new $^{40}\text{Ar}/^{39}\text{Ar}$ age data: Comment. *Geology*, 34(1), 109-110.
126. Robert, H. and Hermans, M. 2000. *Alaska's Natural Wonders: A Guide to the Phenomena*. Graphic Arts Center Publishing Company. 70
127. Robock, Alan and Clifford Mass, 1982: The Mount St. Helens volcanic eruption of 18 May 1980: large short-term surface temperature effects. *Science*, 216, 628-630
128. Robock, A. and Matson, M., 1983. Circumglobal transport of the El Chichón volcanic dust cloud. *Science*, 221(4606), 195-197.
129. Robock, A. and Mao, J., 1992. Winter warming from large volcanic eruptions. *Geophysical Research Letters*, 19(24), 2405-2408.
130. Robock, A. and Free, M.P. 1995. Ice cores as an index of global volcanism from 1850 to the present. *Journal of Geophysical Research: Atmospheres*, 100(D6), 11549-11567

131. Robock, A., 2000. Volcanic eruptions and climate. *Reviews of Geophysics*, 38(2), 191-219.
132. Saemundsson, K., 1974. Evolution of the axial rifting zone in northern Iceland and the Tjörnes fracture zone. *Geological Society of America Bulletin*, 85(4), 495-504.
133. Santer, B., Solomon, S., Ridley, D., Fyfe, J., Beltran, F., Bonfils, C., Painter, J. and Zelinka, M., 2016. Volcanic effects on climate. *Nature Climate Change*, 6(1), 3-4.
134. Scott, K. M., Vallance, J. W., Kerle, N., Luis Macías, J., Strauch, W., & Devoli, G., 2005. Catastrophic precipitation-triggered lahar at Casita volcano, Nicaragua: occurrence, bulking and transformation. *Earth Surface Processes and Landforms*, 30(1), 59-79.
135. Schmid, M.M.E., Dugmore, A.J., Vésteinsson, O. and Newton, A.J. 2017. Tephra isochrons and chronologies of colonisation. *Quaternary Geochronology*, 40, 56-66
136. Schmidt, A., Ostro, B., Carslaw, K.S., Wilson, M., Thordarson, T., Mann, G.W. and Simmons, A.J. 2011. Excess mortality in Europe following a future Laki-style Icelandic eruption. *Proceedings of the National Academy of Sciences of the United States of America*, 108(38), 15710-15715
137. Schmidt, A., 2013. Impact of the 1783–1784 AD Laki Eruption on Global Aerosol Formation Processes and Cloud Condensation Nuclei. In *Modelling Tropospheric Volcanic Aerosol* (65-95). Springer Berlin Heidelberg.
138. Schmidt, A. and Robock, A. 2015. Volcanism, the atmosphere and climate through time. In *Volcanism and Global Environmental Change*, pp. 195-207. Cambridge University Press.
139. Schmidt, P., Lund, B., Hieronymus, C., Maclennan, J., Árnadóttir, T. and Pagli, C., 2013. Effects of present-day deglaciation in Iceland on mantle melt production rates. *Journal of Geophysical Research: Solid Earth*, 118(7), 3366-3379.
140. Schmidt, A., Skeffington, R.A., Thordarson, T., Self, S., Forster, P.M., Rap, A., Ridgwell, A., Fowler, D., Wilson, M., Mann, G.W. and Wignall, P.B., 2016. Selective environmental stress from sulphur emitted by continental flood basalt eruptions. *Nature Geoscience*, 9(10), p.77.
141. Self, S., Rampino, M.R., Zhao, J. and Katz, M.G., 1997. Volcanic aerosol perturbations and strong El Niño events: No general correlation. *Geophysical research letters*, 24(10), 1247-1250.
142. Self, S., Rampino, M.R. and Barbera, J.J., 1981. The possible effects of large 19th and 20th century volcanic eruptions on zonal and hemispheric surface

- temperatures. *Journal of Volcanology and Geothermal Research*, 11(1), 41-60.
143. Self, S., Rampino, M. R., Zhao, J. & Katz, M. G. 1997. Volcanic aerosol perturbations and strong El Niño events: No general correlation. *Geophysical Research Letters*, 24, 1247–1250
144. Self, S., Widdowson, M., Thordarson, T. and Jay, A.E., 2006. Volatile fluxes during flood basalt eruptions and potential effects on the global environment: A Deccan perspective. *Earth and Planetary Science Letters*, 248(1), 518-532.
145. Sigl, M. et al. 2015. Timing and climate forcing of volcanic eruptions for the past 2,500 years. *Nature*, 523(7562), 543-549
146. Sigmundsson, F., 1991. Post-glacial rebound and asthenosphere viscosity in Iceland. *Geophysical Research Letters*, 18(6), 1131-1134.
147. Sigmundsson, F., Pinel, V., Lund, B., Albino, F., Pagli, C., Geirsson, H. and Sturkell, E., 2010. Climate effects on volcanism: influence on magmatic systems of loading and unloading from ice mass variations, with examples from Iceland. *Philosophical Transactions of the Royal Society of London A: Mathematical, Physical and Engineering Sciences*, 368(1919), 2519-2534.
148. Sigvaldason, G.E., Annertz, K. and Nilsson, M., 1992. Effect of glacier loading/deloading on volcanism: postglacial volcanic production rate of the Dyngjufjöll area, central Iceland. *Bulletin of Volcanology*, 54(5), 385-392.
149. Sinton, J., Grönvold, K. and Saemundsson, K., 2005. Postglacial eruptive history of the Western Volcanic Zone, Iceland. *Geochemistry, Geophysics, Geosystems*, 6(12)
150. Slater, L., McKenzie, D.A.N., Grönvold, K. and Shimizu, N., 2001. Melt generation and movement beneath Theistareykir, NE Iceland. *Journal of Petrology*, 42(2), 321-354.
151. Solomon, S., 1999. Stratospheric ozone depletion: A review of concepts and history. *Reviews of Geophysics*, 37(3), 275-316.
152. Stevenson, J., Millington, S., Beckett, F., Thordarson, T. and Swindles, G., 2013, April. Big volcanic ash grains, even from small plumes, travel long distances: implications for satellite remote sensing. In *EGU General Assembly Conference Abstracts*, 15, 9268).
153. Stevenson, J.A., Millington, S.C., Beckett, F.M., Swindles, G.T. and Thordarson, T. 2015. Big Grains Go Far: Reconciling tephrochronology with atmospheric measurements of volcanic ash. *Atmospheric Measurement Techniques* 8, 2069-2091

154. Stothers, R.B., 1984. The great Tambora eruption in 1815 and its aftermath. *Science*, 224(4654), 1191-1198.
155. Stothers, R.B., 1999. Volcanic dry fogs, climate cooling, and plague pandemics in Europe and the Middle East. *Climatic Change*, 42(4), 713-723.
156. Stuiver, M., Grootes, P.M. and Braziunas, T.F. 1995. The GISP $\delta^{18}O$ climate record of the past 16,500 years and the role of the sun, ocean and volcanoes. *Quaternary Research*, 44(3), 341-354
157. Sun, C., Liu, Q., Wu, J., Németh, K., Wang, L., Zhao, Y., Chu, G. and Liu, J., 2016. The first tephra evidence for a Late Glacial explosive volcanic eruption in the Arxan-Chaihe volcanic field (ACVF), northeast China. *Quaternary Geochronology*.
158. Svensen, H., Planke, S., Chevallerier, L., Malthe-Sørenssen, A., Corfu, F. and Jamtveit, B., 2007. Hydrothermal venting of greenhouse gases triggering Early Jurassic global warming. *Earth and Planetary Science Letters*, 256(3), 554-566.
159. Svensson, A., Bigler, M., Blunier, T., Clausen, H.B., Dahl-Jensen, D., Fischer, H., Fujita, S., Goto-Azuma, K., Johnsen, S.J., Kawamura, K. and Kipfstuhl, S., 2013. Direct linking of Greenland and Antarctic ice cores at the Toba eruption (74 ka BP). *Climate of the Past*, 9, 749-766
160. Swindles, G.T. and Roe, H.M., 2006. Reconstruction of Holocene climate change from peatlands in the north of Ireland. In *Geophysical Research Abstracts*, 8, 4778).
161. Swindles, G.T., Lawson, I.T., Matthews, I.P., Blaauw, M., Daley, T.J., Charman, D.J., Roland, T.P., Plunkett, G., Schettler, G., Gearey, B.R. and Turner, T.E., 2013. Centennial-scale climate change in Ireland during the Holocene. *Earth-Science Reviews*, 126, 300-320.
162. Swindles, G.T., De Vleeschouwer, F. and Plunkett, G., 2010. Dating peat profiles using tephra: stratigraphy, geochemistry and chronology. *Mires and Peat*, 7.
163. Swindles, G.T., Lawson, I.T., Savov, I.P., Connor, C.B. and Plunkett, G., 2011. A 7000 yr perspective on volcanic ash clouds affecting northern Europe. *Geology*, 39(9), 887-890.
164. Thordarson, Th., and S. Self, 2003. Atmospheric and environmental effects of the 1783–1784 Laki eruption: A review and reassessment. *Journal of Geophysical Research*, 108(D1), 4011
165. Thouret, J.C. & Lavigne, F., 2000. Lahars: occurrence, deposits and behaviour of volcano-hydrologic flows. *Volcaniclastic rocks from magma to sediments*. Gordon and Breach Science Publishers, 151-174

166. Toohy, M., Krüger, K., Niemeier, U. and Timmreck, C. 2011. The influence of eruption season on the global aerosol evolution and radiative impact of tropical volcanic eruptions. *Atmospheric Chemistry and Physics*, 11, 12351-12367
167. Watson, E.J., Swindles, G.T., Savov, I.P. and Bacon, K.L., 2015. First discovery of Holocene cryptotephra in Amazonia. *Scientific reports*, 5.
168. Watson, E.J., Swindles, G.T., Lawson, I.T. and Savov, I.P., 2016a. Do peatlands or lakes provide the most comprehensive distal tephra records?. *Quaternary Science Reviews*, 139, 110-128.
169. Watson, E.J., Swindles, G.T., Stevenson, J.A., Savov, I. and Lawson, I.T., 2016b. The transport of Icelandic volcanic ash: Insights from northern European cryptotephra records. *Journal of Geophysical Research: Solid Earth*, 121(10), 7177-7192.
170. Watson, E.J., 2016c. Using cryptotephra layers to understand volcanic ash clouds. Doctoral dissertation, University of Leeds.
171. Watson, E.J., Swindles, G.T., Savov, I.P., Lawson, I.T., Connor, C.B. and Wilson, J.A., 2017. Estimating the frequency of volcanic ash clouds over northern Europe. *Earth and Planetary Science Letters*, 460, 41-49.
172. Webster, P.J., 1994. The role of hydrological processes in ocean-atmosphere interactions. *Reviews of Geophysics*, 32(4), 427-476.
173. Wignall, P., 2005. The link between large igneous province eruptions and mass extinctions. *Elements*, 1(5), 293-297.
174. Wilkins, K.L., Watson, I.M., Kristiansen, N.I., Webster, H.N., Thomson, D.J., Dacre, H.F., and Prata, A.J. 2016. Using data insertion with the NAME model to simulate the 8 May 2010 Eyjafjalljökull volcanic ash cloud. *Journal of Geophysical Research: Atmospheres*, 121(1), 306-323
175. Wilson, L. and Huang, T.C., 1979. The influence of shape on the atmospheric settling velocity of volcanic ash particles. *Earth and Planetary Science Letters*, 44(2), 311-324.
176. Zielinski, G.A., Mayewski, P.A., Meeker, L.D., Whitlow, S., Twickler, M.S., Morrison, M., Meese, D.A., Gow, A.J. and Alley, R.B., 2002. Record of volcanism since 7000 BC from the GISP2 Greenland ice core and implications for the volcano-climate system. *Climate Change*, 264, 271.

Chapter 3: Evaluating tephrochronology in permafrost peatlands of Northern Sweden

Claire L. Cooper^{1,2}, Graeme T. Swindles^{1,3}, Elizabeth J. Watson¹, Ivan P. Savov², Mariusz Galka⁴, Angela Gallego-Sala⁵, Werner Borken⁶

¹ School of Geography, University of Leeds, UK, LS2 9JT

² School of Earth and Environment, University of Leeds, UK, LS2 9JT

³ Ottawa-Carleton Geoscience Centre and Department of Earth Sciences, Carleton University, Canada

⁴ Dept. of Biogeography and Palaeoecology, Adam Mickiewicz University, Poland

⁵ School of Geography, University of Exeter, UK, EX4 4RJ

⁶ Dept. of Soil Ecology, University of Bayreuth, Germany

Published in: *Quaternary Geochronology*, 50, 16-28. 2019

Keywords: tephra, peatlands, permafrost, glass preservation, tephrochronology

Highlights

- Six tephra layers are identified in sub-Arctic peatlands at Abisko, Sweden
- Geochemical analyses of glass shards are presented, identifying material belonging to the Hekla 4, Hekla-Selsund, Hekla 1104, and Hekla 1158 eruptions
- Variation in the deposition and preservation of tephra layers across adjacent profiles is identified and discussed

Abstract

Tephrochronology is an increasingly important tool for the dating of sediment and peat profiles for palaeoecological, palaeoclimatic and archaeological research.

However, although much work has been done on tephra in temperate peatlands, there have been very few in-depth investigations of permafrost peatlands. Here we present the analysis of nine peatland cores from Abisko, northern Sweden, and show that the presence of tephra layers may be highly variable even over a scale of < 10 km. Using electron probe microanalysis (EPMA) combined with age-depth profiles compiled from radiocarbon (^{14}C) and ^{210}Pb dating of peat records, we identify the Hekla 1104, Hekla 1158, Hekla-Selsund and the Hekla 4 tephra layers. We also infer the presence of the Askja 1875 tephra, in addition to an unassigned tephra dating from between 1971-1987 AD in two separate cores. Five of the nine analysed cores do not contain distinct tephra layers. Volcanic ash deposits in northern Scandinavia are subject to both regional-scale variations in climate and atmospheric circulation, and local-scale variations on the order of tens of kilometres in topography, vegetation, snow cover, and ground permeability. The extreme inconsistency of tephra preservation within a small study area ($\sim 3000 \text{ km}^2$) brings into question the reliability of tephrochronology within permafrost peatlands, and highlights the necessity of alternative methods for dating peat profiles in this region.

3.1 Introduction

The study of volcanic ash preserved in peatlands and lake sediments is a well-established science, particularly across western Europe and North America (Lowe, 2011; Stivrins et al., 2016; Watson et al., 2016a; Plunkett et al., 2018; Swindles et al., 2018). Light ash particles from volcanic eruptions are carried across continents by atmospheric currents, sometimes being transported thousands of kilometres from their source (Cadle et al., 1976; Palais et al., 1992; Bourne et al., 2016). The fallout from these eruptions may then be preserved in layers in soft sediments such as in peatlands and lakes, providing useful markers and isochrons across multiple sites. Tephra layers linked to particular eruptions allow sediment profiles to be correlated to specific points in time. Assuming that ash deposition occurs approximately simultaneously across multiple sites, applying tephrochronology to a given record allows for precise, high-resolution chronological reconstruction of sediment columns, with a range of environmental and archaeological applications (Lowe et al., 2011; Lane et al., 2014). However, relatively few tephrochronological studies have been performed on permafrost peatlands in Europe compared to temperate peatlands (Watson et al., 2016).

Abisko Scientific Research Station is located in the Scandinavian Arctic, approximately 30 kilometres north of the polar circle at 68°21' N, 18°49'E. The station has a long history of wide-ranging environmental and ecological research, with many recent studies focusing on the observations and effects of climate change in a boreal environment (Alatalo et al., 2016; Lundin et al., 2016; Lett, 2017). Rapid alterations in the local climate over the past 50 years and an increase in the frequency of winter warming events in northern Scandinavia (Vikhamar-Schuler et al., 2016) have caused significant ecological concern. The warmer conditions have been linked to vast reductions in the extent of permafrost in the area (Osterkamp & Romanovsky, 1999; Camill, 2003; Schuur & Abbott, 2011), affecting the surface water pH, water table depth and vegetation in permafrost peatlands (Camill, 1999).

Wetlands have long been acknowledged as playing a significant role in global carbon emissions and sequestration (Lai, 2009). It is therefore increasingly

important for the scientific community to develop an understanding of how permafrost peatlands in this area have changed over time in terms of their ecology, hydrology and carbon accumulation (Swindles et al., 2015b). Accurate and precise chronological control is a crucial component of such investigations into peat archives.

Projections of jet stream currents in the northern hemisphere suggest that, under typical atmospheric circulation conditions, ash particles injected into the stratosphere by Icelandic eruptions should be carried and deposited across much of north-western Europe, including Scandinavia (Woollings et al., 2010; Davies et al., 2010). Past studies have borne this assumption out, and Icelandic tephra has been found across the UK, Ireland, France, Germany, Poland, Belgium, Switzerland, Denmark, Sweden, Norway, and the Faroe Islands (Swindles et al., 2011; Lowe et al., 2011; Watson et al., 2017). However, some disparity between the sediment records of adjacent sites has been noted at several locations (Watson et al., 2016b). Vegetation, local weather at the time of deposition, pH conditions in the sediment, and storm events can all affect the capture and preservation of glass shards (Watson et al., 2016a), resulting in variation across cores, even over distances of a few kilometres. Northern Scandinavia is on the extreme distal edge of most numerical simulations reconstructing Icelandic ash clouds (Davies et al., 2010), making consistent ash fall across wide areas possible, but unlikely. In this paper, we investigate the cryptotephra content (distal tephra < 150µm along the longest axis) of nine cores collected in the vicinity of the Abisko field station. We also discuss the factors affecting shard preservation variability in the area, and consider the implications for future tephrochronological research in this region.

3.2 *Materials and Methods*

3.2.1 *Study Area*

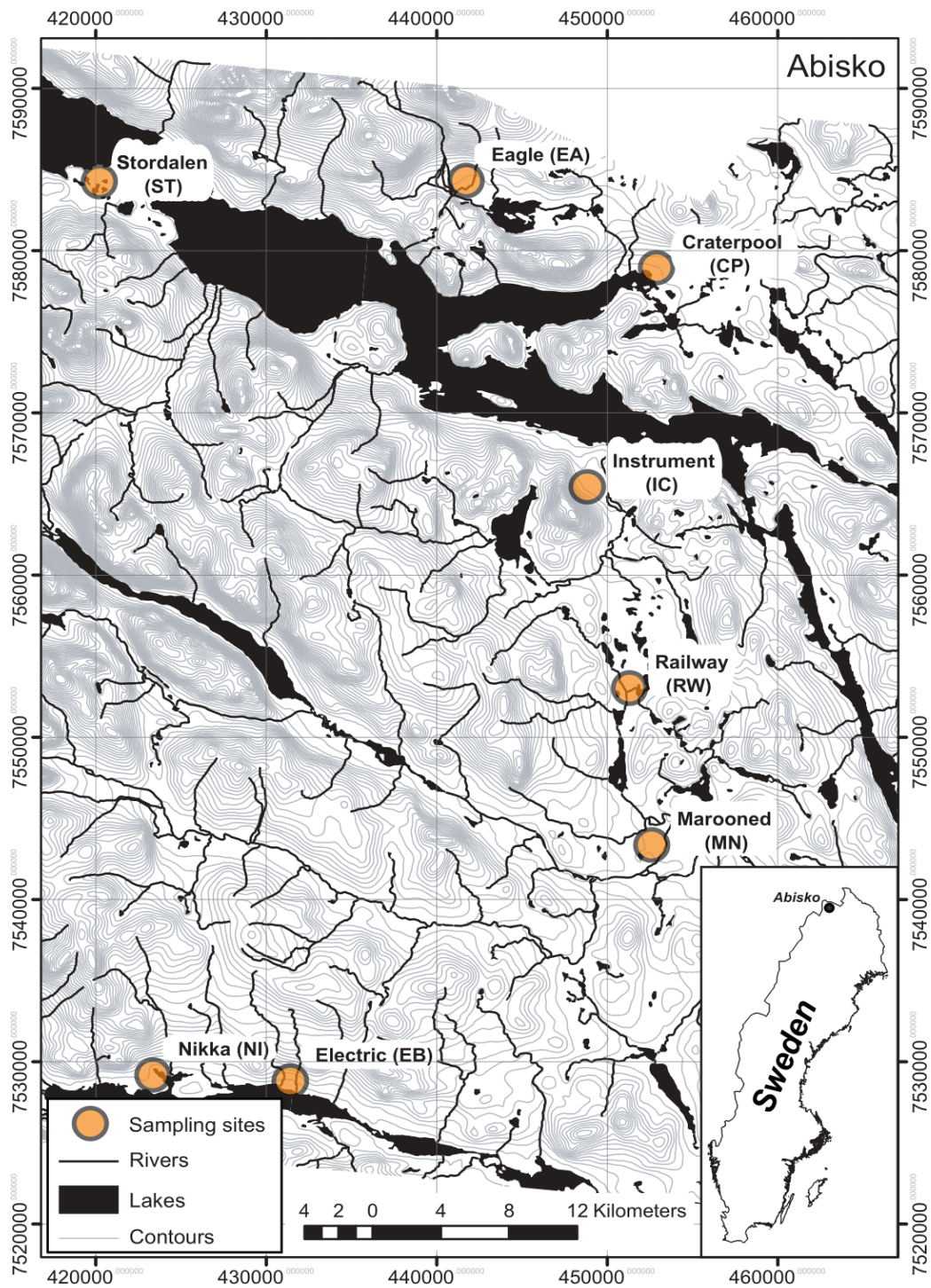


Figure 1: Map of study area, showing local topography and the location of coring sites

Nine samples were collected from peatland sites near Abisko, northern Sweden, seen in Figure 1, using a Russian peat corer. Each sample is between 20-45cm in depth, and is comprised largely of peat, in addition to occasional lenses of organic mud.

Abisko is located within the rain shadow of the Norwegian mountains, and as such receives a relatively small amount of precipitation (332 mm per year; Callaghan et al., 2010), with the highest rainfall occurring during the summer months. Each of the peatlands sampled were part of peat complexes in various stages of permafrost decomposition, from early dome collapse to full inundation after permafrost thaw. The peatlands of the region are primarily composed of ombotrophic bogs, peat plateaus, arctic fens, and palsa mires, many of which are in states of permafrost collapse as a result of rapid warming. Recent studies have shown an increased rate of permafrost decay in some of the Abisko sites, such as Stordalen (Swindles et al., 2015b)

3.2.2 Methods

Coring locations were selected on the basis of physical features, hydrology, and vegetation composition (Swindles et al., 2015a). Sites were deemed suitable if they were situated on relatively flat ground, and could be characterised as fen, bog, or palsa mire landscapes. Full site details may be found in appendix A. The cores were stored in plastic wrap and aluminium foil, and kept at a temperature of 4°C prior to analysis. Extraction of the tephra in these sediment samples was performed following the method detailed by De Vleeschouwer et al., 2010. Each peat core was divided into continuous sections of 1 cm depth, and a sample of 4 cm³ was removed from each. These samples were weighed and dried in ceramic crucibles at 105°C for a minimum of 12 hours. The dry samples were then reduced to ashes in a muffle furnace at 600°C for six hours. After each stage of burning and drying, the samples were weighed to estimate gravimetric water content and mass loss on ignition. These ashes were suspended in 10% hydrochloric acid for 24 hours to remove carbonate material, and then washed with deionised water. The tephra was concentrated at the bottom of the test tubes by placing the aqueous samples in a centrifuge at 3000 r.p.m. for approximately five minutes. This

aqueous material was then sieved through a 10 µm mesh. Petrographic slides were prepared by adding the aqueous solution to a glass slide on a hotplate until the liquid component evaporated. The slides were mounted using Histomount and a glass coverslip, and examined through optical microscopy using 200-400x magnification to assess tephra content. References to several visual and descriptive sources were used to ensure positive tephra identification (Lowe, 2011; Watson et al., 2016a).

Sub-samples which were found to contain more than 10 shards per cm³ were re-sampled and processed using the acid digestion method outlined in Dugmore & Newton (1992), and, later, to density separation, to fully remove problematic organic material and biogenic silica (Blockley et al., 2005). In some cases, tephra was found to exist in irregular, non-continuous, discrete clumps of material rather than in well-defined layers, making repeated extractions from a particular depth within the peat profile problematic. In these instances, optical slides containing tephra were submerged in a xylene solution for 48 hours to dissolve the mounting agent (Ravikumar et al., 2014). This method was found to be highly effective in retaining the tephra and organic material while completely removing the Histomount. Samples for geochemical analysis were then dried, remounted in blocks of resin and subjected to electron probe microanalysis EPMA at the Tephra Analytical Unit, University of Edinburgh. All analysis was performed using a 5µm diameter beam of 15kV with a current of either 2nA (Na, Mg, Al, Si, K, Ca, and Fe) or 80nA (P, Ti, Mn), following the method of Hayward (2012). Lipari and BCR-2G basalt glass standards were used for external calibration (Watson et al., 2015). The standard data generated during geochemical analysis may be found in table B.2 in the appendices. The overall data for the standards returns <1% variability for most major elements.

Radiocarbon signatures of organic material were determined by accelerator mass spectrometry (AMS). Subsamples of 0.8 mg C were combusted in 6 mm sealed quartz tubes with 60 mg CuO oxidizer and 1 cm silver wire for 2 hours at 900°C. The resulting CO₂ was purified from water and non-condensable compounds. Afterwards, CO₂ was reduced to graphite using the zinc reduction method where

TiH₂ and Zn with Fe act as catalysts at 550°C for 7.5 hours (Xu et al., 2007). All preparations took place at the Department of Soil Ecology at the University of Bayreuth. The graphite targets were analysed by the Keck-CCAMS facility of the University of California, Irvine, with a precision of 2–3‰ (‰ deviation is from the ¹⁴C/¹²C ratio of oxalic acid standard in 1950). The samples were corrected to a δ¹³C value of -25‰ to account for any mass dependent fractionation effects (Stuiver & Polach, 1977). Radiocarbon signatures were converted to ¹⁴C age before present (BP) using the IntCal13 calibration curve (Reimer et al., 2013). Full radiocarbon dating results may be found in the appendices.

Further chronological data for the Marooned and Stordalen cores was established through ²¹⁰Pb dating. Peat samples were digested using a combination of concentrated HCl, HNO₃, and H₂O₂. A small amount of ²⁰⁹Po was then added as a tracer. Following the method detailed in Whittle & Gallego-Sala (2016), the material was plated onto silver disks, and alpha spectrometry was performed using an Ortec Octète Plus Integrated Alpha-Spectrometry System at the University of Exeter (UK) Radiometry Lab. ²¹⁰Pb values were derived from the ²¹⁰Po/²⁰⁹Po ratios, and dates were then extrapolated from the ²¹⁰Pb inventory using the constant rate of supply model (Appleby, 2001).

3.3 Results

3.3.1 Tephrostratigraphies

Figure 2 shows the tephra counts per 4 cm³ of the eight peat profiles collected in Abisko, along with the percentage loss on ignition, and age-depth models based on radiocarbon dating of organic material. While four profiles – Stordalen (ST), Marooned (MN), Eagle (EA), and Nikka (NI) – have clear tephra peaks at varying depths, the other profiles have only minimal volcanic ash content, averaging only 1-3 glass shards per section. There is little to no consistency in the presence of tephra with depth across the profiles. The loss-on-ignition for each profile is high, typically between 80 – 90 %, but there is no apparent correlation with the presence of glass. The glass shards themselves were typically between 10-150 µm, though a wide range of morphologies were present, from thin, concave, wisp-like

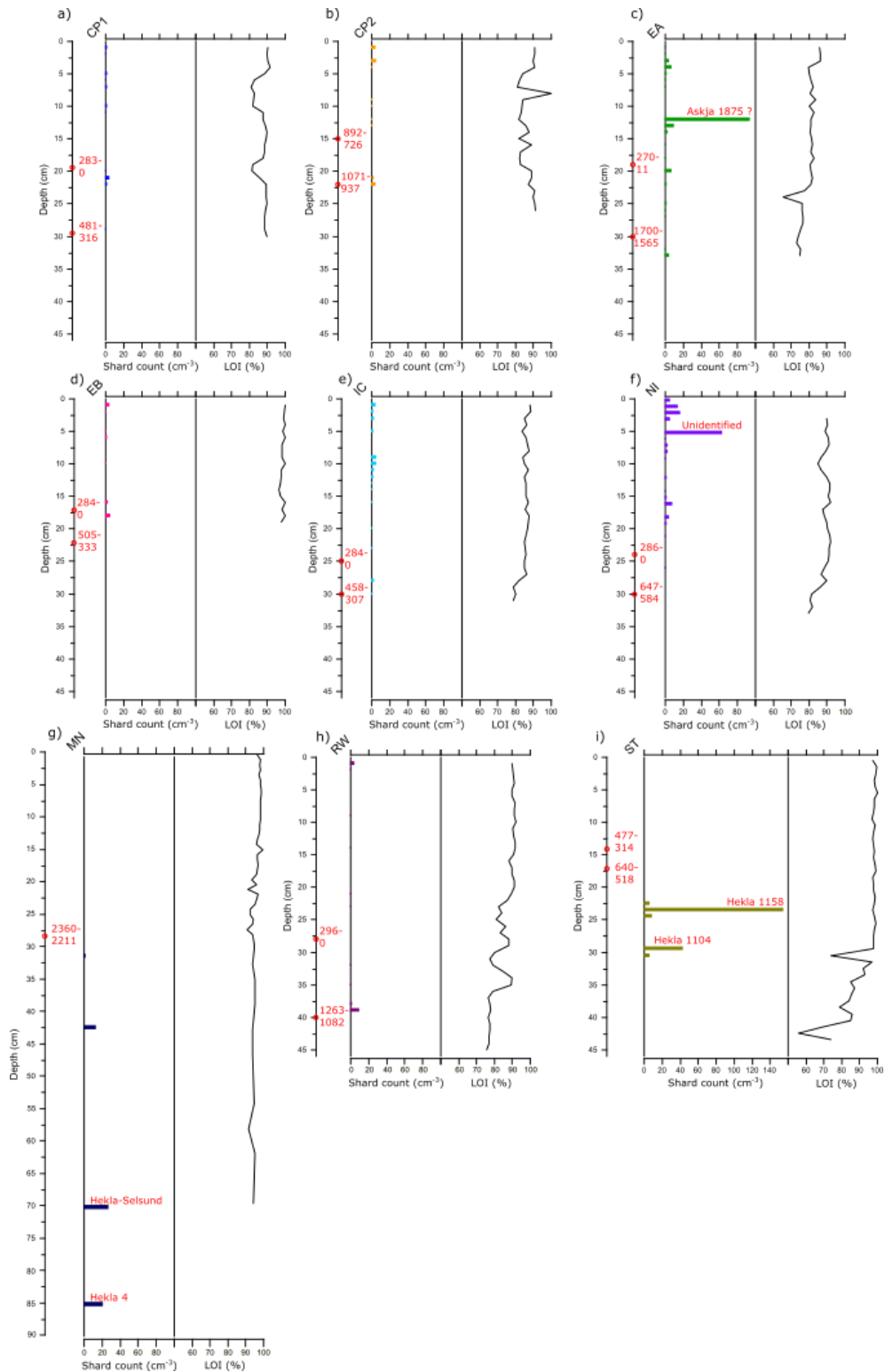


Figure 2: Tephrostratigraphic profiles of Abisko peat cores. Radiocarbon dates (cal BP) are shown in red along the vertical axes. a) Crater Pool 1; b) Crater Pool 2; c) Eagle Bog; d) Electric Bog; e) Instrument Core; f) Nikka Bog; g) Marooned Bog; h) Railway Bog; i) Stordalen Core

structures to larger aggregate shards. As the shards in EA12 and NI8 were found to be too small and sparse to perform EPMA, ^{210}Pb dating of the profiles containing these layers was used to determine their ages. The major element geochemistry of the glass found in the Marooned and Stordalen cores can be found in figure 4. Full geochemistries and profile dates may be found in the appendices.

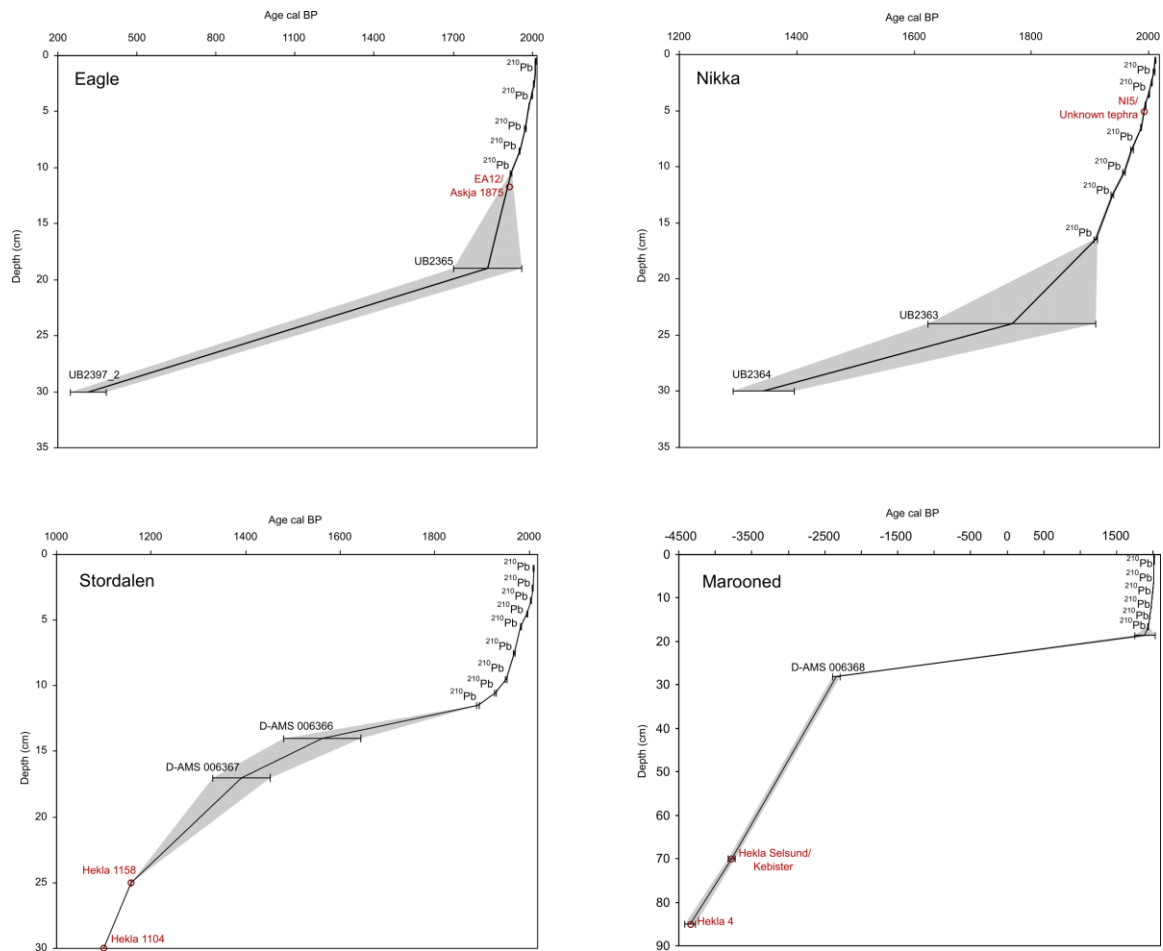


Figure 3: Age-depth models of Eagle, Nikka, and Stordalen peatland profiles. Tephra profiles identified in this paper are marked in red.

3.3.1.1 MN85/Hekla 4

Figure 4 shows the geochemistry of tephra shards found at in the Marooned and Stordalen cores. Shards matching the geochemistry of the Hekla 4 eruption were found at a depth of 85cm in the Marooned bog core. The Hekla 4 eruption represents the most widespread tephra deposit in northern Europe, and relates to a plinian eruption of Hekla occurring between 2395-2297 BC (Pilcher & Hall, 1996;

Watson et al., 2017). Tephra attributed to this deposit occurs across a range of compositions from dacitic to rhyolitic; in the case of the tephra found in Marooned bog, the silica content ranges between 63 – 77 %.

3.3.1.2 MN70/Hekla-Selsund

The Hekla-Selsund tephra, also known as the Kebister tephra, is dated as occurring between 1800-1750BC, and can be found in multiple sites across north-western Europe, including Germany, Great Britain, the Faroe Islands and Scandinavia (Watson et al., 2017). In Abisko, it occurs in the Marooned bog core at a depth of 70cm. This tephra is rhyolitic to dacitic in composition.

3.3.1.3 ST30/Hekla 1104 (Hekla 1)

These glass shards closely match the geochemistry of the Hekla 1104 eruption (also known as the Hekla 1 eruption), with an average SiO₂ content of 63-67%. This tephra has previously been found in multiple sites in northern Scandinavia, including the Sammakovuoma peatland in northern Sweden (Watson et al., 2016a) and the Lofoten Islands in arctic Norway (Pilcher et al., 2005); see figure 5.

3.3.1.4 ST25/Hekla 1158

Several shards with geochemistries similar to Hekla 1158 were found in the Stordalen core at a depth of 23 cm. Tephra from the Hekla 1158 eruption is dacitic in composition, with a silica content of 67-68%. Evidence of this eruption has only recently been found in Europe, in Scandinavian sites in almost all instances (Pilcher et al., 2005; Swindles et al., 2015a).

3.3.1.5 EA12/Askja 1875

Using the combined age-depth profile (figure 3), it can be seen that the layer in EA falls approximately between 1831 and 1920. A likely candidate for this tephra is therefore the Askja 1875 eruption. Ash from this eruption has previously been found in several sites in Scandinavia (Pilcher et al., 2005; Wastegård, 2008; Watson et al., 2016b), suggesting that the tephra cloud was at least partially

carried in a north-easterly heading from the source (the Dyngjufjöll volcanic system). Approximately 0.5km³ of rhyolitic tephra was produced during this eruption (Sigurdsson & Sparks, 1981).

3.3.1.6 NI5 (Unknown tephra)

Using our precise ²¹⁰Pb chronology, the layer in NI appears to fall between 1971 and 1987, and is therefore of a more uncertain origin as no tephra layers from this period have yet been defined in Scandinavia at the time of writing. As stated above, it was not possible to perform geochemical analysis on these shards; however, several potential source eruptions occurred in Iceland during this period. The Hekla and Krafla volcanic systems both exhibited significant activity, although no tephra from the eruptions occurring at Hekla in 1980 and 1981 has yet been reported outside Iceland. The activity from Krafla was almost exclusively effusive with intermittent phreatic explosions (Global Volcanism Program, 2013), making this an unlikely candidate for distal tephra deposition. A minor subglacial eruption of Grímsvötn occurred in 1983, though again this is unlikely to have produced a sufficient tephra cloud to account for the reported layer (Gronvold & Johannesson, 1984). It is therefore possible that this tephra originated from a non-Icelandic source. Tephra attributed to Alaskan volcanoes has previously been found in northern Scandinavia (Watson et al., 2017), and it has recently been suggested that a previously unidentified tephra found in Svartkälsjärn, Sweden (Watson et al., 2016a) may have originated from the Cascades arc in North America (Plunkett & Pilcher, 2018). These findings indicate that, while Iceland is statistically the most likely source of volcanic ash in Scandinavian peatlands, it may be necessary to look further afield to identify more obscure deposits.

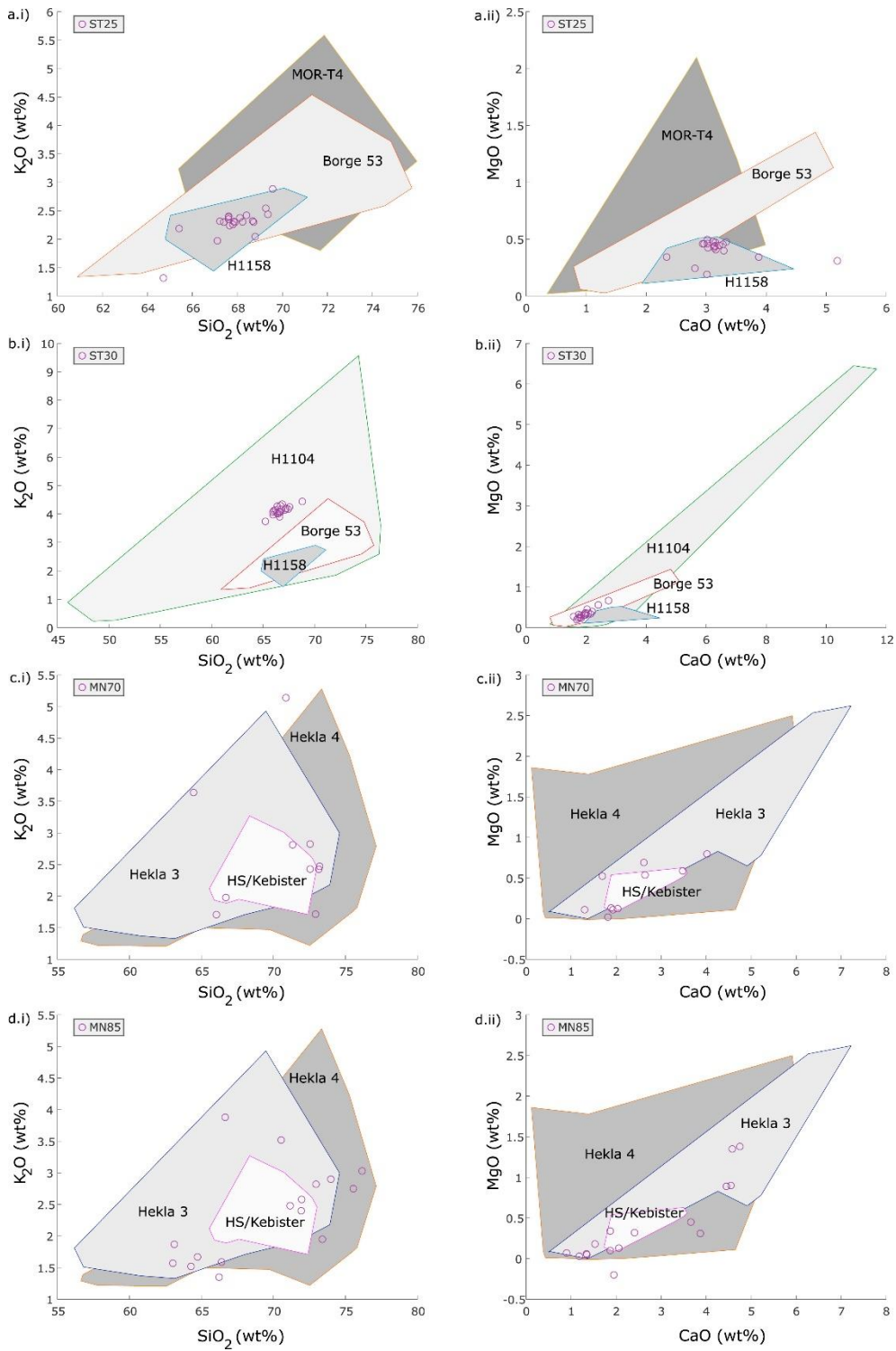


Figure 4: Geochemical bi-plots of glass shards found in the Marooned and Stordalen cores, showing the geochemical type-data envelopes of the eruptions to which they correlate. Also shown are geochemical envelopes for alternative eruptions occurring within a similar timeframe for comparison. a) ST25, b) ST30, c) MN70, d) MN85. EPMA was performed at the Tephra Analysis Unit, University of Edinburgh.

3.4 Discussion

3.4.1 Tephra transport and preservation

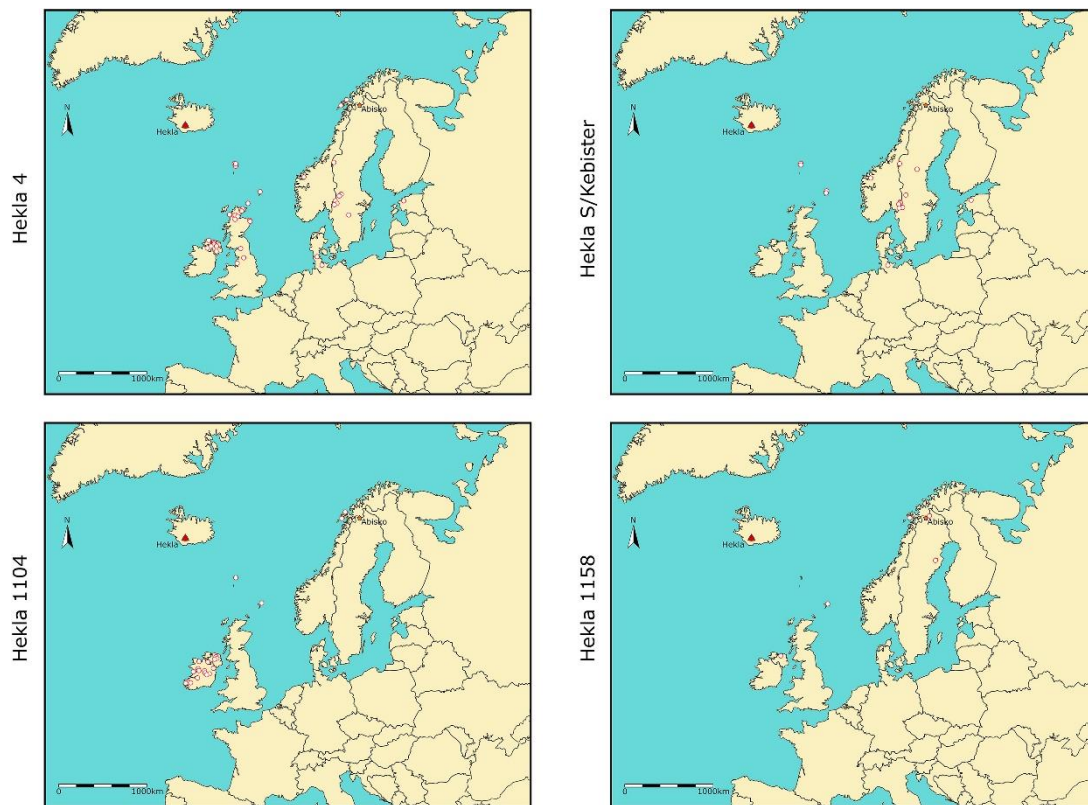


Figure 5: Spatial distributions within Europe of four tephra layers found in the Abisko peatlands. All four originated at Hekla in southern Iceland, and each has previously been found within Scandinavia. (Swindles et al., 2017)

While several distinct deposits of tephra were found within the Abisko region, there is poor correlation of tephra preservation across sites, even between cores separated by < 10 km. A distinct tephra layer can clearly be found in the Eagle bog site, but is not present at the Craterpool bog, despite the two locations being within 12 km of each other. The same is true of the Marooned and Railway bog sites, which are 9 km apart.

There are a number of components influencing the spatial distribution of tephra over a given deposition area. ‘Ash winnowing’, referring to the resorting and redeposition of ash sediments, is a phenomenon which has been previously noted in many volcanological studies, and is typically attributed to erosion by wind- or water-based processes. Analysis of distal ash deposits from the 2008 eruption of

Chaitén, Chile, for example, showed that unsheltered locations occasionally displayed greater degrees of reworking and variability in deposit thickness, and that these anomalies became more frequent with distance from the eruption source (Watt et al., 2009).

The disparities across the stratigraphic columns shown in our results emphasise how a combination of components can cause extreme variability in glass preservation, even over a relatively small area. Many factors are related to local conditions at the time of deposition, while others relate to broader factors such as regional topography and basin drainage systems. Additionally, eruption conditions at the origin volcano can affect glass composition and ash shard morphology, with implications for tephra preservation and transport respectively (Lowe, 2011).

Figure 6 provides a summary of the dominant factors, some of which are explained in greater detail below.

3.4.2 Site analysis

3.4.2.1 Local climate and wind currents

The location of Abisko on the leeward side of the Norwegian mountains results in a significant decline in annual rainfall relative to nearby locations on the windward side (Swindles et al., 2015b). While this may decrease the surface runoff in the region, thus decreasing the likelihood of surface redistribution of fallen tephra, it is also thought that precipitation itself may play a crucial role in the deposition of tephra (Davies et al., 2010). Some studies attribute the patchiness of the Hekla 1947 tephra in many areas of Europe to irregular rain- or snowfall (Salmi, 1948; Thorarinsson, 1967).

Another factor to consider when assessing the impact of precipitation on ash preservation is snow cover. Snow provides a 'shielding' layer above the underlying peatland, enabling redistribution of deposited tephra through surface wind currents (Bergman et al., 2004). Tephra preserved within snow is also subject to transportation should that snow cover melt during seasonal temperature changes.

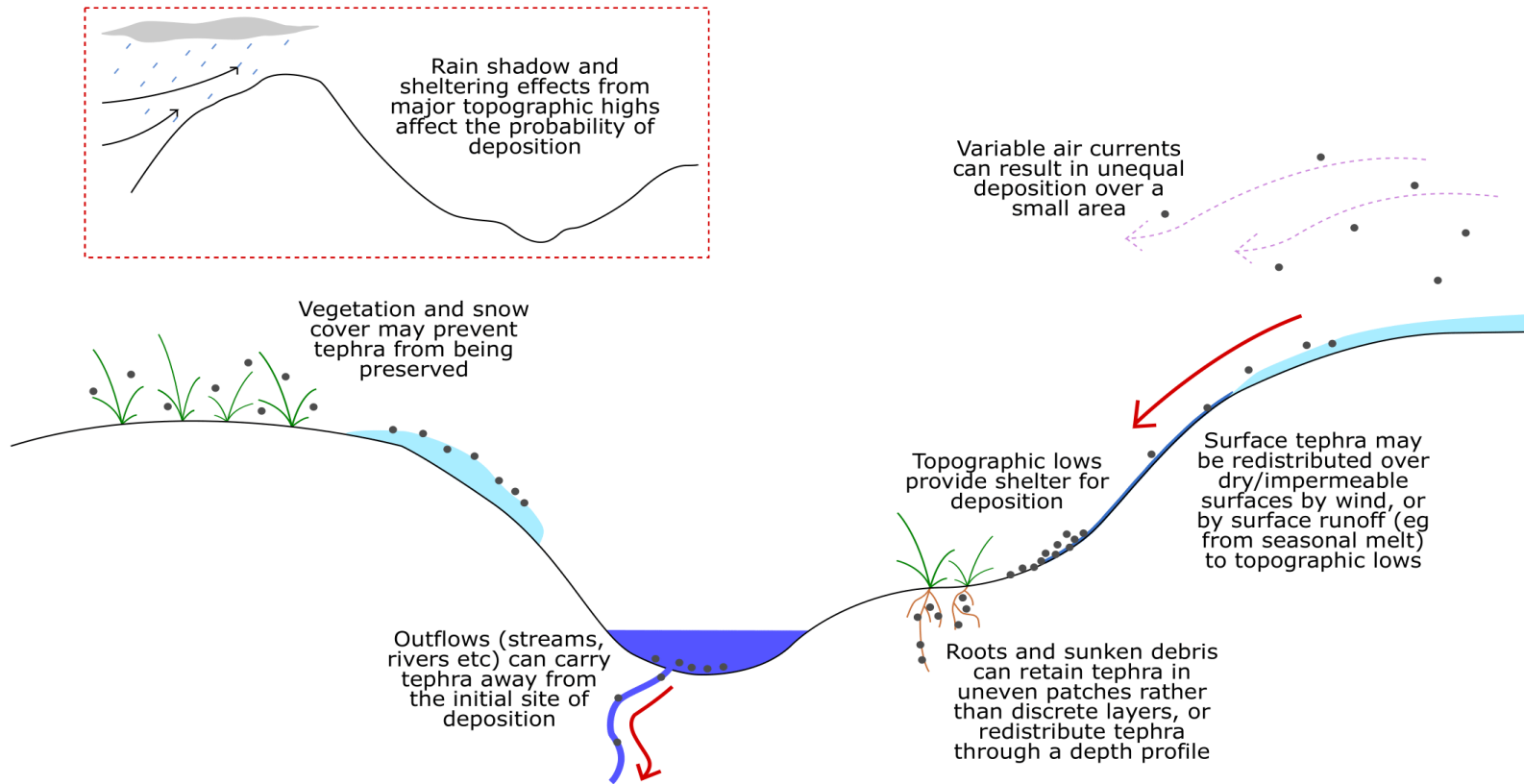


Figure 6: Conceptual diagram of factors influencing tephra preservation in Abisko peatlands.

The variability of air currents over northern Scandinavia is also likely to be a major controlling factor on tephra deposition in the region. Models suggest that seasonal variability in the dominant air currents has a strong influence on tephra transportation, with strong westerlies at high elevations (> 15 km) during autumn and winter, and weak easterlies becoming dominant during spring and summer (Lacasse, 2001). Icelandic eruptions occurring during the latter half of a given year (September-February) are therefore more likely to deposit tephra across Scandinavia. In recent years, however, evidence has emerged that the Earth's warming climate may have a weakening effect on the polar vortex (Kim et al., 2014). If this is proved to be the case, future patterns of tephra distribution in the northern hemisphere may be altered by continuing climate change.

Additionally, it has been suggested that, under the correct conditions, the combination of a variable wind field and changes to the eruption parameters due to fluctuations in the volcanic system may allow for the creation of discrete deposition patterns for different phases of an eruption (Watt et al., 2009; Stevenson et al., 2012). This may provide an explanation for the unusually uniform major element geochemistries seen in some of the deposits found in Abisko, most notably the ST25 and ST30 deposits, attributed to Hekla 1158 and Hekla 1104 respectively. These shard clusters may represent ashfall from a particular phase of those eruptions, though whether the compositional bias in these deposits occurred during transport or through winnowing and preservation processes is unclear.

Studies of ashfall conducted following the 2008 eruption of Chaitén, Chile indicate a complex pattern of ash deposition which was largely attributed to variable wind fields during the course of the week-long eruption, at least on a proximal scale (Watt et al., 2009; Alfano et al., 2010; Durant et al., 2012). However, variations in wind patterns are typically referenced as a cause of regional-scale depositional variations on the order of hundreds of kilometres, as opposed to the local-scale variations observed in Abisko, which occur across areas of < 20 km. While a variable wind field therefore offers a potential explanation for the apparent underrepresentation of many historical Icelandic tephra deposits in Scandinavia

relative to the rest of western mainland Europe, shifting regional air currents are unlikely to have caused the erratic preservation pattern observed at Abisko.

3.4.2.2 Vegetation

Similarly to snow cover, vegetation can provide a shielding effect to underlying sediment. However, a more significant implication for tephra preservation is the effect of root trapping, wherein plant roots capture small packets of sediment, preserving them at a given depth. This has multiple negative consequences for the field of tephrochronology; firstly, the unequal distribution of ash within a given horizon complicates the process of tephra extraction, as it makes the presence of a particular layer at a given depth more uncertain. Additionally, the vertical redistribution of tephra can negatively impact the creation of age-depth profiles for peatlands and lake sediment, as the correlation between tephra layers and dated organic material from the same layer becomes less reliable (Cutler et al., 2016). Dugmore et al., 2018, suggest that uniformly vegetated slopes can produce consistent tephra layers in the stratigraphic record, but areas of sparse or patchy vegetation will result in variability. Many of the Abisko sites were characterised by a uniform top layer of sphagnum moss of between 1-4 cm thickness, with intermittent tussocks of thicker vegetation and herbaceous plants such as cotton sedge (*Eriophorum angustifolium*). Studies of vegetation succession in the Marooned and Stordalen sites also indicate the variable presence of shrub communities over the past millennium (Gałka et al., 2017), making it likely that root trapping could have interfered with tephra preservation in this region.

Ashfall may also be intercepted by vegetation at a sub-aerial level, such as on leaves and branches. However, the sparseness of larger forms of plant life in most sub-Arctic peatland reduces the influence of this factor in this region.

3.4.2.3 Topography

A recent study (Dugmore et al., 2018) based on data from Iceland and Washington State, USA, has shown that tephra layers of 1-10 cm thickness can remain stable on slopes $<35^\circ$, given sufficiently uniform vegetation cover. Slopes of a greater angle are unlikely to produce consistent stratigraphic records, as tephra particles

become concentrated in topographic hollows, resulting in down-slope thickening which can cause differences in thickness as great as an order of magnitude between the peak and the base of a slope (Mairs et al., 2006). Down-slope runoff processes can be mitigated by vegetation and ground cover, resulting in small-scale variation within a given layer.

3.4.2.4 Eruption conditions

Eruption conditions represent a strong control on cryptotephra layers. Very fine ash of the size and density suitable for airborne transport over several thousand kilometres is generated in far greater quantities during explosive silicic eruptions than effusive basaltic eruptions (Rose & Durant, 2009). The effects of ash morphology on airborne tephra transport have been the subject of a great deal of study, as the topic has significant implications for ash cloud modelling techniques. The surface roughness, sphericity and convexity of ash particles all affect the aerodynamic properties of those particles (Riley et al., 2003), which in turn affect the settling velocity, atmospheric residence time, and transport distance. For example, irregular particles with low vesicularity and high surface-to-volume ratios are likely to aggregate due to the high wettability and surface roughness, while flat particles with high long axis to short axis ratios are likely to be transported further from their source (Riley et al., 2003; Cioni et al., 2014). The primary determining factors in ash morphology are magma fragmentation – itself a product of gas content, pressurisation and conduit width, among others – and interaction of the magma and subsequent volcanic plume with water. A greater degree of interaction results in greater fragmentation, giving the tephra a thinner, more concave morphology, with complex implications for transport distance (Freundt & Rosi, 1998).

While a small number of larger (> 150 µm) shards were found some samples in the Stordalen and Marooned cores, the vast majority of tephra found in the Abisko region has a thin, wispy morphology and pale colouration, corresponding with the explosive eruptions to which all of the identified ash layers have been assigned.

3.4.2.5 Other factors

An absence of water outflow is crucial to the successful preservation of a tephra layer. Lakes or fens which have substantial throughflow are typically not suitable for tephrochronological study, as hydrological redistribution of lighter particles is substantially more likely. Dry or impermeable surfaces may also facilitate windblown redistribution of tephra to topographic lows. Particles are therefore preferentially preserved in low areas of damp, permeable terrain. A recent study conducted on thin tephra layers in temperate regions (Blong et al., 2017) suggested that the erosional reworking of tephra layers < 300 mm in thickness, as is the case for many European cryptotephra layers, is highly variable even across relatively homogenous sites. These results may indicate the necessity of large sample sizes and the collection of multiple cores within small areas, although in practice this method is likely to become impractical.

3.5 Conclusions

1. Six distinct tephra layers, the majority of which are likely to be of Icelandic origin, were recorded in the surveyed Abisko peatland cores.
2. Using geochemical analysis, we identify shards belonging to the Hekla 4, Hekla 1104, Hekla 1158 and Hekla-Selsund eruptions in Abisko.
3. From age-depth profiles of two cores, we suggest that the Askja 1875 tephra, and an unidentified, possibly non-Icelandic tephra are present in the Abisko region.
4. We find very little correlation between tephrostratigraphies of adjacent peat cores, suggesting that local-scale variations in topography, vegetation, snow cover, ground permeability, and other factors significantly influence the preservation of windblown tephra in sub Arctic Sweden.
5. The variability of tephra preservation across multiple sites within the study area suggests that northern Scandinavian peatlands may be an unreliable source of volcanic ash deposits due to the increased risks of redeposition and secondary transport, further complicating studies into the tephrochronology of the region.

3.6 Acknowledgements

Claire Cooper acknowledges a Leeds Anniversary Research Scholarship at the University of Leeds, in addition to support from the Climate Research Bursary Fund awarded by the Priestley International Centre for Climate. Elizabeth Watson was funded by NERC funded Doctoral Training Grant NE/K500847/1. We acknowledge the Worldwide University Network (WUN) for funding this project (Project: Arctic Environments, Vulnerabilities and Opportunities). We acknowledge the Abisko Scientific Research Station for assistance with field logistics and Kallax Flyg AB for helicopter support.

References

1. Alatalo, J.M., Jägerbrand, A.K. and Molau, U. 2016. Impacts of different climate change regimes and extreme climatic events on an alpine meadow community. *Scientific Reports*, 6 (21720)
2. Alfano, F., Bonadonna, C., Volentik, A.C., Connor, C.B., Watt, S.F., Pyle, D.M. and Connor, L.J., 2011. Tephra stratigraphy and eruptive volume of the May, 2008, Chaitén eruption, Chile. *Bulletin of Volcanology*, 73(5), pp.613-630.
3. Bergman, J., Wastegård, S., Hammarlund, D., Wohlfarth, B. and Roberts, S. J. 2004. Holocene tephra horizons at Klocka Bog, west-central Sweden: aspects of reproducibility in subarctic peat deposits. *J. Quaternary Sci.*, 19: 241–249. doi:10.1002/jqs.833
4. Blockley, S.P.E. et al. 2005. A new and less destructive laboratory procedure for the physical separation of distal glass tephra shards from sediments. *Quat. Sci. Rev.*, 24, pp. 1952-1960
5. Bourne, A.J., Abbott, P.M., Albert, P.G., Cook, E., Pearce, N.J., Ponomareva, V., Svensson, A. and Davies, S.M., 2016. Underestimated risks of recurrent long-range ash dispersal from northern Pacific Arc volcanoes. *Scientific Reports*, 629837.
6. Cadle, R.D., Kiang, C.S. and Louis, J.-F. 1976. The global scale dispersion of the eruption clouds from major volcanic eruptions. *Journal of Geophysical Research*, 81, 3125-3132
7. Callaghan, T.V., Bergholm, F., Christensen, T.R., Jonasson, C., Kokfelt, U., Johansson, M., 2010. A new climate era in the sub-Arctic: Accelerating climate changes and multiple impacts. *Geophys Res Lett* 37, 14705.
8. Camill, P. 1999. Patterns of boreal permafrost peatland vegetation across environmental gradients sensitive to climate warming. *Canadian Journal of Botany*, 77 (5), 721-733
9. Camill, P. 2004. Permafrost thaw accelerates in boreal peatlands during late-20th century climate warming. *Climatic Change*, 68 (1-2), 135-152
10. Cioni, R. et al. 2014. Insights into the dynamics and evolution of the 2010 Eyjafjallajökull summit eruption (Iceland) provided by volcanic ash textures. *Earth and Planetary Science Letters*, 394, 111-123
11. Davies, S.M. et al. 2010. Widespread dispersal of Icelandic tephra: how does the Eyjafjöll eruption of 2010 compare to past Icelandic events? *Journal of Quaternary Science: Rapid Communication*, 25 (5), 605-611

12. Dugmore, A. J., and Newton, A. J. 1992. Thin tephra layers in peat revealed by X-radiography. *J. Archaeol. Sci.*, 19, 163–170, doi:10.1016/0305-4403(92)90047-7.
13. Dugmore, A., Streeter, R. and Cutler, N. 2018. The role of vegetation cover and slope angle in tephra layer preservation and implications for Quaternary tephrostratigraphy. *Palaeogeography, Palaeoclimatology, Palaeoecology*, 489, 105-116
14. Durant, A.J., Villarosa, G., Rose, W.I., Delmelle, P., Prata, A.J. and Viramonte, J.G., 2012. Long-range volcanic ash transport and fallout during the 2008 eruption of Chaitén volcano, Chile. *Physics and Chemistry of the Earth, Parts A/B/C*, 45, 50-64.
15. Freundt, A. and Rosi, M. 1998. *From magma to tephra : modelling physical processes of explosive volcanic eruptions*. 1st ed. Elsevier, Published Amsterdam ; New York. ISBN: 0444829598
16. Gałka, M. et al. 2017. Vegetation Succession, Carbon Accumulation and Hydrological Change in Subarctic Peatlands, Abisko, Northern Sweden. *Permafrost and Periglac. Process.*, 28, 589–604. doi: 10.1002/ppp.1945.
17. Global Volcanism Program, 1998. Report on Grimsvotn (Iceland). In Wunderman, R (ed.), *Bulletin of the Global Volcanism Network*, 23:11. Smithsonian Institution. <https://dx.doi.org/10.5479/si.GVP.BGVN199811-373010>.
18. Global Volcanism Program, 2000. Report on Hekla (Iceland). In Wunderman, R (ed.), *Bulletin of the Global Volcanism Network*, 25:2. Smithsonian Institution. <https://dx.doi.org/10.5479/si.GVP.BGVN200002-372070>.
19. Global Volcanism Program, 2013. Krafla (373080) In *Volcanoes of the World*, v. 4.6.6. Venzke, E (ed.). Smithsonian Institution. Downloaded 16 Feb 2018 (<http://volcano.si.edu/volcano.cfm?vn=373080>). <https://dx.doi.org/10.5479/si.GVP.VOTW4-2013>
20. Gronvold, K. and Jóhannesson, H., 1984. Eruption in Grímsvötn 1983; course of events and chemical studies of the tephra. *Jökull*, (34), pp.1-8..
21. Kim, B.-M. et al. 2014. Weakening of the stratospheric polar vortex by Arctic sea-ice loss. *Nature Communications*, 5 (4646) doi:10.1038/ncomms5646
22. Lacasse, C. 2001. Influence of climate variability on the atmospheric transport of Icelandic tephra in the subpolar North Atlantic. *Global and Planetary Change*, 29 (1-2), 31-55
23. Lai, D.Y.F., 2009. Methane dynamics in northern peatlands: a review. *Pedosphere*, 19(4), 409-421.

24. Lane, C.S., Cullen, V.L., White, D., Bramham-Law, C.W.F. and Smith, V.C. 2014. Cryptotephra as a dating and correlation tool in archaeology. *Journal of Archaeological Science*, 42, 42-50
25. Lane, C.S., Lowe, D.J., Blockley, S.P.E., Suzuki, T. and Smith, V.C. 2017. Advancing tephrochronology as a global dating tool: Applications in volcanology, archaeology and palaeoclimatic research. *Quaternary Geochronology*, 40, 1-7
26. Larsen, G . 1993 . Nokkur orð um Kötlugjósku. In Larsen, G., ed. *Kötlustefna*, March 27-29, ágrip erinda (abstracts). Reykjavík , Raunvisindastofnun, 6- 7. (Háskólans Fjölrit RH-3-93.)
27. Lett, S. 2017. Mosses as mediators of climate change: implications for tree seedling establishment in the tundra. Doctoral thesis, Umeå University
28. Lowe, D.J. 2011. Tephrochronology and its application: A review. *Quaternary Geochronology*, 6(2), 107-153
29. Lundin, E.J. et al. 2016. Is the subarctic landscape still a carbon sink? Evidence from a detailed catchment balance. *Geophysical Research Letters*, 43 (5), 1988-1995
30. Mairs, K.A., Church, M.J., Dugmore, A.J., Sveinbjarnardóttir, G., Arneborg, J., and Grønnow, B. 2006. Degrees of success: evaluating the environmental impacts of successful long term settlement in south Iceland. In *The Dynamics of Northern Societies*. PNM, Publications from the National Museum, Studies in Archaeology and History, 10, 363-372. ISBN: 87-7602-052-5
31. Osterkamp, T.E. and Romanovsky, V.E. 1999. Evidence for warming and thawing of discontinuous permafrost in Alaska. *Permafrost and Periglacial Processes*, 10 (1), 17-37
32. Palais, J.M., Germani, M.S. and Zielinski, G.A. 1992. Inter-hemispheric transport of volcanic ash from a 1259 A.D. volcanic eruption to the Greenland and Antarctic ice sheets. *Geophysical Research Letters*, 19 (8), 801-804
33. Pilcher, J.R. and Hall, V.A. 1996. Tephrochronological studies in northern England. *The Holocene*, 6 (1), 100-105.
34. Pilcher, J., Bradley, R.S., Francus, P. and Anderson, L., 2005. A Holocene tephra record from the Lofoten Islands, arctic Norway. *Boreas*, 34(2), pp.136-156.
35. Plunkett, G. and Pilcher, J. 2018. Defining the potential source region of volcanic ash in northwest Europe during the Mid- to Late Holocene. *Earth Science Reviews*, 179, 20-37

36. Ravikumar, S., Surekha, R., Thavarajah, R. 2014. Mounting media: An overview. *J. NTR. Univ. Health Sci.*, 3, Suppl S1:1-8
37. Reimer, P.J., et al., 2013. IntCal13 and Marine13 radiocarbon age calibration curves 0–50,000 years cal BP. *Radiocarbon*, 55(4), pp.1869-1887.
38. Riley, C. M., Rose, W. I., and Bluth, G. J. S. 2003. Quantitative shape measurements of distal volcanic ash. *J. Geophys. Res.*, 108, 2504, doi:10.1029/2001JB000818, B10.
39. Rose, W.I. and Durant, A.J., 2009. Fine ash content of explosive eruptions. *Journal of Volcanology and Geothermal Research*, 186(1-2), 32-39.
40. Salmi, M. 1948. The Hekla ash falls in Finland. *Suomen Geologinen Seura* 21: 87–96.
41. Schuur, E.A.G. and Abbott, B. 2011. Climate change: High risk of permafrost thaw. *Nature*, 480, 32-33
42. Stevenson, J.A., et al. 2012. Distal deposition of tephra from the Eyjafjallajökull 2010 summit eruption. *Journal of Geophysical Research: Solid Earth*, 117(B9).
43. Stivirins N., Wulf S., Wastegard S., Lind E.M., Alliksaar T., Gałka M., Andersen T.J., Heinsalu A., Seppa H., Veski S., 2016. Detection of the Askja AD 1875 cryptotephra in Latvia, Eastern Europe. *Journal of Quaternary Science*, 31, 437-441.
44. Swindles, G.T., De Vleeschouwer F. and Plunkett, G. 2010. Dating peat profiles using tephra: stratigraphy, geochemistry and chronology. *Mires and Peat*, 7 (5), 1-9
45. Swindles, G.T., Lawson, I.T., Savov, I.P., Connor, C.B. and Plunkett, G. 2011. A 7000 yr perspective on volcanic ash clouds affecting northern Europe. *Geology*, 39, 887-890
46. Swindles, G.T. et al. 2015a. Evaluating the use of testate amoebae for palaeohydrological reconstruction in permafrost peatlands. *Palaeogeography, Palaeoclimatology, Palaeoecology*, 424, 111–122. <https://doi.org/10.1016/j.palaeo.2015.02.004>
47. Swindles, G.T., et al. 2015b. The long-term fate of permafrost peatlands under rapid climate warming. *Scientific Reports* 5, 17951.
48. Swindles, G.T., Watson, E.J., Savov, I.P., Cooper, C.L., Lawson, I.T., Schmidt, A. and Carrivick, J.L. 2017. Holocene volcanic ash database for Northern Europe. Database. DOI: 10.13140/RG.2.2.11395.60966

49. Swindles, G.T., et al. 2018. Climatic control on Icelandic volcanic activity during the mid-Holocene. *Geology*, 46, 47-50.
50. Thorarinsson, S. 1967. The eruptions of Hekla in historical times: A tephrochronological study. In *The Eruption of Hekla 1947–1948*, Einarsson T, Kjartansson G, Thorarinsson S (eds). *Societas Scientiarum Islandica: Reykjavik*; 1–170.
51. Vikhamer-Schuler, D., Isaksen, K., Haugen, J.E. and Tømmervik, H. 2016. Changes in Winter Warming Events in the Nordic Arctic Region. *Journal of Climate*, 29 (17), 6223-6244.
52. Wastegård, S., Rundgren, M., Schoning, K., Andersson, S., Björck, S., Borgmark, A. and Possnert, G., 2008. Age, geochemistry and distribution of the mid-Holocene Hekla-S/Kebister tephra. *The Holocene*, 18(4), 539-549.
53. Watson, E.J., Swindles, G.T., Lawson, I.T. and Savov, I.P. 2015. Spatial variability of tephra and carbon accumulation in a Holocene peatland. *Quaternary Science Reviews*, 124, 248-264
54. Watson, E.J., Swindles, G.T., Lawson, I.T. and Savov, I.P. 2016a. Do peatlands or lakes provide the most comprehensive distal tephra records? *Quaternary Science Reviews*, 139, 110-128
55. Watson, E.J., Swindles, G.T., Stevenson, J.A., Savov, I. and Lawson, I.T. 2016b. The transport of Icelandic volcanic ash: Insights from northern European cryptotephra records. *Journal of Geophysical Research: Solid Earth*, 121(10), 7177-7192.
56. Watson, E.J., Swindles, G.T., Savov, I., Lawson, I.T., Connor, C. and Wilson, J. 2017. Estimating the frequency of volcanic ash clouds over northern Europe. *Earth and Planetary Science Letters* 460, 41-49.
57. Watt, S.F., Pyle, D.M., Mather, T.A., Martin, R.S. and Matthews, N.E., 2009. Fallout and distribution of volcanic ash over Argentina following the May 2008 explosive eruption of Chaitén, Chile. *Journal of Geophysical Research: Solid Earth*, 114(B4).
58. Woollings, T., Hannachi, A. and Hoskins, B. 2010. Variability of the North Atlantic eddy-driven jet stream. *Quarterly Journal of the Royal Meteorological Society*, 136 (649), 856-868.

Chapter 4: Standard chemical-based tephra extraction methods significantly alter the geochemistry of volcanic glass shards

Claire L. Cooper^{1,2}, Ivan P. Savov², Graeme T. Swindles^{1,3}

¹ School of Geography, University of Leeds, UK, LS2 9JT

² School of Earth and Environment, University of Leeds, UK, LS2 9JT

³ Ottawa-Carleton Geoscience Centre and Department of Earth Sciences, Carleton University, Canada

Published in: Journal of Quaternary Science, 34 (8), 697-707. 2019

Keywords: EPMA, glass preservation, tephrochronology, experimental methods, basaltic

Abstract

The chemical compositions of tephra shards are widely utilised in a myriad of disciplines, including volcanology, petrology, tephrochronology, palaeoecology and climate studies. Previous research has raised concerns over the possible chemical alteration of microscopic (< 100 µm) volcanic glass shards through standard extraction procedures, such as the widely-used acid digestion method. This study subjects ten samples of well-characterised volcanic glasses ranging from basalt to rhyolite to three common methods used in the extraction of volcanic material from lake sediments and peats. The major element geochemistry of each sample was analysed and compared to a control group. The results of this test indicate that basaltic and andesitic glasses are highly susceptible to chemical alteration, particularly to the concentrated corrosive materials used in acid and base digestion techniques.

PERMANOVA analysis of the variation within groups suggests that the oxides most susceptible to variation are alkalis from groups I and II (K_2O , Na_2O , CaO , MgO) and SiO_2 , and the most stable oxides are Al_2O_3 and FeO . Felsic glasses are considerably less susceptible to alteration by both acidic (HCl , HNO_3 , H_2SO_4) and alkaline (KOH) digestions. Our findings have important implications for interpreting the geochemistry of volcanic glasses.

4.1 Introduction

The reliable and non-destructive extraction of tephra is essential for modern applications of tephrochronology and volcanology (Lowe, 2011; Watson et al. 2015). While many methods have been proposed and practiced for the separation of tephra from peat and lake sediments (Hall & Pilcher, 2002; Blockley et al. 2005; Newton et al. 2005), doubts have been raised concerning the geochemical alteration of volcanic glass through these processes. In particular, the use of acid digestion methods has been indicated in the formation of alteration zones around small glass shards, resulting in complications when performing scanning electron microscopy (SEM) or electron probe microanalysis (EPMA) (Blockley et al. 2005). These effects are notably more pronounced in the case of smaller glass shards, producing significant difficulties in the field of tephrochronology where the use of cryptotephra (studies utilising glass shards < 150 µm) is becoming increasingly common for the dating and correlation of sediment and volcanic successions (Watson et al. 2016). Attempts have been made to challenge these claims (Roland et al. 2015); however, this initial case study focused purely on rhyolitic tephra (silica-rich distal deposits of Hekla 4), which comprises slightly more than 75% of the cryptotephra compositions found in western Europe (Swindles et al. 2011; Swindles et al. 2017), and acknowledged that further work on a greater range of glass compositions was required. The ability to accurately compile geochemical profiles of tephra shards is crucial in the identification and correlation of tephra layers to produce isochrons within sediment columns; glass alteration introduces an element of uncertainty which may compromise the reliability of analytical results and their interpretations (Roland et al. 2015; Watson et al. 2016). Several attempts have been made to introduce less chemically destructive techniques, most notably the density separation technique of Blockley et al. (2005). However, the effectiveness of these techniques in removing unwanted biogenic and organic material, such as plant detritus, peat, and biogenic silica, is variable in comparison to traditional chemical digestion-based methods (Brewer et al., 2008; Roland et al., 2015). Therefore, while the original chemical composition of individual shards may be better preserved through density separation techniques, imaging and spectral analysis of samples may still be impaired by

low shard recovery rates produced by repeated separation procedures (Roland et al., 2015). This trade-off between shard concentration and geochemical purity of the glass is the cause of dispute, all the more so as the differing methods have not been thoroughly and comprehensively tested against each other.

Additionally, the apparent preferential preservation of rhyolitic over basaltic tephra in European lake and peatland sites has previously been highlighted by several studies (Wastegård & Davies, 2009; Lawson et al. 2012; Watson et al. 2017). Despite the high frequency of mafic volcanic activity in Iceland (the primary source of European distal tephra deposits (Lawson et al. 2012)), < 3 % of tephra found in western European sites have a basaltic composition (Swindles et al. 2017). Similar distributions of distal tephra are found in other regions globally – a study of tephra found in several Japanese marine cores found that > 80 % of tephra layers contained > 65 % silica (dacites/rhyolites) (Schindlbeck et al. 2018), and of the 3171 tephra reported from the Kamchatsky Peninsula (Far-East Russia; Ponomareva et al. (2017)), only 30% contained < 65 % silica (basalts, andesites and dacites). Several possible explanations have been proposed for this discrepancy – firstly, that basaltic material is often a product of less explosive volcanism, resulting in less widespread distribution (Dugmore et al. 1995); secondly, that the higher density of basaltic tephra shards causes them to deposit as fallout more rapidly than rhyolitic shards, resulting in lower concentrations of mafic material at greater distances (Stevenson et al. 2015); and thirdly, that basaltic glass is more susceptible to alteration and hydration processes in acidic environments, such as those found in peatland or produced during traditional sample preparation techniques (Pollard et al. 2003; Blockley et al. 2005). As the historical tephra record in Europe is relatively well-documented (Swindles, 2011; Lawson et al. 2012), many recent studies have focused on extending the tephra record into older sequences, including tephra from the early Holocene and Younger Dryas periods (Swindles et al. 2017). If the latter hypothesis is correct, many older tephra, particularly those with a more mafic geochemistry, are likely to be more significantly altered from their initial composition.

Here, we examine the latter hypothesis by testing the effects of a range of preparation techniques on the geochemistry and morphology of tephra samples ranging in composition from basaltic to rhyolitic, in order to address the uncertainties presented in many previous tephra studies. We test the hypothesis that mafic glasses are less robust than felsic glasses when exposed to concentrated acidic and alkaline conditions.

4.2 Materials and Methods

4.2.1 Tephra samples

Each analytical method was performed on ten samples of volcanic glass. Seven of the samples are examples of Icelandic glass commonly found in distal deposits across northern Europe, collected from type site exposures in Iceland. Two are proximal deposits collected from lakes near the edifice of Hekla volcano in southern Iceland, and one is a sample of rhyolite obsidian (glass) from the island of Lipari – part of the Aeolian volcanic arc in the Tyrrhenian Sea. Details of each sample can be found in table 1. The silica content of the samples ranges from 47.6 to 75.1 %, and the average size of the shards chosen for EPMA analysis was similar to the common grain sizes of natural samples (~120 - 150 μm). The samples were chosen according to two broad criteria: while some were chosen due to the frequency of their appearance in European (particularly British and Irish) sediments (e.g. Hekla 1947, Hekla-Selsund), the majority were chosen in order to provide a broad range of chemical compositions for comparison. The sample of Lipari obsidian was chosen for inclusion due to its geochemical homogeneity (the sample is extremely low in magnetite and pyroxene inclusions) and comparative resistance to alteration (Hunt & Hill, 1996), while others, such as RL1 and Hekla-Selsund Phase 1, were chosen for their chemical heterogeneity, under the assumption that if one compositional group were preferentially affected by a given treatment, it would be possible to show this within a single sample.

<i>Sample ID</i>	<i>Source Region</i>	<i>Source Volcano</i>	<i>Eruption Age (cal. BP [2000])</i>	<i>Average Silica Content (%)</i>	<i>Min Silica Content (%)</i>	<i>Max Silica Content (%)</i>	<i>Literature Source</i>
Hk1341	Iceland	Hekla	659	56.5	46.3	59.9	<i>Global Volcanism Program (2013)</i>
Ka1357	Iceland	Katla	643	47.6	47.2	48.1	<i>Einarsson et al.(1980)</i>
Hk1991	Iceland	Hekla	9	53.8	47.7	57.3	<i>Gudmundsson et al. (1992)</i>
Hk1947	Iceland	Hekla	53	61.5	60.2	63.9	<i>Rea, Swindles & Roe (2012)</i>
SILK	Iceland	Katla	~3400	66.7	65.5	68.8	<i>Larsen et al. (2001)</i>
HkS P1	Iceland	Hekla	3720	62.5	55.1	74.9	<i>Wastegård et al. (2008)</i>
HkS P2	Iceland	Hekla	3720	53.6	41	72.3	<i>Wastegård et al. (2008)</i>
LipObsidian	Italy	Lipari	Unknown	75.1	74.7	75.4	<i>Hallam et al. (1976)</i>
SL1	Iceland	Unknown	Unknown	61.4	55	65.9	-
RL1	Iceland	Unknown	Unknown	62.4	48.8	76.9	-

Table 1: A summary of the tephra samples used for analysis

4.2.2 Processing methods

4.2.2.1 Control (No treatment)

Samples in the control group were not subjected to any chemical treatment following the combination of the glass with peat. Samples were washed through a 16 µm sieve with deionised water and then dried at 105 °C prior to electron probe analysis. While density separation techniques are becoming a common procedure in the field of tephrochronology, none were performed at any stage in this study as the process is rarely used in combination with acid or base treatments (Blockley et al., 2005).

4.2.2.2 Muffle furnace burning and dilute hydrochloric acid (Method 1)

Following the tephra extraction methods of Hall & Pilcher (2002) and Swindles et al. (2010), the samples subjected to this method were dried overnight at 105 °C, and then burnt in a muffle furnace at 600 °C for six hours. The resulting ashes were then transferred to 15 ml centrifuge tubes, and suspended in 3 ml of 1M hydrochloric acid (HCl) for 24 hours. The tubes were then topped up to 14.5 ml with deionised water, and centrifuged at 3000 rpm for 10 minutes to concentrate the tephra at the base of the tubes. The remaining acid was then removed by washing the samples through a 16 µm sieve with deionised water. While there is some suggestion that the use of the muffle furnace may not be suitable when preparing glass shards for EPMA (Hall & Pilcher, 2002), the method is still commonly used for this purpose (Hang et al, 2006; Swindles, 2010; Watson et al, 2016).

4.2.2.3 Acid digestion (Method 2)

This method follows the modified procedure of Persson (1971), published on 'TephraBase' (http://www.tephrabase.org/tephra_dig.html), where a detailed methodology may be found. The method is also used by Dugmore et al. (1992) and Swindles et al. (2010) and is thought to be most effective in removing organic-rich, ombrotrophic peat sediments (Roland et al. 2015), though it is also used in minerogenic lake samples (Renberg et al., 2002).

The wet samples were placed into 500 ml beakers, and 100 ml of 98 % sulfuric acid (H_2SO_4) was added to cover the samples. The hotplate was then switched on, and turned to maximum ($\sim 300^\circ\text{C}$). Once the initial boiling had subsided (approximately 5 minutes), the samples were left to react for 90 minutes. 10 ml of 68-72% HNO_3 (Standard Laboratory Reagent) was then slowly added, and the contents of the flasks left to simmer for a further 1 hr until the solution became pale yellow or colourless. The hotplate was then switched off, and the samples left to cool to room temperature (approximately 45 minutes). Following this step, 400 ml of distilled water was slowly added until no further vapours were released from the beakers. The samples were then thoroughly washed through a $16\ \mu\text{m}$ sieve, centrifuged at 3000 rpm for 10 minutes, and the supernatant pipetted off.

4.2.2.4 Acid/base digestion (Method 3)

The third method replicated the procedure utilised by Watson et al. (2016) and Matthews-Bird et al. (2017). In the instances described by those studies, the method was used to prepare the samples for radiocarbon analysis.

The samples in this study were placed in 500 ml beakers with 150 ml of 1M HCl, and heated to 80°C for 2 hours. The samples were then cooled to room temperature over the course of 30 minutes and rinsed with deionised water, before being transferred to clean beakers. 150 ml of 0.5M KOH was then added, and the samples were again heated to 80°C for 2 hours. Following this, 10-30 ml of deionised water was added in small increments until no further material was extracted, and the mixtures were then cooled to room temperature as before, and rinsed through a $10\ \mu\text{m}$ mesh with 500 ml of deionised water before being returned to their beakers. A further 150 ml of 1M HCl was then added to the samples, which were then heated again to 80°C for 5 hours. The samples were then cooled and rinsed, washed through a $16\ \mu\text{m}$ sieve, centrifuged at 3000 rpm for 10 minutes, and the supernatant pipetted off.

4.2.3 Electron Probe Microanalysis

The samples were dried and mounted on 25.5 mm disks in Epo-Tek® resin, and finished with a 0.25 µm diamond polish to ensure exposure and a polished surface. EPMA was performed at the Tephra Analysis Unit at the University of Edinburgh, using the “combined analysis method” described in detail in Hayward (2012). All analyses were performed using a 5 µm diameter beam of 15 kV, varying only the current between 2 nA for Na, Mg, Al, Si, K, Ca, and Fe quantities, and 80 nA for Ti and Mn. Secondary (external) glass standards (basalt BCR-2G and Lipari rhyolite) were analysed before each EPMA run, and a PAP correction applied. Analyses were performed as close to the centre of each shard (i.e. the centre point of the x and y axes) as possible in order to ensure accurate geochemical profiling of the glass, in accordance with standard laboratory procedures. Shards that were not sufficiently exposed across the polished surface were excluded.

4.2.4 Statistical Analysis – PERMANOVA

PERMANOVA is a non-parametric multivariate method of statistical analysis. Originally developed as an adaptation of traditional MANOVA methods (Anderson, 2001; McArdle & Anderson, 2005) to better suit the non-normal distributions and discrete (rather than continuous) data values found in ecological datasets (while ecological datasets were the intended target, the developers stated that the method was likely to be applicable across the natural sciences; Anderson, 2001), PERMANOVA is most applicable when handling datasets with asymmetric distributions, and in variables containing multiple zeros. It is therefore useful in the comparison of diverse geochemical profiles, in which element distributions are unlikely to follow a pattern of normal distribution.

The EPMA data were normalised to 100 % (i.e. to an anhydrous basis) prior to multivariate analysis in order to ensure authentic comparison between datasets (Wolde-Gabriel et al., 2005; Pearce et al., 2007).

4.3 Results

4.3.1 Notes on removal of organic material

While both the acid digestion (method 2) and burning/dilute acid (method 1) processes were effective in removing unwanted organic materials from the sample, the process of acid digestion was by far the most thorough in removing the peat, if slightly less time efficient when preparing large batches of samples. However, following method 3, small amounts of organic material remained within the sample, and were visible under an optical microscope. These contaminants were identified as bleached moss and plant material. The organic material was not of a sufficient quantity to obstruct microscope analysis.

4.3.2 Glass Alteration

4.3.2.1 Glass Morphology

Through optical and SEM imagery, a clear difference between the glass morphologies of shards subjected to each treatment can be seen. Alteration rims of between 15-75 μm are immediately visible in most shards subjected to acid digestion (method 2), with most samples displaying a zone of glassy, crystal-rich (typically quartz- and feldspar-rich) material (see figure 1). Alteration rims are also frequently seen in shards subjected to treatment method 1, though they are typically smaller in diameter, between 15-40 μm . However, the most significant changes in shard morphology can be observed following base (KOH) digestion; many shards subjected to this treatment appear substantially degraded, sometimes taking on a pseudo-dendritic appearance (see figure 1 (d)). In the cases of more crystal-rich tephra, the glassy matrix appears to be preferentially dissolved, leaving the plagioclase crystals relatively unaffected (see figure 1 (b. iv.)). Unlike in the acid treatments, these shards do not exhibit a well-defined zone of alteration, with few exceptions.

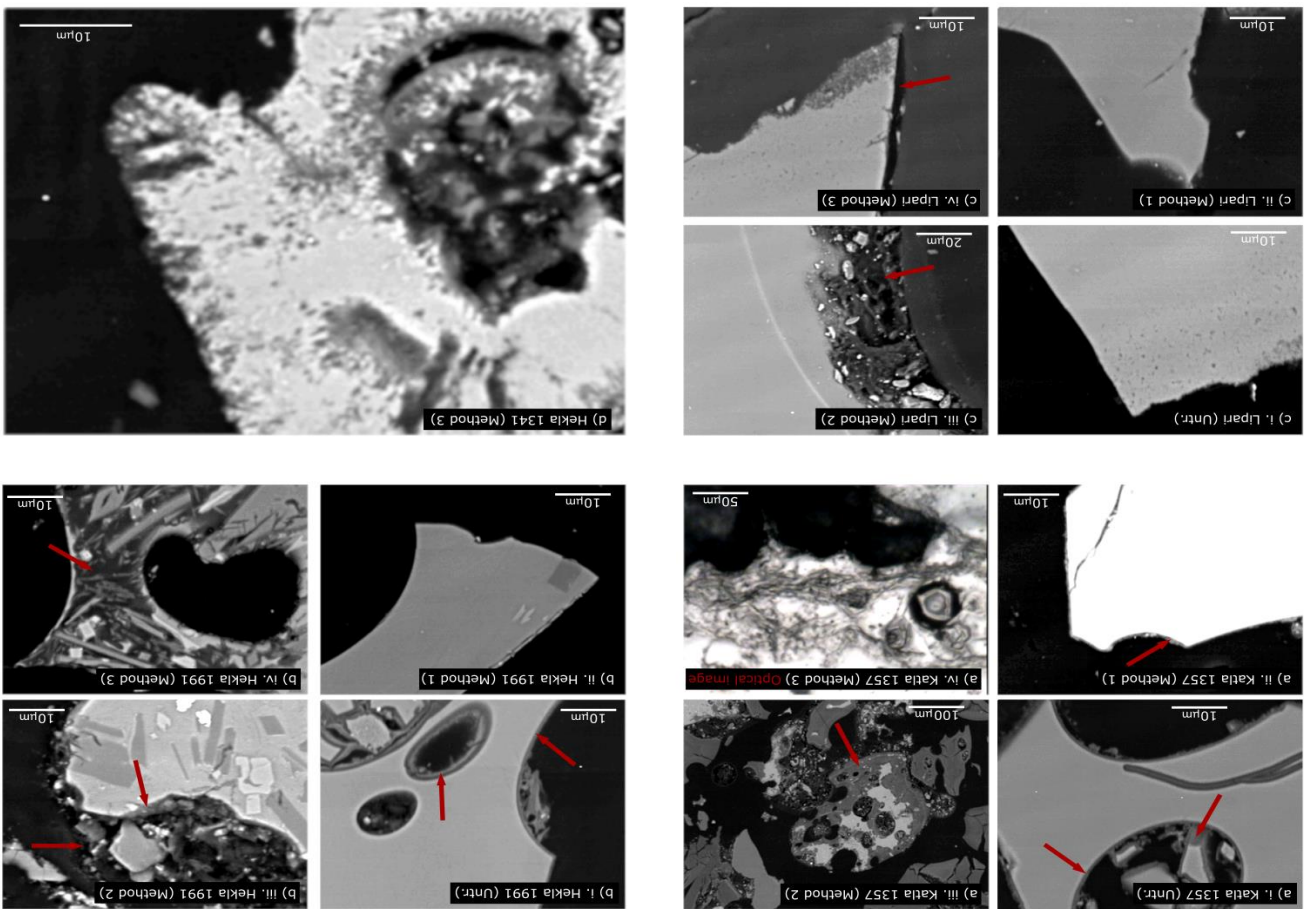


Figure 1: SEM images of volcanic glass belonging to a) Katla 1357; b) Hekla 1991; c) Lipari glass; and analysed following chemical treatments: i) Control group; ii) Acid digestion; iii) Burning + dilute HCl; iv) Base digestion. Red arrows indicate zones of alteration. Image d) shows a pattern of corrosion produced by base digestion on a shard of Hekla 1341 glass. Image a) iv. is an optical image – all useful shards of Katla 1357 were considerably degraded through base digestion, and were not clearly visible through SEM imagery.

The evidence gathered in this study strongly indicates that underlying glass geochemistry plays a role in the degree of shard alteration. Shards from the basaltic Katla 1357 (K1357) eruption (average $\text{SiO}_2 \sim 48$ wt %; figure 1 (a)) show notably greater morphological changes as a result of each treatment than those shards with a higher silica content, such as the andesitic Hekla 1991 (average SiO_2 content 56.48 %; figure 1 (b)), or the rhyolitic Lipari obsidian ($\text{SiO}_2 \sim 75$ wt %; figure 1 (c)). The dissolution of the K1357 shards following base digestion (method 3) was sufficiently extensive to entirely prohibit the use of EPMA in that sample, while the Lipari obsidian was unusual in that it exhibited no alteration rim following weak or concentrated acid treatment, and only a narrow rim of 5-8 μm following base digestion.

4.3.2.2 Geochemistry

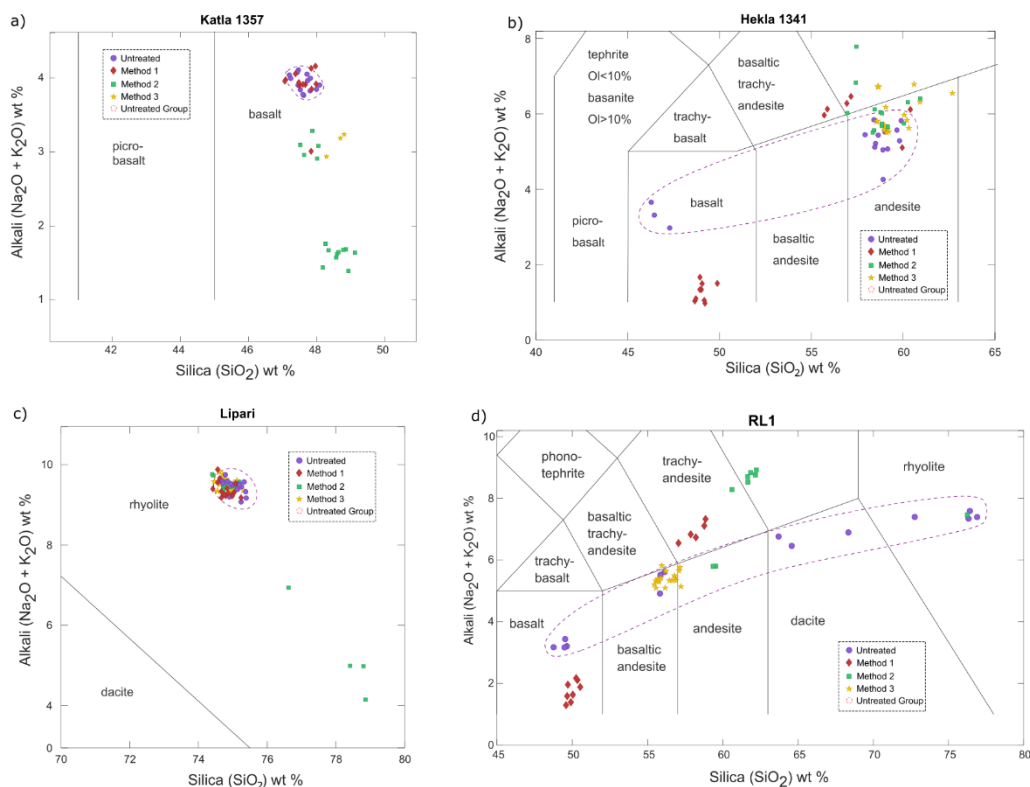


Figure 2: Selected TAS diagrams showing group variations in geochemical classifications following chemical treatments of volcanic glass. Purple circles – control group; red diamonds – burning + dilute HCl; green squares – acid digestion; yellow stars – base digestion. These examples were selected for the clarity of variation from the untreated group across a range of SiO_2 contents. Sample RL1 has been included to variation across initial composition within a single sample. TAS classification after Le Bas et al., 1986.

Our results show a large amount of variability in glass geochemistry following chemical treatment. While many oxide concentrations show significant variation across treatments (discussed further in section 3.3), the most consistently significant differences, both positive and negative, occur in the concentrations of Na₂O, CaO, K₂O, MgO, and SiO₂. While mean relative concentrations of Na₂O and K₂O typically decrease following chemical treatment of the glasses, the relative concentrations of SiO₂, MgO, and CaO typically increase. Additionally, there is a clear and persistent trend across almost all major element oxides wherein variation compared to the control group is greater following acid and base digestions (methods 2 and 3) than those subjected to method 1. The four exceptions to this trend are: the Lipari glass, which displays very few variations in mean oxide concentration to a statistically significant level (5%) of any major element under any tested conditions (the exception being method 2, which produced a 5.52% increase in mean FeO content); and the SL1, RL1, and Hekla 1991 samples, in which the initial geochemistry was found to be variable. In these cases, significant statistical deviations from the control group may simply be a result of variability within the natural glass shard population. A full summary of major element geochemistry and secondary samples can be found in appendix 1.

In addition to the trend described above, we also find a correlation in responses to chemical treatment with initial SiO₂ abundances (i.e. the composition of the control group). The examples shown in figure 3 summarise the geochemical alterations to a basalt, andesite, and rhyolite respectively. In the basaltic K1357 sample (average initial SiO₂ = 47.6 wt %), the mean Na₂O content varies negatively by 61.7 % following acid digestion (method 2) when compared to the control group. In the andesitic Hekla 1947 (average initial SiO₂ = 61.5 wt %), the Na₂O concentration decreases between the control and acid digestion treatment by 5.7 %, and in the rhyolitic Lipari glass (SiO₂ = 75.1 wt %) the decrease in the mean concentration is as low as 0.667 %. Following base digestion (method 3), the Na₂O content deviates negatively from the control group by 26 % for Katla 1357, 38.2 % for Hekla 1947, and 0.48 % for Lipari glass. Both the basalt and the andesite display significantly more variation across groups when compared with the rhyolite.

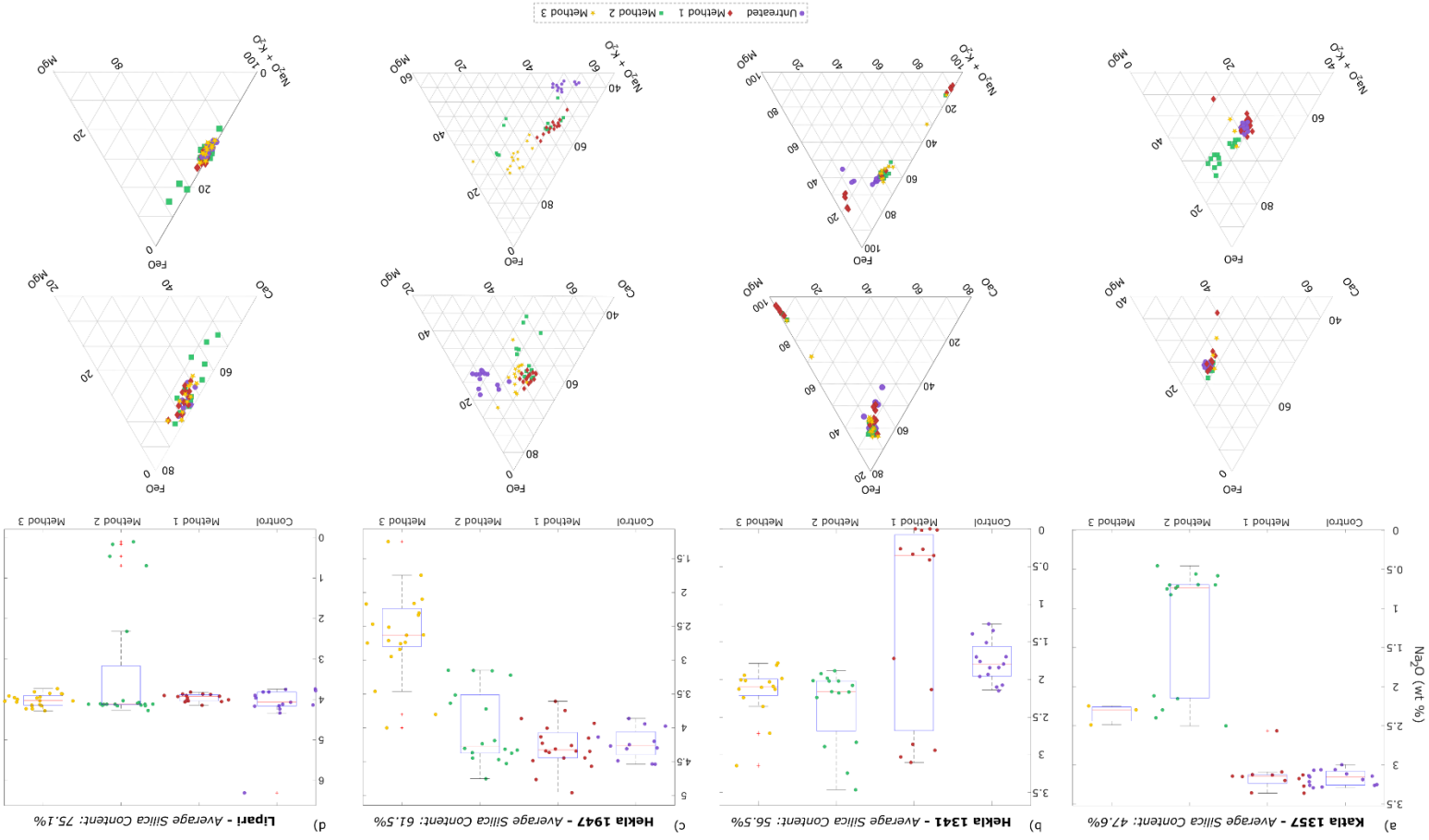


Figure 3: Boxplots and ternary diagrams displaying variations in major element geochemistry for a) Katla 1357; b) Hekla 1947; c) Lipari glass. Symbols are coloured as follows: purple – control group; red – burning + HCl; green – acid digestion; yellow – base digestion.

Certain samples appear to display a trend of 'homogenisation' in the range of observed compositions following chemical treatment. For example, the control groups of Hekla 1341 and Hekla 1991 glass both have a higher range of Si/TA (total alkali) values than in the subsequent treatment groups, particularly those subjected to methods 2 and 3, reflecting an apparent loss of alkali oxides. The affected composition ranges typically occur below ~55 SiO₂ wt% and TA 4-5 wt%. In these instances, the chemical composition of the glasses apparently 'removed' by concentrated chemical treatment are also relatively low in wt %s of network forming cations other than Si. Taking one example of 'removed' material in the Hekla 1341 basalts, TiO₂ (Ti⁴⁺) constitutes < 4 wt% and Al₂O₃ (Al³⁺) < 15 wt% . Likewise, TiO₂ comprises < 0.25 wt% and Al₂O₃ <13 wt% in the Hekla 1991 basalts. The NBO/T ratio of these glasses (a measure of polymerisation; calculated after Mysen et al., 1985), which are not present in the samples subjected to concentrated acid treatment, is subsequently higher than that of the average group composition (Hekla 1341 basalts NBO/T = 2.96 (average 1.77); Hekla 1991 basalts NBO/T = 3.22 (average 2.28)). The lower polymerisation of these glasses would substantially increase their solubility, which may explain their apparent absence in the samples following concentrated solution treatments.

4.3.2.3 PERMANOVA

Table 2 shows the results of the PERMANOVA analysis of each method in comparison to the oxide quantities measured in the control group. In this instance we regard a P value of < 0.01 (1 %) to be statistically significant, i.e. indicating that the wt% of that element has changed to a significant degree. Our results confirm that the most consistently variable oxide is K₂O, which shows a significant within-group variation in 8 out of 30 analyses. CaO and SiO₂ both show significant within-group variation in 7 of 30 analyses, and Na₂O, MgO, MnO, and TiO₂ each show significant variation in 5 of 30. Additionally, samples which show significant variation in at least one oxide across all three chemical treatments show fewer variations, and less significant variance (lower F values), in the method 1 treatment group than in either the acid or base digestion groups (methods 2 and 3).

The PERMANOVA analysis also allows comparison between sample groups. For example, while the Hekla-Selsund Phase 2 sample (average SiO₂ content 53.6 %) shows four statistically significant variations in major element oxide concentrations (K₂O, CaO, SiO₂, and TiO₂) following methods 2 and 3, and two following method 1 (TiO₂ and MnO), the Lipari glass samples do not show statistically significant variations in any oxide following any treatment. Comparison of samples with contrasting SiO₂ content (see table 3), reveals a broad pattern of lower susceptibility to chemical alteration with increasing silica content.

Table 2: PERMANOVA results

Treatment 2: Acid Digestion					Treatment 3: Burn + HCl					Treatment 4: Base Digestion				
		F	TestStatistic	P			F	TestStatistic	P			F	TestStatistic	P
Hekla-Selsund Phase 1	Na	0.17	0.41	0.71	Hekla-Selsund Phase 1	Na	0.77	0.88	0.50	Hekla-Selsund Phase 1	Na	0.98	0.99	0.31
	Mg	1.33	1.15	0.30		Mg	0.08	0.29	0.86		Mg	0.69	0.83	0.44
	Al	5.19	2.28	0.02		Al	2.55	1.60	0.05		Al	0.55	0.74	0.59
	K	0.77	0.88	0.47		K	0.03	0.16	0.86		K	0.00	0.05	0.90
	Ca	0.00	0.01	0.99		Ca	0.37	0.61	0.57		Ca	0.25	0.50	0.32
	Fe	6.65	2.58	0.04		Fe	1.35	1.16	0.23		Fe	0.06	0.25	0.61
	Si	0.03	0.19	0.90		Si	0.77	0.88	0.32		Si	0.12	0.34	0.78
	Ti	4.05	2.01	0.05		Ti	2.13	1.46	0.28		Ti	0.11	0.33	0.64
	Mn	3.42	1.85	0.15		Mn	1.11	1.05	0.42		Mn	0.00	0.06	0.92
Hekla-Selsund Phase 2	Na	11.44	3.38	0.01	Hekla-Selsund Phase 2	Na	0.08	0.28	0.81	Hekla-Selsund Phase 2	Na	11.74	3.43	0.02
	Mg	9.49	3.08	0.03		Mg	0.33	0.57	0.63		Mg	8.81	2.97	0.03
	Al	3.06	1.75	0.16		Al	3.46	1.86	0.13		Al	3.44	1.86	0.09
	K	47.11	6.86	0.00		K	2.43	1.56	0.17		K	41.37	6.43	0.00
	Ca	28.96	5.38	0.00		Ca	6.49	2.55	0.04		Ca	27.57	5.25	0.00
	Fe	5.62	2.37	0.05		Fe	0.19	0.43	0.71		Fe	5.40	2.32	0.06
	Si	21.10	4.59	0.00		Si	0.90	0.95	0.39		Si	22.22	4.71	0.00
	Ti	3.58	1.89	0.00		Ti	44.46	6.67	0.00		Ti	4.03	2.01	0.00
	Mn	9.54	3.09	0.02		Mn	9.14	3.02	0.01		Mn	8.88	2.98	0.01

Hekla 1341	Na	10.80	3.29	0.00	Hekla 1341	Na	0.99	1.00	0.34	Hekla 1341	Na	9.44	3.07	0.01
	Mg	6.00	2.45	0.00		Mg	0.03	0.18	0.86		Mg	5.79	2.41	0.01
	Al	1.79	1.34	0.30		Al	2.90	1.70	0.14		Al	1.74	1.32	0.30
	K	0.20	0.45	0.55		K	9.44	3.07	0.01		K	0.40	0.63	0.52
	Ca	0.27	0.52	0.52		Ca	11.26	3.36	0.02		Ca	0.77	0.88	0.36
	Fe	4.77	2.18	0.04		Fe	0.43	0.66	0.55		Fe	6.33	2.52	0.01
	Si	1.43	1.20	0.39		Si	3.27	1.81	0.15		Si	3.21	1.79	0.04
	Ti	4.13	2.03	0.13		Ti	2.11	1.45	0.27		Ti	4.36	2.09	0.06
	Mn	1.37	1.17	0.40		Mn	7.83	2.80	0.01		Mn	1.36	1.17	0.43
Hekla 1947	Na	0.29	0.54	0.53	Hekla 1947	Na	0.02	0.16	0.64	Hekla 1947	Na	5.79	2.41	0.03
	Mg	0.51	0.72	0.50		Mg	2.19	1.48	0.10		Mg	0.62	0.79	0.52
	Al	4.33	2.08	0.01		Al	3.03	1.74	0.25		Al	4.60	2.14	0.02
	K	4.19	2.05	0.00		K	3.32	1.82	0.00		K	4.11	2.03	0.00
	Ca	12.14	3.48	0.00		Ca	3.14	1.77	0.13		Ca	14.18	3.77	0.00
	Fe	0.39	0.63	0.59		Fe	1.52	1.23	0.33		Fe	0.99	0.99	0.31
	Si	0.65	0.80	0.41		Si	3.96	1.99	0.04		Si	1.10	1.05	0.34
	Ti	4.00	2.00	0.06		Ti	1.26	1.12	0.27		Ti	3.94	1.99	0.07
	Mn	0.36	0.60	0.62		Mn	0.29	0.54	0.76		Mn	0.15	0.38	0.91
Hekla 1991	Na	0.31	0.56	0.66	Hekla 1991	Na	5.50	2.35	0.06	Hekla 1991	Na	31.00	5.57	0.00
	Mg	5.36	2.31	0.07		Mg	8.81	2.97	0.00		Mg	7.77	2.79	0.02
	Al	0.50	0.71	0.47		Al	4.33	2.08	0.05		Al	1.58	1.26	0.21
	K	6.13	2.48	0.01		K	5.30	2.30	0.01		K	1.22	1.10	0.16
	Ca	5.14	2.27	0.06		Ca	7.28	2.70	0.02		Ca	3.44	1.85	0.02

	Fe	1.84	1.36	0.22		Fe	3.78	1.94	0.02		Fe	6.94	2.63	0.00
	Si	3.53	1.88	0.11		Si	10.91	3.30	0.00		Si	5.40	2.32	0.03
	Ti	4.20	2.05	0.12		Ti	5.62	2.37	0.04		Ti	5.66	2.38	0.10
	Mn	8.33	2.89	0.01		Mn	1.83	1.35	0.28		Mn	0.38	0.61	0.58
Katla 1357	Na	54.06	7.35	0.00	Katla 1357	Na	5.09	2.26	0.10	Katla 1357	Na	/	/	/
	Mg	5.37	2.32	0.04		Mg	6.13	2.48	0.01		Mg	/	/	/
	Al	4.20	2.05	0.01		Al	5.73	2.39	0.02		Al	/	/	/
	K	0.13	0.36	0.81		K	4.09	2.02	0.13		K	/	/	/
	Ca	23.56	4.85	0.00		Ca	5.02	2.24	0.12		Ca	/	/	/
	Fe	9.01	3.00	0.00		Fe	5.65	2.38	0.05		Fe	/	/	/
	Si	22.56	4.75	0.00		Si	5.51	2.35	0.06		Si	/	/	/
	Ti	29.80	5.46	0.00		Ti	5.17	2.27	0.09		Ti	/	/	/
	Mn	0.65	0.80	0.51		Mn	4.95	2.22	0.07		Mn	/	/	/
Lipari Obsidian	Na	1.96	1.40	0.21	Lipari Obsidian	Na	0.86	0.93	0.57	Lipari Obsidian	Na	2.10	1.45	0.10
	Mg	2.53	1.59	0.03		Mg	0.23	0.48	0.69		Mg	0.25	0.50	0.49
	Al	7.57	2.75	0.02		Al	5.18	2.28	0.06		Al	4.36	2.09	0.05
	K	0.08	0.28	0.88		K	0.52	0.72	0.67		K	2.10	1.45	0.11
	Ca	0.52	0.72	0.50		Ca	2.58	1.61	0.17		Ca	0.23	0.48	0.65
	Fe	3.85	1.96	0.08		Fe	4.75	2.18	0.05		Fe	0.67	0.82	0.39
	Si	0.73	0.85	0.49		Si	6.14	2.48	0.04		Si	5.77	2.40	0.03
	Ti	2.26	1.50	0.15		Ti	2.01	1.42	0.21		Ti	3.27	1.81	0.11
	Mn	1.81	1.35	0.46		Mn	0.00	0.03	0.98		Mn	0.68	0.82	0.50
SILK	Na	0.01	0.10	0.97	SILK	Na	0.01	0.11	0.92	SILK	Na	3.25	1.80	0.11

	Mg	3.69	1.92	0.11		Mg	2.63	1.62	0.08		Mg	1.34	1.16	0.22
	Al	5.14	2.27	0.01		Al	3.66	1.91	0.03		Al	0.03	0.18	0.16
	K	5.63	2.37	0.01		K	3.82	1.95	0.01		K	11.77	3.43	0.00
	Ca	3.50	1.87	0.16		Ca	1.86	1.36	0.39		Ca	5.29	2.30	0.07
	Fe	6.12	2.47	0.02		Fe	5.03	2.24	0.02		Fe	2.31	1.52	0.22
	Si	4.84	2.20	0.02		Si	5.03	2.24	0.00		Si	16.69	4.09	0.00
	Ti	3.38	1.84	0.25		Ti	2.00	1.41	0.47		Ti	4.43	2.10	0.04
	Mn	5.71	2.39	0.01		Mn	4.34	2.08	0.04		Mn	3.90	1.97	0.02
	Na	7.72	2.78	0.01		Na	12.39	3.52	0.01		Na	0.25	0.50	0.67
	Mg	1.35	1.16	0.32		Mg	0.90	0.95	0.31		Mg	4.40	2.10	0.06
	Al	15.52	3.94	0.00		Al	9.73	3.12	0.01		Al	1.19	1.09	0.28
	K	0.01	0.08	0.91		K	2.29	1.51	0.11		K	7.56	2.75	0.04
SL1	Ca	0.41	0.64	0.52	SL1	Ca	1.78	1.33	0.21	SL1	Ca	9.06	3.01	0.03
	Fe	1.19	1.09	0.37		Fe	0.79	0.89	0.37		Fe	3.83	1.96	0.08
	Si	0.29	0.54	0.60		Si	0.70	0.84	0.40		Si	7.03	2.65	0.03
	Ti	1.61	1.27	0.28		Ti	1.00	1.00	0.28		Ti	4.36	2.09	0.06
	Mn	1.32	1.15	0.29		Mn	1.25	1.12	0.25		Mn	5.61	2.37	0.05
	Na	1.85	1.36	0.24		Na	0.32	0.56	0.64		Na	0.02	0.16	0.83
	Mg	0.86	0.93	0.44		Mg	0.80	0.89	0.50		Mg	0.09	0.30	0.72
	Al	6.03	2.45	0.05		Al	4.53	2.13	0.07		Al	2.07	1.44	0.15
RL1	K	0.04	0.19	0.86	RL1	K	8.06	2.84	0.01	RL1	K	1.12	1.06	0.20
	Ca	0.09	0.30	0.79		Ca	10.00	3.16	0.02		Ca	0.02	0.15	0.82
	Fe	0.58	0.76	0.54		Fe	0.05	0.22	0.85		Fe	0.61	0.78	0.25

	Si	0.14	0.37	0.70		Si	0.00	0.04	0.96		Si	1.94	1.39	0.09
	Ti	1.91	1.38	0.22		Ti	0.10	0.32	0.82		Ti	0.47	0.68	0.27
	Mn	1.41	1.19	0.26		Mn	2.37	1.54	0.18		Mn	2.91	1.71	0.11

Table 3: Summary of variations in relative oxide concentration against average SiO₂ content in control group, NBO/T, and H₂O by difference. Statistically significant ($P < 0.01$) variations are highlighted in bold. As comparisons are drawn between normalised results, constant sum effects should be taken into account.

Sample	Av SiO ₂ % (before treatment)	Observations			NBO/T	H ₂ Odiff (%)
		Method 1	Method 2	Method 3		
Hekla-Selsund Phase 1	62.5	Ti, Fe, Mg, P increase; Al, Na decrease	Al decrease; Fe, P increase	Al, Na decrease	0.72	0.68
Hekla-Selsund Phase 2	53.6	Si, Ti, K, Al, Na increase; Fe, Mg, Ca , P decrease	Ti, Al increase; Fe, Mn, Ca , P decrease	Si, Ti, Al, Na, K increase; Fe, Mn, Mg, Ca decrease	3.33	0.59
Hekla 1341	56.5	Si increase; Fe, Mg decrease	Si, Mn, P decrease; Ti, Ca increase	Si, Na increase; Fe, Mg decrease	1.77	0.11
Hekla 1947	61.5	Si decrease; Ti, Fe, Mg, Ca increase	Fe, Ca increase	Si, Na decrease; Ti, Fe, Mg, Ca, P increase	0.67	0.34

Hekla 1991	53.8	Si, Ti increase; Ca decrease	Si, Ti increase; Fe, Ca, Na decrease	Si, Ti, Al, Mn increase; Fe, Mg decrease	2.28	1.42
Katla 1357	47.6	Si, Ti, Fe increase; Na decrease	No significant changes	(NB Only three analyses possible) Si, Ca increase; P decrease	3.04	0.77
Lipari Obsidian	75.1	No significant changes	No significant changes	No significant changes	0.31	0.31
SILK	66.7	Si decrease; Fe, Ca increase	Si decrease ; Fe, Mg increase	Na increase	0.78	1.04
SL1	61.4	Al increase; P decrease	Mg increase; Na, K, P decrease	Si decrease; Ti, Fe, Mn, Mg, Ca, P increase	1.22	0.37
RL1	62.4	Al, Na increase; Ti, Fe, Mn, Mg decrease	Si, K decrease; Al, Mg, Ca increase	No significant changes	1.16	0.53

4.4 Discussion

This study confirms persistent assertions within tephrochronology that substantial chemical alteration of volcanic glass via commonly used extraction techniques, namely the acid digestion method, is possible, particularly for basaltic and low-silica andesitic tephra (< ~60% SiO₂; Blockley et al., 2005). The assertion of Roland et al. (2015) that no significant geochemical variation could be found following acid digestion is supported by our findings, as the felsic samples (> 63% SiO₂) in our study were among the least susceptible to geochemical alteration. In particular, the highly silicic Lipari glasses were by far the least prone to any chemical perturbation. While the precise mechanisms behind this relationship require further study, we suggest that the increased polymerisation of silica chains in rhyolitic glass may provide a stabilising factor, preventing the leaching of mobile elements (Iler, 1979; Chan, 1989; Dultz et al., 2016). Furthermore, while outside the scope of the data presented in this study, it is likely that volatile content of the tephra could affect the susceptibility of the glasses to alteration, as the formation of molecules such as OH⁻ and CO₃²⁻ (for example) reduce the degree of glass polymerisation.

Additionally, concern has previously been raised over the apparent underrepresentation of basaltic glasses in the European tephra record, compared to the more felsic (evolved) rock varieties sourced from Icelandic (Lawson et al., 2012; Watson et al., 2016; Watson et al., 2017). While basaltic glass is not entirely absent from European peatland and lake records, our results give weight to the theory that this apparent bias may be due in part to either partial alteration or complete destruction of basaltic material during glass shard extraction, as suggested by Watson et al. (2017). Furthermore, it is possible that the acidic conditions present in peat bogs (typically pH 3-4; Sanger et al., 1993; Klavins & Purmalis, 2013) may play a role in creating the apparent bias in the record; a long residence time in such conditions may cause alteration or dissolution of a significant percentage of basaltic shards in a given deposit.

Also of note is the apparently consistent creation in some samples of novel glass geochemistry – in other words, instances in which the combined variation in one or more major element weight percentages is significant enough to place multiple glass shards in new geochemical category when plotting against standard TAS definitions. This is especially relevant for studies concerning cryptotephra < 30-50 µm in diameter (frequently encountered in distal tephra studies; Lowe et al., 2011; Pearce et al., 2014), or those with a high surface area-to-volume ratio, such as tricusate shards or those with multiple bubble walls, as any alteration in those instances is likely to affect a greater percentage of the glass composition in those shards. Particularly important are those compositions which transition from sub-alkaline to alkaline fields. These alkaline compositions are only rarely erupted in Iceland (Wood, 1978; Nicholson et al. 1991; Gudmundsdóttir et al. 2018), yet are occasionally reported in European cryptotephra studies which variably attribute the material to Icelandic eruptions or suggest ultradistal sources, such as the Cascade Range or Alaskan volcanoes of North America (Jensen et al., 2014; van der Bilt et al., 2017; Plunkett & Pilcher, 2018). Figure 4 shows a composite TAS diagram combining several reported Icelandic cryptotephra, overlain with selected anomalous results from this study. While some analyses are clearly distinguishable from the wider trend of Icelandic geochemistry, many of the variations produced by all three treatment methods fall well within the boundaries of reported Icelandic trachyandesites in the European tephra record. Although it is possible that these reported analyses represent the original geochemistry of the tephra shard in question, the control groups for each of the anomalous trachyandesites and trachytes found in this study did not fall into either geochemical category. It is therefore also possible that some reported trachyandesites may have been unintentionally manufactured as a result of chemical alteration during extraction. Great care should therefore be taken in the interpretation of apparently ultra-distal tephra, particularly regarding the relative contents of groups I and II oxides (K₂O, Na₂O, CaO, MgO), which we find to be particularly susceptible to alteration. It is however possible that this same susceptibility may have applications in assessing the validity of volcanic glass datasets,

although the exact nature of any potential statistical test based on that data is beyond the scope of this study.

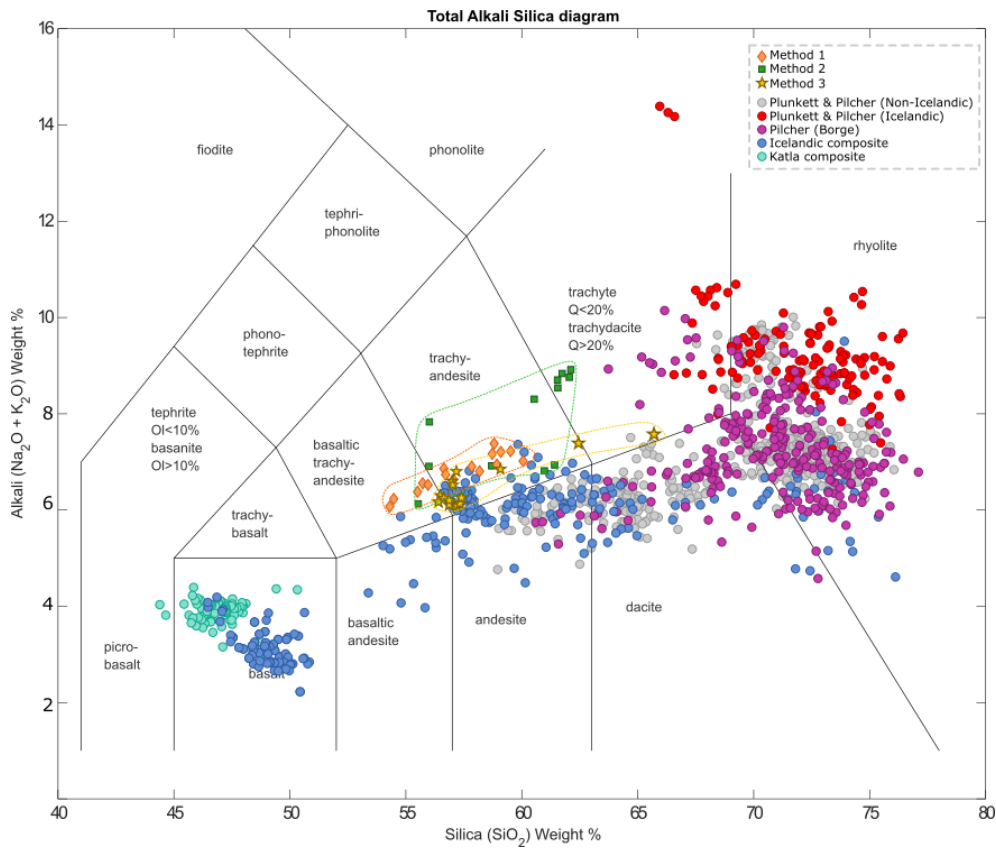


Figure 4. Composite TAS diagram showing the range of reported Icelandic geochemistry against geochemical variations produced by chemical extraction in this study. This study: green squares – acid digestion; orange diamonds – burning + HCl; yellow stars – base digestion. Existing literature is denoted with circle symbols. Grey – Plunkett & Pilcher (2018) (assigned ‘Icelandic’). Red – Plunkett & Pilcher (2018) (assigned ‘non-Icelandic’). Purple – Pilcher et al. (2005) (selected Borge tephtras). Blue – composite Icelandic data from Mangerud et al. (1984); Mangerud, Furnes & Johansen (1986); Pilcher, Hall & McCormac (1996); Boyle (1994); Dugmore et al. (1992); Dugmore, Larsen & Newton (1995); Dugmore & Newton (1997), Larsen, Dugmore et al. (1999); Wastegard et al. (2001); Hall & Pilcher (2002); Chambers et al. (2004); Swindles (2006); Davies et al. (2007); Rea, Swindles & Roe (2012); Ratcliffe et al. (2017). Cyan – composite Katla data from Boyle (1994); Streeter & Dugmore (2014).

The findings of this experiment ultimately suggest that the vulnerability of mafic tephra and cryptotephra to geochemical alteration by laboratory techniques may be greater than previously thought. As basaltic tephra is favoured over more magmatically evolved material in many petrogenetic

studies, the preservation of these tephras in a laboratory setting is increasingly important. Therefore, while non-destructive methods of glass extraction are often more time-consuming and labour-intensive than chemical methods, it may be of greater benefit to future studies to exercise caution and discretion when handling silica-poor glasses, particularly those with a small surface area/perimeter ratio.

4.5 Conclusions

1. The use of burning & dilute HCl, concentrated H₂SO₄ and HNO₃ (as used in the common acid digestion method of tephra preparation), and concentrated KOH in the extraction of volcanic glass are all sufficient to cause statistically significant variations in the less stable element oxides;
2. The oxides most susceptible to variation are K₂O, CaO, SiO₂, and Na₂O. The most statistically stable oxides are Al₂O₃ and FeO.
3. Basaltic and basaltic andesitic glasses are most susceptible to alteration through exposure to concentrated acidic (HNO₃, H₂SO₄) and basic (KOH) conditions;
4. Concentrated acids and bases also cause the destruction of perimeter glass material in volcanic glass, particularly glasses of a mafic composition;
5. These systematic alterations of volcanic glass may have implications for previously published studies of tephra geochemistry and stratigraphy.

Acknowledgements

Claire Cooper acknowledges a New Research Worker's Award from the Quaternary Research Association, in addition to a Climate Research Bursary and a Leeds Anniversary Scholarship from the University of Leeds. The authors thank Dr Chris Hayward at the University of Edinburgh for his assistance in obtaining EPMA results. All EPMA work was performed at the TAU facility at the University of Edinburgh. Additional thanks are given to Miss Sam Walters and Mr James Cooper for their assistance in the field. We thank Dr Tom Roland and Prof Nick Pearce for their assistance and comments on this manuscript.

References

1. Anderson, M.J. (2001) A new method for non-parametric multivariate analysis of variance. *Austral Ecology*, 26: 32-46.
2. Blockley, S.P.E., et al. (2005) A new and less destructive laboratory procedure for the physical separation of distal glass tephra shards from sediments. *Quaternary Science Reviews*, 24(16-17), pp.1952-1960.
3. Boyle, J.E. (1994) Tephra in lake sediments: An unambiguous geochronological marker? PhD. Thesis, University of Edinburgh, Edinburgh
4. Brewer, T. S., Leng, M. J., Mackay, A. W., Lamb, A. L., Tyler, J. J., & Marsh, N. G. (2008). Unravelling contamination signals in biogenic silica oxygen isotope composition: the role of major and trace element geochemistry. *Journal of Quaternary Science: Published for the Quaternary Research Association*, 23(4), 321-330.
5. Chambers, F.M., et al. (2004) Tephrostratigraphy of An Loch Mór, Inis Oírr, western Ireland: implications for Holocene tephrochronology in the northeastern Atlantic region. *Holocene* 14, 703-720.
6. Chan, S. H. (1989). A review on solubility and polymerization of silica. *Geothermics*, 18(1-2), 49-56.
7. Davies, S.M., et al. (2007) Cryptotephra sedimentation processes within two lacustrine sequences from west central Sweden. *Holocene* 17, 319-330.
8. Dugmore, A.J., et al. (1992) Geochemical stability of fine-grained silicic tephra layers in Iceland and Scotland. *Journal of Quaternary Science* 7, 173-183.
9. Dugmore, A.J., Larsen, G.R. and Newton, A.J., (1995) Seven tephra isochrones in Scotland. *The Holocene*, 5(3), pp.257-266.
10. Dugmore, A.J. and Newton, A.J. (1997) Holocene tephra layers in the Faroe Islands. *Froðskaparrit* 45, 141-154.
11. Dultz, S., Behrens, H., Hensch, G., & Deubener, J. (2016). Electrolyte effects on surface chemistry of basaltic glass in the initial stages of dissolution. *Chemical Geology*, 426, 71-84.
12. Einarsson, E. H., Larsen, G., & Thorarinsson, S. (1980). The Sólheimar tephra layer and the Katla eruption of 1357. *Náttúrufræðistofnun Íslands*
13. Global Volcanism Program (2013) Hekla (372070) in *Volcanoes of the World*, v. 4.7.6. Venzke, E (ed.). Smithsonian Institution. Downloaded 18 Mar 2019

(<https://volcano.si.edu/volcano.cfm?vn=372070>).

<https://doi.org/10.5479/si.GVP.VOTW4-2013>

14. Gudmundsdóttir, E. R., Schomacker, A., Brynjólfsson, S., Ingólfsson, Ó., & Larsen, N. K. (2018). Holocene tephrostratigraphy in Vestfirðir, NW Iceland. *Journal of Quaternary Science*, 33(7), 827-839.
15. Gudmundsson, A., et al. (1992). The 1991 eruption of Hekla, Iceland. *Bulletin of Volcanology*, 54(3), 238-246.
16. Hall, V.A. and Pilcher, J.R. 2002. Late-Quaternary Icelandic tephtras in Ireland and Great Britain: detection, characterization and usefulness. *Holocene*, 12, pp. 223-230
17. Hallam, B. R., Warren, S. E., & Renfrew, C. (1976, December). Obsidian in the western Mediterranean: characterisation by neutron activation analysis and optical emission spectroscopy. In *Proceedings of the Prehistoric Society* (Vol. 42, pp. 85-110). Cambridge University Press.
18. Hang, T., Wastegård, S., Veski, S., & Heinsalu, A. (2006). First discovery of cryptotephra in Holocene peat deposits of Estonia, eastern Baltic. *Boreas*, 35(4), 644-649.
19. Hayward, C., (2012) High spatial resolution electron probe microanalysis of tephtras and melt inclusions without beam-induced chemical modification. *The Holocene*, 22(1), pp.119-125.
20. Hunt, J. B., & Hill, P. G. (1996). An inter-laboratory comparison of the electron probe microanalysis of glass geochemistry. *Quaternary International*, 34, 229-241.
21. Iler, Ralph K. (1979). *Chemistry of Silica - Solubility, Polymerization, Colloid and Surface Properties and Biochemistry*. John Wiley & Sons.
22. Jensen, B. J. L., Mackay, H., Pyne-O'Donnell, S., Plunkett, G., Hughes, P. D. M., Froese, D. G., & Booth, R. (2014, December). Exceptionally long distance transport of volcanic ash: implications for stratigraphy, hazards and the sourcing of distal tephra deposits. In *AGU Fall Meeting Abstracts*.
23. Klavins, M., & Purmalis, O. (2013). Properties and structure of raised bog peat humic acids. *Journal of Molecular Structure*, 1050, 103-113.
24. Larsen, G., Dugmore, A., J. and Newton, A.J. (1999) Geochemistry of historic silicic tephtras in Iceland. *The Holocene* 9(4), 463-471

25. Larsen, G., Newton, A. J., Dugmore, A. J., & Vilmundardóttir, E. G. (2001). Geochemistry, dispersal, volumes and chronology of Holocene silicic tephra layers from the Katla volcanic system, Iceland. *Journal of Quaternary Science: Published for the Quaternary Research Association*, 16(2), 119-132.
26. Lawson, I.T., Swindles, G.T., Plunkett, G. and Greenberg, D., (2012) The spatial distribution of Holocene cryptotephra in north-west Europe since 7 ka: implications for understanding ash fall events from Icelandic eruptions. *Quaternary Science Reviews*, 41, pp.57-66.
27. Le Bas, M. L., Maitre, R. L., Streckeisen, A., Zanettin, B., & IUGS Subcommission on the Systematics of Igneous Rocks. (1986). A chemical classification of volcanic rocks based on the total alkali-silica diagram. *Journal of petrology*, 27(3), 745-750.
28. Lowe, D.J. (2011). Tephrochronology and its application: a review. *Quaternary Geochronology*, 6(2), 107-153
29. Mangerud, J., Furnes, H., and Johansen, J. (1986) A 9,000 year old ash bed on the Faroe Islands. *Quaternary Research* 26, 262-265.
30. Mangerud, J., et al. (1984) A Younger Dryas ash bed in western Norway and its possible correlations with tephra in cores from the Norwegian Sea and the North Atlantic. *Quaternary Research* 21, 85-104.
31. Matthews-Bird, et al. (2017) Aquatic community response to volcanic eruptions on the Ecuadorian Andean flank: evidence from the palaeoecological record. *Journal of Paleolimnology*, 58(4), pp.437-453.
32. McArdle, B.H. & Anderson, M.J. (2001) Fitting multivariate models to community data: a comment on distancebased redundancy analysis. *Ecology*, 82, 290-297.
33. Mysen, B. O., Virgo, D., & Seifert, F. A. (1985). Relationships between properties and structure of aluminosilicate melts. *American Mineralogist*, 70(1-2), 88-105.
34. Newton, A.J., Dugmore, A.J. and Gittings, B.M., (2007) TephraBase: tephrochronology and the development of a centralised European database. *Journal of Quaternary Science*, 22(7), pp.737-743.
35. Nicholson, H. et al. (1991) Geochemical and Isotopic Evidence for Crustal Assimilation Beneath Krafla, Iceland, *Journal of Petrology*, 32(5), pp. 1005–1020, <https://doi-org.wam.leeds.ac.uk/10.1093/petrology/32.5.1005>

36. Pearce, N. J., Denton, J. S., Perkins, W. T., Westgate, J. A., & Alloway, B. V. (2007). Correlation and characterisation of individual glass shards from tephra deposits using trace element laser ablation ICP-MS analyses: current status and future potential. *Journal of Quaternary Science*, 22(7), 721-736.
37. Pearce, N. J., Abbott, P. M., & Martin-Jones, C. (2014). Microbeam methods for the analysis of glass in fine-grained tephra deposits: a SMART perspective on current and future trends. *Geological Society, London, Special Publications*, 398(1), 29-46.
38. Persson, C., 1971. Tephrochronological investigation of peat deposits in Scandinavia and on the Faroe Islands. Sveriges reproduktions AB (distr.).
39. Pilcher, J.R., Hall, V.A. and McCormac, F.G. (1996) An outline tephrochronology for the Holocene of the north of Ireland. *Journal of Quaternary Science* 11 (6), 485-494.
40. Plunkett, G., & Pilcher, J. R. (2018). Defining the potential source region of volcanic ash in northwest Europe during the Mid-to Late Holocene. *Earth-Science Reviews*, 179, 20-37.
41. Pollard, A.M., Blockley, S.P.E. and Ward, K.R., (2003) Chemical alteration of tephra in the depositional environment: theoretical stability modelling. *Journal of Quaternary Science*, 18(5), pp.385-394.
42. Ponomareva, V., Portnyagin, M., Pendea, I. F., Zelenin, E., Bourgeois, J., Pinegina, T., & Kozhurin, A. (2017). A full Holocene tephrochronology for the Kamchatsky Peninsula region: Applications from Kamchatka to North America. *Quaternary Science Reviews*, 168, 101-122. doi:10.1016/j.quascirev.2017.04.031
43. Ratcliffe, J., et al. (2017) Contemporary carbon fluxes do not reflect the long-term carbon balance for an Atlantic blanket bog. *The Holocene*, 28(1)
44. Rea, HA, Swindles, GT and Roe, HM (2012) The Hekla 1947 tephra in the north of Ireland: regional distribution, concentration and geochemistry. *Journal of Quaternary Science* 27, 425-431.
45. Renberg, I., Brännvall, M. L., Bindler, R., & Emteryd, O. (2002). Stable lead isotopes and lake sediments—a useful combination for the study of atmospheric lead pollution history. *Science of the Total Environment*, 292(1-2), 45-54.
46. Roland, T.P., Mackay, H. and Hughes, P.D.M., (2015). Tephra analysis in ombrotrophic peatlands: a geochemical comparison of acid digestion and density separation techniques. *Journal of Quaternary Science*, 30(1), pp.3-8.

47. Rose, N.L., Golding, P.N.E. and Battarbee, R.W., (1996) Selective concentration and enumeration of tephra shards from lake sediment cores. *The Holocene*, 6(2), pp.243-246.
48. Sanger, L. J., Billett, M. F., & Cresser, M. S. (1994). The effects of acidity on carbon fluxes from ombrotrophic peat. *Chemistry and Ecology*, 8(4), 249-264.
49. Schindlbeck, J. C., Kutterolf, S., Straub, S. M., Andrews, G. D. M., Wang, K., & Mleneck-Vautravers, M. J. (2018). One million years tephra record at IODP sites U1436 and U1437: Insights into explosive volcanism from the Japan and Izu arcs. *Island Arc*, 27(3), e12244-n/a. doi:10.1111/iar.12244
50. Stevenson, J.A., et al. (2012) Distal deposition of tephra from the Eyjafjallajökull 2010 summit eruption. *Journal of Geophysical Research: Solid Earth*, 117(B9).
51. Streeter, R. and Dugmore, A. (2014) Late-Holocene land surface change in a coupled social ecological system, southern Iceland: a cross-scale tephrochronology approach. *Quaternary Science Reviews* 86, 99-114.
52. Swindles, G. (2006) Reconstructions of Holocene climate change from peatland in the north of Ireland. Unpublished PhD thesis, Queen's University, Belfast
53. Swindles, G. T., De Vleeschouwer, F., & Plunkett, G. (2010). Dating peat profiles using tephra: stratigraphy, geochemistry and chronology. *Mires and Peat*, 7.
54. Swindles, G. T., Lawson, I. T., Savov, I. P., Connor, C. B., & Plunkett, G. (2011). A 7000 yr perspective on volcanic ash clouds affecting northern Europe. *Geology*, 39(9), 887-890.
55. Swindles, G.T. et al. (2017) Holocene volcanic ash database for Northern Europe. Database. DOI: 10.13140/RG.2.2.11395.60966.
56. van der Bilt, W. G., Lane, C. S., & Bakke, J. (2017). Ultra-distal Kamchatkan ash on Arctic Svalbard: towards hemispheric cryptotephra correlation. *Quaternary Science Reviews*, 164, 230-235.
57. Wastegard, S., et al. (2001) The Mjauvotn tephra and other Holocene tephra horizons from the Faroe Islands: a link between the Icelandic source region, the Nordic Seas, and the European continent. *The Holocene* 11(1), 101-109.
58. Wastegård, S., Rundgren, M., Schoning, K., Andersson, S., Björck, S., Borgmark, A., & Possnert, G. (2008). Age, geochemistry and distribution of the mid-Holocene Hekla-S/Kebister tephra. *The Holocene*, 18(4), 539-549.

59. Wastegård, S. and Davies, S.M., (2009) An overview of distal tephrochronology in northern Europe during the last 1000 years. *Journal of Quaternary Science: Published for the Quaternary Research Association*, 24(5), pp.500-512.
60. Watson, E. J., Swindles, G. T., Lawson, I. T., & Savov, I. P. (2015). Spatial variability of tephra and carbon accumulation in a Holocene peatland. *Quaternary Science Reviews*, 124, 248-264.
61. Watson, E.J., Swindles, G.T., Lawson, I.T. and Savov, I.P., (2016) Do peatlands or lakes provide the most comprehensive distal tephra records?. *Quaternary Science Reviews*, 139, pp.110-128.
62. Watson, E.J., Swindles, G.T., Savov, I.P., Lawson, I.T., Connor, C.B. and Wilson, J.A., (2017) Estimating the frequency of volcanic ash clouds over northern Europe. *Earth and Planetary Science Letters*, 460, pp.41-49.
63. WoldeGabriel, G., Hart, W. K., & Heiken, G. (2005). Innovative tephra studies in the East African rift system. *Eos, Transactions American Geophysical Union*, 86(27), 255-255.
64. Wood, D.A. (1978) Major and Trace Element Variations in the Tertiary Lavas of Eastern Iceland and their Significance with respect to the Iceland Geochemical Anomaly, *Journal of Petrology*, 19 (3), pp 393–436,
<https://doi.org/10.1093/petrology/19.3.393>

Chapter 5: Is there a Climatic Control on Icelandic Volcanism?

Claire L. Cooper^{1,2}, Ivan P. Savov², Henry Patton³, Alun Hubbard⁴, Ruza F. Ivanovic², Jonathan L. Carrivick¹, Graeme T. Swindles^{1,5,6}

¹ School of Geography and water@Leeds, University of Leeds, UK

² School of Earth and Environment, University of Leeds, UK

³ Center for Arctic Gas Hydrate, Environment and Climate, Arctic University of Norway, Norway

⁴ Department of Earth Sciences, Aberystwyth University, UK

⁵ Geography, School of Natural and Built Environment, Queen's University Belfast, UK

⁶ Ottawa-Carleton Geoscience Centre and Department of Earth Sciences, Carleton University, Canada

Keywords: unloading effect, isostasy, deglaciation, crustal loading, volcanism

Abstract

The evidence for periods of increased volcanic activity following deglaciation, such as following ice sheet retreat after the Last Glacial Maximum, has been examined in several formerly glaciated areas, including Iceland, Alaska, and the Andean Southern Volcanic Zone. Here we present new evidence supporting the theory that during episodes of cooling in the Holocene, Icelandic volcanic activity decreased. By examining proximal and distal tephra records from Iceland spanning the last 12,500 years, we link two observed tephra minima to documented periods of climatic cooling and glacial advance, at 8.3 to 8 and 5.2 to 4.9 cal kyr BP. We simulate these periods in atmosphere-ocean and ice sheet models to assess the potential validity of the

postglacial 'unloading effect' on Icelandic volcanic systems. We conclude that an increase in glacial cover may have decreased shallow magma ascent rates, thus limiting eruption potential and producing apparent quiescent periods in proximal and distal tephra records. However, several major uncertainties remain regarding the theory, including geographical and temporal preservation biases and the importance of any unloading effects against other factors, and these will require more prolonged investigation in future research.

5.1 Introduction

The effect of reducing sub-aerial loads on crustal strain and lithostatic pressure, often referred to as the ‘unloading effect’, has been intermittently modelled and explored in a number of settings for the past few decades (Jull & McKenzie, 1996; Maclennan et al., 2002; Sigmundsson et al., 2010; Swindles et al., 2018a). In particular, many studies have emphasised the implications for seismic and volcanological hazards (Pagli & Sigmundsson, 2008; Manconi et al., 2009). However, the difficulties and uncertainties involved in modelling deep-crust and shallow-mantle systems have hindered the development of many forward models, resulting in significant ambiguity surrounding the theory, particularly regarding volcanic systems. Here, we present new evidence exploring a possible relationship between periods of glacial advance and reductions in volcanic activity from the Younger Dryas (around 12 ka) to the present day, as seen through several climate proxies and tephrochronological records.

It must be noted that such the existence of such a link between climate, glacial systems, and volcanoes remains highly controversial, most plainly evidenced in the dialogue between Swindles et al., 2018a, Harning et al., 2018b, and Swindles et al., 2018b. In Swindles et al.’s 2018 article ‘Climatic control on Icelandic volcanic activity during the mid-Holocene’, the authors report an apparent decrease in the frequency of known Icelandic eruptions centred on the period 5.5-4.5 ka, visible in both the distal Holocene tephra record and in the volume of lava erupted effusively from several Icelandic volcanoes, including Grímsvötn, Bárðarbunga, and Kverkfjöll. Though they concede that the root cause of volcanic periodicity in Iceland is not currently well understood, the authors also note that variations in rifting regimes have previously been linked to changes in magma upwelling rates (Sigmundsson et al., 2015), which in turn may be affected by increases or decreases in overlying pressure (Jull & McKenzie, 1996; Schmidt et al., 2013). Given the widespread nature of the observed ‘lull’ in activity, the authors posit that an external driver – in this case, alterations to the ice load – caused the observed changes. However, in the subsequent academic discussion of this article, Harning et al., 2018 note some apparent deficiencies in the materials and methods used, arguments that are later refuted by Swindles et al., 2018b.

Criticisms of the original article included limitations of the original tephra dataset, and uncertainties in the reconstructions of Icelandic palaeoclimate. These concerns were addressed in Swindles et al.'s reply, and are further explored in this paper. This manuscript aims to present an objective analysis of the theory, emulating the methods of Swindles et al., 2018a while also providing a critical discussion of the current methodological shortfalls.

One dominant criticism of the 'unloading theory' is rooted in the concept's currently theoretical nature. Physical geological evidence beyond the use of tephrochronology to reconstruct volcanic activity is scarce, primarily due to the timescales on which such phenomena would occur. In the absence of direct observational evidence, some possible geomorphological links have been made – Carrivick et al., 2019 describe a series of sub-glacial volcanic edifices at Kverkfjöll which appear to indicate an increase in explosive volcanic activity synchronous with a thinning of the overlying ice sheet. The research also notes that the same eruptive period seems to be linked to a migration of activity towards the Kverkfjöll central volcano, emphasising that overlying ice may exert a geographic control in addition to a mechanical control on volcanism. However, the vast majority of existing literature on the subject relies either on numerical modelling of the earth systems involved – usually from either a volcano-tectonic perspective, as in Schmidt et al. 2013, or from a glaciological perspective, as in Stevens et al., 2016 – or on the reconstruction of volcanic events using tephra. This latter technique has been applied to similar geospheric theories in the past, setting precedent for the research presented in this paper and in Swindles et al., 2018. McGuire et al., 1997 used a similar method of statistical analysis of tephra layers preserved in deep-sea sediment cores to reconstruct the frequency of explosive activity in the Mediterranean group of volcanoes, which they then linked to variations in local sea level, a factor which is itself linked to climatic change and to the growth or retreat of large ice sheets (McGuire et al., 1997).

Tephrochronology refers to the use of ash particles deposited in discrete layers during volcanic ashfall events to construct a chronological framework for stratigraphy. Distal deposits of volcanic ash from individual events provide useful isochrons across wide areas. Many previous studies have documented individual tephra layers across much of western Europe, and comprehensive

databases of Icelandic tephra have been compiled spanning the last 7,000 years (Newton et al., 2007; Swindles et al., 2011; Swindles et al., 2017). However, tephra layers in the geological record become increasingly sparse with age (Swindles et al., 2011). As a result, studies detailing ash records from the early Holocene and Late Glacial period (12.5 to 6.5 ka) are less common, and typically less successful in identifying the provenance of unknown tephra layers (Watson et al., 2017). As discussed previously in this thesis, there are many mitigating factors which can alter the preservation potential of volcanic glass in a given area. Variable snow cover, vegetation, surface runoff, and ground pH may all have a detrimental effect on tephra preservation, potentially compromising the record of a region. However, by drawing together reported tephras from a very wide geographic area, and by expanding the time frame of the research by several thousand years, we believe this potential bias has been eliminated to the best of our ability. Here we present the first complete tephrostratigraphy of Europe spanning the period 12.5 ka to the present day.

Our study aims to examine the proposed 'unloading effect' of glacial retreat on volcanic systems in Iceland within the Holocene period. The current trends of global climatic change and the rapid retreat and disappearance of Icelandic ice (Björnsson et al., 2013) make this a pertinent topic of conversation for the modern day, as the impacts of Icelandic eruptions in very recent years have had significant implications for European and international aviation (Ulfarsson & Unger, 2011; Budd et al., 2011) and caused subsequent short-term but nonetheless noteworthy economic effects in Europe (O'Regan, 2011). Investigation of this theory is also important as part of a wider effort to understand how the current projections of anthropogenic-driven climate change may affect the field of geohazards in the coming decades and centuries. Much scientific, media, and therefore public attention has been drawn in recent years to the potential impacts of climate change on natural disasters (Van Aalst, 2006; Kousky, 2014; Hallegatte, 2016). The importance of multidisciplinary perspectives on earth system sciences and particularly the study of earth system interactions is becoming increasingly vital to the field, and to that end this paper incorporates several geophysical elements, utilising both the physical tephra record and numerical simulations.

In order to constrain the variability of glacial loading during the identified climate events, our data are coupled with a thermomechanical model of Icelandic ice coverage and a reconstruction of Icelandic palaeoclimate obtained from climate model simulations spanning the period. We show what appears to be a positive connection between periods of glacial advance and greater ice thicknesses and periods of volcanic quiescence, following a variable lag of between < 100-600 years. We also discuss the shortfalls and uncertainties surrounding this theory and the methods used to support it.

5.2 Methods

5.2.1 Tephra

The distal tephra records in this study were compiled from verified sources largely detailed in Swindles et al., 2017, in addition to further references (Óladóttir et al., 2011; Gudmundsdóttir et al., 2012; Gudmundsdóttir et al., 2016; Harning et al., 2018a). The full database of tephra used in this study is included as supplementary material. Tephra ages may have been derived from historical correlations, directly radiocarbon dated, interpolated from age-depth models, wiggle-match radiocarbon dated, or dated through association with another tephra layer. All tephra layers used in this study were verified to have originated at Icelandic sources. While concerns have been raised regarding the reliability and preservation of tephra in geological time, particularly regarding the disparity between rhyolitic and basaltic glasses (detailed more thoroughly in Swindles et al., 2011; Watson et al., 2017), we have endeavoured to be as thorough as possible in collating documented tephra layers, and believe that the comparison of proximal and distal records is sufficient to eliminate the potential effects of preservation bias. Ages presented are in calibrated years before present (1950), and where the same event is reported in multiple sources with varying ages, the median reported age of these events is used to prevent misleading inflation of recorded volcanic activity within a given period.

5.2.2 Atmospheric-Ocean General Circulation Model

The climate model used in this study is the UK Met Office's HadCM3 coupled atmosphere-ocean-vegetation general circulation model (Valdes et al., 2017). For 26 to 21 ka and 21 to 0 ka, model boundary conditions were updated every 1000 and 500 years (respectively) in accordance with the PMIP4 last deglaciation protocol (Ivanovic et al., 2016) using the ICE-6G_C reconstruction of ice sheets and palaeogeography (Argus et al., 2014). Differences with the PMIP4 protocol are pragmatic: the CO₂ curves follow Lüthi et al., 2008 because the protocol had not been finalised at the point of running the simulations, and the simulations are of equilibrium-type rather than being transient (i.e. the boundary conditions were held constant for each 1000/500-year segment) enabling them to be run in parallel. The ocean is not explicitly forced with ice sheet meltwater in these simulations, and water is conserved by forcing global mean ocean salinity to match the ice sheet history, interpolating smoothly between the 1000/500-year timesteps of ICE-6G_C (melt-uniform in the PMIP4 protocol).

The climate means used here are calculated from the last 50 years of each simulation period. Ocean areas were masked out and land data was back-filled using a Poisson equation solver with overrelaxation. The native model grid was then interpolated to a higher resolution (0.5 × 0.5 degrees) using a bi-cubic spline. Bias correction was performed against New et al., 2000. See Morris et al., 2018 for more information on the model setup, downscaling and bias correction.

5.2.3 Ice Sheet Reconstruction

This simulation is a three-dimensional, finite-difference model utilising a 2 km resolution described in detail in Hubbard, 2006. The effects of temperature and precipitation change on ice sheet mass balance are simulated using a degree-day algorithm, chosen for its stability over a long-time scale and the simplicity of its parameterisation. The model acts under the assumptions that climate forcing may be applied uniformly across Iceland, and that the relationships between precipitation and temperature may be considered

constant over time. The degree-day coefficient was calibrated against glacial measurements from Norway, Greenland, and the Vatnajökull and Hofsjökull ice sheets in Iceland. Spatial gradients are introduced to simulate reduced atmospheric moisture during cooling. Ice thickness and flow velocity are coupled to the thermal evolution of the ice sheet via the calculation of absolute temperature and the initiation of basal sliding. Sea level is viewed as an external forcing variable.

Additionally, the model takes into account isostatic bed response to ice loading. This factor is coupled to ice sheet evolution using an elastic lithosphere, which is loaded using the integrated contribution of local and remote loads within a radius of ~100 km (Hubbard, 2006). The unloaded equilibrium topography is estimated through comparison to present-day subglacial topography. The topographic grid is derived from the terrestrial GTOPO30 (<1 km) and ETOPO2 (<4 km) global data sets, merged onto an Albers equal-area conic projection, and incorporating known subglacial topography from Vatnajökull, Mýrdalsjökull and Hofsjökull. The combined DEM was then adjusted assuming steady-state equilibrium.

The boundary conditions of the model reference mean annual temperature and precipitation values taken between 1961 and 1990 by the Icelandic Meteorological Office, interpolated across the model domain. Likewise, geothermal heat flux was derived from Icelandic borehole measurements (Flóvenz & Saemundsson, 1993), and interpolated across the model using a kriging algorithm.

5.3 Results

5.3.1 A correlation between cooling events and lulls in volcanic activity?

It is possible to evaluate the trends of past volcanic activity in Iceland by examining both proximal and distal records of volcanic ash deposits. By combining tephra records retrieved from a range of distances from the volcanic source, we eliminate the bias created by reworking and ‘over-

writing' of deposits by more recent activity (Swindles et al., 2018a), producing a more accurate representation of quiescent and active periods on the island.

The Northern Europe Volcanic Ash database (NEVA) was first published by Swindles et al. 2011, and has since undergone many updates and revisions (Swindles et al., 2017; Watson et al., 2017). This study utilises the newest iteration of the database, in addition to supplemental data spanning a further 5000 years to a maximum age of 12,500 cal kyr BP, as presented in the supplemental material. Additionally, we complement the NEVA distal record with proximal records of Icelandic activity compiled from a number of sources (Óladóttir et al., 2011; Gudmundsdóttir et al., 2012; Gudmundsdóttir et al., 2016; Harning et al., 2018a), including terrestrial and marine shelf data.

In figure 1, we identify three periods in which volcanic activity appears to decline, ending in three tephra minima at 8.3 to 8 cal ka, 5.2 to 4.9 ka, and 3.7 to 3.4 ka. In each instance, the number (*n*) of tephra layers found in western Europe decreases by between 50-60% from previous levels. These declines correlate strongly with periods of rapid temperature decrease, as inferred from variations in 18O isotopes from the GISP2 Greenland cores (Andersen, 2004). In addition this manuscript utilises combined Icelandic sediment accumulation rates and lacustrine C:N ratios (Geirsdóttir et al., 2013). There is an apparent lag period between the onset of cooling and the point of minimum volcanic activity of ~100-600 years, though the onset of volcanic quiescence typically appears to take < 300 years. An apparent sharp increase in *n* that seems to be associated with cooler conditions and increased ice volume within the most recent ~1500 years is attributable to improved preservation and reduced secondary tephra transportation of within this time frame (Swindles et al., 2011; Swindles et al., 2017; Watson et al., 2017).

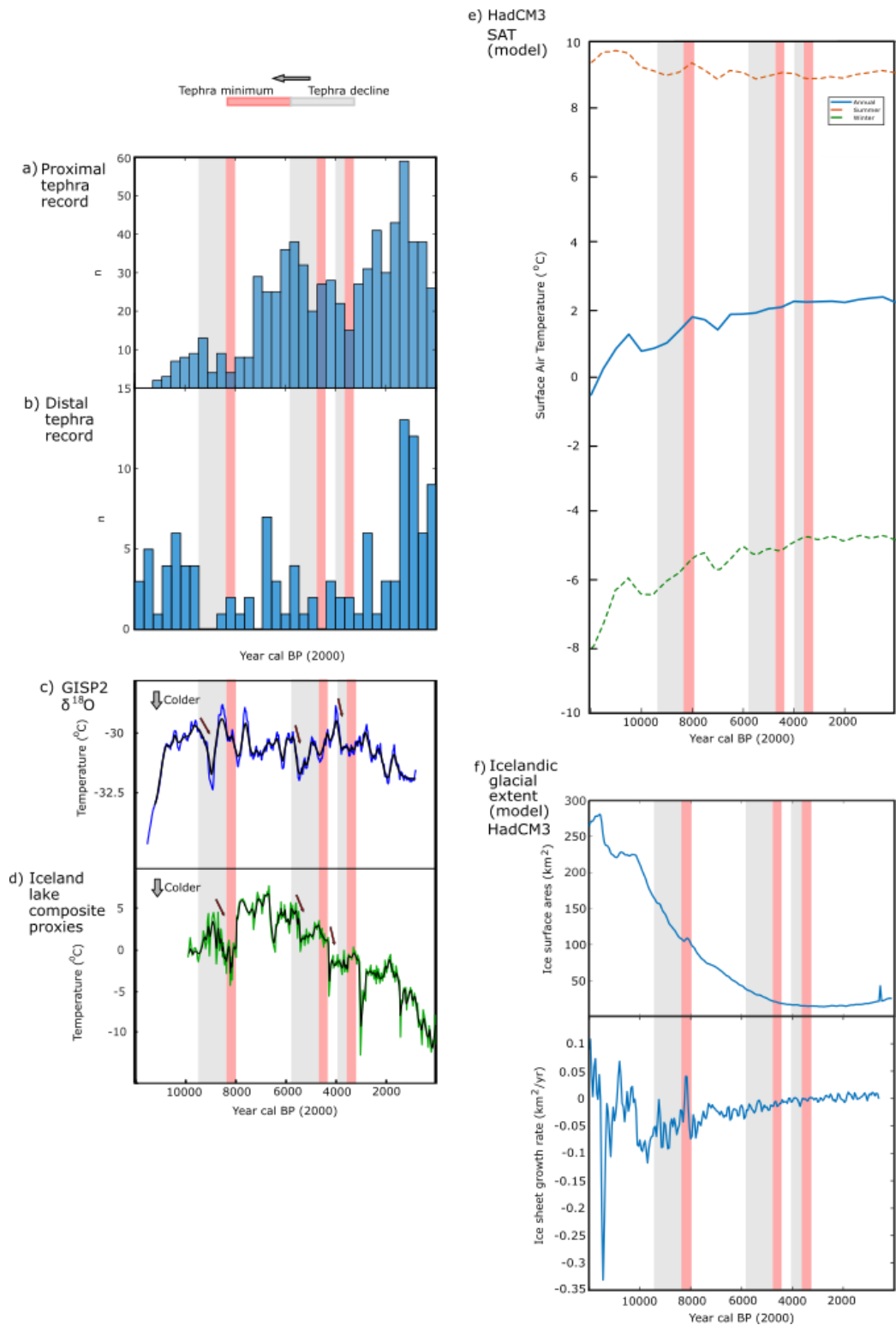


Figure 1: a) Number (n) of Icelandic proximal tephra in 350 year bins (Óladóttir et al., 2011; Gudmundsdóttir et al., 2012; Gudmundsdóttir et al., 2016; Harning et al., 2018a); b) Number of Icelandic distal tephra in 350 year bins; c) Northern Hemisphere mean temperature derived from Gaussian smoothed GISP2 $\delta^{18}O$ concentrations (Andersen et al., 2004); d) Icelandic mean temperature derived from lake composite record (Geirsdóttir et al., 2013); e) Icelandic surface air temperature (SAT) seasonal averages at 500-year resolution from HadCM3 model; f) Modelled ice sheet surface area and growth rate.

The three cooling events which appear to correlate with declines in volcanic activity in Iceland are well-documented and easily observed in climate proxy records. The 8.2 ka event can be seen in climate records across the Northern Hemisphere, and has been linked to widespread influxes of freshwater melt from the Agassiz and Ojibway proglacial lakes (Alley et al., 1997; Wiersma & Renssen, 2006), although accelerated melting of the Laurentide ice sheet may provide a more plausible alternative explanation (Matero et al., 2017). This event is notable for its relatively short duration and well-constrained boundaries (Weirsma & Renssen, 2006), with the most rapid cooling occurring between ~8.3 to 8.0 ka (Quillmann et al., 2012), though many palaeoecological indicators place the initial onset of cooling at around 8.5 to 8.4 ka (Alley et al., 1997; Matero et al., 2017). Likewise, evidence for the 5.2 ka global climate event typically has distinct boundaries, and is generally recognised to be part of a larger trend of climate change spanning from 6 to 5 ka (Roland et al., 2015). While the data concerning a climatic event around 4.3 to 3.4 ka is less coherent, multiple sources suggesting abrupt shifts to globally drier, cooler conditions within that period (such as low-latitude drought conditions (Hoerling & Kumar, 2003), changes to Northern Hemisphere ocean-atmospheric circulation regimes (Bond et al., 2001; Booth et al., 2005; Roland et al., 2014), and lake-level changes around the Mediterranean (Magny et al., 2009)) are often collected under the banner of the 4.2 ka event. These signals are generally recognised to reflect a spatially complex but overall consistent pattern of a climatic shift, occurring globally but most notable in mid- and low latitudes (Walker et al., 2019). Walker et al. (2019) recognise the 4.2 ka event as marking the onset of a new subepoch of the Holocene, termed the Meghalayan Stage. This article reports the use of a speleotherm located in the state of Meghalaya in north-east India as a new Global boundary Stratotype Section and Point (GSSP), and notes that although proxy records of the 4.2 ka event record variable climatic alterations across geographic regions (for example, atmospheric and oceanic cooling in the North Atlantic and Western Canada (Orme et al., 2018) and synchronous aridification across mid- and low-latitudes (Booth et al., 2005; Wanner et al., 2015)), the event appears to have been the 'turning point' for the establishment of a new global climate regime (Walker et al., 2019).

Efforts to determine the underlying factors controlling volcanic and rifting activity in Iceland are often complicated due to uncertainties regarding sporadic rifting rates and mantle plume activity (Larsen et al., 1998; Jones et al., 2002). While periodic variations in magma supply have previously been linked to localised changes to volcanic activity, typically affecting volcanic systems within specific areas (for example, synchronous decreases in activity at several volcanic centres beneath Vatnajökull attributed to a decrease in local magma generation (Óladóttir et al., 2011)), such a widespread and spatially uniform response across multiple volcanic systems suggests the influence of large-scale external forcing.

5.3.2 *Analysing the glacial loading effect in Iceland*

The principle behind the so-called ‘unloading effect’ relies on isostatic adjustment following glacial growth or retreat, with subsequent impacts on subsurface geothermal and mechanical regimes (Jull & McKenzie, 1996; Schmidt et al., 2013) (see figure 2). Under this hypothesis, a reduction in glacial loading would reduce the vertical pressure on both deep and shallow magma storage, resulting in greater quantities of melt (Jull & McKenzie, 1996; Schmidt et al., 2013), potentially increasing the connectivity of the magma ‘plumbing’ system at depth (Eksincho, 2019), thereby increasing the depth of volatile exsolution leading to explosive eruptions (Swindles et al., 2018a). It therefore follows that the reverse scenario may hold true – that an increase in glacial loading would cause compression, and that this could effectively reduce the likelihood of an explosive eruption.

In order to test this reciprocal hypothesis against the observed tephrochronological results, we model Holocene and Late Glacial Icelandic ice sheet coverage and palaeoclimate. The model of ice extent is a three-dimensional, thermomechanically coupled simulation adapted from Hubbard, 2006, relying on sub-glacial topography, bathymetry, geothermal heat flux and surface temperature (Hubbard, 2006; Hubbard et al., 2006).

Palaeoclimate is derived from HadCM3 equilibrium-type climate simulations performed at 1 ka intervals 26 to 21 ka and 500-year intervals 21 to 0 ka,

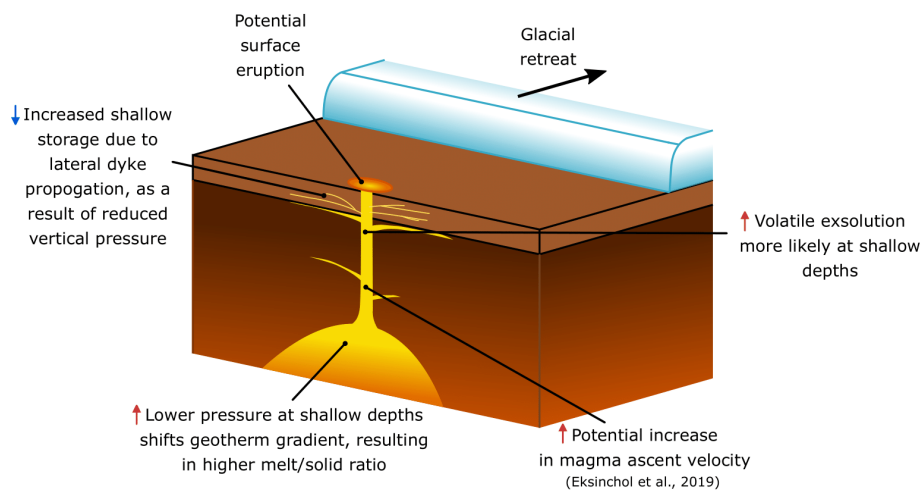
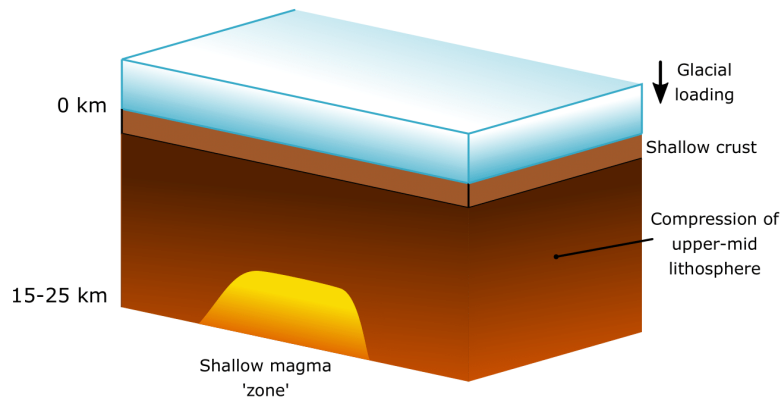


Figure 2: Conceptual model of ice sheet unloading on a volcanic system. In a subglacial system, the overlying weight causes compression of the upper crust, which is subsequently released when the ice sheet (or glacier) retreats. Peripheral volcanic systems then undergo decompression and a potential rapid increase in melt production, significantly increasing the potential for surface eruptions.

broadly following the PMIP4 last deglaciation protocol (Ivanovic et al., 2016). See ‘Methods’ for further information.

From the climate simulations, we infer a decrease in mean Icelandic summer surface air temperatures (SAT) of between 0.2-0.5 °C approximately concurrently with two of the indicated periods, in agreement with previously published works (Geirsdóttir et al., 2009; Morris et al., 2018). In the case of

the tephra minimum observed between 8.3 to 8.0 ka, the model suggests an initial onset of cooling between 10 to 9.5 ka, with a temperature minimum between 9.5 and 9.0 ka. A decrease in recorded distal tephra layers is apparent from approximately 10 ka to the 8.0 ka minimum. However, as the proximal record becomes inherently less reliable towards the early Holocene (Swindles et al., 2011; Watson et al., 2017), this trend is difficult to corroborate. The temporal resolution of the climate simulations does not resolve abrupt climate fluctuations such as the 8.2 climatic event in Iceland (Geirsdóttir et al., 2013), which suggests that the observed decline in volcanic activity may be related to a longer-term trend of cooling and ice sheet advance in the early Holocene (Geirsdóttir et al., 2009; Morris et al., 2018). However, the higher-resolution glacial model records a sharp increase in ice sheet growth rate from a trend of slow retreat to an expansion at the rate of $\sim 0.05 \text{ km}^2/\text{yr}$ coinciding with the tephra minimum at 8.2 ka, indicating an abrupt cooling event which may have precipitated a near-immediate (on the order of a century or less) quiescent response from the volcanic systems.

Further decreases in average summer and winter temperatures are recorded between 6.0 and 5.5 ka, where the climate model indicates an average normalised temperature decrease of $\sim 0.3 \text{ }^\circ\text{C}$ in both summer and winter seasons (see figure 1). The lacustrine and isotope proxy records for this time show a period of cooling of a slightly lower magnitude compared to the 8.2 ka event ($\sim 0.3\text{-}2.0 \text{ }^\circ\text{C}$ compared with $\sim 0.7\text{-}3.0 \text{ }^\circ\text{C}$) over a more sustained period – approximately 500 years compared to 100-200 years. This lengthened timescale of cooling may account for the apparent ‘lag time’ observed between the onset of cooling and the identified tephra minimum. Previous studies have suggested a delay of 500-600 years (Swindles et al., 2018a) between climatic cooling and volcanic response for this event, which is consistent with our results.

Conversely, the climate model records no significant temperature fluctuation associated with the suggested tephra minimum between 3.7 to 3.3 ka. Likewise, the climate proxies for this period provide significantly less

convincing evidence for a coherent pattern of substantial cooling. Therefore, while an apparent decline in volcanic activity is evident in the proximal and distal tephra record for this period, this signal may have instead been caused by non-climatic or non-isostatic factors, such as changes to the regional tectonic or magmatic regimes (Jones et al., 2002; Pagli & Sigmundsson, 2008). Additionally, the climate model indicates an abrupt cooling period at around 7 ka. However, there is little physical evidence to support this in the documented proxies (Óladóttir et al., 2011; Gudmundsdóttir et al., 2012; Gudmundsdóttir et al., 2016; Harning et al., 2018a). This period in fact coincides with current estimates for the Holocene Thermal Maximum in Iceland (Caseldine et al., 2006; Knudsen et al., 2008), suggesting that this data point may be a result of the local climatic conditions are not well represented in the model at this time and may therefore be discounted.

5.4 Discussion and Conclusions

Our results indicate that a glacial control on volcanic activity in Iceland remains theoretically possible, and may be present in the European stratigraphic and palaeoclimate record. Furthermore, we suggest that the magnitude and rapidity of any climate cooling and subsequent glacial loading event would be a strong factor in determining the response time of underlying volcanic systems regarding the onset of quiescence. It follows that the importance of this factor would be as high for a suggested relative increase in volcanic eruption frequency following warming and glacial retreat (Jull & McKenzie, 1996; Licciardi et al., 2007; Sigmundsson et al., 2010; Swindles et al., 2018a). Regional studies focusing on volcanic systems following the last deglaciation (21 – 12.5 ka) indicate increases in productivity that range from a decadal scale subsequent to local ice retreat (Maclennan et al., 2002; Praetorius et al., 2016) to a multi-centennial scale across regional volcanic systems (Huybers & Langmuir, 2009; Watt et al., 2013). Figure 3 shows a simplified model of shallow melt ascent, wherein, following a fifty-year offset period after the onset of warming to allow for glacial response, an initial subglacial melt ascent rate of 30 m/yr (Eksinhol et al., 2019) is increased to 50 m/yr and 100 m/yr, according to current estimates of melt ascent rate (Eksinhol et al., 2019). These ‘melt ascent’ figures may be viewed

as an amalgamation of dyke and conduit transport, shallow melt production within sill storage regions, and influx of magma from depth (Schmidt et al., 2013; Eksinhol et al., 2019). These estimates support a centuries-scale response time of existing magma bodies between 15-25 km depth. This suggests that the more immediate (< 100 year) response observed to more rapid, higher-magnitude cooling events (MacLennan et al., 2002; Praetorius et al., 2016) such as the 8.2 ka event in this study may either represent a much more significant mobilisation of magma, either through increased upwelling due to decompression (Eksinhol et al., 2019) and/or enhanced melt production (Jull & McKenzie, 1996; Schmidt et al., 2013), or represent a rapid utilisation of very shallow (> 15 km) pooled magma stored in the crust during glaciation (MacLennan et al., 2002; Watt et al., 2013).

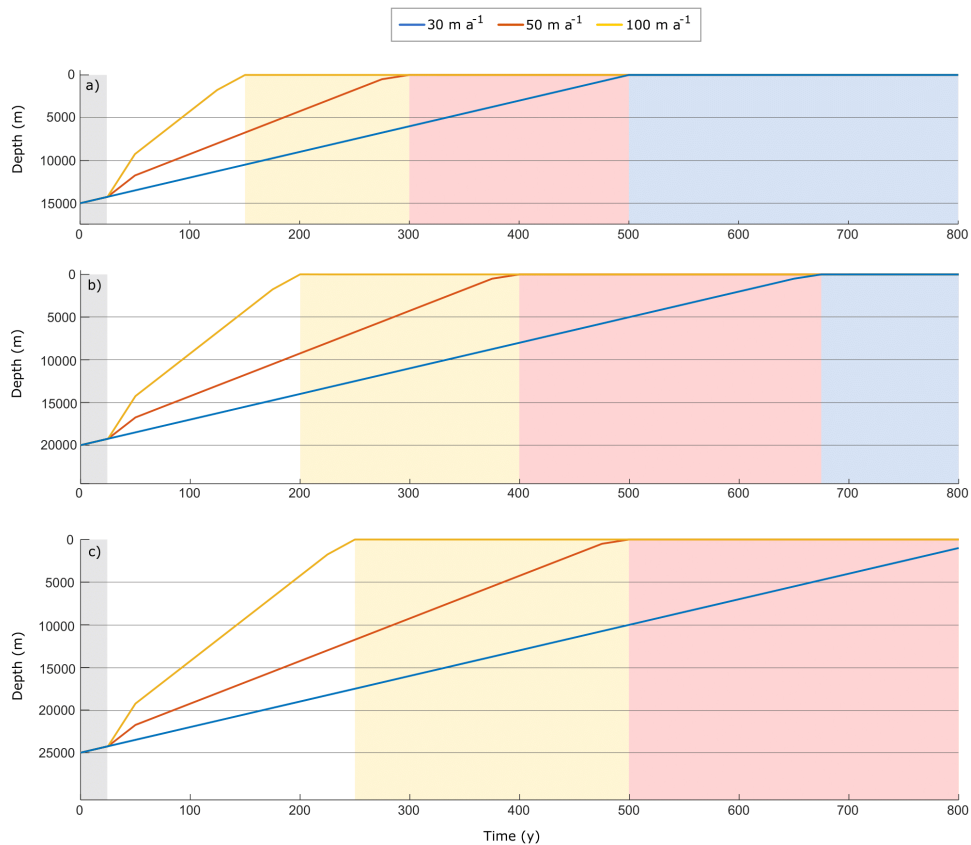


Figure 3: Depth-time models of magma ascent for shallow bodies at a) 15 km, b) 20 km, and c) 25 km depth. Allowing for a steady state of glaciation (grey) for 50 yrs following climate perturbation, the melt ascent velocity is then increased to 50 m a⁻¹ (red) or 100 m a⁻¹ (yellow), or remains constant at 30 m a⁻¹. The corresponding colour screens indicate the period in which each condition would allow melt to be transported to the surface, i.e. the 'lag time' of melt transport.

However, there are a number of factors which still cast doubt on the validity of this theory. While the combination of proximal and distal tephra records may represent the most accurate reconstruction of Icelandic volcanism currently possible (Swindles et al., 2018a) it has been noted that the preservation of prehistoric eruption material decreases dramatically with even short distances from the volcanic source (Thordarson & Höskuldsson, 2008). The unreliable preservation of ashfall material in glaciated Northern Hemisphere regions has previously been highlighted in Cooper et al., 2019, introducing significant uncertainty into the reconstruction of age-distribution patterns of volcanic events. Atmospheric perturbations, ground conditions, and erosion/deposition regimes during various climate periods may all affect the completeness of the tephra record, influencing the accuracy of any frequency reconstruction based on these data. Therefore, while the current compilation of sedimentary records may show variation in favour of the unloading theory, it is possible that the inclusion of events which were not preserved (either due to eruption parameters not favouring tephra production or due to failure to incorporate into local sedimentary records) would change the current understanding of the distribution of Icelandic volcanism through time.

Additionally, there are many instances where it is clear that rapid-onset or high-magnitude cooling events do not coincide with decreases in volcanic activity. One pertinent example is the Little Ice Age (1300 – 1890 AD), which is known to have caused significant glacial advance in Iceland, particularly in the late eighteenth to early nineteenth century (Chenet et al., 2010), but which is not reflected in the tephra records. Multiple other cooling periods during the Holocene, for example at 7, 4.2, and 3 ka (Geirsdóttir et al., 2013) show a similar lack of response by the Icelandic volcanic systems, indicating that, if a climatic control on volcanic activity does exist in this region, it is not often the dominant controlling factor in suppressing volcanism.

In conclusion, while there may be evidence to continue to support the existence of the unloading theory in Iceland, the current degree of

uncertainty regarding the timings and magnitude of fluctuating volcanic activity in this region means that caution must be exercised before firm conclusions may be drawn.

Acknowledgements

C.L. Cooper acknowledges a Leeds Anniversary Research Scholarship in addition to a Climate Research Bursary awarded by the University of Leeds held during the course of this study. The contribution from R.F. Ivanovic was partly supported by a Natural Environment Research Council (United Kingdom) Independent Research Fellowship (NE/K008536/1).

References

1. Alley, R. B. (2000) The Younger Dryas cold interval as viewed from central Greenland. *Quaternary Science Reviews*, 19(1-5), 213-226.
2. Alley, R. B., Mayewski, P. A., Sowers, T., Stuiver, M., Taylor, K. C., & Clark, P. U. (1997) Holocene climatic instability: A prominent, widespread event 8200 yr ago. *Geology*, 25(6), 483-486.
3. Andersen, K.K., Azuma, N., Barnola, J.M., Bigler, M., Biscaye, P., Caillon, N., et al. (2004) High-resolution record of Northern Hemisphere climate extending into the last interglacial period. *Nature*, 431(7005), 147.
4. Argus, D.F., Peltier, W.R., Drummond, R. & Moore, A.W. (2014) The Antarctica component of postglacial rebound model ICE-6G_C (VM5a) based upon GPS positioning, exposure age dating of ice thicknesses, and relative sea level histories. *Geophysical Journal International*, 198(1), 537-563.
5. Björnsson, H., Pálsson, F., Gudmundsson, S., Magnússon, E., Adalgeirsdóttir, G., Jóhannesson, T., Berthier, E., Sigurdsson, O. and Thorsteinsson, T. (2013). Contribution of Icelandic ice caps to sea level rise: Trends and variability since the Little Ice Age. *Geophysical Research Letters*, 40(8), pp.1546-1550.
6. Bond, G., Kromer, B., Beer, J., Muscheler, R., Evans, M.N., Showers, W. et al. (2001) Persistent solar influence on North Atlantic climate during the Holocene. *Science*, 294(5549), 2130-2136.
7. Booth, R. K., Jackson, S. T., Forman, S. L., Kutzbach, J. E., Bettis III, E. A., Kreigs, J., & Wright, D. K. (2005) A severe centennial-scale drought in midcontinental North America 4200 years ago and apparent global linkages. *The Holocene*, 15(3), 321-328.
8. Budd, L., Griggs, S., Howarth, D. and Ison, S. (2011). A fiasco of volcanic proportions? Eyjafjallajökull and the closure of European airspace. *Mobilities*, 6(1), pp.31-40.
9. Carrivick, J.L., Russell, A.J., Rushmer, E.L., Tweed, F.S., Marren, P.M., Deeming, H. and Lowe, O.J. (2009) Geomorphological evidence towards a de-glacial control on volcanism. *Earth Surface Processes and Landforms*, 34(8), 1164-1178
10. Caseldine, C., Langdon, P., & Holmes, N. (2006) Early Holocene climate variability and the timing and extent of the Holocene thermal maximum (HTM) in northern Iceland. *Quaternary Science Reviews*, 25(17-18), 2314-2331.
11. Chenet, M., Roussel, E., Jomelli, V., & Grancher, D. (2010). Asynchronous Little Ice Age glacial maximum extent in southeast Iceland. *Geomorphology*, 114(3), 253-260.

12. Cooper, C. L., Swindles, G. T., Watson, E. J., Savov, I. P., Gałka, M., Gallego-Sala, A., & Borken, W. (2019). Evaluating tephrochronology in the permafrost peatlands of northern Sweden. *Quaternary Geochronology*, 50, 16-28.
13. Eksinçol, I., Rudge, J. F., & Maclennan, J. (2019) Rate of Melt Ascent beneath Iceland from the Magmatic Response to Deglaciation. *Geochemistry, Geophysics, Geosystems*.
14. Flóvenz, Ó. G., & Saemundsson, K. (1993) Heat flow and geothermal processes in Iceland. *Tectonophysics*, 225(1-2), 123-138.
15. Geirsdóttir, Á., Miller, G. H., Axford, Y., & Ólafsdóttir, S. (2009) Holocene and latest Pleistocene climate and glacier fluctuations in Iceland. *Quaternary Science Reviews*, 28(21-22), 2107-2118.
16. Geirsdóttir, Á., Miller, G. H., Larsen, D. J., & Ólafsdóttir, S. (2013) Abrupt Holocene climate transitions in the northern North Atlantic region recorded by synchronized lacustrine records in Iceland. *Quaternary Science Reviews*, 70, 48-62.
17. Gudmundsdóttir, E. R., Larsen, G., & Eiríksson, J. (2012) Tephra stratigraphy on the North Icelandic shelf: extending tephrochronology into marine sediments off North Iceland. *Boreas*, 41(4), 719-734.
18. Gudmundsdóttir, E. R., Larsen, G., Björck, S., Ingólfsson, Ó., & Striberger, J. (2016) A new high-resolution Holocene tephra stratigraphy in eastern Iceland: Improving the Icelandic and North Atlantic tephrochronology. *Quaternary Science Reviews*, 150, 234-249.
19. Hallegatte, S. (2016) *Natural disasters and climate change*. Springer International Pu.
20. Harning, D.J., Thordarson, T., Geirsdóttir, Á., Zalzal, K. and Miller, G.H. (2018a) Provenance, stratigraphy and chronology of Holocene tephra from Vestfirðir, Iceland. *Quaternary Geochronology*, 46, 59-76.
21. Harning, D. J., Geirsdóttir, Á., Thordarson, T., & Miller, G. H. (2018b). Climatic control on Icelandic volcanic activity during the mid-Holocene: COMMENT. *Geology*, 46(5), e443-e443.
22. Hoerling, M., & Kumar, A. (2003) The perfect ocean for drought. *Science*, 299(5607), 691-694.
23. Hubbard, A. (2006) The validation and sensitivity of a model of the Icelandic ice sheet. *Quaternary Science Reviews*, 25(17-18), 2297-2313.
24. Hubbard, A., Sugden, D., Dugmore, A., Norddahl, H., & Pétursson, H. G. (2006) A modelling insight into the Icelandic Last Glacial Maximum ice sheet. *Quaternary Science Reviews*, 25(17-18), 2283-2296.

25. Huybers, P., & Langmuir, C. (2009) Feedback between deglaciation, volcanism, and atmospheric CO₂. *Earth and Planetary Science Letters*, 286(3-4), 479-491.
26. Ivanovic, R., Gregoire, L., Kageyama, M., Roche, D., Valdes, P., Burke, A. et al. (2016) Transient climate simulations of the deglaciation 21-9 thousand years before present (version 1)-PMIP4 Core experiment design and boundary conditions. *Geoscientific Model Development*, 9, 2563-2587.
27. Jones, S. M., White, N., & Maclennan, J. (2002) V-shaped ridges around Iceland: Implications for spatial and temporal patterns of mantle convection. *Geochemistry, Geophysics, Geosystems*, 3(10), 1-23.
28. Jull, M., and McKenzie, D. (1996) The effect of deglaciation on mantle melting beneath Iceland. *Journal of Geophysical Research: Solid Earth* 101.B10 21815-21828.
29. Knudsen, K. L., Søndergaard, M. K. B., Eiriksson, J., & Jiang, H. (2008) Holocene thermal maximum off North Iceland: Evidence from benthic and planktonic foraminifera in the 8600–5200 cal year BP time slice. *Marine Micropaleontology*, 67(1-2), 120-142.
30. Kousky, C., (2014) Informing climate adaptation: A review of the economic costs of natural disasters. *Energy Economics*, 46, 576-592.
31. Larsen, G., Gudmundsson, M. T., & Björnsson, H. (1998) Eight centuries of periodic volcanism at the center of the Iceland hotspot revealed by glacier tephrostratigraphy. *Geology*, 26(10), 943-946.
32. Licciardi, J.M., Kurz, M.D., and Curtice, J.M. (2007) Glacial and volcanic history of Icelandic table mountains from cosmogenic ³He exposure ages. *Quaternary Science Reviews*, 26, 1529–1546, doi:10.1016/j.quascirev.2007.02.016.
33. Lüthi, D., Le Floch, M., Bereiter, B., Blunier, T., Barnola, J. M., Siegenthaler, U. et al. (2008) High-resolution carbon dioxide concentration record 650,000–800,000 years before present. *Nature*, 453(7193), 379.
34. Maclennan, J., Jull, M., McKenzie, D., Slater, L., & Grönvold, K. (2002) The link between volcanism and deglaciation in Iceland. *Geochemistry, Geophysics, Geosystems*, 3(11), 1-25
35. Magny, M., Vannière, B., Zanchetta, G., Fouache, E., Touchais, G., Petrika, L., et al. (2009) Possible complexity of the climatic event around 4300—3800 cal. BP in the central and western Mediterranean. *The Holocene*, 19(6), 823-833.
36. Manconi, A., Longpré, M. A., Walter, T. R., Troll, V. R., & Hansteen, T. H. (2009) The effects of flank collapses on volcano plumbing systems. *Geology* 37.12, 1099-1102.

37. Matero, I. S. O., Gregoire, L. J., Ivanovic, R. F., Tindall, J. C., & Haywood, A. M. (2017) The 8.2 ka cooling event caused by Laurentide ice saddle collapse. *Earth and Planetary Science Letters*, 473, 205-214.
38. McGuire, W.J., Howarth, R.J., Firth, C.R., Solow, A.R., Pullen, A.D., Saunders, S.J., Stewart, I.S. and Vita-Finzi, C. (1997) Correlation between rate of sea-level change and frequency of explosive volcanism in the Mediterranean. *Nature*, 389(6650), 473-476.
39. Meeker, L. D., & Mayewski, P. A. (2002). A 1400-year high-resolution record of atmospheric circulation over the North Atlantic and Asia. *The Holocene*, 12(3), 257-266.
40. Morris, P. J., Swindles, G. T., Valdes, P. J., Ivanovic, R. F., Gregoire, L. J., Smith, M. W., et al. (2018) Global peatland initiation driven by regionally asynchronous warming. *Proceedings of the National Academy of Sciences*, 115(19), 4851-4856.
41. New, M., Hulme, M., & Jones, P. (2000) Representing twentieth-century space–time climate variability. Part II: Development of 1901–96 monthly grids of terrestrial surface climate. *Journal of Climate*, 13(13), 2217-2238.
42. Newton, A. J., Dugmore, A.J., and Gittings, B.M. (2007) Tephrobase: tephrochronology and the development of a centralised European database. *Journal of Quaternary Science* 22.7, 737-743.
43. Óladóttir, B. A., Larsen, G., & Sigmarsson, O. (2011) Holocene volcanic activity at Grímsvötn, Bárðarbunga and Kverkfjöll subglacial centres beneath Vatnajökull, Iceland. *Bulletin of Volcanology*, 73(9), 1187-1208.
44. Orme, L.C., Miettinen, A., Divine, D., Husum, K., Pearce, C., Van Nieuwenhove, N., Born, A., Mohan, R. and Seidenkrantz, M.S. (2018). Subpolar North Atlantic sea surface temperature since 6 ka BP: Indications of anomalous ocean-atmosphere interactions at 4-2 ka BP. *Quaternary Science Reviews*, 194, 128-142.
45. Pagli, C., and Sigmundsson, F. (2008) Will present day glacier retreat increase volcanic activity? Stress induced by recent glacier retreat and its effect on magmatism at the Vatnajökull ice cap, Iceland. *Geophysical Research Letters* 35.9
46. Praetorius, S., Mix, A., Jensen, B., Froese, D., Milne, G., Wolhowe, M., et al. (2016) Interaction between climate, volcanism, and isostatic rebound in Southeast Alaska during the last deglaciation. *Earth and Planetary Science Letters*, 452, 79-89.
47. Quillmann, U., Marchitto, T.M., Jennings, A.E., Andrews, J.T., and Friestad, B.F. (2012) Cooling and freshening at 8.2 ka on the NW Iceland Shelf recorded in paired $\delta^{18}\text{O}$ and Mg/Ca measurements of the benthic foraminifer *Cibicides lobatulus*. *Quaternary Research*, 78, 528–539, doi:10.1016/j.yqres.2012.08.003.

48. O'Regan, M. (2011). On the edge of chaos: European aviation and disrupted mobilities. *Mobilities*, 6(1), pp.21-30.
49. Roland, T. P., Caseldine, C. J., Charman, D. J., Turney, C. S. M., & Amesbury, M. J. (2014) Was there a '4.2 ka event' in Great Britain and Ireland? Evidence from the peatland record. *Quaternary Science Reviews*, 83, 11-27.
50. Roland, T.P., Daley, T.J., Caseldine, C.J., Charman, D.J., Turney, C.S.M., Amesbury, M.J., et al. (2015) The 5.2 ka climate event: Evidence from stable isotope and multi-proxy palaeoecological peatland records in Ireland. *Quaternary Science Reviews*, 124, 209-223.
51. Schmidt, P., Lund, B., Hieronymus, C., Maclennan, J., Árnadóttir, T., & Pagli, C. (2013) Effects of present-day deglaciation in Iceland on mantle melt production rates. *Journal of Geophysical Research: Solid Earth*, 118(7), 3366-3379.
52. Sigmundsson, F., Pinel, V., Lund, B., Albino, F., Pagli, C., Geirsson, H., & Sturkell, E. (2010) Climate effects on volcanism: influence on magmatic systems of loading and unloading from ice mass variations, with examples from Iceland. *Philosophical Transactions of the Royal Society of London A: Mathematical, Physical and Engineering Sciences* 368, 2519-2534.
53. Sigmundsson, F., Hooper, A., Hreinsdóttir, S., Vogfjörð, K.S., Ófeigsson, B.G., Heimisson, E.R., Dumont, S., Parks, M., Spaans, K., Gudmundsson, G.B. and Drouin, V. (2015) Segmented lateral dyke growth in a rifting event at Bárðarbunga volcanic system, Iceland. *Nature*, 517(7533), 191-195.
54. Stevens, N.T., Parizek, B.R. and Alley, R.B., (2016) Enhancement of volcanism and geothermal heat flux by ice-age cycling: A stress modeling study of Greenland. *Journal of Geophysical Research: Earth Surface*, 121(8), 1456-1471.
55. Swindles, G. T., Lawson, I. T., Savov, I. P., Connor, C. B., & Plunkett, G. (2011) A 7000 yr perspective on volcanic ash clouds affecting northern Europe. *Geology* 39.9, 887-890
56. Swindles, G.T., Watson, E.J., Savov, I.P., Cooper, C.L., Lawson, I.T., Schmidt, A. and Carrivick, J.L. (2017) Holocene volcanic ash database for Northern Europe. *ResearchGate*, Database DOI: 10.13140/RG.2.2.11395.60966.
57. Swindles, G.T., Watson, E.J., Savov, I.P., Lawson, I.T., Schmidt, A., Hooper, A., et al. (2018a) Climatic control on Icelandic volcanic activity during the mid-Holocene. *Geology* 46.1, 47-50.
58. Swindles, G. T., Savov, I. P., Schmidt, A., Hooper, A., Connor, C. B., & Carrivick, J. L. (2018b). Climatic control on Icelandic volcanic activity during the mid-Holocene: REPLY. *Geology*, 46(5), e444-e444.
59. Thordarson, T., & Höskuldsson, Á. (2008). Postglacial volcanism in Iceland. *Jökull*, 58(198), 228.

60. Ulfarsson, G.F. and Unger, E.A. (2011). Impacts and responses of Icelandic aviation to the 2010 Eyjafjallajökull volcanic eruption: case study. *Transportation research record*, 2214(1), pp.144-151.
61. Valdes, P. J., Armstrong, E., Badger, M. P., Bradshaw, C. D., Bragg, F., Davies-Barnard, T. et al. (2017) The BRIDGE HadCM3 family of climate models: HadCM3@Bristol v1.0. *Geoscientific Model Development*, 10(10), 3715–3743. <https://doi.org/10.5194/gmd-10-3715-2017>
62. Van Aalst, M.K., (2006) The impacts of climate change on the risk of natural disasters. *Disasters*, 30(1), 5-18.
63. von Grafenstein, U., Erlenkeuser, H., Brauer, A., Jouzel, J., & Johnsen, S. J. (1999) A mid-European decadal isotope-climate record from 15,500 to 5000 years BP. *Science*, 284(5420), 1654-1657.
64. Walker, M., Head, M.J., Lowe, J., Berkelhammer, M., Björck, S., Cheng, H., Cwynar, L.C., Fisher, D., Gkinis, V., Long, A. and Newnham, R., (2019). Subdividing the Holocene Series/Epoch: formalization of stages/ages and subseries/subepochs, and designation of GSSPs and auxiliary stratotypes. *Journal of Quaternary Science*, 34(3), 173-186.
65. Wanner, H., Mercolli, L., Grosjean, M., & Ritz, S. P. (2015). Holocene climate variability and change; a data-based review. *Journal of the Geological Society*, 172(2), 254-263.
66. Watson, E. J., Swindles, G. T., Savov, I. P., Lawson, I. T., Connor, C. B., & Wilson, J. A. (2017) Estimating the frequency of volcanic ash clouds over northern Europe. *Earth and Planetary Science Letters* 460, 41-49.
67. Watt, S. F., Pyle, D. M., & Mather, T. A. (2013) The volcanic response to deglaciation: Evidence from glaciated arcs and a reassessment of global eruption records. *Earth-Science Reviews*, 122, 77-102.
68. Wiersma, A. P., & Renssen, H. (2006) Model–data comparison for the 8.2 ka BP event: confirmation of a forcing mechanism by catastrophic drainage of Laurentide Lakes. *Quaternary Science Reviews*, 25(1-2), 63-88.

Chapter 6: Discussion & Conclusions

In this chapter I will summarise and critically examine the findings of the previous chapters in order to synthesise overall conclusions. I will also connect the results of the studies described above to the aims and objectives of this thesis as outlined in Chapter 1, and explain their significance to the wider scientific community. For the sake of clarity, the stated aim of this thesis was as follows:

'To examine the foundations of the data commonly used in defence of the unloading theory, and, having determined its validity, to assess the potential for a change in volcanic eruption frequency as a result of isostatic uplift.'

In order to fulfil this aim, I compartmentalised the research into two objectives. Firstly, I aimed to establish the legitimacy of the methods used to examine the unloading effect in the Holocene. The first objective was met through:

- 1) Reviewing previous studies and accepted scientific methods (Chapter 2)
- 2) A case study of distal tephrochronology based in Northern Sweden, which established the high variability of tephra preservation across a geographic range of < 3000 km² due to irregular snow cover, vegetation, topography, and secondary transportation (Chapter 3)
- 3) A lab-based comparison of chemical-based tephra extraction methods commonly used on peat and lake sediments, which found that prolonged exposure to concentrated acids and bases has the potential to geochemically alter low-silica glasses through leaching of alkali oxides (Chapter 4)

The second objective examined whether there is evidence to support the occurrence of the unloading effect in Europe within that timeframe. This objective was fulfilled in three ways:

- 1) Through establishing new tephrochronological records in previously underrepresented areas, namely the Abisko region of Northern Sweden (Chapter 3)
- 2) Compiling Icelandic tephra records from across North-western Europe spanning into the Younger Dryas (Chapter 5)
- 3) Reconstructing Holocene palaeoclimate and Icelandic glacial extent using numerical simulations and climate proxies, and comparing the results of these to the volcanism record (Chapter 5)

In the course of this thesis, I have challenged current understandings of the environmental processes and research methods relevant to the field of tephrochronology. My identification of the Hekla 4, Hekla-Selsund, Hekla 1104,

and Hekla 1158 tephras in Northern Sweden substantially extended the distribution patterns of these eruptions. Furthermore, the discovery that the preservation of these tephras varied significantly over distances of < 10 km suggested that tephrochronology in permafrost peatlands is more likely to be affected by secondary transport and redeposition of material than previously thought. Additionally, my research has extended the existing database of palaeotephra records by more than 3,000 years, fully spanning the Holocene. Chapter 4, '*Standard chemical-based tephra extraction methods significantly alter the geochemistry of volcanic glass shards*', represents the first truly comprehensive comparative study of the use of concentrated chemicals in the extraction of basaltic to rhyolitic glass from peat. The findings of this research have strong implications for future tephrochronological studies, and also raise new uncertainties regarding the validity of some exotic tephra compositions previously reported in Europe, discussed further in section 6.1.1.

Most crucially, by integrating physical tephra records and palaeoclimatological data with numerical simulations I was able to prove the potential of the unloading effect as an important factor in the fluctuation of Icelandic volcanic activity throughout the Holocene. This manuscript represents the first truly holistic approach to examining the phenomenon, taking into account estimations of magma transport and storage, atmosphere-ocean reconstructions, and models of ice sheet extent. My findings showed that the observed volcanic quiescence following periods of ice sheet growth and subsequent increase in eruption frequency following ice retreat was likely to be due to either increased upwelling as a result of decompression or rapid utilisation of shallow 'pooled' magma. This has many implications, not only for scientific understanding of earth systems processes in the Holocene, but also for volcanological studies in the coming decades, discussed further in section 6.3.

6.1 Research Synthesis

6.1.1. Objective 1 – Establish the legitimacy of the methods used to examine the unloading effect in the Holocene

The purpose of this aspect of the research was to investigate the utility and potential pitfalls of methods used in previous research regarding the unloading

effect. The primary focus of these manuscripts was the use of tephrochronology, which is sometimes cited as providing physical evidence of fluctuating volcanic activity in Iceland during the Holocene (Watson et al., 2016a; Swindles et al., 2018). My studies examined both the physical processes influencing the creation and preservation of tephra layers in the sedimentological record, and the laboratory methods commonly used to extract and analyse the glass shards.

In Chapter 3, *'Evaluating tephrochronology in permafrost peatlands in Northern Sweden'*, I analysed nine sediment cores of peatland material sourced from the Abisko region of Sweden, less than 100 km below the Arctic Circle. From these cores, I identified six distinct tephra layers, five of which I attributed as belonging to the Hekla 4, Hekla 1104, Hekla 1158 and Hekla-Selsund, and Askja 1875 Icelandic eruptions. The sixth layer remains unidentified, as its position within the age-depth profile of the core does not correlate with any known Icelandic eruptions which have created observable tephra layers in Europe. Unfortunately, the glass shards in this layer were found to be both too small and too sparse to perform geochemical analysis and obtain meaningful results. This study was one of the first examples of tephrochronology to be performed at such high latitudes in Europe (Pilcher et al., 2005; Vorren et al., 2009; Watson et al., 2016b).

Though the discovery and firm identification of several tephra layers in Abisko contributed significantly to the understanding of Icelandic tephra distribution patterns over mainland Europe by filling a previous geographic gap (Lawson et al., 2012), the primary goal of this research was to provide an in-depth analysis of natural factors influencing the deposition and preservation of tephra in sub-Arctic peatlands. As stated in Chapter 3, Northern Sweden was previously thought to be an unlikely candidate for frequent ashfall from Icelandic eruptions, according to reconstructions of fallout patterns based on other documented tephra layers (Davies et al., 2010). The findings of my research bore this assumption out; of the nine analysed sediment cores, five did not contain tephra, and the remaining four contained volcanic glass in only trace amounts. Furthermore, the variation of preservation even between adjacent cores was very high; even sediment cores separated by distances of < 10 km did not contain correlating tephra layers. Our conclusion following this new observation was that local environmental factors have a much greater impact on the tephra preservation potential of a given site

than previously thought, with significant ramifications for tephrochronology as a discipline.

This research found that local climate and wind currents were perhaps the greatest factor in determining the preservation status of ashfall within a region, in addition to local topography and the permeability of target surfaces. The combination of these influences led me to suggest that northern Scandinavian peatlands may represent an unsuitable prospect for future tephrochronological studies, due to the high risk of redeposition. The major implication of this finding for tephrochronology as a discipline is that reconstruction of historic or pre-historic eruption patterns from the tephra records of even a relatively large geographic area may be subject to preservation biases. This highlights the importance of considering data on a continental scale in such research; studies such as Swindles et al., 2018 and Watson et al., 2017 take into account tephrochronological data collated from several countries when attempting to characterise Icelandic volcanic activity, thereby reducing the risk of possible misrepresentation from areas of poor preservation.

In Chapter 4, 'Standard chemical-based tephra extraction methods significantly alter the geochemistry of volcanic glass shards', I compared the chemical impacts of three commonly used methods of tephra extraction on glass shards of various compositions ranging from silica-poor basalts to very silica-rich obsidian. This study was the first to truly compare the effects of both dilute and concentrated chemical (acid and base) solutions on multiple tephra compositions, making it a vital contribution to the scientific field. Crucially, this research found that chemical methods of tephra extraction could change the geochemical composition of glass shards. Many previous studies investigating this possibility had come to differing conclusions; while Roland et al., 2015 found that rhyolitic glasses produced no significant chemical variation following acid digestion treatment, studies focusing solely on basaltic glasses found evidence of chemical changes (Blockley et al., 2005). However, the findings of my research conclusively show that initial glass composition is a key determining factor in the susceptibility of tephra to chemical alteration. In this study, I found that glasses with an initial silica content of < 55 % showed significantly greater amounts of mobile element leaching following chemical treatment. Likewise, glasses with initial SiO₂ concentrations of > 65 %

were exceptionally stable when subjected to even highly concentrated acids and bases at heat.

This finding provides a plausible explanation for the observation by many previous studies that basalts are considerably underrepresented in the tephrochronological records of many geographic regions when compared to the geochemical outputs of the relevant volcanic systems (Wastegård & Davies, 2009; Lawson et al., 2012; Watson et al., 2017). Many of these studies hypothesised that basalts may undergo post-deposition degradation in acidic environments, such as those found in peatland (Pollard et al. 2003; Blockley et al. 2005). My research indicates that this scenario is highly likely – given that the more basaltic glasses examined in Chapter 4 (Katla 1357, Hekla-Selsund Phase 2) showed chemical variation from the control group in response to even dilute HCl treatment over a period of 24 hours, it seems reasonable to suggest that a residence time of several decades or centuries within a low-pH environment would cause substantial geochemical alteration. The study found that alkaline oxides, such as K_2O , CaO , and Na_2O , were consistently more susceptible to variation than non-alkaline metal oxides such as Al_2O_3 and FeO . While the exact cause and mechanism of this is yet to be determined as it was outside the scope of this research project, it is likely that this finding will be of importance to the field in future studies, as it has implications for the relationship between the geochemical compositions of in situ proximal erupted materials and their distal counterparts.

A secondary implication of these findings is that some tephras found in European sites and reported with novel or non-European geochemical provenances may in fact have been altered from their original compositions through analytical or extraction techniques. In particular, some tephras found in European sites have been attributed to transatlantic sources including Alaska (Mt Churchill; the White River Ash (WRA))(Jensen et al., 2014), the Cascade range of North America (Plunkett & Pilcher, 2018), and to some sources as far south as Mexico (Plunkett & Pilcher, 2018). If it is possible for commonly used methods such as the acid digestion technique to significantly alter basaltic and intermediate volcanic glasses (as was found in the research detailed in Chapter 4), then it is conceivable that the unusual geochemical compositions described in those studies are the unintended result of chemical alteration of some glass shards. Reported trachydacitic and trachyandesitic compositions are particularly questionable when considered with

the results of the research in Chapter 4; my research indicated that, while basalts were more susceptible to total destruction by concentrated chemical techniques, a small number of shards in mid-range andesite samples (55-65 wt% SiO₂) showed an apparent relative increase in the concentrations of Na₂O and K₂O via the leaching of CaO and MgO. This alteration in composition was sufficient to reclassify the shards as trachyandesites and trachydacites.

In most cases, the chemical alterations caused by standard techniques were not of a high enough magnitude to warrant geochemical reclassification, particularly among the more silicic compositions. However, as modern tephrochronology relies heavily on drawing comparisons and correlations between the geochemical compositions of geographically disparate shards, even minor variations in glass geochemistry have the potential to hinder the success of future research.

6.1.2. Objective 2 – Has the unloading effect occurred in Europe within the Holocene?

This compartment of the research focused on drawing together the data and arguments compiled under Objective 1, and assessing their value as evidence for or against the unloading effect in Iceland. Additionally, further data in the form of historic tephra and climate records were collected in an extensive database and used as the foundation for numerical simulations of palaeoclimate and Icelandic glacial extent within the Holocene and Late Glacial periods. The combination of these aspects represents the most comprehensive and multidisciplinary study of this phenomenon in Iceland thus far, drawing together many elements, some of which had previously been considered separately (Jull & McKenzie, 1996; Sigmundsson et al., 2010) but not in concert. By linking physical data with earth system simulations, this work produces a clear and coherent visualisation of Iceland's volcanic history, and connects it to established fluctuations in local and regional climate within the Holocene.

The first step in assessing the evidence for the unloading effect occurring in Europe during the Holocene was to compile a comprehensive database of Icelandic distal tephra deposits. Other works with similar goals include Watson et al., 2017 and the NEVA tephra database currently listed on ResearchGate (Swindles et al., 2017). However, my research greatly extends the time frame of

previous compilations through the Holocene and into the Late Glacial period, to a maximum age of 14,550 cal BP. The new database collects tephra records from across western Europe, including sites as far north as sub-Arctic Sweden (some of which were first presented in Chapter 3), and as far east as Poland. The database records over 100 discrete Icelandic volcanic events, each with multiple records as the tephra is preserved across geographic regions. When these records are collated as part of individual events, the resulting data may be used as a proxy for the frequency of Icelandic ashfall over Europe within the last geological period.

In Chapter 5, 'Is there a climatic control on Icelandic volcanism?', I brought together the arguments made in previous chapters and combined them with new data to address the central question of this thesis. In addition to the distal tephra record described above, I examined several proximal records of Icelandic volcanism, in an attempt to eliminate the biases introduced by both patchy preservation at a distal range (Watson et al., 2016b) and the overwriting of deposits by new activity at proximal sites (Swindles et al., 2018). The combination of these sources produced a clear image of Holocene Icelandic volcanic activity, and also produced a consensus on the presence and timings of several peaks and troughs in volcanism during this period. These records were presented alongside new results of numerical simulations recreating northern hemisphere Holocene climatic conditions and Icelandic ice sheet extents, in addition to physical palaeoclimate data obtained from a range of sources, detailed fully in Chapter 5. The integration of physical data and numerical models introduces a degree of ground-truthing often absent in previous purely theoretical studies examining the unloading phenomenon.

The results of this study indicated that, while a positive relationship between local climate fluctuations and quiescent periods in Icelandic volcanism could not be conclusively proven, there is still substantial evidence that such a link may exist. In particular, two periods of atmospheric cooling, at approximately 8.2 kya and 5.7 kya, correlate strongly with troughs in European tephra layer frequency. However, the study also identifies other (weaker or shorter) periods of cooling which are not apparently connected to any significant decrease in volcanic activity. Likewise, there is one tephra minimum indicated at around 3.5 kya which is not associated with any contemporary climate fluctuation, suggesting the quiescence may have

been a result of other influencing factors, such as a regional stress regime change caused by tectonic influences, or a temporary decrease in magma supply.

The implication of this finding is that although a correlation between glacial loading and volcanism in this location remains a possibility, there are likely to be many other factors exerting a relatively stronger control on the frequency of explosive volcanic activity in Iceland. The relative importance of any climatic influence would certainly be determined by the magnitude and duration of the temperature fluctuation in question. However, as the atmospheric influence on volcanic systems is indirect, instead being transmitted through ice sheet response which carries with it an inherent time delay, even large atmospheric perturbations are significantly offset. As a result, more direct changes to the volcanic systems, either on a local or regional scale (such as upwelling rates, water availability, or changes to magma composition (Schmidt et al., 2013; Ekinschol et al., 2019) will exert a much greater control.

A final inference that can be made from the results of this research relates to the depth of material that could potentially be affected by the proposed unloading mechanism. With reference to the work of Ekinschol et al., 2019 on melt ascent rates in Iceland, it is implied that the initial 'spike' in volcanic activity observed in Chapter 5 and in previous works (Swindles et al., 2018) which occurs between 100-200 years after the cessation or reversal of atmospheric cooling would be drawing only on shallow material (> 15 km depth). This in turn implies that the quiescence observed during high magnitude, rapid onset cooling events is a result of magma pooling at a shallow depth within crustal storage, as explosive eruptive activity may have been suppressed through increased overlying pressure. This hypothesis is in line with the observation that underlying geological inputs are likely to exert a greater control on volcanic activity than unloading. It has previously been argued that most Holocene cooling events would not have caused a great enough perturbation to magma bodies at depth to be responsible for the observed variations in volcanic eruption frequency, despite the temporal correlation (Harning et al., 2018). However, if the observed spikes utilise only materials brought to the near-surface by existing volcanic systems, then the rapid removal of pressure by ice sheet retreat once more becomes a viable cause of increased eruption frequency through alteration of the local pressure regime.

6.2 Research Implications

Tephrochronology is a rapidly advancing discipline with applications both new and established in a wide range of fields. Its potential as a dating tool across large geographic areas is of particular importance, though from a geological standpoint, cryptotephra layers are a highly important resource in their own right, as they represent one of the few stratigraphic and geochemical records of pre-historic ash clouds (Watson, 2016a). It is therefore crucial that the uncertainties and disputes regarding extraction and analytical techniques are resolved, and the results of the work detailed in this research project are a significant advance towards that end.

During this project, six tephra layers (Hekla 4, Hekla-Selsund, Hekla 1104, Hekla 1158, and two unidentified tephra, one of which is tentatively inferred to be the Askja 1875 ash) were identified in a new geographic region, filling a significant spatial gap in the European tephra record. Additionally, this element of the work furthered the understanding of tephra preservation in permafrost peatland, an essential requirement for future work conducted at high latitude sites.

Furthermore, this project has contributed a vital addition to the methodologies of tephra extraction, a topic which has been (and remains) a source of controversy for many years (Blockley et al., 2005; Roland et al., 2015). This work represented the most geochemically comprehensive study of its type conducted on volcanic glass. The results conclusively showed that basaltic and andesitic glasses are significantly more susceptible to chemical alteration than rhyolites, strongly suggesting that many commonly-used chemical-based extraction methods (particularly the acid digestion method) are inappropriate for use on low-silica glasses. Finally, our findings regarding the potential validity of the unloading effect in glaciated areas have potential ramifications for other geographic regions containing a similar convergence of ice loading and active volcanism, such as the northern volcanoes of the Aleutian arc in Alaska, volcanoes of the Kamchatka peninsula of Eastern Russia, and some volcanoes located in the Southern and Austral Andean Volcanic Zones.

A greater understanding of the processes governing the emplacement and preservation of volcanic ash layers will be of great importance to scientists working on or utilising tephrochronology in their fields of study, which might include archaeologists, palaeoecologists, or atmospheric scientists. Likewise, our findings on the unloading effect in Iceland are likely to be highly relevant to

volcanologists, glaciologists, and climate scientists, as the phenomenon itself transcends many traditional disciplinary boundaries. In light of the Earth's changing climate in the coming centuries, this research is also likely to be of note to some civil authorities, notably aviation authorities, local governments, and the general public.

6.2.1 *Advances in methods and understanding*

- The discovery of six tephra layers – four identified as belonging to specific Icelandic eruptions, as detailed above and in Chapter 3, and two unidentified tephra – in the Abisko region of Northern Sweden filled a significant spatial gap in the European Holocene tephra record, and extended the accepted distribution patterns of those ash clouds into higher latitudes (Chapter 3)
- The lack of continuity between even adjacent peat cores in the Abisko region suggests that, due to a number of local and regional geographic factors, permafrost peatlands may be unreliable and therefore potentially unsuitable sources of tephrochronological data (Chapter 3)
- The finding that the use of burning & dilute HCl, concentrated H₂SO₄ and HNO₃, and concentrated KOH in the extraction of tephra from peat material are all individually sufficient to alter the geochemistry of low-silica volcanic glasses will have significant implications for the future of tephrochronology as a field (Chapter 4)

6.2.2 *Novel approaches*

- Thorough comparison of the reactions of a range of volcanic glasses from basaltic through to rhyolitic compositions to both strong and weak chemical conditions showed conclusive differences in the behaviours of low silica vs high silica materials (Chapter 4)
- Combining physical tephra records with climate proxies and numerical simulations of Icelandic palaeoclimate suggests that centuries-scale changes in climate may have affected volcanic activity in the region (Chapter 5)

6.3 *Prospects for Future Research*

The findings presented in this thesis pose a number of further questions which could prompt several lines of further research. Chapter 3 represents one of the few existing tephrochronological studies conducted in permafrost peatland – it is important that more such studies are performed in similar geographic areas in order to establish whether the same factors negatively influence tephra

preservation across the region as in Abisko. Such a finding would have major ramifications for the validity of tephrochronology performed at high latitudes.

The use of concentrated chemical agents as a means of tephra extraction from organic material has been a point of contention for many years, and while the research presented in Chapter 4 is a substantial advance in terms of supplying evidence to the argument, there are more questions yet to be answered. What is the exact geochemical mechanism of glass damage? Do the leachates produced during extraction contain useful chemical information on original glass composition? Are there unexplored alternatives that balance the retention of material seen in density separation methods with the effectiveness in removing organic material and the time efficiency of acid digestion? These questions are crucial to the future of tephrochronology on an international level, and must be answered if the discipline is to retain its validity as a versatile and multidisciplinary tool.

In Chapter 5, a new database of European Holocene tephra was presented, extending the oldest records of previous compilations by an additional 3,000 years and including new geographic sites, including those first presented in Chapter 3. However, while comprehensive, this record is by no means complete, and much work is still required to build a full view of Icelandic tephra deposition over mainland Europe and the surrounding islands. This will require extensive campaigns of data collection in the field, and a concerted effort from the international tephrochronology community.

Finally, while the results of Chapter 5 are a step forwards in combining physical and simulated data to investigate the unloading effect, and extend the scope of the proposed phenomenon up to the Late Glacial period, there is still a great deal of remaining uncertainty and contrary evidence surrounding the theory. More work is required to specifically examine how the rate and magnitude of any warming might affect isostatic rebound through glacial unloading, as inferred from the results presented in Chapter 5. There is also potential in investigating whether this phenomenon is observable in other parts of the world as has been previously suggested (Watt et al., 2013; Rawson et al., 2016), and, perhaps more topically, whether the current trend of global mean temperature rise would be theoretically sufficient to cause the suggested short-term increase in volcanic activity through the ongoing documented patterns of ice sheet retreat.

References

1. Blockley, S.P.E., et al. (2005) A new and less destructive laboratory procedure for the physical separation of distal glass tephra shards from sediments. *Quaternary Science Reviews*, 24(16-17), pp.1952-1960
2. Davies, S.M. et al. 2010. Widespread dispersal of Icelandic tephra: how does the Eyjafjöll eruption of 2010 compare to past Icelandic events? *Journal of Quaternary Science: Rapid Communication*, 25 (5), 605-611
3. Harning, D.J., Geirsdóttir, Á., Thordarson, T. and Miller, G.H., 2018. Climatic control on Icelandic volcanic activity during the mid-Holocene: COMMENT. *Geology*, 46(5), pp.e443-e443.
4. Jensen, B., Pyne-O'Donnell, S., Plunkett, G., Froese, D.G., Hughes, P.D.M., Sigl, M., McConnell, J.R. et al. 2014. Transatlantic distribution of the Alaskan White River Ash, *Geology*, 42, 875-878
5. Jull, M., and McKenzie, D. 1996. The effect of deglaciation on mantle melting beneath Iceland. *Journal of Geophysical Research: Solid Earth* 101.B10 21815-21828.
6. Lawson, I.T., Swindles, G.T., Plunkett, G., Greenberg, D., 2012. The spatial distribution of Holocene cryptotephra in north-west Europe since 7 ka: implications for understanding ash fall events from Icelandic eruptions. *Quaternary Science Reviews* 41, 57-66
7. Plunkett, G. and Pilcher, J.R., 2018. Defining the potential source region of volcanic ash in northwest Europe during the Mid-to Late Holocene. *Earth-science reviews*, 179, pp.20-37.
8. Pollard, A.M., Blockley, S.P.E. and Ward, K.R., (2003) Chemical alteration of tephra in the depositional environment: theoretical stability modelling. *Journal of Quaternary Science*, 18(5), pp.385-394.
9. Rawson, H., Pyle, D.M., Mather, T.A., Smith, V.C., Fontijn, K., Lachowycz, S.M. and Naranjo, J.A., 2016. The magmatic and eruptive response of arc volcanoes to deglaciation: Insights from southern Chile. *Geology*, 44(4), pp.251-254.
10. Roland, T.P., Mackay, H. and Hughes, P.D.M., (2015). Tephra analysis in ombrotrophic peatlands: a geochemical comparison of acid digestion and density separation techniques. *Journal of Quaternary Science*, 30(1), pp.3-8.
11. Schmidt, P., Lund, B., Hieronymus, C., Maclennan, J., Árnadóttir, T., & Pagli, C. (2013) Effects of present-day deglaciation in Iceland on mantle melt production rates. *Journal of Geophysical Research: Solid Earth*, 118(7), 3366-3379.

12. Sigmundsson, F., Pinel, V., Lund, B., Albino, F., Pagli, C., Geirsson, H., & Sturkell, E. 2010. Climate effects on volcanism: influence on magmatic systems of loading and unloading from ice mass variations, with examples from Iceland. *Philosophical Transactions of the Royal Society of London A: Mathematical, Physical and Engineering Sciences* 368, 2519-2534.
13. Swindles, G.T., Watson, E.J., Savov, I.P., Cooper, C.L., Lawson, I.T., Schmidt, A. and Carrivick, J.L. 2017b. Holocene volcanic ash database for Northern Europe. Database. DOI: 10.13140/RG.2.2.11395.60966
14. Swindles, G.T., Watson, E.J., Savov, I.P., Lawson, I.T., Schmidt, A., Hooper, A., Cooper, C.L., Connor, C.B., Gloor, M. and Carrivick, J.L., 2018. Climatic control on Icelandic volcanic activity during the mid-Holocene. *Geology*, 46(1), pp.47-50.
15. Vorren, KD, Elverland, E, Blaauw, M, Ravna, EK and Jensen, CAH 2009 Vegetation and climate c. 12 300-9000 cal. yr BP at Andøya, NW Norway. *Boreas* 38, 401-420
16. Wastegård, S. and Davies, S.M., (2009) An overview of distal tephrochronology in northern Europe during the last 1000 years. *Journal of Quaternary Science: Published for the Quaternary Research Association*, 24(5), pp.500-512.
17. Watson, E.J., 2016a. Using cryptotephra layers to understand volcanic ash clouds. Doctoral dissertation, University of Leeds.
18. Watson, E.J., Swindles, G.T., Lawson, I.T. and Savov, I.P. 2016b Do peatlands or lakes provide the most comprehensive distal tephra records?. *Quaternary Science Reviews* 139, 110-128
19. Watson, E.J., Swindles, G.T., Savov, I.P., Lawson, I.T., Connor, C.B. and Wilson, J.A., 2017. Estimating the frequency of volcanic ash clouds over northern Europe. *Earth and Planetary Science Letters*, 460, 41-49.
20. Watt, S.F., Pyle, D.M. and Mather, T.A., 2013. The volcanic response to deglaciation: Evidence from glaciated arcs and a reassessment of global eruption records. *Earth-Science Reviews*, 122, pp.77-102

Appendix

Suppl. Chapter 3: Evaluating tephrochronology in the permafrost peatlands of northern Sweden

Table A.1.1. Radiocarbon dates of Abisko peat profiles

Site	Lab Code	Depth (cm)	¹⁴ C Age	1σ Error	Material dated	Cal range 2σ (BP)	Cal Median Age (BP)
Electric	UB2359	17	165	20	<i>Dicranum bergerii</i> + <i>Dicranum elongatum</i> stems with leaves	166–225	187
	UB2360	22	390	20	<i>Sphagnum</i> stems + leaves	434–505	476
Crater Pool I	UB2358	15	860	20	<i>Sphagnum russowii</i> stems with leaves	726–796	763
	Poz-80223	22	1110	30	<i>Sphagnum riparium</i> stems with leaves	937–1071	1014
Crater Pool II	UB2356	19	160	20	<i>Betula nana</i> leaf remains + fruits scale, <i>Empetrum nigrum</i> seed remains, <i>Andromeda polifolia</i> leaves and seeds, <i>Sphagnum fuscum</i> stems with leaves	167–224	187
	UB2357	29	345	20	<i>Sphagnum fuscum</i> stems with leaves, <i>Oxycoccus palustris</i> leaves, <i>Betula nana</i> leaf remains	316–407	386
Railway	UB2366	28	200	20	<i>Oxycoccus palustris</i> leaves, <i>Betula nana</i> leaf remains, <i>Sphagnum russowii</i> stems with leaves	146–189	172

Site	Lab Code	Depth (cm)	¹⁴ C Age	1σ Error	Material dated	Cal range (BP)	Cal Median Age (BP)
	UB2398_2	40	1240	20	Bulk	1196–1263	1211
Eagle	UB2365	19	130	20	<i>Dicranum elongatum</i> stems with leaves, <i>Pleurozium schreberii</i> stems with leaves	59–149	119
	UB2397_2	30	1725	25	Bulk	1565–1700	1635
Nikka	UB2363	24	180	20	<i>Sphagnum fuscum</i> stems with leaves	142–219	183
	UB2364	30	595	20	<i>Sphagnum fuscum</i> stems with leaves	584–647	606
Instrument	UB2361	25	165	20	<i>Dicranum elongatum</i> stems with leaves	166–224	187
	UB2362	30	320	20	<i>Dicranum elongatum</i> stems with leaves	348–458	387
Stordalen	D-AMS006366	14	340	24	<i>Sphagnum</i>	477–518	388
	D-AMS006367	17	553	31	<i>Sphagnum</i>	640–518	559
Marooned	D-AMS006368	28	2317	26	<i>Sphagnum</i> , herb epidermis	2360–2211	2342

Table A.1.2. ²¹⁰Pb dating of Abisko peat profiles

Site	Cumul. ²¹⁰ Pb_ex inventory (Bq/m ²)	±	Residual ²¹⁰ Pb_ex (Bq/m ²)	±	Age (year)	YEAR (AD)	±
	19.02	1.68	3632.39	26.67	0.17	2011.83	1.00
	116.57	6.13	3534.84	26.62	1.04	2010.96	1.02
	273.73	8.11	3377.68	25.96	2.50	2009.50	1.06
	504.43	11.26	3146.97	25.41	4.77	2007.23	1.08
Marooned	833.18	14.73	2818.22	24.17	8.32	2003.68	1.12
	1263.37	18.20	2388.03	22.23	13.64	1998.36	1.17
	1942.68	21.82	1708.73	19.49	24.39	1987.61	1.25
	2485.15	23.74	1166.26	15.33	36.65	1975.35	1.35
	3073.40	25.72	578.01	12.15	59.19	1952.81	1.61
	3359.58	26.35	291.83	7.05	81.14	1930.86	1.75
	3582.02	26.53	69.39	4.14	127.27	1884.73	2.89
	3651.40	26.67	0.00	2.76			
	3651.40	26.85					
	3611.87	26.91					
	3618.02	31.04					
	3556.55	33.89					
Eagle	47.57	4.29	3602.81	45.06	0.42	2011.58	1.01
	166.11	7.75	3484.27	44.85	1.50	2010.50	1.04
	553.84	18.48	3096.54	44.38	5.28	2006.72	1.10
	1239.81	25.69	2410.57	41.09	13.33	1998.67	1.25
	1923.16	30.09	1727.22	37.01	24.03	1987.97	1.43

Site	Cumul. ²¹⁰ Pb_ex inventory (Bq/m ²)	±	Residual ²¹⁰ Pb_ex (Bq/m ²)	±	Age (year)	YEAR (AD)	±
	2521.79	40.57	1128.59	33.53	37.70	1974.30	1.71
	3064.50	43.78	585.89	19.60	58.75	1953.25	1.97
	3441.33	44.64	209.05	10.63	91.84	1920.16	2.59
	3650.38	45.06	0.00	6.09			
	3650.38	45.48					
	3606.77	45.52					
	3580.58	45.59					
	3511.91	45.65					
	3254.74	45.99					
	2968.36	47.14					
	2868.03	48.93					
	2579.98	51.08					
	129.65	12.70	2517.20	28.58	1.61	2010.39	1.02
	328.28	16.64	2318.57	25.61	4.25	2007.75	1.16
	600.43	18.59	2046.42	23.24	8.26	2003.74	1.22
	1018.88	20.87	1627.98	21.71	15.61	1996.39	1.28
	1599.29	23.67	1047.56	19.53	29.77	1982.23	1.44
Nikka	1971.58	27.37	675.27	16.03	43.87	1968.13	1.64
	2248.59	28.20	398.26	8.23	60.82	1951.18	1.65
	2455.75	28.40	191.10	4.65	84.40	1927.60	1.80
	2584.36	28.51	62.50	3.23	120.30	1891.70	2.66
	2646.85	28.58	0.00	2.05			

Site	Cumul. ²¹⁰ Pb_ex inventory (Bq/m ²)	±	Residual ²¹⁰ Pb_ex (Bq/m ²)	±	Age (year)	YEAR (AD)	±
	2646.85	28.75					
	2618.05	29.25					
	2607.31	29.73					
	2594.90	31.04					
	2556.27	31.43					
	129.65	12.70	2517.20	28.58	1.61	2010.39	1.02
	328.28	16.64	2318.57	25.61	4.25	2007.75	1.16
	600.43	18.59	2046.42	23.24	8.26	2003.74	1.22
	1018.88	20.87	1627.98	21.71	15.61	1996.39	1.28
	1599.29	23.67	1047.56	19.53	29.77	1982.23	1.44
	1971.58	27.37	675.27	16.03	43.87	1968.13	1.64
	2248.59	28.20	398.26	8.23	60.82	1951.18	1.65
Stordalen	2455.75	28.40	191.10	4.65	84.40	1927.60	1.80
	2584.36	28.51	62.50	3.23	120.30	1891.70	2.66
	2646.85	28.58	0.00	2.05			
	2646.85	28.75					
	2618.05	29.25					
	2607.31	29.73					
	2594.90	31.04					
	2556.27	31.43					

Table A.1.3. Non-normalised major element glass geochemistry of Abisko peat profiles

Core	Depth (cm)	SiO ₂	TiO ₂	Al ₂ O ₃	FeO	MnO	MgO	CaO	Na ₂ O	K ₂ O	P ₂ O ₅	Total
Marooned	85	70.54	0.45	13.10	4.65	0.19	0.18	1.53	4.89	3.52	0.05	99.09
		76.16	0.24	11.91	2.06	0.08	0.07	0.90	4.19	3.03	0.03	98.69
		73.40	0.28	14.28	3.43	0.12	0.32	2.41	4.91	1.95	0.05	101.19
		71.93	0.24	13.25	2.98	0.12	-0.20	1.95	5.25	2.40	0.03	97.96
		63.12	0.85	14.63	7.49	0.23	0.89	4.45	4.17	1.87	0.28	97.98
		64.73	0.85	15.19	7.59	0.24	0.90	4.55	4.78	1.67	0.29	100.75
		73.99	0.14	12.80	2.01	0.08	0.05	1.35	5.02	2.90	0.01	98.38
		66.65	0.52	15.15	4.41	0.20	0.34	1.87	5.54	3.88	0.07	98.65
		72.96	0.13	12.14	1.94	0.09	0.03	1.18	4.67	2.82	0.00	95.98
		66.40	0.57	15.02	5.22	0.17	0.45	3.66	5.69	1.59	0.16	98.92
		66.23	0.59	15.03	4.04	0.11	0.31	3.87	5.64	1.35	0.19	97.34
		71.16	0.24	13.29	3.09	0.11	0.13	2.06	5.06	2.48	0.02	97.67
		71.96	0.23	12.95	2.84	0.11	0.10	1.87	4.71	2.58	0.02	97.41
		63.02	1.18	15.07	7.17	0.20	1.38	4.75	4.41	1.57	0.40	99.09
		64.28	1.18	14.04	7.17	0.21	1.35	4.58	4.48	1.52	0.39	99.11
	75.55	0.20	12.23	1.73	0.07	0.06	1.34	4.34	2.75	0.03	98.36	
Stordalen	25	69.57	0.46	13.51	5.23	0.14	0.34	2.34	4.97	2.88	0.10	99.54
		69.36	0.42	15.53	4.17	0.11	0.19	3.01	5.34	2.44	0.10	100.68
		69.26	0.50	14.28	4.83	0.19	0.24	2.81	5.49	2.54	0.10	100.25
		68.79	0.47	15.19	5.09	0.15	0.40	3.29	5.47	2.05	0.09	100.99
		68.72	0.46	15.23	5.52	0.17	0.43	3.13	5.27	2.30	0.11	101.34

Core	Depth (cm)	SiO ₂	TiO ₂	Al ₂ O ₃	FeO	MnO	MgO	CaO	Na ₂ O	K ₂ O	P ₂ O ₅	Total
		68.68	0.47	15.41	5.46	0.17	0.47	3.15	5.12	2.32	0.10	101.35
		68.40	0.48	14.09	5.48	0.19	0.42	3.03	5.06	2.42	0.10	99.68
		68.23	0.48	14.53	5.48	0.17	0.48	3.33	5.16	2.31	0.09	100.26
		68.11	0.47	15.35	5.70	0.18	0.46	2.96	5.30	2.38	0.10	101.01
		67.90	0.47	14.36	5.31	0.18	0.44	3.14	5.54	2.30	0.11	99.75
		67.84	0.48	14.88	5.75	0.17	0.45	3.22	5.12	2.31	0.11	100.32
		67.84	0.47	14.52	5.83	0.15	0.46	3.28	4.81	2.31	0.12	99.77
		67.80	0.48	15.01	5.75	0.19	0.50	3.02	4.78	2.26	0.08	99.97
		67.66	0.46	15.06	5.70	0.18	0.46	2.94	5.71	2.24	0.09	100.51
		67.62	0.45	14.22	5.39	0.14	0.50	3.02	5.44	2.41	0.11	99.30
		67.60	0.46	14.83	5.76	0.16	0.44	3.14	5.43	2.35	0.10	100.29
		67.60	0.48	15.22	5.65	0.19	0.44	3.14	5.09	2.39	0.10	100.31
		67.39	0.46	15.04	6.06	0.17	0.46	3.02	5.55	2.30	0.11	100.56
		67.22	0.45	14.85	5.61	0.17	0.48	3.11	5.39	2.32	0.11	99.71
		67.11	0.41	16.93	4.25	0.15	0.34	3.88	5.87	1.97	0.09	101.00
		65.41	0.07	13.85	5.66	0.11	0.41	3.16	4.04	2.19	0.07	95.20
		64.71	0.27	20.15	3.10	0.07	0.31	5.19	6.36	1.32	0.06	101.54
Stordalen	30	67.63	0.38	16.11	4.01	0.16	0.26	1.78	5.73	4.18	0.05	100.29
		67.49	0.40	15.75	4.05	0.19	0.27	1.82	6.16	4.22	0.06	100.40
		67.48	0.39	16.25	4.23	0.18	0.24	1.85	6.22	4.21	0.06	101.12
		67.41	0.39	15.78	4.42	0.16	0.33	1.76	5.92	4.16	0.05	100.38
		67.28	0.47	15.85	4.69	0.19	0.46	2.05	5.97	3.94	0.09	101.01
		67.20	0.43	15.84	4.75	0.20	0.36	2.09	5.73	4.11	0.64	100.76

Core	Depth (cm)	SiO ₂	TiO ₂	Al ₂ O ₃	FeO	MnO	MgO	CaO	Na ₂ O	K ₂ O	P ₂ O ₅	Total
		66.98	0.34	15.68	3.76	0.15	0.23	1.71	6.01	4.21	0.06	99.12
		66.96	0.46	16.59	4.48	0.19	0.40	2.24	5.99	4.13	0.08	101.52
		66.76	0.43	15.94	4.34	0.16	0.37	1.98	6.14	4.07	0.06	100.25
		66.66	0.43	16.64	4.14	0.17	0.32	1.96	5.87	4.02	0.07	100.28
		66.50	0.36	16.14	4.28	0.15	0.28	1.58	6.14	4.28	0.06	99.73
		66.44	0.33	14.26	3.60	0.15	0.19	1.63	5.64	4.29	0.04	96.56
		66.27	0.41	15.63	4.34	0.18	0.35	1.99	6.25	4.06	0.07	99.53
		65.85	0.47	14.11	5.66	0.28	0.66	2.73	5.49	4.12	0.08	99.46
		65.83	0.57	16.08	5.60	0.23	0.57	2.43	5.74	3.78	0.12	100.94
		65.73	0.38	15.60	4.07	0.16	0.31	1.80	5.92	4.27	0.07	98.31
		65.41	0.46	15.62	4.53	0.18	0.31	1.96	6.07	3.98	0.07	98.60
		65.13	0.46	15.79	4.61	0.17	0.34	2.12	6.13	3.92	0.08	98.74
		64.89	0.40	15.78	4.17	0.18	0.31	1.89	5.89	4.18	0.07	97.76
		63.34	0.43	15.82	4.25	0.16	0.31	1.87	5.71	3.95	0.06	95.91
Marooned	70	72.02	0.62	14.51	2.45	0.16	0.53	1.71	6.08	2.84	0.10	100.96
		64.63	0.77	15.68	5.58	0.24	0.54	2.65	6.43	3.65	0.16	100.27
		72.73	0.64	13.28	3.17	0.15	0.69	2.61	4.65	1.71	0.13	99.73
		71.16	0.25	13.54	3.02	0.12	0.12	1.98	4.66	2.36	0.03	97.28
		70.33	0.31	13.18	3.82	0.17	0.11	1.29	4.87	5.10	0.04	99.24
		65.73	0.67	14.49	6.32	0.21	0.58	3.43	4.99	1.95	0.20	98.55
		71.67	0.25	13.34	3.00	0.12	0.13	1.85	5.08	2.42	0.02	97.90
		71.40	0.23	13.42	2.98	0.14	0.02	1.79	5.64	2.78	0.01	98.42
		64.60	0.77	14.05	7.17	0.23	0.78	3.93	4.40	1.67	0.24	97.82

Core	Depth (cm)	SiO ₂	TiO ₂	Al ₂ O ₃	FeO	MnO	MgO	CaO	Na ₂ O	K ₂ O	P ₂ O ₅	Total
		72.28	0.24	13.55	3.13	0.12	0.11	1.92	5.84	2.42	0.03	99.63

Table A.1.4. EMPA of Lipari and BCR-2G glass standards prior to Abisko glass shard analysis

DataSet	SiO₂	TiO₂	Al₂O₃	FeO	MnO	MgO	CaO	Na₂O	K₂O	P₂O₅	Total	Comment	Mean Z
1/1.	55.20	2.30	13.56	12.15	0.20	3.60	6.93	3.21	1.79	0.36	99.29	BCR2g	12.70
2/1.	54.41	2.26	13.38	12.48	0.17	3.72	7.13	3.28	1.74	0.38	98.96	BCR2g	12.70
3/1.	54.54	2.26	13.16	12.58	0.21	3.75	6.91	3.32	1.88	0.39	99.00	BCR2g	12.72
4/1.	53.96	2.26	13.23	12.38	0.20	3.77	7.03	3.52	1.79	0.38	98.51	BCR2g	12.64
5/1.	74.43	0.07	12.70	1.76	0.07	0.04	0.81	4.18	5.23	0.00	99.30	Lipari	11.27
6/1.	74.04	0.08	12.68	1.63	0.07	0.04	0.71	4.16	4.96	0.01	98.36	Lipari	11.13
7/1.	74.78	0.07	12.99	1.59	0.07	0.06	0.72	4.27	5.21	0.00	99.76	Lipari	11.29
8/1.	74.50	0.07	12.80	1.65	0.07	0.02	0.79	4.01	5.24	0.00	99.15	Lipari	11.24
9/1.	54.11	2.26	13.23	12.50	0.18	3.69	6.99	3.21	1.86	0.36	98.40	BCR2g	12.64
10/1.	54.70	2.27	13.33	12.72	0.20	3.76	7.09	3.42	1.76	0.36	99.60	BCR2g	12.80
11/1.	54.92	2.26	13.41	12.62	0.19	3.66	7.11	3.42	1.81	0.38	99.77	BCR2g	12.81
12/1.	54.22	2.28	13.08	11.70	0.20	3.80	7.00	3.25	1.86	0.35	97.74	BCR2g	12.48

Table A.1.5. Site information

Site name	Codes	Latitude (°N)	Longitude (°E)	Peatland type	Number of samples	Water table depth range (cm)	pH range
Craterpool	P1-7	68°19'10.1"	19°51'27.2"	Palsa	7	-5 to 45	3.76– 4.77
Eagle	E1-6	68°21'56.5"	19°35'02.9"	Fen and bog	6	0 to 29	4.52– 6.74
Electric	L1-6	67°51'56.1"	19°22'06.4"	Palsa	6	0 to 45	3.66– 6.95
Instrument	I1-6	68°11'52.4"	19°45'56.2"	Palsa	6	0 to 36	3.43– 5.32
Marooned	M1-7	67°57'24.0"	19°59'11.4"	Fen and bog	7	-1 to 29	3.24– 4.21
Nikka	N1-6	67°52'02.2"	19°10'42.5"	Fen and bog	6	-1 to 40	4.02– 5.27
Railway	R1-7	68°05'12.6"	19°49'52.9"	Palsa	7	0 to 40	3.25– 6.35
Stordalen	S1-40	68°21'24.3"	19°02'53.5"	Palsa and fen	40	-7 to 50	2.99– 3.80

**Suppl. Chapter 4: Standard chemical-based tephra extraction methods
significantly alter the geochemistry of volcanic glass shards**

A.2.1. PERMANOVA testing

The Euclidean distance between data points in each variable set was calculated, and these distance measures for each data group were used in the construction of the test statistic (F -ratio) and the calculation of permutation (P) values. The F -ratio is calculated as follows:

$$F = \frac{SS_A / (a-1)}{SS_W / (N-a)} \quad (1)$$

where SS_W is equal to the sum of the squared Euclidean distances between each data point and the corresponding group centroid, and SS_T represents the sum of squared distances in the Euclidean half matrix divided by N (total number of observations) (Anderson, 2001). a = the number of groups.

$$SS_W = \frac{1}{n} \sum_{i=1}^{N-1} \sum_{j=i+1}^N d_{ij}^2 \varepsilon_{ij} \quad (2)$$

$$SS_T = \frac{1}{N} \sum_{i=1}^{N-1} \sum_{j=i+1}^N d_{ij}^2 \quad (3)$$

$$SS_A = SS_T - SS_W \quad (4)$$

The purpose of the F -ratio is to test the degree of variance within groups against variance between groups; in this instance, the variance within the control group of each element oxide versus the groups subjected to each of the three treatments. The greater the value of F , the less likely the condition of a null hypothesis (i.e. no difference between the treatments and the control values for

that element oxide). Calculation of the P -values is a further measure of confidence in this regard; the statistic is calculated under the assumption that, in the scenario of a true null hypothesis, values within groups could be permuted across groups with negligible impact on the F -ratio. P is therefore calculated as:

$$P = \frac{(\text{No. of } F^\pi = F)}{\text{Total no. } F^\pi} \quad (5)$$

where F^π is the value of the F -ratio under any given permutation. The P -value represents an evaluation of how well the sample data matches the criteria of the null hypothesis; in short, the greater the value of P , the more likely the case of a null hypothesis. All equations are after Anderson (2001).

Table A.2.1. Major element geochemistry of tephra analyses for each chemical treatment, normalised to 100%. Analyses with an original total oxide count of < 97 % have been removed.

Control (Untreated)											
	SiO ₂	TiO ₂	Al ₂ O ₃	FeO	MnO	MgO	CaO	Na ₂ O	K ₂ O	P ₂ O ₅	Original Analytical Total
Hekla-Selsund Phase 1	64.99	0.03	20.96	0.85	0.02	0.02	4.69	7.46	0.97	0.00	102.03
	55.49	0.02	27.88	0.48	0.01	0.03	10.15	5.77	0.17	0.01	101.64
	55.76	0.02	27.68	0.32	0.01	0.02	10.39	5.61	0.18	0.01	100.74
	55.14	0.03	27.88	0.51	0.02	0.05	10.47	5.75	0.15	0.01	101.93
	74.98	0.19	13.29	2.57	0.09	0.11	1.45	4.20	3.11	0.02	100.25
	74.80	0.18	13.56	2.71	0.09	0.12	1.48	4.06	2.99	0.01	100.22
	65.57	0.64	14.41	7.74	0.20	0.85	3.74	5.15	1.46	0.24	100.03
	62.83	0.79	15.13	8.84	0.24	0.96	4.55	4.80	1.53	0.32	99.97
	55.94	0.87	22.75	6.96	0.22	1.22	5.33	4.42	1.84	0.46	100.43
	61.31	0.62	21.91	4.88	0.19	0.91	3.92	4.17	1.80	0.29	101.85
	60.84	0.38	20.52	4.52	0.09	0.50	6.66	5.58	0.72	0.19	99.51
	62.89	0.92	14.40	9.42	0.24	1.18	4.28	3.83	2.45	0.38	99.50
<i>Average</i>	<i>62.54</i>	<i>0.39</i>	<i>20.03</i>	<i>4.15</i>	<i>0.12</i>	<i>0.50</i>	<i>5.59</i>	<i>5.07</i>	<i>1.45</i>	<i>0.16</i>	
Hekla-Selsund Phase 2	56.86	2.04	13.94	11.68	0.29	2.50	6.39	3.82	1.41	1.08	99.54
	57.38	2.09	13.56	11.30	0.27	2.62	6.25	4.06	1.43	1.06	99.71
	57.65	2.08	13.36	11.58	0.29	2.55	6.25	3.74	1.42	1.07	99.43
	54.99	0.08	27.42	0.61	0.01	0.11	11.27	5.29	0.19	0.02	101.17

	55.60	0.07	27.47	0.54	0.01	0.08	10.65	5.37	0.19	0.02	100.42
	49.73	0.35	1.60	20.87	0.81	8.17	18.20	0.30	0.00	0.00	101.41
	40.97	0.26	1.47	15.65	0.65	6.31	25.19	0.19	0.06	9.26	100.13
	50.09	0.33	1.35	19.74	0.76	8.68	18.77	0.27	0.00	0.00	100.19
	50.38	0.35	1.44	19.39	0.70	8.64	18.88	0.22	0.01	0.00	101.49
	50.51	0.33	1.36	19.34	0.72	8.66	18.78	0.30	0.00	0.00	100.68
	50.08	0.27	1.05	21.09	0.81	7.97	18.46	0.26	0.00	0.01	101.03
	49.43	0.26	1.00	22.10	0.83	7.37	18.79	0.24	0.00	0.01	101.31
	50.16	0.31	1.22	19.87	0.75	8.52	18.88	0.29	0.00	0.00	101.64
	57.83	1.94	13.08	11.52	0.29	2.98	6.12	3.85	1.37	1.01	100.08
<i>Average</i>	52.26	0.77	8.52	14.66	0.51	5.37	14.49	2.01	0.43	0.97	
Hekla 1341	58.41	1.67	14.15	11.47	0.29	2.01	5.37	4.28	1.57	0.79	100.31
	59.14	1.51	14.18	11.51	0.28	2.23	5.37	3.40	1.67	0.69	98.11
	59.79	1.63	14.06	10.87	0.29	1.85	5.44	3.60	1.69	0.78	99.81
	46.28	3.46	14.27	15.33	0.24	5.75	10.66	3.03	0.63	0.36	100.96
	46.45	3.29	14.61	15.54	0.24	5.92	10.29	2.70	0.61	0.35	101.21
	59.65	1.62	14.07	10.71	0.29	2.10	5.21	3.68	1.89	0.78	100.57
	58.89	1.70	13.84	11.89	0.30	2.18	5.39	3.40	1.64	0.76	100.79
	59.88	1.65	13.19	11.36	0.29	1.75	5.15	3.87	1.96	0.91	98.88
	58.50	1.64	13.96	11.74	0.30	2.31	5.61	3.69	1.53	0.72	100.11
	58.91	1.66	14.23	11.85	0.30	2.35	5.69	2.78	1.49	0.74	99.70
	58.98	1.50	14.41	10.91	0.27	2.16	5.56	4.16	1.37	0.68	100.97
	58.65	1.58	13.86	11.55	0.28	2.27	5.62	3.92	1.51	0.75	99.42
	58.45	1.71	13.32	12.24	0.35	2.39	5.63	3.52	1.60	0.78	100.06

	57.92	0.83	17.13	9.96	0.15	1.81	6.36	4.20	1.24	0.40	100.13
	47.29	2.43	15.67	12.88	0.19	7.48	10.84	2.52	0.45	0.26	100.67
<i>Average</i>	<i>56.48</i>	<i>1.86</i>	<i>14.33</i>	<i>11.99</i>	<i>0.27</i>	<i>2.97</i>	<i>6.55</i>	<i>3.52</i>	<i>1.39</i>	<i>0.65</i>	
Hekla 1947	60.76	1.29	14.68	5.02	0.27	1.93	1.87	3.97	1.87	0.51	99.88
	60.22	1.31	14.82	5.01	0.26	1.97	1.75	3.86	1.75	0.53	100.86
	60.52	1.21	15.32	5.28	0.25	1.76	1.56	4.29	1.56	0.49	100.19
	60.76	1.29	14.84	4.89	0.25	1.93	1.86	3.94	1.86	0.53	101.27
	63.85	1.05	14.72	4.52	0.24	1.06	2.01	4.25	2.01	0.34	98.12
	63.21	0.91	15.27	4.63	0.23	1.24	1.77	4.53	1.77	0.30	100.92
	63.00	0.93	15.09	4.71	0.24	1.17	1.75	4.53	1.75	0.31	99.95
	60.73	1.33	14.29	4.95	0.27	1.83	1.68	4.31	1.68	0.55	101.12
	60.82	1.28	14.54	4.90	0.27	1.75	1.89	4.20	1.89	0.54	100.98
	61.73	1.28	14.33	4.74	0.22	1.70	1.83	4.26	1.83	0.54	99.51
	61.14	1.24	13.92	4.99	0.26	2.08	1.63	4.13	1.63	0.52	100.48
	60.85	1.20	15.42	5.38	0.23	1.63	1.51	4.48	1.51	0.54	100.77
<i>Average</i>	<i>61.46</i>	<i>1.19</i>	<i>14.77</i>	<i>4.92</i>	<i>0.25</i>	<i>1.67</i>	<i>1.76</i>	<i>4.23</i>	<i>1.76</i>	<i>0.47</i>	
Hekla 1991	48.10	0.24	12.79	14.73	0.24	4.97	10.01	3.08	0.70	0.63	98.62
	47.74	0.23	12.75	15.05	0.23	5.09	9.86	3.09	0.75	0.65	98.66
	47.95	0.23	12.52	14.90	0.23	5.16	9.73	3.29	0.79	0.63	98.61
	48.19	0.24	12.53	14.89	0.24	5.01	9.80	3.09	0.82	0.64	97.93
	56.74	0.31	12.54	12.58	0.31	2.71	6.24	3.90	1.55	1.13	97.43
	56.45	0.33	12.48	13.29	0.33	3.06	6.12	3.31	1.56	1.06	98.99
	57.31	0.30	12.44	12.54	0.30	2.52	6.03	3.81	1.58	1.13	98.52
	56.63	0.31	12.70	12.74	0.31	2.60	6.13	3.77	1.57	1.17	98.61

	56.51	0.30	12.98	12.93	0.30	2.83	5.86	3.60	1.60	1.04		99.46
	56.75	0.31	14.07	12.32	0.31	3.05	6.72	2.43	1.33	0.94		99.32
	56.51	0.31	13.58	12.45	0.31	2.99	6.44	3.21	1.40	0.99		98.53
	56.89	0.33	12.17	13.59	0.33	2.27	6.18	3.13	1.81	1.17		98.27
<i>Average</i>	<i>53.82</i>	<i>0.29</i>	<i>12.80</i>	<i>13.50</i>	<i>0.29</i>	<i>3.52</i>	<i>7.43</i>	<i>3.31</i>	<i>1.29</i>	<i>0.93</i>		
Katla 1357	47.62	4.81	12.88	15.16	0.23	5.06	9.74	3.06	0.70	0.73		98.84
	47.46	4.80	12.37	15.59	0.22	5.19	9.76	3.07	0.83	0.70		99.09
	47.47	4.79	12.76	15.16	0.24	5.21	9.59	3.26	0.85	0.70		99.73
	47.20	4.80	12.60	15.60	0.23	5.07	9.76	3.29	0.75	0.70		98.90
	47.81	4.78	12.38	15.61	0.24	4.96	9.70	3.06	0.77	0.70		99.44
	47.43	4.84	12.57	15.25	0.26	5.11	9.75	3.25	0.82	0.71		98.80
	47.24	4.80	12.70	15.63	0.24	5.03	9.64	3.19	0.81	0.71		99.59
	47.60	4.84	12.93	15.07	0.24	5.10	9.72	3.00	0.78	0.71		98.64
	47.44	4.77	12.72	15.36	0.24	5.07	9.60	3.26	0.82	0.72		99.53
	47.74	4.78	12.47	15.28	0.23	5.02	9.81	3.22	0.75	0.70		99.42
	48.09	4.76	12.47	15.12	0.23	4.92	9.78	3.14	0.76	0.72		99.26
	47.52	4.86	12.83	15.12	0.23	5.05	9.82	3.14	0.71	0.72		98.06
	47.82	4.81	12.68	15.01	0.23	5.13	9.64	3.16	0.84	0.69		98.76
	48.00	4.76	12.59	15.26	0.23	4.98	9.63	3.12	0.73	0.70		100.36
	47.72	4.77	12.63	15.13	0.25	5.10	9.67	3.28	0.77	0.68		100.08
<i>Average</i>	<i>47.61</i>	<i>4.80</i>	<i>12.64</i>	<i>15.29</i>	<i>0.24</i>	<i>5.07</i>	<i>9.71</i>	<i>3.17</i>	<i>0.78</i>	<i>0.71</i>		
Lipari Obsidian	74.77	0.08	13.17	1.36	0.07	0.04	0.76	3.90	5.84	0.00		99.51
	74.72	0.08	13.28	1.56	0.06	0.04	0.74	3.82	5.70	0.00		100.96
	74.86	0.08	13.02	1.62	0.06	0.05	0.74	3.74	5.82	0.00		99.73

	75.33	0.08	12.69	1.51	0.05	0.03	0.74	3.81	5.75	0.01	100.51
	74.96	0.08	13.10	1.56	0.05	0.03	0.70	3.75	5.77	0.01	101.10
	75.24	0.09	13.24	1.56	0.06	0.02	0.71	6.31	2.77	0.00	98.12
	75.11	0.08	13.05	1.50	0.06	0.05	0.71	3.78	5.64	0.01	100.25
	74.98	0.08	12.98	1.64	0.07	0.04	0.71	4.24	5.26	0.00	101.67
	75.37	0.08	12.96	1.41	0.07	0.05	0.72	4.12	5.21	0.01	101.04
	75.08	0.08	12.99	1.49	0.07	0.04	0.72	4.33	5.18	0.01	100.64
	74.90	0.08	13.21	1.68	0.06	0.05	0.81	3.96	5.23	0.02	101.21
	75.39	0.08	12.94	1.51	0.07	0.06	0.77	4.07	5.10	0.01	99.82
	75.24	0.08	12.90	1.42	0.05	0.07	0.78	4.17	5.28	0.01	100.53
	74.70	0.08	13.10	1.66	0.06	0.04	0.76	4.15	5.44	0.01	99.04
	75.13	0.08	13.18	1.43	0.07	0.01	0.71	4.14	5.25	0.00	100.50
	75.05	0.08	13.05	1.53	0.06	0.04	0.74	4.15	5.28	0.01	
<i>Average</i>	67.30	1.37	14.23	6.19	0.20	1.28	3.48	2.85	2.74	0.37	97.75
SILK	66.75	1.38	13.92	5.61	0.19	1.21	3.16	4.74	2.68	0.36	98.37
	66.56	1.38	13.90	5.61	0.18	1.13	3.30	4.89	2.68	0.37	98.76
	65.74	1.39	13.81	6.31	0.20	1.29	3.39	4.86	2.63	0.39	100.59
	66.68	1.41	14.48	5.98	0.19	1.28	3.34	3.48	2.79	0.36	99.36
	65.73	1.36	13.79	6.32	0.21	1.30	3.61	4.77	2.55	0.37	100.40
	67.25	1.41	13.99	4.96	0.17	1.17	3.03	4.84	2.82	0.36	99.60
	65.60	1.37	13.75	6.38	0.22	1.48	3.68	4.54	2.62	0.36	99.32
	67.22	1.40	14.57	6.47	0.21	1.43	3.50	2.21	2.63	0.36	98.45
	65.91	1.38	14.04	5.91	0.18	1.35	3.57	4.68	2.59	0.38	98.26
	65.90	1.38	14.03	6.04	0.20	1.40	3.44	4.54	2.69	0.37	97.48

	65.46	1.35	14.05	6.23	0.20	1.43	3.64	4.71	2.58	0.36	99.1827
<i>Average</i>	66.34	1.38	14.05	6.00	0.20	1.31	3.43	4.26	2.67	0.37	
SL1	65.51	0.84	14.99	6.56	0.18	1.33	4.38	4.15	1.74	0.30	100.50
	65.11	0.81	15.07	6.80	0.17	1.17	4.60	4.37	1.64	0.27	101.57
	65.91	0.84	15.14	6.19	0.16	1.15	4.21	4.32	1.81	0.27	100.71
	65.11	0.84	14.90	6.88	0.18	1.32	4.48	4.31	1.70	0.28	101.28
	54.96	2.30	14.02	12.71	0.27	3.24	6.74	3.13	1.35	1.27	100.06
	55.10	2.12	14.47	11.93	0.27	3.07	6.61	4.04	1.26	1.14	100.19
	55.86	2.07	14.31	11.34	0.27	3.11	6.80	3.82	1.31	1.12	99.91
	55.72	2.06	14.50	11.69	0.27	3.04	6.53	3.86	1.27	1.07	100.69
	55.49	2.06	14.20	12.12	0.28	3.12	6.43	3.82	1.38	1.10	99.84
	56.66	2.13	14.03	11.30	0.28	2.93	6.24	3.83	1.48	1.13	100.179
	65.07	0.81	15.20	6.84	0.17	1.24	4.39	4.31	1.69	0.29	99.9944
	65.66	0.80	15.17	6.28	0.15	1.15	4.26	4.45	1.79	0.27	100.0378
	64.30	0.72	16.68	5.54	0.15	0.95	5.28	4.78	1.35	0.26	100.0082
	65.25	0.78	15.41	6.33	0.14	1.17	4.32	4.62	1.71	0.27	100.0078
	65.25	0.84	14.95	6.69	0.18	1.15	4.33	4.55	1.80	0.26	100.61
<i>Average</i>	61.40	1.33	14.87	8.61	0.21	1.94	5.31	4.16	1.55	0.62	
RL1	49.64	3.05	13.22	14.64	0.24	5.76	9.92	2.77	0.44	0.33	100.01
	72.75	0.21	14.07	3.32	0.11	0.09	2.03	4.76	2.63	0.02	99.50
	49.53	2.65	16.78	11.97	0.20	4.27	10.87	3.09	0.35	0.29	99.35
	48.76	3.06	13.44	15.19	0.25	5.69	10.09	2.71	0.46	0.34	99.18
	49.48	3.08	13.15	14.78	0.24	5.56	10.19	2.71	0.46	0.35	99.07
	64.58	0.64	15.66	6.87	0.17	0.62	4.80	5.42	1.04	0.20	99.53

	63.70	0.70	14.78	8.79	0.26	0.83	3.96	4.55	2.22	0.20	99.87
	56.13	2.06	15.80	10.01	0.27	2.43	6.68	4.36	1.25	1.01	99.84
	55.82	1.65	18.41	8.72	0.23	1.85	7.64	3.88	1.04	0.76	99.96
	55.86	1.72	16.66	9.49	0.25	2.19	7.49	4.45	1.07	0.82	99.41
	76.90	0.07	12.47	1.87	0.07	0.06	1.17	4.50	2.89	0.00	99.77
	76.33	0.08	13.00	1.77	0.08	0.04	1.35	4.50	2.84	0.01	100.46
	76.42	0.08	12.66	1.86	0.06	0.01	1.32	4.77	2.82	0.00	99.08
	68.34	0.41	14.60	5.67	0.19	0.40	3.40	4.69	2.21	0.09	98.76
	71.83	0.42	15.47	5.94	0.18	0.39	3.50	0.06	2.12	0.10	98.26
<i>Average</i>	<i>62.41</i>	<i>1.33</i>	<i>14.68</i>	<i>8.06</i>	<i>0.19</i>	<i>2.01</i>	<i>5.63</i>	<i>3.81</i>	<i>1.59</i>	<i>0.30</i>	

Method 1: Burn + HCl

	SiO ₂	TiO ₂	Al ₂ O ₃	FeO	MnO	MgO	CaO	Na ₂ O	K ₂ O	P ₂ O ₅	Original Analytical Total
Hekla-Selsund Phase 1	63.50	0.79	15.08	8.85	0.24	1.09	4.00	5.05	1.08	0.33	99.71
	64.42	0.74	15.79	6.92	0.16	0.74	4.85	5.16	0.92	0.29	100.21
	63.31	0.78	15.14	9.12	0.26	1.17	3.64	5.33	0.96	0.29	100.24
	63.48	0.78	15.19	8.51	0.22	1.07	4.06	5.13	1.27	0.28	100.57
	69.64	0.32	14.76	4.87	0.15	0.27	2.87	4.84	2.24	0.06	100.72
	62.45	0.79	15.78	8.82	0.24	1.07	4.39	5.29	0.85	0.32	101.03
	66.22	0.49	15.15	6.50	0.18	0.50	3.56	4.96	2.29	0.15	99.92
	66.84	0.50	15.14	6.07	0.18	0.55	3.67	4.69	2.21	0.15	99.83
	66.91	0.49	15.13	6.03	0.17	0.59	3.40	4.84	2.28	0.16	99.78
	56.68	0.13	26.50	0.66	0.00	0.04	9.18	6.25	0.55	0.02	99.89
	55.97	0.13	26.94	0.86	0.01	0.05	9.56	6.00	0.44	0.03	100.06
	56.75	0.12	26.66	0.73	0.00	0.06	9.00	6.20	0.47	0.02	101.34

	66.49	0.52	15.33	6.72	0.19	0.60	3.66	4.43	1.91	0.15	100.02
	66.18	0.55	15.13	6.48	0.19	0.65	3.87	4.76	2.02	0.17	99.37
	62.47	0.92	14.59	9.53	0.25	1.16	4.30	4.78	1.63	0.37	100.01
	62.30	0.91	15.13	9.35	0.24	1.12	4.24	4.80	1.53	0.37	99.94
	65.05	0.95	15.12	9.38	0.25	1.13	4.51	1.77	1.46	0.38	97.96
Hekla-Selsund Phase 2	47.82	3.97	13.38	15.25	0.22	5.65	11.16	1.53	0.62	0.41	98.76
	48.30	4.00	13.30	15.00	0.22	5.75	11.05	1.34	0.63	0.42	98.53
	47.91	3.97	13.53	15.45	0.22	5.66	10.92	1.37	0.56	0.42	99.63
	48.24	4.00	13.31	14.98	0.22	5.83	10.97	1.47	0.54	0.43	98.73
	47.66	4.03	13.79	14.82	0.23	5.81	11.18	1.45	0.60	0.43	97.98
	47.20	2.51	15.51	12.93	0.20	7.33	11.21	2.42	0.44	0.27	97.68
	46.72	2.43	15.83	12.96	0.21	7.50	11.15	2.54	0.43	0.23	99.16
	47.02	2.47	15.89	12.43	0.20	7.60	11.25	2.52	0.39	0.24	98.64
	46.58	2.45	16.11	12.81	0.20	7.53	11.14	2.46	0.45	0.26	98.89
	58.06	2.10	13.59	12.15	0.30	2.35	6.13	2.99	1.28	1.06	99.96
	58.44	2.18	13.60	11.76	0.30	2.54	6.18	2.62	1.25	1.13	98.73
	57.48	2.12	13.66	11.80	0.30	2.44	6.04	3.66	1.41	1.09	99.29
	57.42	2.12	13.57	11.23	0.28	2.52	6.32	4.03	1.42	1.08	99.61
	56.85	2.10	13.96	11.62	0.29	2.49	6.18	3.98	1.43	1.09	99.43
	73.02	0.19	13.94	3.17	0.11	0.12	1.93	4.96	2.53	0.02	99.67
	73.10	0.19	14.06	3.01	0.12	0.14	2.20	4.72	2.45	0.02	99.91
	58.64	0.01	25.87	0.32	0.00	0.01	7.89	7.00	0.25	0.01	100.21
	59.07	0.01	25.47	0.39	0.01	0.00	7.78	7.02	0.24	0.01	99.91
	58.47	0.01	26.19	0.26	0.00	0.01	8.08	6.74	0.23	0.01	100.85

	67.28	0.47	14.96	5.94	0.18	0.57	3.47	4.89	2.12	0.13	99.72
	67.51	0.47	15.18	6.05	0.17	0.54	3.52	4.46	1.97	0.14	99.88
Hekla 1341	49.88	4.69	12.53	15.32	0.24	5.05	10.18	0.70	0.79	0.62	99.10
	55.89	0.06	27.07	0.61	0.00	0.08	10.13	5.88	0.25	0.03	100.17
	55.71	0.05	27.22	0.49	0.00	0.06	10.49	5.72	0.25	0.02	99.43
	56.94	0.06	26.52	0.68	0.01	0.07	9.42	6.06	0.22	0.02	99.31
	59.97	1.35	15.58	10.06	0.26	1.81	5.28	3.44	1.67	0.58	99.51
	60.41	1.28	15.19	10.20	0.25	1.81	4.22	4.27	1.85	0.51	97.37
	57.16	0.10	25.82	0.89	0.00	0.14	9.37	6.20	0.26	0.05	99.82
	48.65	5.13	11.51	18.38	0.26	4.32	9.97	0.00	1.03	0.76	98.00
	49.17	5.12	11.60	18.14	0.28	4.14	9.68	0.02	1.02	0.83	98.52
	48.72	5.11	11.97	18.05	0.28	4.29	9.68	0.03	1.06	0.81	98.39
	49.20	5.12	11.64	18.08	0.28	4.33	9.59	0.00	0.98	0.79	98.82
	48.96	4.73	13.03	15.71	0.25	5.14	10.25	0.53	0.82	0.58	97.62
	49.01	4.66	13.16	16.03	0.22	4.98	9.99	0.53	0.81	0.60	99.04
	49.06	4.68	13.25	15.51	0.26	5.09	10.08	0.67	0.82	0.59	99.12
	48.93	4.74	12.94	15.40	0.24	5.20	10.26	0.82	0.84	0.62	97.63
Hekla 1947	61.65	1.13	15.35	9.02	0.24	1.55	4.87	4.23	1.53	0.43	99.11
	60.84	1.20	15.55	9.23	0.25	1.69	5.26	4.00	1.47	0.51	98.99
	60.08	1.28	15.69	9.39	0.23	1.79	5.43	3.93	1.60	0.57	99.89
	63.22	0.92	14.72	8.34	0.24	1.23	4.73	4.57	1.72	0.31	99.28
	63.85	0.93	15.11	7.27	0.23	1.16	4.37	4.96	1.83	0.30	100.29
	61.55	1.20	15.31	9.33	0.25	1.68	5.15	3.61	1.45	0.47	99.54
	61.43	1.13	15.70	8.72	0.24	1.57	4.88	4.34	1.53	0.45	100.58

	60.15	1.34	15.06	9.90	0.26	2.01	5.35	3.74	1.61	0.58	100.00
	63.13	0.94	15.02	8.20	0.23	1.29	4.76	4.48	1.62	0.33	100.06
	63.62	0.94	14.82	8.50	0.26	1.28	4.40	4.13	1.76	0.31	98.58
	63.06	0.96	15.37	8.62	0.24	1.37	4.57	3.86	1.62	0.33	99.14
	64.30	0.92	14.76	7.80	0.22	1.20	4.49	4.31	1.70	0.30	99.74
	63.33	0.92	14.97	8.43	0.25	1.32	4.48	4.26	1.73	0.31	100.23
	63.66	0.93	15.53	7.66	0.23	1.17	4.56	4.15	1.80	0.31	99.85
	63.00	0.91	15.22	8.40	0.24	1.21	4.52	4.36	1.82	0.30	100.02
	61.35	1.21	15.17	8.66	0.23	1.59	4.91	4.76	1.62	0.50	99.66
	60.47	1.26	15.07	9.47	0.24	1.84	4.92	4.44	1.76	0.53	99.03
	63.90	0.94	15.33	7.78	0.23	1.20	4.13	4.34	1.80	0.34	99.91
	63.37	0.93	15.28	8.43	0.23	1.25	4.00	4.34	1.85	0.33	99.58
	63.33	0.94	15.38	8.13	0.24	1.28	4.23	4.44	1.70	0.34	99.84
Hekla 1991	56.86	2.36	13.08	13.45	0.31	2.65	6.42	2.11	1.55	1.21	98.32
	57.37	2.35	13.34	12.97	0.32	2.68	6.16	2.16	1.41	1.26	98.19
	56.86	2.33	13.25	13.15	0.31	2.56	6.30	2.56	1.51	1.17	97.59
	57.18	2.35	13.05	13.37	0.32	2.62	6.25	2.33	1.36	1.17	98.51
	57.43	2.35	12.92	12.99	0.33	2.60	6.50	2.25	1.37	1.27	99.12
	57.38	2.34	13.38	12.67	0.29	2.59	6.12	2.45	1.56	1.22	98.88
	57.03	2.31	13.25	13.27	0.32	2.71	6.26	2.10	1.48	1.25	99.08
	57.11	2.35	13.56	13.13	0.31	2.76	6.10	2.05	1.42	1.20	99.05
	60.11	1.83	13.55	10.53	0.25	1.57	4.31	4.29	2.64	0.92	99.84
	60.39	1.78	13.00	10.28	0.26	1.87	4.18	4.75	2.62	0.88	100.27
	56.92	2.37	13.10	12.94	0.32	2.67	6.04	2.58	1.80	1.25	98.66

	58.25	2.52	12.47	12.99	0.31	2.47	6.12	1.96	1.61	1.31	98.15
	56.83	2.15	13.92	12.97	0.31	3.02	6.19	1.95	1.59	1.07	99.80
	56.83	2.10	13.79	12.29	0.29	2.89	6.32	2.90	1.58	1.02	99.38
	57.03	2.42	12.72	12.82	0.30	2.43	5.45	2.75	2.85	1.23	99.22
	57.18	2.00	14.74	11.56	0.26	2.68	6.47	2.85	1.28	0.98	99.30
	57.06	2.05	14.49	11.74	0.28	2.78	6.68	2.67	1.26	1.00	98.38
	57.20	2.04	14.37	11.68	0.28	2.70	6.85	2.55	1.30	1.03	98.29
	56.88	2.03	14.58	11.80	0.29	2.67	6.91	2.50	1.34	1.00	98.17
	57.03	2.00	15.13	11.12	0.28	2.70	6.88	2.77	1.13	0.96	98.89
	56.83	2.04	14.51	11.71	0.30	2.88	6.89	2.54	1.30	1.00	98.62
	56.32	2.06	14.86	12.03	0.30	2.91	6.70	2.49	1.33	0.99	98.65
Katla 1357	47.98	4.72	13.03	13.95	0.23	5.05	10.11	3.36	0.85	0.72	98.62
	47.86	4.84	12.90	14.54	0.25	4.83	9.89	3.36	0.82	0.72	98.67
	47.10	4.84	12.57	15.51	0.25	5.01	10.02	3.20	0.81	0.68	97.85
	47.87	4.84	12.32	15.36	0.24	5.10	9.71	3.13	0.75	0.69	98.13
	47.51	4.84	12.40	15.85	0.23	4.91	9.64	3.18	0.75	0.69	98.13
	47.68	4.84	12.46	15.51	0.23	4.95	9.72	3.15	0.79	0.67	99.59
	47.07	4.90	12.57	15.62	0.23	4.91	10.00	3.12	0.87	0.71	99.79
	47.62	4.80	12.16	15.64	0.25	5.03	9.82	3.09	0.86	0.74	98.96
	47.49	4.84	12.71	15.49	0.22	4.85	9.72	3.14	0.83	0.71	99.96
	47.39	4.83	12.94	15.35	0.23	4.65	9.76	3.27	0.83	0.75	98.00
	48.00	4.88	12.77	14.36	0.22	4.85	10.25	3.13	0.82	0.71	98.45
	47.86	3.99	12.20	12.44	0.23	6.73	12.87	2.56	0.41	0.71	98.00
Lipari Obsidian	74.94	0.09	13.18	1.55	0.08	0.07	0.78	3.97	5.34	0.01	99.98

	75.07	0.08	13.02	1.52	0.06	0.04	0.67	4.06	5.46	0.01	99.36
	75.00	0.08	13.14	1.69	0.07	0.00	0.75	4.03	5.23	0.01	100.18
	75.05	0.07	13.08	1.61	0.08	0.05	0.76	3.90	5.41	0.00	99.90
	74.65	0.08	13.26	1.43	0.06	0.07	0.77	4.05	5.62	0.01	99.17
	74.74	0.08	13.33	1.55	0.06	0.07	0.88	3.87	5.42	0.01	97.98
	74.43	0.08	13.43	1.69	0.05	0.04	0.87	3.92	5.48	0.00	98.35
	74.58	0.08	13.27	1.63	0.06	0.07	0.75	4.01	5.55	0.00	99.20
	74.83	0.08	13.30	1.71	0.07	0.03	0.74	3.82	5.41	0.01	100.25
	75.26	0.08	13.03	1.64	0.05	0.05	0.72	3.87	5.31	0.00	100.72
	74.58	0.07	12.98	1.66	0.06	0.05	0.72	4.14	5.74	0.01	99.23
	74.67	0.08	13.36	1.67	0.06	0.01	0.81	3.90	5.43	0.00	98.98
	75.02	0.08	13.07	1.66	0.08	0.05	0.75	3.93	5.36	0.01	99.60
	74.70	0.09	13.33	1.83	0.07	0.06	0.73	3.88	5.32	0.00	100.23
	74.86	0.09	13.12	1.62	0.08	0.04	0.79	4.03	5.37	0.00	99.12
SILK	65.51	1.37	13.82	5.98	0.20	4.98	3.70	4.98	2.77	0.38	99.52
	65.45	1.37	13.92	6.37	0.20	4.91	3.50	4.91	2.58	0.35	100.45
	65.58	1.39	13.93	6.18	0.19	4.96	3.51	4.96	2.53	0.38	99.45
	49.71	4.55	13.11	15.11	0.23	0.68	10.18	0.68	0.74	0.55	98.33
	49.38	4.51	13.03	15.12	0.22	0.97	10.08	0.97	0.93	0.56	98.54
	65.47	1.38	14.01	6.50	0.19	4.75	3.27	4.75	2.62	0.38	99.29
	65.38	1.38	13.98	6.28	0.20	4.88	3.53	4.88	2.65	0.36	99.53
	65.08	1.38	14.16	6.77	0.22	4.80	3.12	4.80	2.63	0.37	99.39
	65.82	1.38	14.03	6.37	0.21	4.51	3.36	4.51	2.60	0.37	99.60
	65.50	1.37	14.38	6.21	0.20	4.65	3.40	4.65	2.55	0.36	100.52

	65.34	1.37	13.96	6.43	0.20	4.71	3.67	4.71	2.52	0.39	99.93
	66.20	1.40	14.01	6.31	0.21	4.55	2.79	4.55	2.80	0.39	98.06
	65.45	1.37	13.89	6.17	0.20	4.74	3.78	4.74	2.60	0.36	99.47
	65.64	1.38	13.82	6.45	0.20	4.57	3.58	4.57	2.63	0.38	99.27
	65.37	1.38	13.94	6.09	0.19	4.83	3.77	4.83	2.68	0.38	99.33
SL1	55.59	2.21	15.05	12.05	0.27	3.11	7.10	2.23	1.19	1.21	98.02
	55.85	2.17	15.19	11.60	0.29	3.15	7.13	2.09	1.31	1.22	99.20
	55.66	2.21	14.75	12.19	0.28	3.18	7.02	2.21	1.23	1.26	98.10
	55.48	2.23	15.10	12.03	0.27	3.31	6.98	2.09	1.31	1.21	98.51
	55.76	2.25	14.93	11.41	0.29	3.09	6.78	3.05	1.18	1.26	97.70
	62.12	1.39	15.41	8.62	0.20	1.97	5.43	2.84	1.38	0.64	98.74
	56.43	2.09	14.86	11.84	0.29	3.18	6.75	1.93	1.49	1.15	98.95
	59.03	1.68	15.63	9.80	0.22	2.32	6.03	3.00	1.46	0.84	98.43
	55.75	2.19	14.88	12.91	0.30	3.41	7.05	1.43	0.81	1.26	98.56
	65.17	0.82	15.27	6.42	0.17	1.20	4.33	4.56	1.78	0.27	98.96
	65.33	0.81	15.19	6.49	0.17	1.09	4.37	4.54	1.70	0.29	99.16
	64.75	0.82	15.55	6.73	0.19	1.25	4.30	4.41	1.73	0.27	99.34
	65.20	0.82	15.21	6.63	0.17	1.20	4.33	4.48	1.68	0.26	99.46
	65.43	0.82	14.96	6.69	0.16	1.17	4.24	4.49	1.76	0.28	99.65
	65.31	0.82	15.40	6.42	0.16	1.12	4.20	4.53	1.74	0.28	99.14
RL1	57.09	0.01	26.76	0.33	0.01	0.01	9.24	6.36	0.18	0.00	99.88
	57.90	0.02	26.16	0.22	0.01	0.03	8.84	6.61	0.22	0.00	100.27
	58.81	0.02	25.71	0.30	0.01	0.05	8.01	6.88	0.22	0.00	99.25
	58.89	0.01	25.45	0.29	0.00	0.03	8.00	7.07	0.25	0.01	101.50

58.25	0.01	26.12	0.28	0.00	0.02	8.61	6.50	0.22	0.00	100.66
49.92	4.60	13.25	15.08	0.25	4.96	9.96	0.47	0.89	0.60	98.08
49.60	4.62	13.53	15.46	0.23	4.97	9.74	0.36	0.91	0.58	97.83
49.68	4.58	13.44	15.21	0.24	4.93	9.78	0.69	0.88	0.59	97.92
49.72	1.88	14.05	13.37	0.23	6.68	11.95	1.70	0.24	0.18	98.84
50.36	1.87	14.05	13.13	0.22	6.51	11.60	1.85	0.24	0.17	99.28
50.28	1.89	13.65	13.32	0.22	6.63	11.69	1.95	0.19	0.19	99.00
50.06	1.96	14.08	13.95	0.24	6.50	11.41	1.39	0.22	0.20	99.35
50.55	1.92	13.94	13.08	0.23	6.50	11.73	1.65	0.21	0.19	100.92

Method 2: Acid Digestion

	SiO ₂	TiO ₂	Al ₂ O ₃	FeO	MnO	MgO	CaO	Na ₂ O	K ₂ O	P ₂ O ₅	Original Analytical Total
Hekla-Selsund Phase 1	70.83	0.25	14.37	4.07	0.11	0.29	2.50	4.75	2.80	0.04	100.33
	64.33	0.77	16.35	6.03	0.17	0.55	4.54	5.19	1.73	0.33	99.98
	64.12	0.72	15.05	8.06	0.22	0.96	4.22	4.52	1.87	0.26	98.82
	63.94	0.72	15.09	8.29	0.20	0.96	4.35	4.29	1.91	0.25	99.84
	64.67	0.72	15.20	7.55	0.21	0.88	4.27	4.38	1.86	0.26	99.81
	46.91	4.24	13.35	15.58	0.25	5.22	10.47	2.18	1.28	0.52	99.15
	47.07	4.26	13.52	15.61	0.25	5.21	10.34	2.06	1.20	0.49	98.03
	63.83	0.67	14.72	7.78	0.21	0.89	4.99	4.99	1.68	0.24	99.22
	63.00	0.83	15.04	8.69	0.23	1.11	4.24	5.13	1.42	0.31	98.89
	58.80	0.09	25.02	1.15	0.01	0.08	7.95	6.46	0.38	0.05	100.43
	61.12	0.48	20.02	4.32	0.12	0.56	6.40	5.58	1.15	0.23	98.89
	61.57	0.49	20.26	3.79	0.10	0.26	6.36	5.58	1.28	0.31	99.54
	62.98	0.94	14.88	9.22	0.24	1.19	4.35	4.32	1.50	0.39	99.30

	62.58	0.96	14.66	9.29	0.26	1.14	4.48	4.55	1.70	0.37	98.96
	62.82	0.92	14.41	9.63	0.25	1.14	4.24	4.37	1.85	0.37	100.41
Hekla-Selsund Phase 2	57.49	2.17	13.41	11.82	0.29	2.43	5.92	3.84	1.50	1.13	98.25
	57.02	2.15	13.65	12.01	0.30	2.39	6.03	3.80	1.53	1.13	98.29
	57.61	2.19	13.53	11.38	0.28	2.51	6.10	3.81	1.49	1.09	100.03
	57.64	2.09	13.66	11.52	0.27	2.45	6.16	3.63	1.48	1.11	97.16
	67.23	0.47	15.17	6.11	0.16	0.57	3.39	4.79	1.99	0.12	99.94
	59.26	2.04	13.43	10.80	0.26	1.92	5.26	3.95	2.00	1.07	100.15
	68.10	0.44	15.19	5.54	0.17	0.53	3.17	4.68	2.08	0.10	98.03
	68.24	0.44	14.69	5.63	0.17	0.50	3.24	4.94	2.04	0.11	90.94
	57.68	2.14	13.07	11.76	0.29	2.48	6.14	3.83	1.51	1.10	98.78
	57.12	2.14	13.43	12.00	0.29	2.48	5.88	4.03	1.54	1.10	98.48
	73.18	0.19	14.06	3.06	0.09	0.15	1.97	4.76	2.53	0.02	98.12
	73.60	0.18	13.98	2.93	0.10	0.13	2.06	4.60	2.42	0.01	97.46
	73.22	0.19	14.11	3.03	0.10	0.16	1.89	4.88	2.41	0.03	98.11
	73.18	0.19	14.12	3.08	0.10	0.18	2.01	4.75	2.38	0.03	98.01
	67.05	0.49	15.19	6.22	0.17	0.58	3.42	4.79	1.95	0.14	99.58
Hekla 1341	58.86	1.53	14.87	10.52	0.27	1.99	5.53	4.32	1.41	0.68	99.96
	57.45	0.11	25.71	1.05	0.02	0.12	8.68	6.49	0.34	0.05	99.45
	58.79	1.95	13.40	11.74	0.29	1.64	5.23	4.04	1.99	0.92	98.24
	60.05	1.61	13.82	10.94	0.27	1.81	5.05	3.97	1.78	0.70	99.66
	56.98	0.10	26.19	0.86	0.01	0.08	9.73	5.78	0.24	0.03	100.58
	60.27	1.64	12.94	11.21	0.30	1.53	4.93	4.05	2.26	0.88	98.11
	60.94	1.56	13.42	10.51	0.30	1.31	4.75	4.33	2.07	0.80	99.31

	58.85	1.52	14.85	10.58	0.28	2.01	5.20	4.47	1.54	0.69		100.09
	59.17	1.54	15.17	10.11	0.27	2.07	5.31	4.15	1.50	0.71		98.55
	58.37	1.55	14.77	11.24	0.30	2.10	5.47	3.84	1.66	0.71		99.26
	58.44	1.69	13.98	11.61	0.29	2.12	5.51	3.77	1.79	0.80		98.71
	58.87	1.63	14.50	10.53	0.29	2.06	5.67	4.03	1.64	0.78		99.46
	58.46	1.74	14.09	11.08	0.29	2.02	5.40	4.36	1.75	0.81		98.07
Hekla 1947	48.51	4.62	12.87	14.84	0.24	4.79	9.60	3.16	0.78	0.60		98.45
	47.95	4.66	12.59	15.36	0.22	4.80	9.76	3.15	0.90	0.60		97.72
	48.12	4.61	13.00	14.83	0.24	4.79	9.82	3.22	0.75	0.60		98.27
	48.01	4.61	12.97	14.94	0.23	4.91	9.82	3.15	0.76	0.59		98.44
	60.80	1.17	15.45	8.95	0.24	1.61	5.17	4.47	1.65	0.49		99.79
	60.67	1.20	15.31	9.11	0.24	1.66	5.21	4.44	1.66	0.49		99.30
	60.75	1.17	15.26	9.10	0.25	1.79	5.23	4.33	1.62	0.51		99.52
	63.14	0.93	15.33	7.88	0.23	1.17	4.46	4.75	1.78	0.33		100.29
	61.54	1.20	14.98	9.06	0.24	1.69	4.96	4.19	1.63	0.51		99.66
	63.49	0.93	14.94	8.01	0.23	1.20	4.48	4.52	1.86	0.33		99.30
	60.80	1.20	15.36	8.97	0.26	1.73	5.23	4.37	1.58	0.50		98.62
	61.32	1.19	15.14	8.69	0.24	1.72	5.25	4.36	1.60	0.49		98.47
	61.23	1.21	14.99	8.95	0.25	1.72	5.40	4.23	1.53	0.50		98.92
	61.58	1.21	15.09	8.49	0.25	1.72	5.21	4.30	1.61	0.54		99.10
Hekla 1991	56.79	2.35	12.56	12.81	0.32	2.65	6.53	3.32	1.50	1.18		99.18
	56.79	2.46	13.30	12.46	0.29	2.51	6.20	3.16	1.60	1.22		99.43
	55.49	2.41	13.24	13.07	0.35	2.83	6.43	3.50	1.55	1.14		97.62
	55.60	2.39	12.86	13.71	0.31	2.88	6.19	3.45	1.48	1.14		99.07

	56.20	2.37	13.03	12.81	0.33	2.75	6.44	3.35	1.58	1.15	98.65
	55.90	2.35	12.92	13.21	0.31	2.85	6.23	3.47	1.62	1.15	99.10
	55.54	2.35	13.02	13.56	0.32	2.89	6.25	3.37	1.53	1.17	98.89
	55.84	2.35	12.93	13.36	0.32	2.89	6.36	3.29	1.50	1.16	99.05
	56.27	2.34	12.88	13.10	0.31	2.93	6.28	3.20	1.57	1.13	100.22
	56.53	2.51	12.91	12.46	0.31	2.60	6.11	3.66	1.65	1.26	98.47
	56.47	2.44	12.97	13.02	0.32	2.67	6.08	3.26	1.53	1.23	98.10
	56.55	2.44	12.38	13.03	0.36	2.44	5.82	3.51	2.20	1.28	98.41
	60.92	1.80	12.29	11.47	0.28	1.71	4.86	3.74	2.09	0.83	99.14
	61.04	1.87	12.74	11.11	0.27	1.49	4.86	3.66	2.07	0.90	99.00
	55.94	2.54	13.10	12.97	0.33	2.65	6.32	3.23	1.62	1.29	94.97
Katla 1357	48.60	4.91	12.91	15.79	0.25	5.35	10.01	0.58	0.85	0.74	98.5113
	48.20	5.04	12.60	17.14	0.23	5.02	9.77	0.56	0.73	0.72	97.6744
	48.96	4.95	12.98	15.65	0.24	5.32	9.92	0.45	0.78	0.73	99.84
	48.89	4.91	12.71	15.87	0.25	5.09	10.01	0.75	0.80	0.71	99.62
	48.04	4.94	12.53	15.74	0.24	5.09	9.84	2.12	0.75	0.71	100.13
	47.65	4.86	12.65	15.77	0.23	5.28	9.94	2.15	0.77	0.70	100.03
	47.89	4.85	12.51	15.52	0.23	5.02	10.00	2.50	0.77	0.70	98.60
	48.07	4.88	12.98	15.29	0.23	5.04	9.75	2.30	0.75	0.71	98.52
	47.53	4.82	12.91	15.72	0.23	5.23	9.81	2.40	0.67	0.68	99.59
	48.81	4.91	13.47	15.28	0.24	5.06	9.96	0.74	0.80	0.73	99.85
	48.62	4.88	12.89	15.83	0.26	5.19	10.09	0.70	0.79	0.76	98.29
	48.28	4.89	12.84	15.75	0.23	5.40	10.22	0.82	0.81	0.75	100.02
	48.67	4.87	12.97	15.82	0.23	5.07	10.12	0.69	0.82	0.75	90.97

Lipari Obsidian

74.60	0.08	13.24	1.60	0.07	0.06	0.79	4.12	5.45	0.00	98.69
75.19	0.08	13.22	1.10	0.05	0.05	0.74	4.03	5.53	0.01	98.90
74.78	0.08	13.00	1.66	0.07	0.06	0.83	4.27	5.24	0.00	99.00
78.80	0.08	14.01	1.27	0.05	0.02	0.77	0.11	4.88	0.01	97.95
78.41	0.10	14.26	1.24	0.05	0.11	0.81	0.17	4.83	0.01	99.56
74.77	0.08	13.20	1.60	0.07	0.03	0.65	4.12	5.48	0.00	99.08
74.44	0.09	13.35	1.51	0.05	0.04	0.78	4.14	5.58	0.00	100.14
74.40	0.08	13.42	1.47	0.07	0.04	0.75	4.14	5.62	0.01	99.77
75.02	0.09	13.18	1.41	0.07	0.04	0.70	4.12	5.38	0.01	99.39
75.06	0.08	13.06	1.47	0.07	0.08	0.71	4.07	5.41	0.01	99.48
74.99	0.08	13.21	1.39	0.07	0.03	0.71	4.11	5.41	0.01	99.89
74.75	0.08	13.43	1.42	0.07	0.05	0.74	4.15	5.30	0.01	98.93
74.91	0.09	13.19	1.62	0.07	0.03	0.79	4.09	5.21	0.01	100.36
74.80	0.07	13.35	1.58	0.06	0.04	0.71	4.11	5.28	0.01	99.19
74.83	0.09	13.21	1.40	0.06	0.07	0.74	4.12	5.48	0.00	99.30
74.73	0.09	13.34	1.61	0.05	0.04	0.79	4.12	5.22	0.00	99.02
74.92	0.08	12.96	1.72	0.07	0.04	0.77	4.16	5.27	0.01	99.64
76.62	0.08	14.15	1.13	0.04	0.07	0.95	2.32	4.62	0.02	99.83

SILK

65.46	1.38	14.12	6.15	0.21	1.47	3.59	4.57	2.69	0.37	95.68
65.08	1.39	13.89	6.49	0.22	1.45	3.95	4.64	2.51	0.37	97.67
64.77	1.37	14.00	6.95	0.22	1.37	3.90	4.62	2.43	0.37	99.05
67.18	1.33	13.69	5.68	0.21	1.14	2.94	4.51	2.98	0.36	96.19
68.30	1.37	13.93	6.11	0.20	1.12	3.01	3.07	2.57	0.32	95.45
68.18	1.35	14.11	5.94	0.19	1.22	2.97	3.21	2.49	0.34	96.23

	47.53	4.79	12.65	15.19	0.24	5.18	9.93	3.10	0.71	0.69	98.43
	46.65	4.81	13.30	15.32	0.23	5.22	10.09	2.97	0.70	0.69	97.99
	46.51	4.83	13.33	15.31	0.24	5.27	10.04	3.04	0.71	0.72	97.94
	65.88	1.39	13.54	6.26	0.20	1.37	3.67	4.74	2.59	0.36	99.53
	65.04	1.37	14.36	6.40	0.20	1.34	3.53	4.80	2.58	0.37	99.37
	65.43	1.38	14.22	6.20	0.19	1.34	3.43	4.82	2.60	0.39	98.73
	65.65	1.38	14.23	6.04	0.19	1.27	3.39	4.76	2.72	0.37	98.68
	66.99	1.37	14.35	5.08	0.18	1.15	3.03	4.70	2.78	0.36	100.08
	65.71	1.37	13.89	6.17	0.20	1.28	3.56	4.73	2.71	0.37	99.50
SL1	58.08	1.67	14.68	10.43	0.24	2.48	6.05	4.14	1.45	0.77	98.64
	57.92	1.65	15.10	10.40	0.26	2.54	5.87	4.05	1.41	0.81	100.36
	58.52	1.66	15.10	9.61	0.22	2.36	5.65	4.70	1.37	0.81	98.51
	60.25	1.25	15.99	8.26	0.19	1.90	5.66	4.46	1.47	0.57	98.90
	60.72	1.30	14.83	9.20	0.21	2.05	5.39	4.16	1.57	0.56	98.70
	60.06	1.17	15.56	9.05	0.21	1.94	5.51	4.42	1.57	0.51	99.67
	61.08	1.15	15.94	8.43	0.19	1.76	5.52	4.08	1.32	0.53	99.42
	60.49	1.19	16.84	7.18	0.21	1.58	5.99	4.88	1.13	0.52	100.54
	65.04	0.84	15.36	6.46	0.18	1.25	4.46	4.41	1.72	0.29	98.57
	65.03	0.82	15.74	6.54	0.18	1.15	4.10	4.45	1.72	0.27	99.93
	64.59	0.82	15.43	6.86	0.19	1.32	4.42	4.38	1.73	0.26	99.95
	65.33	0.83	15.58	6.19	0.15	1.10	4.06	4.61	1.87	0.29	100.36
	64.75	0.83	15.32	6.77	0.18	1.20	4.47	4.52	1.68	0.28	100.29
	65.17	0.83	15.03	6.76	0.18	1.21	4.42	4.46	1.65	0.29	99.37
	64.24	1.01	15.85	6.31	0.18	1.38	4.45	4.52	1.70	0.36	99.62

RL1	63.26	0.98	15.94	6.92	0.16	1.45	4.68	4.57	1.69	0.35	99.38
	63.36	0.99	15.41	7.24	0.18	1.45	4.79	4.50	1.70	0.39	99.36
	62.65	0.99	15.89	7.53	0.18	1.53	4.83	4.43	1.61	0.38	99.17
	61.63	0.00	23.84	0.33	0.00	0.00	5.72	8.16	0.35	0.00	101.16
	60.58	0.01	24.70	0.27	0.00	0.01	6.15	7.95	0.32	0.01	100.44
	61.82	0.00	23.88	0.21	0.01	0.00	5.27	8.43	0.40	0.00	101.12
	62.20	0.00	23.63	0.28	0.01	0.01	4.97	8.53	0.37	0.00	99.32
	62.14	0.00	23.60	0.24	0.00	0.00	5.27	8.33	0.41	0.01	99.04
	61.62	0.00	24.13	0.21	0.02	0.00	5.35	8.29	0.39	0.00	100.40
	76.23	0.08	12.98	1.88	0.07	0.03	1.26	4.57	2.88	0.01	99.32
	59.50	1.34	15.07	9.89	0.26	2.02	5.55	4.28	1.51	0.58	101.12
	59.33	1.33	15.12	9.94	0.26	1.97	5.71	4.34	1.43	0.57	100.47
Method 3: Base Digestion											
	SiO₂	TiO₂	Al₂O₃	FeO	MnO	MgO	CaO	Na₂O	K₂O	P₂O₅	Original Analytical Total
Hekla-Selsund Phase 1	57.09	0.02	26.75	0.37	0.01	0.02	9.31	6.28	0.15	0.00	99.35
	56.71	0.01	26.84	0.38	0.00	0.01	9.75	6.11	0.19	0.00	100.05
	56.63	0.02	27.23	0.35	0.01	0.04	9.54	5.99	0.20	0.00	100.37
	56.93	0.02	26.89	0.36	0.00	0.04	9.66	5.92	0.18	0.00	101.06
	56.58	0.02	26.87	0.41	0.01	0.04	9.76	6.13	0.18	0.00	100.13
	65.95	0.50	15.58	6.06	0.18	0.58	3.50	4.51	3.01	0.14	100.27
	63.33	0.90	15.16	8.09	0.23	0.89	4.51	4.73	1.79	0.37	98.99
	65.21	0.65	15.22	7.38	0.20	0.81	3.75	4.49	2.08	0.21	99.20
	65.23	0.63	15.36	7.01	0.20	0.84	3.83	4.49	2.18	0.23	98.34
	64.49	0.65	15.34	7.58	0.19	0.83	4.10	4.59	2.00	0.23	99.17

	62.62	0.41	20.40	2.81	0.06	0.16	6.04	6.26	1.07	0.16	98.70
	64.50	0.62	16.44	6.08	0.19	0.71	4.48	5.22	1.53	0.21	99.07
	65.02	0.64	15.24	7.33	0.19	0.79	4.10	4.59	1.89	0.21	99.22
	68.17	0.65	15.60	7.57	0.21	0.79	4.08	0.56	2.15	0.21	97.60
	67.55	0.66	15.81	7.92	0.21	0.85	4.16	0.68	1.94	0.22	97.07
	65.52	0.57	15.53	6.62	0.19	0.66	3.88	4.96	1.86	0.20	99.21
	68.01	0.65	15.52	7.59	0.22	0.86	3.81	0.88	2.24	0.22	97.50
	62.86	0.73	15.19	8.76	0.22	1.04	4.40	5.20	1.31	0.29	100.34
	63.75	0.74	15.41	7.68	0.21	0.96	5.00	4.68	1.28	0.29	99.59
	64.45	0.76	15.23	7.43	0.19	0.92	3.66	5.39	1.69	0.27	99.41
Hekla-Selsund Phase 2	57.72	2.13	13.42	11.48	0.28	2.48	6.07	3.95	1.39	1.06	98.64
	57.61	2.06	13.80	11.57	0.29	2.37	6.01	3.74	1.50	1.06	99.68
	57.80	2.10	13.68	11.37	0.27	2.35	6.09	3.82	1.45	1.07	98.07
	57.53	2.13	13.51	11.53	0.28	2.51	6.03	3.96	1.48	1.05	98.07
	67.78	0.45	15.07	5.74	0.17	0.50	3.34	4.71	2.12	0.11	98.20
	67.89	0.45	15.18	5.75	0.17	0.47	3.21	4.72	2.03	0.11	98.91
	67.72	0.44	15.01	5.58	0.17	0.53	3.26	4.95	2.25	0.10	99.21
	68.20	0.43	14.75	5.74	0.17	0.50	3.34	4.66	2.09	0.11	98.74
	68.35	0.43	14.79	5.62	0.17	0.47	3.36	4.60	2.10	0.11	98.68
	57.26	2.04	13.84	11.30	0.29	2.62	6.24	4.02	1.33	1.06	98.77
	56.63	2.03	14.14	11.63	0.28	2.59	6.14	4.00	1.49	1.08	98.58
	57.53	2.03	13.90	11.07	0.29	2.61	6.27	3.77	1.44	1.10	98.64
	57.19	2.01	13.93	11.28	0.29	2.63	6.21	4.03	1.36	1.08	97.90
	57.64	2.06	13.67	11.27	0.28	2.55	6.06	3.97	1.44	1.05	99.10

	57.27	2.09	13.75	11.22	0.26	2.42	6.28	4.20	1.47	1.05	98.36
	57.50	2.06	13.55	11.55	0.27	2.42	6.08	4.03	1.42	1.10	99.17
	57.60	2.10	13.63	11.28	0.28	2.52	6.09	4.00	1.44	1.07	97.87
	57.54	2.11	13.68	11.29	0.29	2.61	6.09	3.96	1.31	1.12	97.54
Hekla 1341	60.20	1.77	12.73	11.52	0.30	1.66	5.05	3.62	2.22	0.93	97.89
	58.66	0.14	25.14	1.06	0.01	0.08	8.13	6.29	0.43	0.06	101.57
	59.12	1.48	15.09	10.12	0.28	2.01	5.64	3.98	1.60	0.69	99.77
	59.20	1.50	15.24	9.84	0.28	2.01	5.69	4.03	1.51	0.70	99.21
	59.06	1.52	14.73	10.01	0.26	1.99	5.55	4.48	1.69	0.71	98.97
	59.06	1.56	14.58	10.56	0.28	2.12	5.59	4.02	1.51	0.72	99.71
	60.32	1.72	12.39	11.94	0.30	1.51	5.03	3.57	2.06	1.16	99.14
	60.60	1.78	13.03	10.05	0.27	1.79	4.83	4.71	2.05	0.87	97.73
	60.93	0.30	22.26	2.80	0.06	0.25	6.95	5.43	0.86	0.15	100.91
	60.06	1.75	12.15	12.31	0.35	1.97	4.73	3.89	2.09	0.71	98.82
	58.99	1.51	14.88	10.28	0.27	1.98	5.71	4.21	1.49	0.68	97.24
	58.59	1.49	14.93	10.40	0.26	2.03	5.83	4.25	1.54	0.68	99.14
	58.57	1.51	15.06	10.33	0.27	2.07	5.72	4.19	1.60	0.69	98.35
	58.96	1.54	14.72	10.57	0.28	1.97	5.65	4.06	1.54	0.70	97.23
	62.70	1.31	13.64	9.31	0.27	1.27	4.35	4.25	2.27	0.63	98.46
Hekla 1947	56.74	2.00	14.94	11.74	0.28	2.81	6.93	2.30	1.26	1.00	98.64
	56.31	2.78	12.06	14.12	0.36	2.43	6.11	2.63	1.67	1.53	97.86
	56.71	2.07	14.42	11.95	0.29	2.85	6.44	2.84	1.44	0.99	99.25
	56.81	2.08	14.22	11.94	0.29	2.97	6.62	2.74	1.30	1.02	99.09
	56.54	2.00	14.73	12.01	0.28	2.76	6.93	2.47	1.28	0.99	99.47

	56.99	2.23	13.72	12.58	0.31	2.60	6.35	2.76	1.32	1.15	99.09
	57.05	2.29	13.37	12.60	0.29	2.78	6.27	2.75	1.46	1.16	98.81
	56.63	2.24	13.33	13.04	0.32	2.82	6.14	2.95	1.38	1.15	98.56
	56.59	2.31	13.08	13.81	0.33	2.93	6.38	2.17	1.28	1.14	97.69
	66.35	2.59	16.03	0.00	0.00	2.27	7.83	2.10	1.61	1.23	99.25
	50.70	2.96	13.28	14.64	0.23	5.84	10.27	1.25	0.49	0.34	98.94
	57.03	2.08	14.74	11.73	0.29	2.91	6.60	2.33	1.32	0.98	98.26
	57.34	2.29	13.33	12.56	0.31	2.68	6.20	2.71	1.36	1.24	99.57
	56.91	2.09	14.62	10.87	0.26	2.73	5.95	4.00	1.54	1.03	98.24
	57.54	2.57	12.83	13.08	0.30	2.47	3.98	3.80	2.06	1.37	98.20
	57.50	2.48	12.63	13.64	0.34	2.63	6.23	1.75	1.49	1.31	99.36
	57.04	2.47	12.61	13.77	0.33	2.25	5.86	2.63	1.75	1.31	98.78
	56.31	2.01	14.86	11.95	0.30	2.90	6.95	2.51	1.24	0.97	98.83
	56.30	2.26	13.87	12.05	0.30	2.88	5.64	3.46	2.13	1.10	97.86
	56.07	2.59	13.06	13.51	0.33	2.91	6.54	2.16	1.43	1.38	101.06
Hekla 1991	56.45	1.99	15.87	9.81	1.99	2.18	6.29	4.97	1.23	0.98	99.95
	56.21	2.38	13.02	12.81	2.38	2.73	5.99	3.97	1.40	1.18	98.72
	56.62	2.43	12.46	12.16	2.43	2.92	5.77	4.42	1.72	1.20	99.17
	56.39	0.23	26.52	0.93	0.23	0.14	9.60	5.82	0.24	0.09	100.48
	56.87	2.37	12.79	12.33	2.37	2.70	5.86	3.99	1.60	1.19	99.80
	57.19	2.41	12.94	11.59	2.41	2.62	5.86	4.31	1.66	1.15	99.13
	57.33	2.41	13.12	10.96	2.41	2.59	6.09	4.44	1.58	1.22	99.06
	56.01	2.35	12.87	12.99	2.35	2.81	6.30	3.84	1.37	1.14	98.67
	56.32	2.39	12.92	12.28	2.39	2.82	6.10	4.08	1.63	1.15	99.26

	57.40	2.39	12.61	11.47	2.39	2.69	5.84	4.50	1.65	1.14	98.82
	56.87	2.44	12.71	12.50	2.44	2.23	5.62	3.97	2.03	1.29	98.33
	56.99	2.33	13.15	10.72	2.33	2.50	6.37	4.87	1.64	1.17	99.44
	58.52	2.42	13.43	12.69	2.42	2.83	5.85	1.20	1.51	1.22	98.79
	56.68	0.28	25.66	1.58	0.28	0.28	9.52	5.48	0.36	0.13	100.22
	57.68	2.28	13.55	11.57	2.28	2.55	5.96	3.43	1.58	1.13	98.49
	58.76	2.46	13.20	12.25	2.46	2.77	6.14	1.22	1.67	1.25	97.78
Katla 1357	48.83	4.50	12.42	14.61	0.24	5.17	10.43	2.49	0.73	0.57	99.94
	48.31	4.62	13.18	15.51	0.25	4.72	9.94	2.25	0.65	0.58	99.66
	48.72	4.59	12.86	13.33	0.23	5.42	11.10	2.30	0.87	0.60	99.52
Lipari Obsidian	75.21	0.08	12.87	1.40	0.07	0.04	0.80	3.85	5.66	0.01	99.57
	74.62	0.08	13.25	1.40	0.07	0.03	0.73	4.06	5.77	0.01	98.85
	74.48	0.08	13.40	1.59	0.08	0.03	0.77	4.00	5.58	0.00	99.66
	75.32	0.08	13.06	1.40	0.07	0.04	0.67	3.87	5.49	0.01	99.25
	75.16	0.08	13.16	1.37	0.07	0.03	0.72	3.81	5.60	0.00	99.81
	74.63	0.08	13.25	1.71	0.07	0.02	0.73	3.96	5.54	0.00	100.22
	74.48	0.08	13.39	1.59	0.07	0.04	0.78	3.93	5.64	0.01	99.42
	74.69	0.08	13.40	1.34	0.04	0.04	0.74	3.95	5.70	0.00	99.37
	74.57	0.08	13.74	1.35	0.06	0.07	0.80	3.86	5.48	0.01	100.28
	74.98	0.07	13.10	1.55	0.08	0.07	0.75	3.73	5.65	0.01	99.76
	74.72	0.07	13.14	1.47	0.06	0.05	0.75	4.03	5.71	0.01	99.78
	74.75	0.07	12.95	1.77	0.07	0.08	0.70	3.91	5.69	0.00	99.53
	74.99	0.08	13.13	1.58	0.06	0.06	0.74	4.16	5.20	0.00	100.22
	74.80	0.08	13.20	1.39	0.07	0.06	0.75	4.28	5.36	0.01	99.86

SILK

74.91	0.08	13.23	1.52	0.06	0.03	0.79	4.23	5.15	0.01	99.77
74.92	0.09	13.37	1.60	0.06	0.03	0.69	4.13	5.10	0.01	99.34
75.03	0.07	13.29	1.30	0.05	0.03	0.68	4.14	5.39	0.02	99.12
74.96	0.08	13.21	1.65	0.07	0.03	0.74	4.03	5.22	0.01	99.94
75.13	0.08	12.89	1.43	0.07	0.04	0.75	4.23	5.37	0.00	100.96
74.77	0.09	13.28	1.50	0.08	0.05	0.77	4.15	5.32	0.00	99.81
74.99	0.08	12.93	1.66	0.07	0.06	0.90	4.04	5.25	0.01	100.04
65.63	1.38	14.01	6.15	0.21	1.31	3.55	4.78	2.63	0.36	99.50
66.03	1.38	14.14	5.75	0.20	1.36	3.51	4.59	2.68	0.37	98.65
65.20	1.40	14.31	6.05	0.21	1.27	3.72	4.82	2.68	0.36	98.21
65.88	1.37	13.83	6.19	0.20	1.38	3.46	4.73	2.61	0.35	99.39
66.14	1.38	13.76	5.97	0.21	1.44	3.57	4.55	2.63	0.36	98.99
65.25	1.37	14.13	6.01	0.21	1.39	4.06	4.68	2.55	0.35	100.14
65.81	1.37	13.98	5.85	0.21	1.33	4.06	4.52	2.51	0.36	99.82
65.65	1.38	13.87	6.19	0.21	1.26	3.76	4.73	2.58	0.37	99.03
66.26	1.38	13.74	5.99	0.20	1.38	3.59	4.51	2.58	0.36	99.31
65.44	1.38	14.27	6.01	0.20	1.42	3.64	4.66	2.62	0.37	99.52
65.49	1.37	14.18	6.29	0.19	1.30	3.58	4.62	2.59	0.37	99.50
65.83	1.38	14.02	6.08	0.21	1.33	3.56	4.61	2.61	0.37	99.09
65.34	1.37	14.10	6.36	0.20	1.45	4.00	4.37	2.44	0.37	100.01
66.57	1.40	14.21	5.60	0.19	1.35	3.63	4.14	2.54	0.37	100.19
66.09	1.38	14.08	5.79	0.20	1.40	3.67	4.47	2.59	0.34	98.88
65.84	1.39	13.68	6.11	0.21	1.33	3.48	4.90	2.69	0.36	99.37
65.42	1.37	14.13	6.24	0.20	1.41	3.58	4.66	2.62	0.37	99.52

	65.49	1.35	14.22	6.21	0.21	1.34	3.66	4.61	2.53	0.38		99.63
	66.01	1.37	13.73	6.13	0.20	1.41	3.60	4.56	2.62	0.36		99.66
	65.40	1.34	14.10	6.25	0.22	1.42	3.65	4.73	2.56	0.35		100.15
	65.84	1.37	13.77	6.10	0.22	1.40	3.71	4.58	2.65	0.36		98.87
SL1	55.67	1.83	14.80	11.50	0.26	2.91	6.78	3.95	1.38	0.92		98.61
	56.25	1.87	14.82	10.99	0.25	2.75	6.49	4.30	1.34	0.94		99.45
	57.26	1.87	15.32	10.15	0.25	2.64	6.42	3.75	1.39	0.96		99.12
	57.12	1.89	14.88	10.28	0.26	2.64	6.31	4.29	1.36	0.96		98.04
	56.88	1.84	14.82	10.64	0.27	2.72	6.45	4.06	1.37	0.95		99.46
	55.97	1.86	14.95	10.92	0.27	2.72	6.55	4.42	1.39	0.96		98.96
	57.18	1.90	14.71	10.47	0.24	2.60	6.18	4.28	1.48	0.97		98.80
	56.82	1.82	14.60	10.95	0.25	2.65	6.48	4.24	1.25	0.94		99.69
	56.92	1.87	14.85	10.77	0.26	2.72	6.32	3.94	1.39	0.95		99.02
	56.65	1.93	14.84	10.66	0.25	2.84	6.50	3.99	1.34	0.99		98.82
	56.20	1.99	14.51	11.05	0.28	2.97	6.83	3.84	1.26	1.07		99.35
	55.93	1.98	14.80	11.23	0.26	2.82	6.50	4.09	1.33	1.05		98.91
	55.79	2.01	14.75	11.35	0.27	2.79	6.72	3.98	1.32	1.02		99.10
	55.58	2.06	14.33	11.52	0.26	3.04	6.79	3.93	1.40	1.09		97.92
	55.48	2.00	14.68	11.63	0.27	3.03	6.69	3.87	1.33	1.02		99.66
	55.60	2.02	14.66	11.58	0.27	2.97	6.72	3.83	1.27	1.10		98.69
	55.76	2.07	14.71	11.34	0.27	2.98	6.52	3.87	1.43	1.06		98.52
	55.70	1.99	14.48	11.32	0.27	3.02	6.76	4.00	1.39	1.06		98.93
	56.48	2.05	14.21	11.01	0.26	3.02	6.54	4.01	1.32	1.09		99.26
RL1	48.66	4.16	13.35	15.56	0.22	4.34	9.24	3.05	0.92	0.51		99.47

49.70	2.20	13.70	12.05	0.18	7.01	12.02	2.63	0.28	0.22	100.78
49.18	2.22	14.08	13.05	0.20	6.51	11.66	2.66	0.22	0.22	100.24
49.76	2.27	13.74	12.02	0.19	7.13	11.99	2.38	0.29	0.22	100.20
50.34	2.25	13.65	11.28	0.18	7.45	12.21	2.30	0.14	0.19	100.55
67.28	0.48	15.05	5.84	0.20	0.45	3.68	4.79	2.11	0.12	99.23
72.55	0.19	14.44	3.10	0.11	0.14	1.97	4.91	2.49	0.11	97.65
72.83	0.19	13.95	3.36	0.12	0.13	1.99	4.76	2.66	0.02	100.01
73.27	0.19	13.77	3.01	0.12	0.09	2.08	4.86	2.60	0.02	98.95
72.49	0.19	14.26	3.21	0.12	0.15	2.12	4.89	2.55	0.02	98.53
72.79	0.17	13.80	3.14	0.10	0.16	2.06	5.11	2.66	0.02	97.83
72.90	0.19	14.05	3.08	0.11	0.15	2.12	4.79	2.59	0.02	96.16

Table A.2.2. Secondary glass standards for EPMA (non-normalised)

DataSet/Point	SiO₂	TiO₂	Al₂O₃	FeO	MnO	MgO	CaO	Na₂O	K₂O	P₂O₅	Total	Standard
1	53.9346	2.2666	13.7207	12.7276	0.1827	3.6812	7.2985	3.1962	1.6988	0.3697	99.0766	BCR-2G
2	54.1304	2.2913	13.5067	12.6721	0.2026	3.6168	7.0971	3.0944	1.8108	0.3383	98.7605	BCR-2G
3	54.2393	2.2711	13.0686	12.6245	0.2074	3.6552	7.2742	3.2742	1.7855	0.3293	98.7292	BCR-2G
4	76.2592	0.0794	12.8869	1.5706	0.0727	0.0521	0.7584	4.0109	5.2082	0.0139	100.9123	Lipari
5	75.7437	0.0815	12.7646	1.5353	0.0724	0.0398	0.6935	4.1173	5.2115	0.0099	100.2694	Lipari
6	73.9441	0.0804	12.6063	1.5064	0.0451	0.033	0.7022	4.0831	5.2511	0.0132	98.2648	Lipari
7	74.3367	0.0831	12.9576	1.4698	0.0585	0.0717	0.6994	4.1114	5.1438	0.0109	98.9429	Lipari
8	74.4902	0.0773	13.0603	1.5235	0.0664	0.0397	0.8205	4.1376	5.1785	0.0268	99.4209	Lipari
9	5.0383	0.0875	13.0399	73.8443	0.0703	0.0308	1.5303	3.9363	0.7198	0.0143	98.3119	Lipari
10	5.057	0.0717	13.3174	73.9403	0.0637	0.0451	1.5113	4.1062	0.7521	0.014	98.8788	Lipari
11	5.0911	0.0865	13.0887	74.1761	0.0646	0.0225	1.5593	4.1588	0.7511	0.0159	99.0146	Lipari
12	5.3085	0.0754	13.1362	74.7009	0.0688	0.0463	1.3735	4.0991	0.8141	0.011	99.6338	Lipari
13	5.1982	0.0764	12.6631	73.6932	0.0711	0.0554	1.4085	3.9761	0.6972	0.0116	97.8508	Lipari
14	5.1711	0.0807	12.8907	74.3177	0.0648	0.0607	1.6695	4.0816	0.7505	0.013	99.1003	Lipari
15	1.9011	2.2907	13.5603	54.5861	0.1967	3.5944	12.5752	3.2212	7.1205	0.3666	99.4129	BCR-2G
16	1.7229	2.2778	13.423	54.6984	0.1978	3.6425	12.7114	3.03	7.4121	0.3575	99.4733	BCR-2G
17	1.8297	2.2895	13.3652	54.6558	0.2015	3.6252	12.4978	3.1735	7.448	0.3873	99.4735	BCR-2G
18	1.7382	2.2843	13.3038	54.733	0.2072	3.6056	12.0074	3.2616	7.0451	0.3678	98.554	BCR-2G
19	1.7886	2.2919	13.6545	54.821	0.2069	3.6032	12.4013	3.1996	7.1527	0.3732	99.4929	BCR-2G
20	1.7539	2.2791	13.4331	54.4521	0.2024	3.5302	12.6881	3.1832	7.3348	0.3657	99.2227	BCR-2G
21	1.7522	2.3023	13.5628	55.7709	0.1926	3.7345	12.8941	1.1644	7.1172	0.376	98.867	BCR-2G

22	1.7624	2.295	13.7449	56.2914	0.2011	3.6634	12.4957	1.1911	7.2871	0.365	99.2972	BCR-2G
23	1.9114	2.3048	13.7837	55.3051	0.1938	3.5628	12.7506	1.2498	7.3091	0.3692	98.7402	BCR-2G
24	3.5014	0.0812	13.7538	77.1316	0.0559	0.049	1.6245	0.2924	0.7165	0.0194	97.2257	Lipari
25	3.301	0.0846	13.5992	78.502	0.0668	0.0139	1.6986	0.1998	0.7579	0.0115	98.2352	Lipari
26	3.2686	0.086	13.4583	77.1331	0.0619	0.0616	1.7058	0.0736	0.7683	0.0203	96.6375	Lipari

Suppl. Chapter 5: Is there a Climatic Control on Icelandic volcanism?

Table A.3. NEVA database v.2.0

Name	Method	Mid age cal BC/AD	Mid age cal age BP (2000)	Mid age cal BP (1950)	Source	Region	Mean age of event deposit cal age BP (1950)	¹⁴ C Median Age (where applicable)
Hekla 1947	H	1947	53	3	Hekla	Great Britain		
Hekla 1947	H	1947	53	3	Hekla	Great Britain		
Hekla 1947	H	1947	53	3	Hekla	Ireland		
Hekla 1947	H	1947	53	3	Hekla	Ireland		
Hekla 1947	H	1947	53	3	Hekla	Ireland		
Hekla 1947	H	1947	53	3	Hekla	Ireland		
Hekla 1947	H	1947	53	3	Hekla	Ireland		
Hekla 1947	H	1947	53	3	Hekla	Ireland		
Hekla 1947	H	1947	53	3	Hekla	Ireland		
Hekla 1947	H	1947	53	3	Hekla	Ireland		
Hekla 1947	H	1947	53	3	Hekla	Ireland		
Hekla 1947	H	1947	53	3	Hekla	Ireland		
Hekla 1947	H	1947	53	3	Hekla	Ireland		
Hekla 1947	H	1947	53	3	Hekla	Ireland		
Hekla 1947	H	1947	53	3	Hekla	Ireland		
Hekla 1947	H	1947	53	3	Hekla	Ireland		3

Hekla 1947	H	1947	53	3	Hekla	Ireland	
Hekla 1947	H	1947	53	3	Hekla	Ireland	
Hekla 1947	H	1947	53	3	Hekla	Ireland	
Hekla 1947	H	1947	53	3	Hekla	Ireland	
Hekla 1947	H	1947	53	3	Hekla	Great Britain	
Hekla 1947	H	1947	53	3	Hekla	Ireland	
Askja 1875	R	1845	95	75	Askja	Poland	
Askja 1875	H	1875	125	75	Askja	Poland	
Askja 1875	H	1875	125	75	Askja	Germany	
Askja 1875	H	1875	125	75	Askja	Scandinavia	
Askja 1875	H	1875	125	75	Askja	Poland	
Askja 1875	H	1875	125	75	Askja	Scandinavia	
Askja 1875	H	1875	125	75	Askja	Scandinavia	
Askja 1875	H	1875	125	75	Askja	Scandinavia	
Askja 1875	H	1875	125	75	Askja	Germany	
Askja 1875	H	1875	125	75	Askja	Scandinavia	
Askja 1875	H	1875	125	75	Askja	Scandinavia	
Askja 1875	H	1875	125	75	Askja	Scandinavia	
Askja 1875	H	1875	125	75	Askja	Scandinavia	
Askja 1875	H	1875	125	75	Askja	Scandinavia	
Askja 1875	H	1875	125	75	Askja	Scandinavia	
Askja 1875	H	1875	125	75	Askja	Scandinavia	
Askja 1875	H	1875	125	75	Askja	Scandinavia	75

Askja 1875	W	833	1167	75	Askja	Scandinavia	
Hekla 1845	H	1845	155	105	Hekla	Great Britain	
Hekla 1845	H	1845	155	105	Hekla	Ireland	
Hekla 1845	H	1845	155	105	Hekla	Ireland	
Hekla 1845	H	1845	155	105	Hekla	Ireland	
Hekla 1845	H	1845	155	105	Hekla	Faroes	
Hekla 1845	H	1845	155	105	Hekla	Ireland	
Hekla 1845	H	1845	155	105	Hekla	Ireland	
Hekla 1845	H	1845	155	105	Hekla	Ireland	105
BRACSH-1	I	1804	196	146	Grímsvötn?	Ireland	146
QUB-384/G1: Borge unknown 1 cf. Loch Portain B	I	1700	300	250	Unknown (Iceland)	Scandinavia	250
QUB-384/G3: Borge unknown 2	I	1700	300	250	Unknown (Iceland)	Great Britain	
QUB-384/G3: Borge unknown 2	I	1700	300	250	Unknown (Iceland)	Scandinavia	250
QUB-384/G4: Borge unknown 3	I	1700	300	250	Unknown (Iceland)	Great Britain	
QUB-384/G4: Borge unknown 3	I	1700	300	250	Unknown (Iceland)	Scandinavia	250
Hekla 1693?	H	1693	307	257	Hekla	Ireland	
Hekla 1693?	H	1693	307	257	Hekla	Ireland	257
SLU-5	I	1650	350	300	Unknown (Iceland)	Ireland	300
Hekla 1510	H	1510	490	440	Hekla	Ireland	
Hekla 1510	H	1510	490	440	Hekla	Great Britain	
Hekla 1510	H	1510	490	440	Hekla?	Great Britain	
Hekla 1510	H	1510	490	440	Hekla	Great Britain	
Hekla 1510	H	1510	490	440	Hekla	Ireland	440

Hekla 1510	H	1510	490	440	Hekla	Ireland	
Hekla 1510	H	1510	490	440	Hekla	Ireland	
Hekla 1510	H	1510	490	440	Hekla	Ireland	
Hekla 1510	H	1510	490	440	Hekla	Ireland	
Hekla 1510	H	1510	490	440	Hekla	Ireland	
Hekla 1510	H	1510	490	440	Hekla	Ireland	
Hekla 1510	H	1510	490	440	Hekla	Ireland	
Hekla 1510	H	1510	490	440	Hekla	Ireland	
Hekla 1510	H	1510	490	440	Hekla	Great Britain	
Hekla 1510	H	1510	490	440	Hekla	Ireland	
Hekla 1510	H	1510	490	440	Hekla	Ireland	
Hekla 1510	H	1510	490	440	Hekla	Great Britain	
Hekla 1510	H	1510	490	440	Hekla	Ireland	
Hekla 1510	H	1510	490	440	Hekla	Great Britain	
Hekla 1510	H	1510	490	440	Hekla	Ireland	
Hekla 1510	H	1510	490	440	Hekla	Ireland	
Hekla 1510	H	1510	490	440	Hekla	Ireland	
Hekla 1510	H	1510	490	440	Hekla	Ireland	
Loch Portain B tephra	A	1510	490	440	Hekla?	Great Britain	
Loch Portain B tephra	A	1510	490	440	Hekla?	Great Britain	440
MOR-T1 / Veiðivötn 1477	I	1477	523	473	Veiðivötn	Ireland	
Veiðivötn 1477	H	1477	523	473	Veiðivötn	Scandinavia	473
Öræfajökull 1362	H	1362	638	588	Öræfajökull	Ireland	588

Öræfajökull 1362	H	1362	638	588	Öræfajökull	Ireland	
Öræfajökull 1362	H	1362	638	588	Askja	Scandinavia	
Öræfajökull 1362	H	1362	638	588	Askja	Scandinavia	
Öræfajökull 1362	H	1362	638	588	Öræfajökull	Ireland	
Öræfajökull 1362	H	1362	638	588	Öræfajökull	Ireland	
Öræfajökull 1362	H	1362	638	588	Askja	Scandinavia	
Öræfajökull 1362	H	1362	638	588	Öræfajökull	Ireland	
Öræfajökull 1362	H	1362	638	588	Öræfajökull	Ireland	
Öræfajökull 1362	H	1362	638	588	Öræfajökull	Ireland	
QUB-385/G1: Borge unknown 4	A	1362	638	588	Unknown (Iceland)	Scandinavia	588
GB4-50	I	1250	750	700	Unknown (Iceland)	Ireland	700
Hekla 1158	H	1158	842	792	Hekla	Scandinavia	
Hekla 1158	H	1158	842	792	Hekla	Scandinavia	
Hekla 1158	H	1158	842	792	Hekla	Scandinavia	
Hekla 1158	H	1158	842	792	Hekla	Scandinavia	792
GB4-57	I	1150	850	800	Unknown (Iceland)	Ireland	800
BGMT1	I	1157	843	830	Unknown (Iceland)	Great Britain	830
Hekla 1104	H	1104	896	846	Hekla	Ireland	
Hekla 1104	H	1104	896	846	Hekla	Ireland	
Hekla 1104	H	1104	896	846	Hekla	Scandinavia	
Hekla 1104	H	1104	896	846	Hekla	Scandinavia	
Hekla 1104	H	1104	896	846	Hekla	Scandinavia	
Hekla 1104	H	1104	896	846	Hekla	Scandinavia	946

Hekla 1104	H	1104	896	846	Hekla	Ireland	
Hekla 1104	H	1104	896	846	Hekla	Ireland	
Hekla 1104	H	1104	896	846	Hekla	Ireland	
Hekla 1104	H	1104	896	846	Hekla	Ireland	
Hekla 1104	H	1104	896	846	Hekla	Ireland	
Hekla 1104	H	1104	896	846	Hekla	Scandinavia	
Hekla 1104	H	1104	896	846	Hekla	Faroes	
Hekla 1104	H	1104	896	846	Hekla	Ireland	
Hekla 1104	H	1104	896	846	Hekla	Ireland	
Hekla 1104	H	1104	896	846	Hekla	Ireland	
Hekla 1104	H	1104	896	846	Hekla	Ireland	
Hekla 1104	H	1104	896	846	Hekla	Ireland	
Hekla 1104	H	1104	896	846	Hekla	Ireland	
Hekla 1104	H	1104	896	846	Hekla	Ireland	
Hekla 1104	H	1104	896	846	Hekla	Ireland	
Hekla 1104	H	1104	896	846	Hekla	Ireland	
Hekla 1104	H	1104	896	846	Hekla	Ireland	
Hekla 1104	H	1104	896	846	Hekla	Ireland	
Hekla 1104	H	1104	896	846	Hekla	Ireland	
Hekla 1104	H	1104	896	846	Hekla	Ireland	
Hekla 1104	H	1104	896	846	Hekla	Ireland	
Hekla 1104	H	1104	896	846	Hekla	Ireland	
Hekla 1104	H	1104	896	846	Hekla	Scandinavia	
Hekla 1104	H	1104	896	846	Hekla	Ireland	
MOR-T4	I	1000	1000	950	Unknown (Iceland)	Ireland	
MOR-T4	I	1000	1000	950	Unknown (Iceland)	Ireland	950

MOR-T4	I	1000	1000	950	Unknown (Iceland)	Great Britain		
MOR-T4	I	1000	1000	950	Unknown (Iceland)	Ireland		
BMR-90	I	920	1080	1030	Unknown (Iceland)	Ireland	1030	
BIP-24a	I	900	1100	1050	Unknown (Iceland)	Scandinavia		
BIP-24a	I	900	1100	1050	Unknown (Iceland)	Scandinavia	1050	
QUB-389/G2: Borge unknown 5	I	900	1100	1050	Unknown (Iceland)	Scandinavia	1050	
QUB-389/G4: Borge unknown 6	I	900	1100	1050	Unknown (Iceland)	Scandinavia	1050	
MOR-T5	I	890	1110	1060	Unknown (Iceland)	Ireland	1060	
TSK11_B1u_137e142_T	V	873	1127	1077	Grímsvötn?	Germany	1077	
Landnám	GRIP Ice core	871	1129	1079	Veiðivötn/Torfajökull	Scandinavia		
Landnám	GRIP ice core	871	1129	1079	Veiðivötn/Torfajökull	Faroes		
Landnám	GRIP Ice core	871	1129	1079	Veiðivötn/Torfajökull	Great Britain		
Landnám	GRIP ice core	871	1129	1079	Veiðivötn/Torfajökull	Faroes	1079	
Tjørnuvík	I	850	1150	1100	Hekla	Faroes		
Tjørnuvík	I	850	1150	1100	Hekla	Faroes		
Tjørnuvík	I	850	1150	1100	Hekla	Faroes	1100	
MOR-T6	I	840	1160	1110	Hekla	Ireland	1110	
AD 860 A	W	833	1167	1117	Grímsvötn?	Great Britain		
AD 860 A	W	833	1167	1117	Grímsvötn?	Great Britain		
AD 860 A	W	833	1167	1117	Grímsvötn?	Ireland		
AD 860 A	W	833	1167	1117	Grímsvötn?	Ireland	1117	

AD 860 A	W	833	1167	1117	Grímsvötn?	Ireland	
AD 860 A	W	833	1167	1117	Grímsvötn?	Great Britain	
AD 860 A	W	833	1167	1117	Grímsvötn?	Ireland	
QUB-571/G3: Borge unknown 7	A	785	1215	1165	Unknown (Iceland)	Scandinavia	1165
GA4-85	I	750	1250	1200	Katla?	Ireland	
GA4-85	I	750	1250	1200	Katla?	Ireland	
GA4-85	I	750	1250	1200	Katla?	Ireland	
GA4-85	I	750	1250	1200	Katla?	Ireland	1200
SN-1	I	?	1279	1229	Snæfellsjökull	Scandinavia	
SN-1	I	?	1279	1229	Snæfellsjökull	Scandinavia	1229
OWB-105	I	700	1300	1250	Unknown (Iceland)	Scandinavia	
OWB-105	I	700	1300	1250	Unknown (Iceland)	Ireland	1250
QUB-570/G2: Borge unknown 9	I	659	1341	1291	Unknown (Iceland)	Scandinavia	1291
Tjörnuvík B	I	650	1350	1300	Hekla	Scandinavia	1300
QUB-570/G1: Borge Unknown 8	I	650	1350	1300	Unknown (Iceland)	Scandinavia	1300
DOM-3	I	650	1350	1300	Unknown (Iceland)	Germany	
DOM-3	I	650	1350	1300	Unknown (Iceland)	Germany	
DOM-3	I	650	1350	1300	Unknown (Iceland)	Germany	1300
QUB-569/G1: Borge unknown 10	I	625	1375	1325	Unknown (Iceland)	Scandinavia	1325
QUB-568/G3: Borge unknown 11	I	600	1400	1350	Unknown (Iceland)	Scandinavia	1350
QUB-567/G1: Borge unknown 12	I	450	1550	1500	Unknown (Iceland)	Scandinavia	1500
QUB-567/G2: Borge unknown 13	I	450	1550	1500	Unknown (Iceland)	Scandinavia	1500
DOM-4	I	400	1600	1550	Unknown (Iceland)	Germany	1550

DOM-4	I	400	1600	1550	Unknown (Iceland)	Germany		
JC09_B2_170e173_T/JC09_B2_155e158_T	V	25	1975	1925	Unknown (Iceland)	Poland	1925	
Stömyren (?= different phase of Glen Garry)	I	-150	2150	2100	Unknown (Iceland)	Scandinavia	2100	
Stömyren (?= different phase of Glen Garry)	I	-150	2150	2100	Unknown (Iceland)	Scandinavia		
Glen Garry?	W	-226	2226	2176	Unknown (Iceland)	Germany	2176	
Glen Garry	W	-226	2226	2176	Unknown (Iceland)	Great Britain		
Glen Garry	W	-226	2226	2176	Unknown (Iceland)	Great Britain		
Glen Garry	W	-226	2226	2176	Unknown (Iceland)	Great Britain		
Glen Garry	W	-226	2226	2176	Unknown (Iceland)	Great Britain		
Glen Garry	W	-226	2226	2176	Unknown (Iceland)	Great Britain		
Glen Garry	W	-226	2226	2176	Unknown (Iceland)	Great Britain		
Glen Garry	W	-226	2226	2176	Unknown (Iceland)	Germany		
Glen Garry	W	-226	2226	2176	Unknown (Iceland)	Germany		
Glen Garry	W	-226	2226	2176	Unknown (Iceland)	Great Britain		
Glen Garry	W	-226	2226	2176	Unknown (Iceland)	Great Britain		
Glen Garry	W	-226	2226	2176	Unknown (Iceland)	Great Britain		
Glen Garry	W	-226	2226	2176	Unknown (Iceland)	Great Britain		
Glen Garry	W	-226	2226	2176	Unknown (Iceland)	Germany		
Glen Garry	W	-226	2226	2176	Unknown (Iceland)	Great Britain		
Glen Garry	W	-226	2226	2176	Unknown (Iceland)	Great Britain		
Glen Garry	W	-226	2226	2176	Unknown (Iceland)	Great Britain		
Glen Garry	W	-226	2226	2176	Unknown (Iceland)	Great Britain		
Glen Garry	W	-226	2226	2176	Unknown (Iceland)	Great Britain		2176

Glen Garry	W	-226	2226	2176	Unknown (Iceland)	Great Britain		
Glen Garry	W	-226	2226	2176	Unknown (Iceland)	Great Britain		
Glen Garry	W	-226	2226	2176	Unknown (Iceland)	Great Britain		
Glen Garry	W	-226	2226	2176	Unknown (Iceland)	Great Britain		
Glen Garry	W	-226	2226	2176	Unknown (Iceland)	Great Britain		
Glen Garry	W	-226	2226	2176	Unknown (Iceland)	Great Britain		
Glen Garry	W	-226	2226	2176	Unknown (Iceland)	Great Britain		
Glen Garry	W	-226	2226	2176	Unknown (Iceland)	Great Britain		
Glen Garry	W	-226	2226	2176	Unknown (Iceland)	Great Britain		
QUB-565/G2: Borge unknown 15	I	-300	2300	2250	Unknown (Iceland)	Scandinavia	2250	
BMR-190	W	-645	2645	2595	Hekla	Ireland		
BMR-190	W	-645	2645	2595	Hekla	Ireland		
BMR-190	W	-645	2645	2595	Hekla	Ireland		
BMR-190	W	-645	2645	2595	Hekla	Ireland		
BMR-190	W	-645	2645	2595	Hekla	Ireland		
BMR-190	W	-645	2645	2595	Hekla	Ireland		
BMR-190	W	-645	2645	2595	Hekla	Ireland	2595	
QUB490 Unknown Garry	?	-675.5	2676	2626	Unknown (Iceland)	Ireland	2626	
BGMT3 = Microlite	W	-697	2697	2647	Snæfellsjökull	Great Britain		
Microlite	W	-717.5	2718	2668	Snæfellsjökull	Great Britain		
Microlite	W	-717.5	2718	2668	Snæfellsjökull	Ireland		
Microlite	W	-717.5	2718	2668	Snæfellsjökull	Ireland	2667	

Microlite	W	-717.5	2718	2668	Snæfellsjökull	Ireland	
Microlite	W	-717.5	2718	2668	Snæfellsjökull	Germany	
Microlite	W	-717.5	2718	2668	Snæfellsjökull	Germany	
Microlite	W	-717.5	2718	2668	Snæfellsjökull	Ireland	
Microlite	W	-717.5	2718	2668	Snæfellsjökull	Ireland	
Microlite	W	-717.5	2718	2668	Snæfellsjökull	Ireland	
Microlite	W	-717.5	2718	2668	Snæfellsjökull	Germany	
Microlite	W	-717.5	2718	2668	Snæfellsjökull	Germany	
Microlite	W	-717.5	2718	2668	Snæfellsjökull	Ireland	
Microlite	W	-717.5	2718	2668	Snæfellsjökull	Ireland	
Microlite	W	-717.5	2718	2668	Snæfellsjökull	Ireland	
Microlite	W	-717.5	2718	2668	Snæfellsjökull	Ireland	
Microlite	W	-717.5	2718	2668	Snæfellsjökull	Ireland	
OMH-185 Population 2	W	-717.5	2718	2668	Unknown (Iceland)	Great Britain	
OMH-185 Population 2	W	-717.5	2718	2668	Unknown	Ireland	
OMH-185 Population 2	W	-717.5	2718	2668	Unknown	Ireland	
OMH-185 Population 2	W	-717.5	2718	2668	Unknown	Ireland	
OMH-185 Population 2	W	-717.5	2718	2668	Unknown	Ireland	2668
Gullbergby	I	-750	2750	2700	Torfajökull?	Scandinavia	2700
GB4-150 (~SILK-UN)	W	-779	2779	2729	Katla	Ireland	
GB4-150 (~SILK-UN)	W	-779	2779	2729	Katla	Ireland	
GB4-150 (~SILK-UN)	W	-779	2779	2729	Katla	Ireland	
GB4-150 (~SILK-UN)	W	-779	2779	2729	Katla	Ireland	2729

GB4-150 (~SILK-UN)	W	-779	2779	2729	Katla	Ireland		
GB4-150 (~SILK-UN)	W	-779	2779	2729	Katla	Ireland		
GB4-150 (~SILK-UN)	W	-779	2779	2729	Katla	Ireland		
GB4-150 (~SILK-UN)	W	-779	2779	2729	Katla	Ireland		
Hekla 3	W	-1046.5	3046	2996	Hekla	Scandinavia		
Hekla 3	W	-1046.5	3046	2996	Hekla	Faroes		
Hekla 3	W	-1046.5	3046	2996	Hekla	Ireland		
Hekla 3	W	-1046.5	3046	2996	Hekla	Germany		
Hekla 3	W	-1046.5	3046	2996	Hekla	Germany		
Hekla 3	W	-1046.5	3046	2996	Hekla	Scandinavia		
Hekla 3	W	-1046.5	3046	2996	Hekla	Scandinavia		
Hekla 3	W	-1046.5	3046	2996	Hekla	Germany		
Hekla 3	W	-1046.5	3046	2996	Hekla	Scandinavia		
Hekla 3	W	-1046.5	3046	2996	Hekla	Scandinavia		
Hekla 3	W	-1046.5	3046	2996	Hekla	Scandinavia		
Hekla 3	W	-1046.5	3046	2996	Hekla	Scandinavia		
Hekla 3	W	-1046.5	3046	2996	Hekla	Scandinavia	2996	
GB4-182	I	-1350	3350	3300	Unknown (Iceland)	Ireland	3300	
LBA-2 ?= Sn-2 = "x" tephra of Dyngjufjöll region	W	-1650	3650	3600	Snæfellsjökull	Scandinavia	3600	
Hekla-S/Kebister	W	-1775	3770	3720	Hekla	Scandinavia		
Hekla-S/Kebister	W	-1775	3770	3720	Hekla	Scandinavia		
Hekla-S/Kebister	W	-1775	3770	3720	Hekla	Scandinavia	3723	

Hekla-S/Kebister	W	-1775	3770	3720	Hekla	Scandinavia		
Hekla-S/Kebister	W	-1775	3770	3720	Hekla	Scandinavia		
Hekla-S/Kebister	W	-1775	3770	3720	Hekla	Scandinavia		
Hekla-S/Kebister	W	-1775	3770	3720	Hekla	Scandinavia		
Hekla-S/Kebister	W	-1775	3770	3720	Hekla	Scandinavia		
Hekla-S/Kebister	W	-1775	3770	3720	Hekla	Scandinavia		
Hekla-S/Kebister	W	-1775	3770	3725	Hekla	Scandinavia		
Hekla-S/Kebister	W	-1775	3775	3725	Hekla	Faroes		
Hekla-S/Kebister	W	-1775	3775	3725	Hekla	Germany		
Hekla-S/Kebister	W	-1775	3775	3725	Hekla	Germany		
Hekla-S/Kebister	W	-1775	3775	3725	Hekla	Great Britain		
Hekla-S/Kebister	W	-1775	3775	3725	Hekla	Faroes		
Hekla-S/Kebister	W	-1775	3775	3725	Hekla	Faroes		
Hekla-S/Kebister	W	-1775	3775	3725	Hekla	Faroes		
Hekla-S/Kebister	W	-1775	3775	3725	Hekla	Faroes		
Hekla-S/Kebister	W	-1775	3775	3725	Hekla	Faroes		
Hekla-S/Kebister	W	-1775	3775	3725	Hekla	Great Britain		
SILK A1 (?)	R	-1869	3869	3819	Katla	Faroes	3819	5000
Unknown	R	-2096	4196	4146	Unknown (Iceland)	Ireland	4146	3790
BGMT-4 (= Silk-N2)	A	-2337	4337	4287	Katla	Great Britain		
SILK-N2?	A	-2337	4337	4287	Katla	Ireland	4287	
Hekla 4	W	-2337	4337	4287	Hekla	Germany		
Hekla 4	W	-2337	4337	4287	Hekla	Ireland	4287	

Hekla 4	W	-2337	4337	4287	Hekla	Scandinavia	
Hekla 4	W	-2337	4337	4287	Hekla	Great Britain	
Hekla 4	W	-2337	4337	4287	Hekla	Scandinavia	
Hekla 4	W	-2337	4337	4287	Hekla	Scandinavia	
Hekla 4	W	-2337	4337	4287	Hekla	Ireland	
Hekla 4	W	-2337	4337	4287	Hekla	Great Britain	
Hekla 4	W	-2337	4337	4287	Hekla	Great Britain	
Hekla 4	W	-2337	4337	4287	Hekla	Scandinavia	
Hekla 4	W	-2337	4337	4287	Hekla	Ireland	
Hekla 4	W	-2337	4337	4287	Hekla	Great Britain	
Hekla 4	W	-2337	4337	4287	Hekla	Scandinavia	
Hekla 4	W	-2337	4337	4287	Hekla	Scandinavia	
Hekla 4	W	-2337	4337	4287	Hekla	Faroes	
Hekla 4	W	-2337	4337	4287	Hekla	Ireland	
Hekla 4	W	-2337	4337	4287	Hekla	Great Britain	
Hekla 4	W	-2337	4337	4287	Hekla	Ireland	
Hekla 4	W	-2337	4337	4287	Hekla	Ireland	
Hekla 4	W	-2337	4337	4287	Hekla	Germany	
Hekla 4	W	-2337	4337	4287	Hekla	Germany	
Hekla 4	W	-2337	4337	4287	Hekla	Faroes	
Hekla 4	W	-2337	4337	4287	Hekla	Great Britain	
Hekla 4	W	-2337	4337	4287	Hekla	Great Britain	
Hekla 4	W	-2337	4337	4287	Hekla	Scandinavia	

Hekla 4	W	-2337	4337	4287	Hekla	Ireland	
Hekla 4	W	-2337	4337	4287	Hekla	Ireland	
Hekla 4	W	-2337	4337	4287	Hekla	Great Britain	
Hekla 4	W	-2337	4337	4287	Hekla	Germany	
Hekla 4	W	-2337	4337	4287	Hekla	Great Britain	
Hekla 4	W	-2337	4337	4287	Hekla	Scandinavia	
Hekla 4	W	-2337	4337	4287	Hekla	Scandinavia	
Hekla 4	W	-2337	4337	4287	Hekla	Great Britain	
Hekla 4	W	-2337	4337	4287	Hekla	Great Britain	
Hekla 4	W	-2337	4337	4287	Hekla	Great Britain	
Hekla 4	W	-2337	4337	4287	Hekla	Great Britain	
Hekla 4	W	-2337	4337	4287	Hekla	Ireland	
Hekla 4	W	-2337	4337	4287	Hekla	Great Britain	
Hekla 4	W	-2337	4337	4287	Hekla	Faroes	
Hekla 4	W	-2337	4337	4287	Hekla	Scandinavia	
Hekla 4	W	-2337	4337	4287	Hekla	Scandinavia	
Hekla 4	W	-2337	4337	4287	Hekla	Great Britain	
Hekla 4	W	-2337	4337	4287	Hekla	Scandinavia	
Hekla 4	W	-2337	4337	4287	Hekla	Faroes	
Hekla 4	W	-2337	4337	4287	Hekla	Great Britain	
Hekla 4	W	-2337	4337	4287	Hekla	Ireland	
Hekla 4	W	-2337	4337	4287	Hekla	Ireland	
Hekla 4	W	-2337	4337	4287	Hekla	Great Britain	

Hekla 4	W	-2337	4337	4287	Hekla	Scandinavia		
Hekla 4	W	-2337	4337	4287	Hekla	Faroes		
Hekla 4	W	-2337	4337	4287	Hekla	Scandinavia		
Hekla 4	W	-2337	4337	4287	Hekla	Ireland		
Tv-5	R, I, A	-2940	4940	4890	Unknown	Iceland	4890	6000
HÖ	R	-3030	5030	4980	Hekla	Iceland	4980	6060
SILK-A7	R, I	-3197	5197	5147	Unknown	Faroes	5147	6200
Mjáuvøtn A	I	-3550	5550	5500	Unknown (Iceland)	Faroes		
Mjáuvøtn A	I	-3550	5550	5500	Unknown (Iceland)	Faroes		
Mjáuvøtn A	I	-3550	5550	5500	Unknown (Iceland)	Faroes	5500	
QUB-598/G1: Borge unknown 16	I	-3850	5850	5800	Unknown (Iceland)	Scandinavia	5800	
QUB-598/G3: Borge unknown 17	I	-3850	5850	5800	Unknown (Iceland)	Scandinavia	5800	
QUB-598/G5: Borge unknown 18	I	-3850	5850	5800	Unknown (Iceland)	Scandinavia	5800	
Hov	R	-3950	5950	5900	Grímsvötn	Faroes	5900	5170
QUB-600/G1: Borge unknown 20	I	-4420	6420	6370	Unknown (Iceland)	Scandinavia	6370	
QUB-600/G2: Borge unknown 21	I	-4420	6420	6370	Unknown (Iceland)	Scandinavia	6370	
Hoy	R	-4425	6425	6375	Torfajökull	Ireland		5600
Hoy	R	-4425	6425	6375	Torfajökull	Ireland		
Hoy	R	-4425	6425	6375	Torfajökull	Ireland		
Hoy	R	-4425	6425	6375	Torfajökull	Great Britain		
Hoy	R	-4425	6425	6375	Torfajökull	Great Britain	6375	
Hekla DH	SAR	-4650	6700	6650	Hekla	Iceland	6650	
MOR-T10	I, A	-4700	6700	6650	Torfajökull	Ireland	6650	

MOR-T10	I, A	-4700	6700	6650	Torfajökull	Ireland		
QUB-601/G1: Borge unknown 22	I	-4700	6700	6650	Unknown (Iceland)	Scandinavia	6650	
QUB-601/G2: Borge unknown 23	I	-4700	6700	6650	Unknown (Iceland)	Scandinavia	6650	
Lairg B	A	-4676	6676	6626	Unknown	Ireland	6670	
Lairg B	A	-4676	6676	6626	Unknown	Ireland		
Lairg B	W	-4725.5	6726	6676	Torfajökull	Germany		
Lairg B	W	-4725.5	6726	6676	Torfajökull	Ireland		
Lairg B	W	-4725.5	6726	6676	Torfajökull	Great Britain		
Lairg B	W	-4725.5	6726	6676	Torfajökull	Great Britain		
Lairg B	W	-4725.5	6726	6676	Torfajökull	Ireland		
Lairg B	W	-4725.5	6726	6676	Torfajökull	Ireland		
Lairg B	W	-4725.5	6726	6676	Torfajökull	Ireland		
Lairg B	W	-4725.5	6726	6676	Torfajökull	Ireland		
Lairg B	W	-4725.5	6726	6676	Torfajökull	Ireland		
Lairg B	W	-4725.5	6726	6676	Torfajökull	Ireland		
Lairg B	W	-4725.5	6726	6676	Torfajökull	Ireland		
Lairg B	W	-4725.5	6726	6676	Torfajökull	Germany		
Lairg B	W	-4725.5	6726	6676	Torfajökull	Germany		
Lairg B	W	-4725.5	6726	6676	Torfajökull	Great Britain		
Lairg B	W	-4725.5	6726	6676	Torfajökull	Ireland		
Lairg B	W	-4725.5	6726	6676	Torfajökull	Ireland		
Hekla 5	A, I	-4800	6800	6750	Hekla	Sweden	6900	
Hekla 5	A, I	-4800	6800	6750	Hekla	Sweden		
Hekla 5	I	-5100	7100	7050	Hekla	Iceland		
Hekla 5	A, R	-5050	7100	7050	Hekla	Iceland		
								6185

Lairg A	I, W, A	-4900	6900	6850	Hekla	Ireland	
Lairg A	A, I	-4900	6900	6850	Unknown	Ireland	
Lairg A	A	-4900	6900	6900	Hekla	Ireland	
Lairg A	W	-4949.5	6950	6900	Hekla	Ireland	
Lairg A	W	-4949.5	6950	6900	Hekla	Ireland	
Lairg A	W	-4949.5	6950	6900	Hekla	Scandinavia	
Lairg A	W	-4949.5	6950	6900	Hekla	Great Britain	
Lairg A?	W	-4949.5	6950	6900	Hekla	Scandinavia	
Lairg A	W	-4949.5	6950	6900	Hekla	Great Britain	
Lairg A	W	-4949.5	6950	6900	Hekla	Ireland	
Lairg A	W	-4949.5	6950	6900	Hekla	Ireland	
Lairg A	W	-4949.5	6950	6900	Hekla	Scandinavia	
Lairg A	W	-4949.5	6950	6900	Hekla	Ireland	
Lairg A	W	-4949.5	6950	6900	Hekla	Ireland	
Lairg A	W	-4949.5	6950	6900	Hekla	Germany	
Lairg A	W	-4949.5	6950	6900	Hekla	Germany	
Lairg A	W	-4949.5	6950	6900	Hekla	Scandinavia	
Lairg A	W	-4949.5	6950	6900	Hekla	Great Britain	
Lairg A	W	-4949.5	6950	6900	Hekla	Ireland	
Lairg A	W	-4949.5	6950	6900	Hekla	Scandinavia	
Lairg A	W	-4949.5	6950	6900	Hekla	Great Britain	6895
MOR-T12	A, I	-5350	7350	7300	Hekla?	Ireland	7300
SSn	I	-5550	7550	7500	Unknown (Snaefellsjokull?)	Sweden	7500

SSn	I	-5550	7550	7500	Unknown (Snaefellsjokull?)	Sweden		
Suderoy	I	-6000	8000	7950	Katla	Iceland		
Suderoy	A,I	-6066	8066	8016	Katla	Faroe Islands	7983	
Tv-4	I, A	-7100	8141	8091	Unknown	Iceland	8091	8900
Högstorpssmossen	R, A	-7118	8296	8246	Unknown (Snaefellsjokull?)	Sweden	8246	9000
Tv-3	I, A	-7200	8440	8390	Unknown	Iceland	8390	9200
Saksunarvatn	A, I	-7050	9050	9000	Grimsvotn	Faroe Islands		
Saksunarvatn	R	-7350	9350	9300	Grimsvotn	Shetland Islands		
Saksunarvatn	R	-8022	10022	9972	Grimsvotn	Norway		10210
Saksunarvatn	A	-8150	10150	10100	Grimsvotn	Orkney Islands		
Saksunarvatn	Ice core, A	-8230	10230	10180	Unknown (Grimsvotn?)	Greenland		
Saksunarvatn	R	-8230	10230	10180	Grimsvotn	Greenland		
Saksunarvatn	I, A	-8230	10230	10180	Grimsvotn	Scotland		
Saksunarvatn	I, A	-8260	10260	10210	Grimsvotn	Orkney Islands		
Saksunarvatn	I	-8300	10300	10250	Grimsvotn	Iceland		
Saksunarvatn	A, R	-8300	10350	10300	Unknown (Grimsvotn?)	Iceland		
Saksunarvatn	R, A	-8397	10397	10347	Grimsvotn	Greenland		
Saksunarvatn	I, Ice core	-8400	10400	10350	Grimsvotn	Faroe Islands	10031	
Askja-S	I, A	-7592	9592	9542	Dyngjufjöll	Ireland		10000
Askja-S	A, I	-8475	10475	10425	Askja	Sweden	10474	

Askja-S	I	-8475	10475	10425	Askja	Faroe Islands		
Askja-S	A, I	-8860	10860	10810	Askja	Sweden		
Askja-S	A, R	-8810	10860	10810	Askja	Iceland		
Askja-S	I, A	-8880	10880	10830	Askja	Orkney Islands		
An Druim	I	-6590	9610	9560	Torfajökull	Scotland	9560	
QM1 133	I, A	-7721	9721	9671	Grimsvotn	Orkney Islands	9671	
Høvdarhagi	I	-7775	9775	9725	Unknown (Torfajökull?)	Faroe Islands	9725	
Skopun	I	-7800	9800	9750	Unknown	Faroe Islands	9750	
LL1755	R	-7990	10089	10039	Veidivötn-Bardabunga	Iceland	10039	
Vedde	R	-8080	10080	10030	Katla	Sweden		
Vedde	R	-8173	10173	10123	Katla	Scotland		10300
Vedde	R, A	-8265	10265	10215	Katla	Sweden		10350
Vedde	R, A	-8350	10350	10300	Katla	Russia		
Vedde?	A	-8650	10650	10600	Katla	Norway		
Vedde	R	-9980	11980	11930	Katla	Sweden		
Vedde	R	-10005	12005	11955	Katla	Norway		12067
Vedde	Ice core, A	-10030	12030	11980	Katla	Greenland		
Vedde	R	-10030	12030	11980	Katla	Greenland		
Vedde	A	-10060	12060	12010	Katla	Sweden		
Vedde	I, A	-10073	12073	12023	Katla	Orkney Islands		
Vedde	I	-10120	12120	12070	Katla	Iceland	11527	

Vedde	A, R	-10120	12170	12120	Katla	Iceland		
Vedde	A, I	-10171	12171	12121	Katla	Sweden		
Vedde	R	-10171	12171	12121	Katla	Scotland		
Vedde	R, A	-10221	12221	12171	Katla	Greenland		
Vedde	I, A	-10260	12260	12210	Katla	Scotland		
QM1 154	I, A	-8185	10185	10135	Grimsvotn	Orkney Islands	10135	
QM1 160	I, A	-8207	10207	10157	Grimsvotn	Orkney Islands	10157	
Fosen	I	-8250	10250	10200	Unknown (Öraefajökull?)	Norway	10200	
L-274	I	-8275	10275	10225	Unknown	Faroe Islands	10225	
QM1 187	I, A	-8450	10450	10400	Torfajökull?	Orkney Islands	10400	
CRUM1 444	I, A	-8526	10526	10476	Grimsvotn	Orkney Islands	10476	
Hovsdalur	R, I	-8550	10550	10500	Snaefellsjokull	Faroe Islands	10500	
Tv-1	I, A	-8750	10813	10763	Unknown	Iceland	10763	10800
QM1 188	I, A	-8860	10860	10810	Askja	Orkney Islands	10810	
CRUM1 510	I, A	-8887	10887	10837	Grimsvotn	Orkney Islands	10837	
Ashik	A, I	-8055	10890	10840	Unknown (Iceland)	Scotland	10840	
Sandoy B	I	-9280	11280	11230	Unknown (Bardabunga?)	Faroe Islands	11230	
Hässeldalen	A, I	-9380	11380	11330	Unknown (Snaefellsjokull?)	Sweden	11349	

Hässeldalen	I	-9380	11380	11330	Unknown (Snaefellsjökull?)	Faroe Islands		
Hässeldalen	I, A	-9437	11437	11387	Snaefellsjökull	Orkney Islands		
Sandoy A	I	-9380	11380	11330	Unknown (Bardabunga?)	Faroe Islands	11330	
QM1 192	I, A	-9438	11438	11388	Snaefellsjökull?	Orkney Islands	11388	
AF555	I, A	-9545	11545	11495	Unknown (Katla?)	Scotland	11495	
Roddans Port A	R	-9948	11948	11898	Unknown	Ireland	11898	12000
Roddans Port B	R	-9948	11948	11898	Unknown	Ireland	11898	12000
Vallensgård Mose	I, A	-9948	11948	11898	Unknown	Denmark	11898	12000
QM1 198	I, A	-10058	12058	12008	Unknown	Orkney Islands	12008	
Bld_T122	A, I	-10171	12171	12121	Katla?	Slovenia	12121	
Borrobol	I	-10500	12500	12450	Unknown	Sweden		
Borrobol-type	I, A	-10507	12507	12457	Unknown	Orkney Islands		
Borrobol	I	-10500	12658	12608	Unknown	Scotland		12450
Borrobol	A, I	-10830	12830	12780	Unknown	Scotland		12500
Borrobol-type	A, R	-11640	13690	13640	Unknown	Iceland		
Borrobol	R, I	-12095	14095	14045	Unknown	Scotland		
Borrobol	I, A	-12148	14148	14098	Unknown	Orkney Islands		
Borrobol	I, A	-12450	14450	14400	Unknown	Scotland		
Borrobol	I	-12550	14550	14500	Unknown	Iceland		
Borrobol-type	A, R	-12550	14600	14550	Unknown	Iceland	13553	

LT2	A	-11140	13140	13090	Unknown	France	13090	
LT3	A	-11265	13265	13215	Unknown	France	13215	
Dimna	R	-11340	13340	13290	Unknown	Norway	13290	12800
QM1 213	I, A	-11500	13500	13450	Unknown	Orkney Islands	13450	
QM1 218	I, A	-11500	13500	13450	Unknown	Orkney Islands	13450	
Penifiler	I	-11920	13920	13870	Unknown	Scotland		
Penifiler	I, A	-12039	14039	13989	Unknown	Orkney Islands	13930	
KOL-GS-2	A, I	-12230	14230	14180	Unknown	Iceland	14180	13400